INSTITUT POLYTECHNIQUE DE PARIS

NNT : *to be defined*

Thèse de doctorat

ÉCOLE POLYTECHNIQUE

IP PARIS

A Multi-Scale Analysis of Biodiversity Decline

From Farmer Decisions to Global Food Systems

Thèse de doctorat de l'Institut Polytechnique de Paris
préparée à l'École polytechnique

École doctorale n°626 École doctorale de l'Institut Polytechnique de Paris (EDIPP)

Spécialité de doctorat: Physique

Thèse présentée et soutenue à Palaiseau, le 5 Octobre 2026, par

Elia Moretti

Composition du Jury :

Mauro Napoletano Université Côte d'Azur	Rapporteur
Elisa Thébault Institut d'Écologie et des Sciences de l'Environnement de Paris	Rapporteure
Antoine Mandel Université Paris 1 Panthéon-Sorbonne	Examinateur
Marco Pangallo CENTer for AI, CENTAI	Examinateur
Michael Benzaquen CNRS & École Polytechnique & Capital Fund Management	Directeur de thèse

Acknowledgments

In nature, resilience comes from interconnected networks rather than isolation. Writing the final words of this thesis, I realize how true this is for my own journey. This PhD is not something I achieved alone. It is the result of the guidance, support, and encouragement of a wonderful community, and I am deeply grateful to everyone who helped me along the way.

My deepest thanks go to Michael Benzaquen, who has been a true mentor in both research and life. His constant support gave me the freedom and confidence to pursue my ideas. Michael always listened patiently, never dismissing an idea as too ambitious, but instead pushing me to explore it further. I am especially grateful for his help in organizing my thoughts before speaking—lessons in clarity that will stay with me far beyond academia.

I am just as grateful to Jean-Philippe Bouchaud. Even though he often stayed out of the spotlight, his support behind the scenes was a constant anchor for me. I deeply admire his humility and endless curiosity. These are qualities I want to carry with me, shaping the kind of researcher—and person—I hope to become.

A special thanks goes to my collaborators. Connecting complex systems, economics, and ecology is a team effort, and I appreciate your patience in listening to my ideas. To Michel Loreau, Andrea Roventini, and Francesco Lamperti: thank you for trusting me, especially during uncertain times when few others did. Your belief in my potential made this work possible.

A huge thank you to Max Knicker, truly "my man" throughout this PhD. Going through the ups and downs of this journey together has been a privilege. His insights and drive to always push the limits have made him not just a great colleague, but a friend for life.

Thank you to Ortensia Forni for her close friendship and for showing me that hard work and discipline can overcome any obstacle. I also want to thank Guillaume Maitrier, whose contagious positivity brightened the office every day, and with whom I shared unforgettable adventures outside the lab.

My time doing this PhD was made so much better by the entire Econophysics Lab. I won't list everyone by name, because the lab's spirit comes from everyone who is here now and everyone who has been here in the past. To all my colleagues, past and present: thank you for creating such a welcoming and stimulating environment. The daily chats, shared lunches, and great company made these last three years truly special.

On a personal note, looking back at these past three years, I can't forget the deep love and support from my family, my girlfriend (and future wife) Maria Chiara, and my lifelong friends. Through the inevitable challenges of this journey, your love has been the sturdy ship upon which I navigated the winding, tempestuous seas of life, forever propelled forward by my desire for truth.

Foreword

The journey behind this thesis began on a foggy November afternoon in Milan. Then a Master's student in Physics at the University of Milan, deep into the elegant but "abstract" equations of statistical mechanics, I felt a growing restlessness. I loved the pure rigor of physics, but I harbored a persistent desire to step beyond theoretical constructs and have a tangible impact on the pressing challenges of our time. This drive to bridge the gap between elegant theory and the urgent, messy reality of the world led me to pack my bags for Paris, where I was given the opportunity to pursue an internship at the Econophysics Lab.

Transitioning into econophysics felt like stepping into a vast, uncharted territory. It was thrilling to apply the rigorous tools of the physical sciences to the behaviors of firms network. Yet, while the work was intellectually stimulating, I still felt a lingering sense of searching—a feeling that I had not yet found the precise frontier where my background could be of the greatest use.

The true turning point arrived somewhat unexpectedly. During a conference, I stumbled upon a talk by Michel Loreau. He spoke with stark, urgent clarity about the critical importance of biodiversity preservation and the monumental scientific work that still needed to be done to understand and halt ecological collapse. Listening to him, the pieces finally fell into place: the ongoing environmental crisis was the defining challenge of our generation, and it demanded the very tools of complexity and systemic thinking that I had spent years studying.

With this newfound focus, and thanks to Michael's unwavering trust in my pivot toward bio-economics, I embarked on this doctoral journey. Stepping into the intersection of physics, economics, and ecology was undeniably daunting. I began this endeavor with a quiet but persistent fear of not finding my true space in the academic world—of being caught between established disciplines without a clear home or a definitive voice.

Looking back at that initial apprehension, I now understand that finding one's place in the world does not mean fitting perfectly into a pre-existing mold. Rather, it is about having the courage to build bridges where none previously existed. I realize now that the most urgent problems we face do not respect disciplinary boundaries, and the space I was so anxious to find was exactly here: at the vital, complex intersection where human systems meet the natural world. This thesis is the culmination of that realization.

Abstract

The ongoing collapse of global biodiversity is a paramount systemic risk, inextricably linked to the structural and economic evolution of agricultural landscapes. Mitigating this crisis requires moving beyond static, single-discipline approaches. The central contribution of this thesis is a suite of parsimonious, scale-adapted bio-economic models. Rejecting a single monolithic framework, this research bridges complexity science, theoretical econophysics, and applied ecology to tailor specific architectures to the distinct realities of three interconnected case studies: the European agricultural sector [1, 2], the Brazilian Cerrado [3], and the global food system [4].

At the micro-level within Europe, the reality of the agricultural sector is defined by intense structural pressure and land consolidation. Adapting to this scale, a spatially implicit Agent-Based Model [1] demonstrates that isolated environmental mandates—such as blanket pesticide reductions—can paradoxically accelerate biodiversity loss. By compressing smallholder profit margins without providing economic safeguards, such policies drive market exits and landscape homogenization. Advancing to a spatially explicit framework [2], the analysis maps the mechanics of natural pest control, revealing that while ecological intensification is viable for small-to-medium farms, it faces hard spatial constraints in large-scale, consolidated operations due to the limited dispersal ranges of natural predators.

As consolidation reshapes established landscapes, the pressure of commodity production shifts outward to active frontiers like the Brazilian Cerrado. To capture the spatial reality of this specific scale, the analysis employs a spatially explicit cellular automata model [3] to evaluate frontier expansion as a percolation process driven by local economic incentives. The model strongly suggests that standalone conservation policies—whether supply-chain embargoes or singular financial incentives—are easily bypassed by the spatial fluidity of agricultural expansion. Halting systemic deforestation strictly requires a synergistic policy portfolio: coupling spatial friction (removing agricultural subsidies on newly cleared land) with targeted positive incentives (Payments for Environmental Services) to optimize landscape architecture and generate a net bio-economic surplus.

Finally, navigating the macroeconomic reality of the global food system, the research [4] dynamically couples consumption patterns with the physical limits of spatial expansion. Demonstrating the limited effects of isolated supply-side technological improvements, the proposed model shows that the global food system will continue to expand beyond its biophysical limits unless the underlying aggregate demand for resource-intensive commodities (specifically animal-based proteins) is actively reduced.

Ultimately, this thesis demonstrates that true agricultural sustainability defies isolated technological fixes. It demands a socio-economically coupled approach that deploys tailored interventions across scales—simultaneously addressing the micro-economic realities of the individual farmer, capturing the spatial dynamics of capital flow at the frontier, and structurally diminishing the macro-level global demand for resource-intensive commodities.

Résumé

L'effondrement de la biodiversité mondiale est un risque systémique majeur lié à l'évolution socio-économique des paysages agricoles. Pour dépasser les approches monodisciplinaires, cette thèse développe une suite de modèles bioéconomiques parcimonieux adaptés à différentes échelles. Alliant science de la complexité, éconophysique théorique et écologie appliquée, cette recherche propose des architectures spécifiques adaptées aux réalités de trois cas interconnectés : le secteur agricole européen [1, 2], le Cerrado brésilien [3] et le système alimentaire mondial [4]. Cette modélisation intégrée permet notamment de saisir les propriétés émergentes issues des boucles de rétroaction non linéaires entre choix économiques et dégradation environnementale.

Au niveau microéconomique européen, marqué par une forte concentration foncière, un modèle à base d'agents (ABM) spatialement implicite [1] montre que des contraintes environnementales isolées — comme des réductions de pesticides sans garanties économiques — peuvent paradoxalement accélérer la perte de biodiversité en éliminant les petites exploitations. En élargissant cela à un cadre spatialement explicite [2], l'analyse du contrôle naturel des ravageurs révèle que l'intensification écologique se heurte à des limites physiques de dispersion des prédateurs au sein des structures hautement consolidées à grande échelle.

À la frontière active du Cerrado brésilien, l'expansion agricole est appréhendée via un modèle d'automates cellulaires [3] comme un processus de percolation dicté par les incitations locales. Le modèle suggère fortement que les politiques de conservation isolées (moratoires ou incitations financières uniques) sont facilement contournées par la fluidité spatiale de l'expansion. Contenir la déforestation exige un portefeuille politique synergique, combinant friction spatiale (suppression des subventions sur les terres défrichées) et incitations positives ciblées (Paiements pour Services Environnementaux) pour optimiser l'architecture paysagère et générer un surplus bioéconomique net.

Enfin, à l'échelle macroéconomique mondiale, la recherche [4] couple les modes de consommation aux limites physiques de l'espace disponible. Face à l'impact limité des seuls progrès technologiques du côté de l'offre, le modèle montre que le système alimentaire mondial dépassera ses limites biophysiques sans une réduction structurelle de la demande pour les produits à forte intensité de ressources, en particulier les protéines animales.

In fine, cette thèse prouve que la durabilité agricole appelle une approche socio-économique intégrée, déployant des interventions sur mesure : soutenir la viabilité de l'agriculteur au niveau micro, maîtriser la dynamique des flux de capitaux à la frontière spatiale et réguler structurellement la demande mondiale au niveau macro. Par conséquent, elle ouvre la voie à une gouvernance environnementale renouvelée, capable de concilier la viabilité financière des producteurs avec la préservation à long terme des fonctionnalités écologiques.

List of Publications

[1] **Moretti, E.** and Benzaquen, M. (2025). Mitigating farmland biodiversity loss: A bio-economic model of land consolidation and pesticide use. *Royal Society Open Science*, vol. 12, no. 12.

[2] **Moretti, E.**, Loreau, M., and Benzaquen, M. (2025). Farm size matters: A spatially explicit ecological-economic framework for biodiversity and pest management. *Journal of Environmental Management*, vol. 396, p. 128111.

[3] **Moretti, E.**, Marcolin, J. V. S., Coronese, M., Lamperti, F., Roventini, A., and Benzaquen, M. (2026). Policies for halting deforestation via fragmentation reduction and economic value creation. *Working paper*, Jun. 2026.

[4] **Moretti, E.**, Loreau, M., and Benzaquen, M. (2025). A global systems perspective on food demand, deforestation and agricultural sustainability. *arXiv preprint arXiv:2510.14720*.

Contents

Introduction

1 Introduction **2**
- 1.1 The biological baseline: The sixth mass extinction . . . 2
  - 1.1.1 The windshield phenomenon . . . 2
  - 1.1.2 Magnitude and velocity of the current extinction . . . 3
  - 1.1.3 The ecological framework: Defining biodiversity . . . 4
  - 1.1.4 The drivers: Agriculture . . . 5
  - 1.1.5 The consequences: From life to function . . . 7
- 1.2 Lack of parsimonious bio-economic frameworks . . . 9
- 1.3 Thesis structure . . . 10
  - 1.3.1 Research scales: From local frontiers to global demand . . . 10
  - 1.3.2 Methodological evolution . . . 11

I A European Perspective: The Role of Farm Intensification

2 Farmland biodiversity decline in Europe **14**
- 2.1 The importance of farm intensification and land consolidation . . . 14
- 2.2 The CAP . . . 15
- 2.3 Our contribution . . . 15

3 An agent-based model of land consolidation and pesticide use **18**
- 3.1 Introduction to agent-based model . . . 18
- 3.2 Model overview . . . 20
  - 3.2.1 Production of goods . . . 21
  - 3.2.2 Goods market . . . 21
  - 3.2.3 Technology adoption . . . 22
  - 3.2.4 Land rental market . . . 23
  - 3.2.5 Pesticide use . . . 24
  - 3.2.6 Biodiversity update . . . 24
- 3.3 Real data and numerical simulations . . . 25
  - 3.3.1 Data sourcing . . . 25
  - 3.3.2 Calibration . . . 25
  - 3.3.3 Initialization . . . 27
  - 3.3.4 Simulation . . . 28
- 3.4 Results . . . 28
  - 3.4.1 Baseline scenario . . . 28
  - 3.4.2 Pesticide reduction . . . 30

3.4.3 Subsidies . . . 30
3.4.4 Combined policy: Pesticide reduction and subsidies reallocation . . . 31
3.5 Discussion . . . 32
3.5.1 Main findings and mechanisms . . . 33
3.5.2 Policy implications in the current French context . . . 34
3.5.3 Limitations and future directions . . . 34
3.6 Supplementary materials . . . 36
3.6.1 Calibration procedure and sensitivity analysis . . . 36
3.6.2 Biodiversity influence on yield . . . 36
3.6.3 Technological advances and sustainable farming . . . 37

4 An ecological-economic framework for biodiversity and pest management 41
4.1 Literature review . . . 41
4.2 Model and methods . . . 43
4.2.1 Model overview . . . 43
4.2.2 Landscape construction . . . 43
4.2.3 Natural enemies' abundance . . . 45
4.2.4 Farmers' economic performance . . . 47
4.2.5 Parameter specification . . . 48
4.2.6 Computational implementation . . . 48
4.3 Results . . . 49
4.3.1 Landscape structure, pesticide use, and natural enemy abundance . . . 49
4.3.2 Policy impacts on yield and income across farm sizes . . . 51
4.3.3 Economic potential of natural pest protection without pesticides . . . 54
4.4 Discussion . . . 55
4.5 Supplementary materials . . . 59
4.5.1 Landscape generation . . . 59
4.5.2 Calibration procedure and parameters value . . . 60
4.5.3 Rationale for using physical farm size . . . 61
4.5.4 Scenario exploration for fixed parameters . . . 62

II A Brazilian Perspective: The Role of Deforestation

5 Land-use change in the Cerrado and the Soy Republic 72
5.1 The displacement of ecological debt . . . 72
5.2 Brazil: The epicenter of the global agro-export boom . . . 73
5.3 The Cerrado: The active agricultural frontier . . . 74

6 A cellular-automata model of landscape transformation 76
6.1 Literature review . . . 76
6.2 Model and methods . . . 79
6.2.1 Model overview . . . 79
6.2.2 Production . . . 80
6.2.3 Ecosystem service provision . . . 80
6.2.4 Costs, revenues, and profitability . . . 81
6.2.5 Land market and farm consolidation . . . 82

6.2.6 Deforestation decision . . . 83
6.2.7 Intensification decision . . . 84
6.2.8 Abandonment decision . . . 85
6.2.9 Parameter specification and numerical experiments . . . 85
6.3 Results . . . 86
6.3.1 Business-as-usual projections (2025–2050) . . . 88
6.3.2 Policy counterfactuals: Efficacy and bio-economic synergies . . . 90
6.3.3 Policy optimization: Maximizing bio-economic efficiency . . . 92
6.3.4 Fiscal feasibility and the monetization of ecological dividends . . . 95
6.4 Discussion . . . 95
6.4.1 Systemic evaluation of frontier dynamics . . . 95
6.4.2 The structural necessity of spatial targeting . . . 96
6.4.3 Structuring a synergistic policy portfolio . . . 97
6.4.4 Maximizing bio-economic efficiency and fiscal sustainability . . . 97
6.4.5 Methodological limitations and future research . . . 98
6.4.6 Conclusion . . . 99
6.5 Supplementary materials . . . 100
6.5.1 Detailed initialization procedure . . . 100
6.5.2 Exogenous inputs: Commodity price dynamics and enforcement probability . . . 101
6.5.3 Parameterization . . . 102
6.5.4 Computational calibration of behavioral parameters . . . 104
6.5.5 Sensitivity analysis . . . 105

III A Global Perspective: The Role of Food Demand

7 Ecological limits, resilience, and societal vulnerability 112
7.1 Societal collapse discussion . . . 112
7.2 The *limits to growth* discussion . . . 113
7.3 Economic incentives behind ecological dynamics . . . 113
7.4 Our contribution . . . 114

8 A stylized, spatially explicit model of global food demand and production 116
8.1 Literature review . . . 116
8.2 Model . . . 117
8.2.1 Model overview . . . 117
8.2.2 Demand: Economic and population growth . . . 118
8.2.3 Production: Crop and livestock systems . . . 119
8.2.4 Landscape and natural ecosystem integrity . . . 122
8.2.5 Parameter specification and numerical experiments . . . 123
8.3 Results . . . 124
8.3.1 Business-as-usual scenario . . . 124
8.3.2 Effects of single policy measures . . . 127
8.3.3 Synergies and trade-offs in policy portfolios . . . 128
8.4 Discussion . . . 131
8.4.1 Beyond the supply-side: Systemic barriers to sustainability . . . 131

8.4.2 Structural need for demand reductions . . . 131
8.4.3 Integrated approaches and systemic solutions . . . 133
8.4.4 Limitations and unaccounted aspects . . . 133
8.5 Conclusion . . . 134
8.6 Supplementary materials . . . 136
8.6.1 Initialization . . . 136
8.6.2 Calibration procedure and parameter values . . . 136

Conclusion and Perspectives

9 Conclusion and perspectives 141
9.1 Conclusion . . . 141
9.1.1 Part I: The European context . . . 141
9.1.2 Part II: The Brazilian Cerrado . . . 142
9.1.3 Part III: The global scale . . . 142
9.2 Perspectives . . . 143
9.2.1 The limits of behavioral and cognitive simplifications . . . 143
9.2.2 Ecological homogeneity and simplified biophysical dynamics . . . 143
9.2.3 The absence of global trade feedbacks . . . 144
9.2.4 The omission of alternative farming paradigms . . . 144
9.2.5 The omission of distributional impacts . . . 144
9.3 Final remarks . . . 145

Appendix

A Externality costs of agricultural production and the organic alternative 148
A.1 Introduction . . . 148
A.2 The paradigm and trajectory of organic farming in Europe . . . 149
A.3 Methodology . . . 151
A.4 Results . . . 156
A.4.1 National-level cost structure . . . 156
A.4.2 Regional distribution and typology of damages . . . 157
A.4.3 Scenario analysis: The imperative of spatial targeting . . . 158
A.5 Discussion and limitations . . . 160
A.6 Conclusion . . . 160
A.7 Supplementary materials . . . 162

References 164

Introduction

1. Introduction

> "Sune Boye Riis was on a bike ride with his youngest son, enjoying the sun slanting over the fields and woodlands near their home north of Copenhagen, when it suddenly occurred to him that something about the experience was amiss. Specifically, something was missing. It was summer. He was out in the country, moving fast. But strangely, he wasn't eating any bugs. [...] Where had all those insects gone? And when? And why hadn't he noticed?"
>
> — Brooke Jarvis, *The insect apocalypse is here*, The New York Times Magazine [5]

1.1 The biological baseline: The sixth mass extinction

1.1.1 The windshield phenomenon

The term "windshield phenomenon" denotes the observed long-term reduction in the density of insect remnants accumulated on the surfaces of moving motor vehicles. While historically categorized as an anecdotal or localized observation, this phenomenon has increasingly been recognized in conservation biology as a visible, qualitative indicator of systemic arthropods decline. Within contemporary ecological literature, the transition of this observation from informal consensus to empirical hypothesis has served as a catalyst for systematic macro-ecological assessments.

The empirical validation of these qualitative accounts was significantly advanced by long-term, standardized longitudinal monitoring. A first 20-year study [6] measured the number of dead insects on car windshields on two stretches of road in Denmark from 1997 until 2017. Adjusted for variables such as time of day, date, temperature, and wind speed, the research found an 80% decrease in the number of insects impacting cars. Later, Hallmann et al. (2017) [7] documented a 76.7% decline in seasonal flying insect biomass over a 27-year observation period within protected areas in Germany. By utilizing standardized Malaise traps, this study demonstrated that the observed biomass reduction was neither an artifact of changing vehicle aerodynamics nor a localized consequence of intensive agricultural environments. Instead, these findings provided robust quantitative evidence supporting the hypothesis that widespread biomass contractions are occurring partially independent of localized land-use variations, signaling a broader macro-ecological shift.

Since insect communities function as critical nodes within terrestrial ecosystems—mediating essential services such as pollination [8], natural pest control [9], and foundational energy transfer [10]—this magnitude of biomass loss introduces severe, cascading vulnerabilities into global food webs. Yet, the dramatic contraction of arthropod populations provides only a

glimpse into a far more profound systemic unravelling. Rather than an isolated ecological anomaly, this loss is a less visible symptom of a broader, multi-trophic crisis that is destabilizing diverse functional groups simultaneously. Ultimately, this synchronized, cross-trophic collapse constitutes the core functional mechanic of what many ecologists now term the Sixth Mass Extinction [11, 12].

1.1.2 Magnitude and velocity of the current extinction

The scientific discourse surrounding a potential Sixth Mass Extinction is firmly grounded in the quantitative tracking of global biodiversity loss. By relying on macroscopic indicators, researchers can systematically map the accelerating contraction of the biosphere. Foremost among this evidence is the staggering, long-term decline in wild terrestrial mammal biomass, a metric widely used as a proxy for the structural richness of the animal kingdom (discussed extensively by [14–16]). As illustrated in Fig. 1.1, quantitative estimates reveal that total wild mammalian biomass has suffered a profound 85% collapse since the emergence of anatomically modern humans.

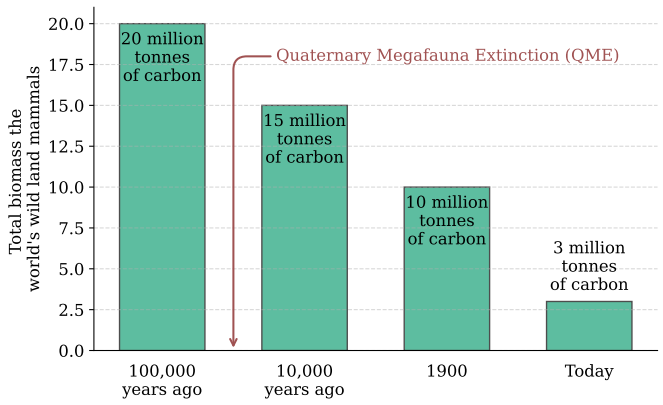


Figure 1.1 Data from [13]. Long-run decline of global wild mammal biomass.

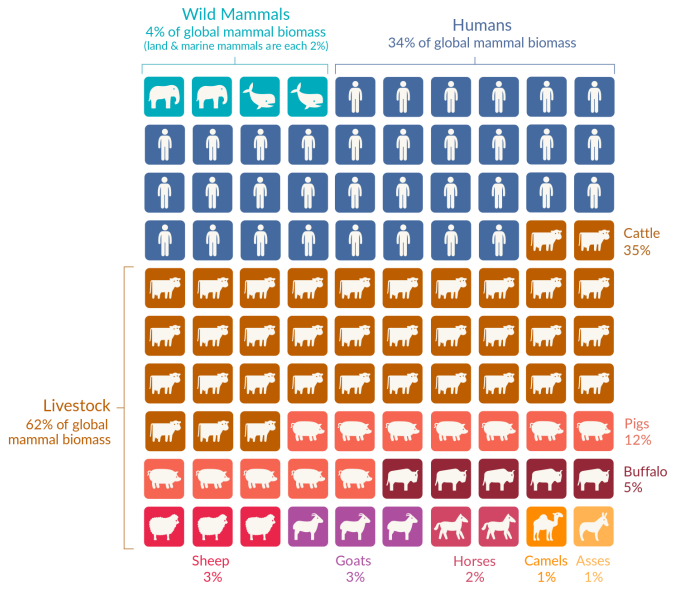


Figure 1.2 Source: [17]. Contemporary asymmetric distribution of global mammalian biomass.

Equally alarming is the sheer velocity of recent losses. Merely since 1900, terrestrial wild mammals have experienced an additional 70% decline in biomass. This modern contraction compresses what historically manifested as a protracted, multi-millennial collapse—such as the Quaternary Megafauna Extinction—into little more than a single century.

This historical hollowing out of the natural world has culminated in a drastically asymmetric distribution of contemporary mammalian life (Fig. 1.2). Current assessments [16] show that wild terrestrial and marine mammals now account for a mere 4% of global mammalian biomass. The remaining 96% consists entirely of humans and our in-

dustrialized livestock. This unprecedented appropriation of the Earth's metabolic capacity firmly links the current biodiversity crisis to modern food production systems—a core dynamic that will be analyzed in detail in Section 1.1.4.

While historical biomass data captures the absolute scale of ecological displacement, other indicators measure the real-time velocity of the crisis. For instance, the Living Planet Index (LPI) [19] shifts the analytical focus away from binary species extinctions and toward the continuous decline of population abundance. Frequently cited but often misinterpreted [20], the LPI calculates the geometric mean of proportional changes across more than 30,000 monitored vertebrate populations. It reveals a devastating 73% average decline in global vertebrate population sizes since 1970 (Fig. 1.3). By tracking abundance rather than simply counting lost species, this metric exposes the rapid demographic erosion occurring across distinct geographic regions and trophic levels.

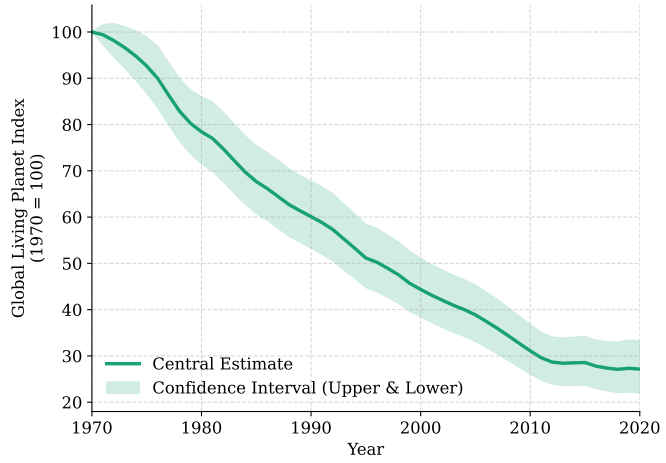


Figure 1.3 Data from [18]. Global Living Planet Index.

Crucially, this widespread drop in population abundance is not merely a retrospective observation; it acts as an active precursor to future extinction. The systematic thinning of local populations translates directly into severe taxonomic vulnerability. Data from the International Union for Conservation of Nature (IUCN) Red List demonstrates a steady upward migration of entire taxonomic groups into high-risk categories [21]. With a growing proportion of species now officially classified as "Critically Endangered," it is clear that stable evolutionary clades are fracturing under anthropogenic pressure, shifting the baseline of planetary biology from historical abundance to systemic precarity.

1.1.3 The ecological framework: Defining biodiversity

While the narrative of a "Sixth Mass Extinction" powerfully communicates the magnitude of contemporary ecological loss, its reliance on terminal extinction metrics can inadvertently flatten the complexity of the crisis. Indeed, significant academic critique has recently emerged regarding this framing. Paleobiological benchmarks establish that a mass extinction event is characterized by a profound taxonomic contraction—specifically, the loss of approximately 75% of global species within a geologically compressed window [22]. While contemporary absolute extinction counts have not yet reached this terminal threshold [23], adopting this binary metric as the primary indicator of ecological health is analytically flawed because it ignores the gradual disruption of functional species that precede terminal extinctions and therefore limits proactive intervention [24]. To rigorously model anthropogenic impacts on ecosystems—and to move

beyond monolithic narratives—it is necessary to deconstruct the multidimensional architecture of biodiversity. Within theoretical ecology, biodiversity is not a singular, static inventory, but rather a hierarchical, dynamic system evaluated through three intersecting lenses: taxonomic, functional, and genetic.

Taxonomic diversity Taxonomic diversity represents the most traditional axis of ecological measurement, encompassing both species richness (the absolute count of distinct species) and species evenness (the relative abundance of individuals across those species). While this dimension provides the foundational nomenclature for tracking global biosphere changes, relying solely on taxonomic inventories risks reducing complex ecological networks to mere catalogues [25]. A system can technically maintain high species richness while suffering severe demographic collapse and rapid species turnover, masking underlying structural instabilities [26].

Functional diversity Consequently, modern systems ecology increasingly prioritizes functional diversity [27]. This dimension quantifies the range of behavioral, physiological, and metabolic traits that species exhibit within an ecosystem [28]. It defines the specific, operational roles species play—from primary production and nutrient cycling to pest regulation and entomophilous pollination. Ecosystem stability and resilience are primarily governed not by the sheer number of species present, but by functional redundancy and complementarity [29]. The erosion of functional diversity is often the most immediate, tangible threat to ecosystem services, as the extirpation of key functional groups can precipitate severe trophic cascades long before terminal taxonomic extinctions are officially recorded [30].

Genetic diversity Underpinning both the taxonomic and functional tiers is genetic diversity, which captures the intraspecific variation within populations. This allelic diversity constitutes the evolutionary reservoir that enables populations to adapt to shifting anthropogenic pressures, disease vectors, and climatic volatility [31]. As populations undergo rapid demographic contractions, they suffer profound genetic bottlenecks, leading to loss of genetic variation, inbreeding depression, and increased fixation of deleterious alleles [32, 33]. This hidden erosion compromises the intrinsic resilience of populations, locking them into an extinction vortex even if their absolute numbers temporarily appear stable.

Current ecological literature confirms a synchronized, downward trajectory across all three of these organizational levels [34–36]. It is within this multi-dimensional degradation that the conceptual limitations of the Sixth Mass Extinction framework become apparent. By fixating on terminal taxonomic death, the mass extinction narrative risks ignoring the profound, insidious hollowing out of functional networks and population abundance that occurs over the preceding decades. As synthesized by recent global assessments [37, 38], waiting for the definitive metric of absolute extinction is inadequate for research focused on socio-ecological resilience; the true crisis lies in the continuous, systemic degradation of biological complexity and the resulting collapse of nature's contributions to human systems.

1.1.4 The drivers: Agriculture

If the multi-dimensional degradation of biological complexity is the defining symptom of the current ecological crisis, it cannot be viewed strictly as a modern phenomenon. Rather, it is the

culmination of a deep-time historical interaction between human demographic expansion and the Earth's natural carrying capacity. To contextualize the structural collapse of biodiversity as discussed previously, it is critical to trace the bio-economic drivers responsible for historical biomass loss (see Fig. 1.1), which collectively set the stage for the transformative legacy of the Green Revolution.

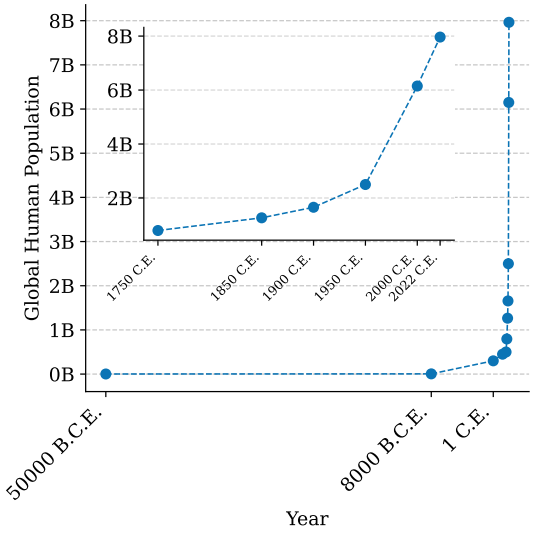


Figure 1.4 Data from [39].The size of the global human population over the long run.

In a world defined by finite resources, human survival has inherently necessitated competition with wild species. Early in our evolutionary history, subsequent to foundational socio-metabolic transitions such as the control of fire, this competition took the form of direct predation, triggering the initial anthropogenic collapse of global megafauna, such as the woolly mammoth (*Mammuthus primigenius*) and the giant ground sloth (*Megatherium*) [40, 41]. Subsequently, the Neolithic agricultural revolution initiated a profound shift in how this biophysical pressure was exerted. Instead of relying on direct hunting, human societies began to outcompete wild populations through land-use modification—systematically clearing primeval forests [42], altering hydrological flows, and establishing permanent settlements [43]. During this era, as depicted in Fig. 1.4, the global human population began to systematically rise, albeit at a severely constrained growth rate. Indeed, demographic expansion was fundamentally capped by the carrying capacity of local ecosystems, locking early agrarian societies into the structural constraints of the Malthusian trap [44].

Formulated at the close of the eighteenth century, the Malthusian trap outlines a fundamental biophysical constraint: human populations possess the capacity for exponential demographic growth, whereas traditional agricultural production—reliant on fixed land availability and endogenous solar energy—tends to expand only linearly [45]. Historically, this dynamic structurally bounded human populations to local carrying capacities, where ecological overshoot was periodically regulated by resource scarcity and demographic contractions. However, the onset of the Industrial Revolution initiated a gradual decoupling from these localized limits [46]. The transition to fossil-based energy regimes facilitated early agricultural mechanization and spurred unprecedented economic expansion, generating the capital and infrastructure required to support global population expansion [47].

Building upon this industrialized economic foundation, the subsequent Green Revolution in the mid-twentieth century fundamentally altered the biophysical boundaries of global food production. By adopting a paradigm of severe agricultural intensification—most notably through the Haber-Bosch synthesis of atmospheric nitrogen [48] and the development of broad-spectrum synthetic pesticides [49]—agronomic yields increased dramatically. This massive influx of exogenous chemical inputs allowed for a higher production of resources on existing cultivated land. Together, these sequential socio-metabolic transitions successfully uncoupled human population dynamics from historical ecological constraints, expanding the planetary carrying capacity.

However, as populations expanded and per capita incomes rose, the global food system became stucked in a well-documented bio-economic dynamic known as the efficiency trap, or the Jevons Paradox [50]. While agronomic innovations drastically increased the yield efficiency of agricultural land, these technological gains rarely resulted in a proportional reduction of aggregate resource use [51]. Instead, increased efficiency lowered the marginal cost of production, driving higher market demand and ultimately leading to an expansion of total resource extraction [52]. Consequently, the drive to feed a growing, increasingly wealthy population continuously pushed the agricultural frontier outward, effectively neutralizing any localized land-sparing benefits.

Ultimately, the Green Revolution transitioned agriculture from an ecologically integrated practice into a highly industrialized, extractive process. This historical paradigm locked the global food system into a specialized, path-dependent trajectory characterized by chemical dependency and severe biological simplification [53, 54]. Decades later, the systemic legacy of this socio-technical lock-in is all the more evident worldwide, manifesting as the chronic degradation of long-term soil fertility, widespread water table depletion, and the systematic extirpation of natural biodiversity.

1.1.5 The consequences: From life to function

The preceding sections have established that, while the rhetoric surrounding a "Sixth Mass Extinction" can sometimes overstate the current magnitude of ecological decline, the empirical reality of the crisis is rigorously documented. It manifests as a systemic erosion of biological complexity across its taxonomic, functional, and genetic dimensions. This multi-tiered degradation is inextricably linked to the biophysical consequences of humanity's escape from the Malthusian trap. Propelled by the economic acceleration of the Industrial and Green Revolutions, the exponential expansion of the human population and the subsequent bio-economic lock-in of industrialized, extractive agriculture have catalyzed an unprecedented appropriation of planetary biomass. We have delineated both the multidimensional nature of this ecological collapse and the historical drivers that propel it. It is now necessary to examine the profound structural consequences of this trajectory. Specifically, we must focus on how the rupture of the Biodiversity-Ecosystem Functioning (BEF) [55] relationship translates ecological degradation into acute agronomic failures and macroeconomic instability.

The core premise of the BEF framework is that an ecosystem's overall stability, productivity, and resilience are directly governed by its internal functional diversity [56]. Industrial agriculture fundamentally short-circuits this relationship by replacing self-regulating ecological interactions—such as biological pest control and natural nutrient cycling—with exogenous chemical inputs. This ongoing substitution systematically strips the landscape of its "functional redundancy": the critical presence of multiple diverse species capable of performing the same ecological role. Consequently, as landscapes are homogenized into vast monocultures, the natural buffering capacity provided by these overlapping ecological networks collapses. The resulting biophysical architecture becomes highly fragile, stripped of its innate ability to absorb external shocks and critically vulnerable to cascading trophic failures [57].

Consequently, this rupture transcends localized ecological degradation, threatening macroscopic socio-economic stability. As critical functional groups vanish, the foundational biophysical flows that underwrite human survival—such as primary production, soil nutrient cycling, entomophilous pollination, and localized climate regulation—become dangerously volatile. Within a rigorous bio-economic framework, it becomes evident that the human economy cannot be

accurately modeled as an independent, closed-loop entity capable of endlessly substituting natural capital with technological alternatives. Rather, the economy is an entirely embedded, dependent subsystem of the biosphere [58]. When the underlying ecological functions that regulate the Earth system destabilize, the socio-economic structures built upon them are inevitably pulled into the same trajectory of collapse, shifting the ecological crisis from an environmental externality to a paramount systemic risk.

This systemic destabilization is no longer a theoretical projection; empirical manifestations of this socio-ecological rupture are already evident, bifurcating into acute agronomic failures and profound public health crises. At the agronomic level, the historical reliance on severe intensification has begun to yield diminishing marginal returns [59, 60], directly threatening farmer livelihoods and macroeconomic food security [61]. This production instability is often correlated with the simplification of natural capital, specifically the collapse of underlying soil microbiome functionality [62] and the acute deficit of wild pollinators [63]. Beyond pollination, the loss of biological pest control vividly illustrates the financial burden of this ecological degradation. Recent empirical evaluations demonstrate that when insectivorous bat populations collapsed across North America due to invasive pathogens, farmers were forced to compensate by drastically increasing synthetic insecticide applications, absorbing massive, unanticipated financial shocks simply to maintain baseline yields [64].

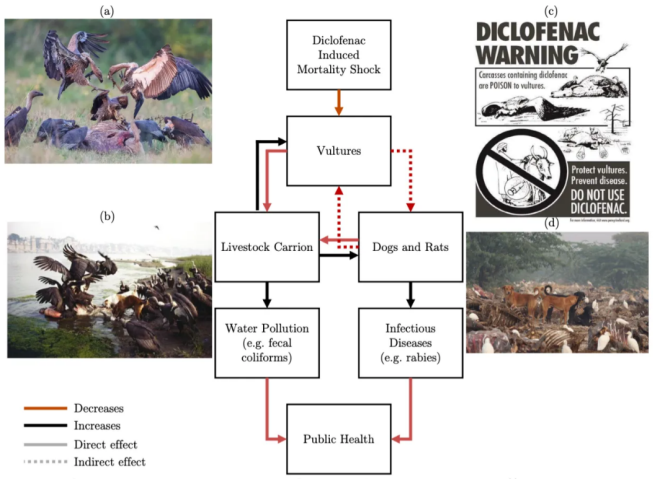


Figure 1.5 Source: [65]. The figure summarizes the key components of the coupled natural-human system used in the original study, illustrating how interactions between carrion, vultures, dogs, and rats impact public health and the environment.

Crucially, the consequences of these socio-technical substitutions do not remain confined to the agricultural sector; they cascade outward as severe societal externalities. For example, in the previously discussed bat collapse scenario, the massive influx of exogenous agrochemicals deployed to replace bat predation significantly increased human infant mortality in the affected counties [64]. Concurrently, the biophysical simplification of landscapes has fundamentally eroded the natural epidemiological buffering capacity of broader ecosystems. Just as the loss of bats forced a dangerous and toxic chemical dependency, the collapse of native amphibian populations in Central America severed a critical ecological control loop for mosquito larvae. This specific loss of functional biodiversity directly exacerbated the transmission of vector-borne diseases, causing severe, prolonged spikes in human malaria incidence [66, 67].

This dynamic of epidemiological buffering failure is perhaps most devastatingly illustrated by another recent functional extinction: the collapse of Indian vulture populations [65]. Following the widespread veterinary use of the painkiller diclofenac, vulture populations—which historically provided critical environmental sanitation by rapidly scavenging millions of live-

stock carcasses—declined by over 95%. The sudden removal of this keystone functional group triggered a massive negative shock to regional sanitation: feral dog populations surged, water quality severely deteriorated, and zoonotic disease transmission spiked. Recent macroeconomic evaluations reveal that this single functional extinction is associated with an estimated 104,000 additional human deaths annually, translating to nearly $69.4 billion per year in mortality damages.

Ultimately, these contemporary disruptions confirm that the biosphere's limits are actively binding. By forcing agricultural systems to substitute vanished biological functions with costly and potentially toxic anthropogenic alternatives, the degradation of biodiversity internalizes what were once considered distant environmental externalities into immediate, structural economic liabilities and acute human health crises.

1.2 Lack of parsimonious bio-economic frameworks

Despite growing consensus on the severe socio-economic consequences of biological simplification, the translation of this awareness into actionable policy remains trapped in a conceptual stalemate [68]. To transition from diagnosing the ecological crisis to engineering resilient solutions, we must establish a rigorous framework capable of bridging distinct disciplines.

Historically, this paralysis stems from a polarized binary between two dominant paradigms. On one side, traditional conservation ecology frequently advocates for an immediate cessation of anthropogenic pressures [69]. While biophysically sound, this stance often ignores the rigid structural dependencies of global food security [70]. Conversely, orthodox environmental economics relies on "weak sustainability," implicitly assuming that natural capital can be infinitely substituted by technological innovation [71]. By treating ecological degradation as a mere market failure correctable via optimized pricing, this paradigm attempts to preserve continuous economic growth while ignoring the Earth system's non-linear thresholds or tipping points [72]. Ultimately, putting absolute ecological preservation against orthodox economic expansion has proven analytically insufficient and politically intractable.

To move beyond this impasse, this thesis adopts a fundamentally integrated, "nested" ecological-economic framework. Drawing from complexity science [73, 74] and ecological economics [75, 76], the human economy is not modeled in isolation; it is understood strictly as a dependent subsystem embedded within, and constrained by, the ecosystem services provision. Reconciling this nested reality requires abandoning monolithic policy prescriptions that either ignore economic realities or violate biological limits.

The analytical contribution of this research lies in deploying rigorous systemic reasoning to map the interactions across these nested layers. Crucially, addressing this socio-ecological complexity does not necessitate the imposition of entirely novel or hyper-abstract model structures. Instead, it requires distilling the system to its foundational mechanisms. By rigorously calibrating these key extracted features to empirical historical trends, it becomes possible to accurately capture the heterogeneous feedback loops driving agricultural practices, land-use dynamics, and biodiversity outcomes.

The deployment of stylized, parsimonious models—grounded in data-driven calibration to reproduce historical trajectories—forms the methodological core of this thesis. This empirical grounding enables the identification of nuanced policy portfolios and behavioral shifts that can halt environmental degradation, while explicitly internalizing the macroeconomic costs and benefits associated with such transitions. Ultimately, this integrated framework replaces the

paralyzing binary debate with a search for calibrated, pragmatic interventions—interventions that are precisely tailored to the specific spatial and temporal scales of the socio-ecological systems under investigation.

1.3 Thesis structure

To effectively unravel the complex mechanisms driving contemporary biodiversity loss, this thesis is organized along two complementary axes: a thematic progression that scales from regional land systems to global networks, and a methodological evolution that progressively integrates spatial topology and socio-economic complexity.

1.3.1 Research scales: From local frontiers to global demand

In terms of scale, this work progresses from localized drivers of landscape homogenization to the macroscopic pressures of global consumption, a trajectory that defines the three main parts of the thesis.

Part I: A European perspective The first part narrows the analytical focus to the mature agricultural systems of Europe, where biodiversity decline is driven by gradual farm intensification and the systematic erasure of landscape complexity. Rather than viewing this as a purely ecological issue, this section investigates the socio-economic behavioral drivers at the individual farmer level. Through the analysis of farmer decision-making in France, it explores the tightly coupled dynamics of land consolidation and pesticide reliance. It details how the pursuit of short-term economic efficiency and risk aversion incentivizes the removal of semi-natural habitats (such as hedgerows), which in turn compromises the ecological networks necessary for ecosystem services like natural pest control. This creates a bio-economic lock-in, where simplified landscapes necessitate ever-increasing chemical inputs, further degrading regional biodiversity.

Part II: A Brazilian perspective Shifting the focus from a mature, intensive system to an active agricultural frontier, the second part investigates the Brazilian Cerrado. Here, the ecological crisis manifests through the violent dual threat of rapid land-use intensification and massive, systemic deforestation in highly biodiverse ecosystems. This section models the spatial displacement of ecological debt, demonstrating how localized decisions to clear native vegetation are not isolated events, but are inextricably linked to a broader process of capitalization, land speculation, and structural frontier expansion. It clarifies the mechanics of how market signals translate into physical landscape transformations at the active edges of the agricultural network.

Part III: A Global perspective The final part broadens the scope to the macro-systemic level, integrating the demand side of the global food system to close the causal loop. This section examines how global dietary trajectories and consumption patterns act as the ultimate catalysts for the local ecological collapses modeled in Parts I and II. By explicitly modeling the structural limits to growth, this section challenges the assumption that supply-side technological improvements and localized conservation efforts are sufficient. It questions whether global

biophysical boundaries can be respected without fundamentally altering aggregate demand and consumption behaviors.

1.3.2 Methodological evolution

While the foundational logic of the parsimonious bio-economic approach remains consistent across all models presented in this work, bridging these diverse spatial and thematic scales, the maturity of the analytical framework and the specific features it necessitates have evolved significantly over time. As the research questions transition from observing baseline socio-ecological interactions to capturing complex, real-world structural transformations, the models progressively incorporate greater spatial and temporal resolution. This step-wise evolution reflects a continuous refinement of the methodological toolkit, ensuring that each phase introduces only the specific architectural features required by the scale and dynamics of the system under study.

Phase 1: Spatially implicit The analytical journey begins with the deployment of spatially implicit Agent-Based Models (ABM). This foundational phase is designed to isolate and observe fundamental economic-ecological feedback loops—such as the cyclical relationship between pest pressure, crop yield, and pesticide application. By utilizing heuristic behavioral rules grounded in aggregate statistical data, this approach captures core systemic attractors without the computational overhead of resolving explicit spatial constraints.

Phase 2: Spatially explicit / static economic Recognizing that ecological resilience is inherently tied to landscape topology, the methodology advances to integrate physical space. This spatially explicit framework acknowledges , for example, that the distance to semi-natural habitats (like hedgerows) dictates ecological outcomes. By introducing a spatial grid, the model captures the localized effects of farmer decisions on neighboring plots, mapping the physical fragmentation of the European agricultural landscape.

Phase 3: Dynamic-spatial-economic To accurately capture the volatile nature of the Brazilian agricultural frontier, the modeling approach evolves further to combine dynamic economic descriptions with spatial frameworks. Unlike the relatively static land tenure of Europe, the Cerrado requires simulating structural change over time: the accumulation of capital, the aggregation of landholdings, and the moving boundary of the frontier itself. This phase dynamically links economic capitalization directly to spatial expansion.

Policy evaluation: Across these varying spatial and temporal models, the thesis culminates in qualitative and quantitative policy evaluations. It assesses a spectrum of structural interventions, moving beyond theoretical critique to test the efficacy of specific mechanisms, and evaluating the true leverage of the current strategies.

Part I

A European Perspective: The Role of Farm Intensification

Part I is adapted from Moretti et al. (2024) [1], *Mitigating farmland biodiversity loss: a bio-economic model of land consolidation and pesticide use*, and Moretti et al. (2025) [2], *Farm size matters: A spatially explicit ecological-economic framework for biodiversity and pest management*. Minor modifications have been made to the original texts to align them with the narrative and context of this thesis.

2. Farmland biodiversity decline in Europe

Chapter 1 provided a general overview of biodiversity decline and its main drivers. In the present chapter, we narrow the focus to the European agricultural context and situate our contribution within this literature. To do so, we first present a spatially implicit agent-based model for France. We then motivate the development of a second, spatially explicit bio-economic model aimed at providing a more accurate representation of pest-management processes and their ecological and economic implications.

2.1 The importance of farm intensification and land consolidation

As in many other regions of the world, in recent decades, Europe has witnessed a dramatic reduction in biodiversity [77], with significant declines in both the overall biomass [78] and the number of different species [79]. Likewise, the number of species at risk of extinction has risen [80]. Unlike in several other world regions, where deforestation remains a central driver of biodiversity loss, in Europe forest area has, on average, slightly increased over recent decades and some forest-related indicators have shown local improvements. Nevertheless, biodiversity decline remains substantial, and it is particularly pronounced in farmland ecosystems, where bird populations have shrunk [81], the number of pollinators has dwindled [82], and invasive species are increasingly infiltrating agro-ecosystems [83]. As discussed in the general introduction, modern agriculture is widely recognized as the primary driver of this trend [84, 85]. In particular, in Europe, the scientific literature points to two primary drivers of this decline [86]: the simplification of agricultural landscapes through land consolidation and the widespread use of synthetic pesticides.

The expansion of field sizes, removal of linear landscape features such as hedgerows, and reduction of permanent grasslands have diminished the availability of diverse habitats essential for a rich array of species [87, 88]. Simultaneously, the extensive application of synthetic pesticides, intended to maximize yields by controlling crop pests, has had significant side-effects, directly impacting beneficial insect populations and raising concerns about human health and environmental contamination [89, 90]. The unintended consequences of these practices are now becoming increasingly apparent. The reduction in the number of natural enemies of crop pests, coupled with the emergence of pesticide-resistant pest populations, has begun to contribute to a worrying trend of stagnating yields in some agricultural systems [59, 60, 91, 92]. Furthermore, in the face of ongoing climate change, many scientific projections suggest that the vulnerability of these simplified and chemically reliant agricultural systems will likely be exacerbated, potentially leading to further ecological and economic instability if current farming practices persist [9].

Underlying these ecological trends is a broader socio-economic transformation within agriculture itself. A persistent drive for economies of scale—in pursuit of higher productivity, profitability, and mechanization—has led to structural changes across much of the agricultural sector. Farm consolidation has become widespread [93, 94], notably in developed regions such as Europe, where the shift from smaller, family-run farms towards fewer, larger holdings has been particularly pronounced [95–97]. Agricultural statistics for the European Union (EU) show that, over the last decades, the number of farms has been decreasing and the average operated area has been increasing. This ongoing concentration of landholdings not only alters the rural socio-economic landscape—impacting farm viability, demographic structure, and farmer well-being—but also raises pressing questions regarding the environmental sustainability and resilience of large-scale, monocultural farming systems.

2.2 The CAP

Faced with these complex and interrelated challenges, both policymakers and researchers have sought to guide agricultural systems onto a more sustainable path. Within Europe, the Common Agricultural Policy (CAP) has been a fundamental driver in shaping rural landscapes and agricultural practices since its establishment in the early 1960s [98]. The CAP's initial focus was on increasing food production, stabilizing markets, and safeguarding farmers' livelihoods, but these priorities were largely pursued through policies that promoted intensification and land consolidation [99, 100]—often overlooking environmental concerns. As the negative consequences of these strategies, including biodiversity loss and other ecological externalities, became more apparent, the CAP underwent successive rounds of reform [101]. Over time, these reforms progressively expanded the role of environmental objectives within agricultural policy, thereby moving the CAP from a predominantly productivist framework towards a broader, though still contested, sustainability-oriented agenda.

These policy changes introduced agri-environmental schemes and "greening" measures with the aim of encouraging more sustainable land management and integrating environmental objectives into mainstream agricultural policy [102–104]. In its current form, the CAP also relies on a broader set of instruments, including conditionality requirements and eco-schemes, intended to reward the provision of environmental public goods and to promote more sustainable farming practices. However, despite these policy shifts, major hurdles remain: farmland biodiversity, including insect populations[79] and other key indicators[105], continues to decline at an alarming pace. As a result, questions persist regarding the real-world effectiveness of these reforms. A critical policy debate has thus emerged around identifying the most effective tools for simultaneously restoring and maintaining ecosystem health in agricultural landscapes, while also ensuring the economic sustainability of farms in a sector characterized by considerable diversity in farm structure and scale.

2.3 Our contribution

The academic literature addressing this question is broad and interdisciplinary, spanning ecology, agronomy, economics, and rural sociology. Empirical investigations have examined the ecological benefits of agri-environmental schemes, diversified crop rotations, and field margins for species richness and ecosystem services [102, 106, 107]. Landscape-level analyses

have emphasized how spatial configuration and connectivity shape biodiversity outcomes and ecological resilience [88, 108]. Yet, their results are often context-dependent, limiting the transferability of insights across systems [109, 110]. Complementing these ecological perspectives, socio-economic studies have explored farmer attitudes, risk perceptions, and behavioral barriers to the adoption of sustainable practices [111, 112], revealing the importance of social and institutional drivers alongside biophysical factors.

Substantial efforts have been made to curb ongoing environmental degradation, including through the design and evaluation of policy interventions. Nevertheless, many of the models currently used to study agro-environmental systems remain rooted predominantly in either ecological or economic disciplines. Accordingly, and consistent with the objective stated in the introduction of jointly accounting for ecological–economic interactions, dynamic feedbacks, and spatial structure, we present two complementary studies that address the two key processes emphasized above: land consolidation and pesticide use.

In the first study [1], we develop a minimal bio-economic agent-based model for France. Its purpose is not thorough prediction, but rather to provide a transparent simulation laboratory in which policy interventions that may mitigate farmland biodiversity decline can be explored qualitatively. By combining the economic incentives that may lead to environmental degradation with the ecological consequences of such degradation, the model allows us to examine trade-offs, potential economic costs, and feedback loops emerging between the economic and ecological components. However, in order to preserve simplicity and transparency, this first framework is spatially implicit. To address this limitation and to analyze the importance of landscape configuration, the second study [2] introduces a spatially explicit bio-economic model with a richer representation of ecosystem-service dynamics, focusing in particular on natural pest control. In line with a growing body of literature recognizing the importance of landscape heterogeneity in supporting biodiversity and ecosystem services in agricultural systems, see *e.g.*, [113–117], this model provides a stylized description of flying generalist natural enemies (*e.g.*, ladybirds) feeding on herbivorous insect pests (*e.g.*, aphids) in annual crop systems (*e.g.*, winter wheat). We then use this framework to study how the spatial configuration of the agricultural landscape, in combination with different pesticide-use regimes, affects both the abundance of beneficial predatory arthropods and the resulting economic outcomes for farmers.

Key Takeaways

- **The biodiversity crisis:** Farmland biodiversity is severely declining across Europe, driven primarily by agricultural intensification, chemical reliance, and the systematic removal of semi-natural habitats.
- **Policy limitations:** Despite introducing agri-environmental measures, the Common Agricultural Policy (CAP) has historically prioritized productivity and remains structurally insufficient to halt ecological degradation.
- **Methodological approach:** To untangle these dynamics, this part of the thesis comprises two distinct papers employing different modeling frameworks to tackle the problem from two complementary angles: one focusing on the macroscopic socio-economic drivers of farm consolidation, and the other detailing the spatially explicit ecological dynamics of natural pest control.

3. An agent-based model of land consolidation and pesticide use

In this chapter, we introduce a modeling framework to (i) understand the dynamics of agricultural landscapes in relation to biodiversity, and (ii) evaluate policy instruments for supporting biodiversity conservation. Specifically, we address two questions: How do pesticide use and land consolidation influence biodiversity levels and ecological stability? Which policy instruments may be effective in curbing biodiversity degradation at large scales? We employ a macroscopic approach grounded in real data, ensuring our model replicates historical trends in farm structure (including average farm size and farm size distribution), pesticide application, and biodiversity indicators. We adopt this macroscopic framework because biodiversity decline operates over long timeframes ($\geq$ 10 years) at pan-European scales, transcending regional differences—a scale that fine-grained models cannot adequately capture due to their limited spatial and temporal resolution and sparse calibration data.

The chapter is structured as follows: in Section 3.2, we detail the model's structure and mathematical formulation. Section 3.3 presents the model initialization and numerical simulation setup. In Section 3.4 we present predictions under a "business as usual" scenario, demonstrating that further declines in biodiversity occur due to continued farmland consolidation. Finally, we evaluate different policy options and show that the most effective approach for achieving both environmental and economic sustainability involves a combination of tighter pesticide regulations and support programs for small farms. In Section 3.5, we conclude.

3.1 Introduction to agent-based model

Standard economic approaches rely on strict, well-defined rules to characterize economic agents and their interactions. Specifically, standard economic models use the concept of "representative farms" and market equilibrium conditions to describe the behavior and characteristics of a group of farms. As an example, Mouysset *et al.* [118] developed a bio-economic model to study sustainable biodiversity management, combining the community dynamics of 34 bird species with a representative farmer who makes decisions about land use over time under market equilibrium assumptions. Although widely adopted, such modeling approaches face criticism for relying on a single representative agent, whereas the real agricultural landscape consists of a diverse mosaic of agents shaped by their interactions and behavioral biases [119–121].

In this context, agent-based models (ABMs) emerge as more promising candidates [122]. Indeed, by representing farmers as interacting autonomous agents, each with unique goals, resources, and constraints, ABMs can effectively capture the diversity of agricultural practices and their impact on land use and biodiversity [119, 123]. This capability makes ABMs particularly

suitable for evaluating the dynamics of agro-ecological systems, where understanding the variability in farmers' behaviors is crucial [124–126].

The literature on agricultural ABMs has expanded rapidly, encompassing diverse areas such as (i) land use and management [127, 128], (ii) economic and market dynamics [129, 130], (iii) technological adoption and innovation [121, 131], (iv) social and behavioral aspects [124, 132], and (v) environmental and ecological interactions [122, 126, 128, 133]. Of particular interest to our study is the latter category [123]. Within this ABM literature, a variety of decision-making models are employed [125, 130, 134], ranging from microeconomic rules [135], where agents maximize profit or utility, to psychosocial and cognitive models [124], where decisions rely on cognitive abilities or intentions, and heuristic rules [121, 136], where agents decision is based on simple adaptive rules.

While microeconomic and psychosocial/cognitive models can serve as robust tools for quantitative policy exploration due to their realism in decision-making elements, they also come with challenges of their own. Their detailed granular nature often limits their spatial and temporal resolution to a few years and square kilometers [133, 135]. Then, calibrating these types of ABMs is consistently challenging, as it requires comprehensive data that are often scarce at these scales [137]. Moreover, biodiversity decline in agricultural landscapes occurs over long timeframes – typically at least 10 years – and is a pan-European phenomenon that emerges clearly at the macroscopic level, regardless of national differences in specific farming systems and regional economic conditions [77, 78, 80].

In this regard, the use of simple heuristic rules for describing farmer decision-making appears to be an adequate approach. While the simplicity of this choice does not enable precise quantitative forecasts for real-world scenarios, it may offer a comprehensive understanding of the feedback loops that are pivotal to ecosystem degradation. This approach aligns with the methodological foundation proposed by Bouchaud, who advocates for the use of ABMs as explanatory tools to ascertain the plausibility of the existence of "Black Swans" or "Dark Corners" – discontinuity lines beyond which runaway instabilities may emerge [138, 139]. Furthermore, this type of model allows for the extension of the simulation horizon both spatially and temporally, leading to a macroscopic description where aggregate properties exhibit minimal fluctuations, thereby making the results more robust against changes in microscopic details.

We draw from this extensive body of literature to propose a new minimal bio-economic agent-based model designed to capture both macroscopic trends and individual farmer behavior. However, unlike existing models [121, 140], ours uniquely combines heuristic rules with aggregate data to approximate real-world scenarios. By employing relatively simple decision-making processes, our model successfully replicates historical trends in biodiversity loss, pesticide reduction, and farm size increases over the past 30 years, using French data. The novelty of our approach lies in its ability to strategically distill key factors influencing farmer decisions to replicate macro trends. This provides a simulation laboratory to investigate qualitatively the policy interventions that can mitigate farmland biodiversity decline. Indeed, the absence of clear large-scale evidence of the effectiveness of usual agri-environmental policy instruments [141, 142] advocates the need to conceive new models and policies to this end.

3.2 Model overview

The model includes the following entities: farmers[1] and biodiversity. Farmers produce a single standardized good, making decisions on two critical production factors: utilized agricultural land and pesticide use. We assume that farmers adjust their pesticide use to achieve specific yield targets, taking economic conditions into account. Profitability results from a combination of internal factors (pesticide efficiency, farm size) and external influences (market conditions, policies, and pest pressure). When profitable, farmers can invest in improving efficiency, potentially reducing pesticide use, and adjust their land holdings by renewing, terminating, or establishing new rental contracts[2].

On the ecological side, a rescaled bird population index is used as an overall indicator for biodiversity. Indeed, bird population trends are often reliable indicators of environmental health [144] as they occupy high trophic levels in food chains and reflect systemic changes [81]. In line with existing literature [145, 146], we characterize bird population evolution taking into account the degrading contribution of pesticide use [90] and increased farm size [147]. Increased farm size contributes to bird population decline via the reduction of field margins which are vital nesting sites. The biodiversity level determines potential pest damage which directly affects farmers' yield. Indeed, with greater biodiversity comes a lower risk of major pest outbreaks and the potential for higher crop yields [148–151].

Regarding temporal resolution, a time step in the model represents one crop cycle (typically one year), and simulations cover the timeframe from 1990 to 2075[3]. The spatial resolution is at the national level, with no explicit spatial description;[4] the scale refers to the number of farmers considered. The model's general characteristics are informed by the French agricultural sector, serving as a case study due to its significance in the European context. Economic aspects of farmers, considered constant such as production costs and economies of scale, are derived from field-crop businesses[5], whereas agronomic characteristics are modeled on wheat.[6] Free parameters have been calibrated to replicate historical trends for key variables, including the biodiversity index, average pesticide use, average farm size, farm size distribution, average yield, and market price.

Key processes in the model, repeated at each time step, include land consolidation, changes

[1]Throughout this discussion, we will use the terms "farms" and "farmers" interchangeably.

[2]Note that land in the model is rented, in line with the fact that 80% of utilized agricultural land in France is indeed rented [143]

[3]We select 2075 as a suitable temporal horizon, distant enough to explore long-term effects given the model's inherent inertia, yet close enough for our approximations to remain reasonable throughout the period.

[4]On the ecological side, this assumption can be partially justified by the fact that birds typically cover wider ranges compared to other species (such as insects or bees), making them less sensitive to region-specific details. On the economic side, we describe broader economic flows rather than localized spatial interactions to have a consistent macro level description in total land use and goods production. We acknowledge that this approach may simplify the complexities associated with biodiversity degradation and land consolidation. Therefore, we intend to explore ways of incorporating a spatial description in future versions of our model. However, considering that our model is intended as an exploratory tool for national-level dynamics, we believe that those assumptions do not significantly compromise the model's results.

[5]Field-crop farming is the most extended land use in France by occupying about 30% of the utilized agricultural area [152]

[6]Wheat is the most cultivated cereal in France as it occupies 16% of all agricultural land [152]

in pesticide use, and ecological responses (also illustrated in Fig. 3.1). Farmers adjust pesticide use and land holdings based on economic outcomes, while ecological components reflect these adjustments through changes in biodiversity indicators. Interactions among farmers emerge only in the land and goods markets, where the dynamics depend on collective actions.

The central design concept of the model is the integration of a microscopic representation of farmer decision-making with an aggregate biodiversity indicator. This approach allows biodiversity trends to emerge from agricultural practices and facilitates the development of effective policy instruments that may impact such trends.

We now present the model's components and their interactions, following the model's temporal sequence illustrated in Fig. 3.1. We outline the underlying hypotheses and provide the mathematical equations governing the dynamics.

3.2.1 Production of goods

The total production $Y_{i,t}$ of farmer i at time t is computed by multiplying his land area $L_{i,t}$ by his yield per hectare $y_{i,t}$:

$$Y_{i,t} = L_{i,t} y_{i,t}. \tag{3.1}$$

The latter is assumed to be given by a Mitcherliche-Baul production function [153]:

$$y_{i,t} = y_{\max}\left[1 - \pi_t \exp\left(-\frac{e_{i,t}P_{i,t}}{P_{\text{ref}}}\right)\right](1 + \xi_{i,t}), \tag{3.2}$$

where $y_{\max}$ denotes the maximum attainable yield, according to agronomic choices not explicitly detailed here. $P_{i,t}$ denotes the pesticide application rate aimed at protecting the yield from pest damage π_t (see Eq. 3.16), while $e_{i,t}$ reflects the efficiency of pesticide use, with P_{ref} serving as a normalizing reference level. The efficiency $e_{i,t}$ encompasses variability in modern technology use (see below). Finally, $\xi_{i,t}$ is a white Gaussian noise accounting for further inter and intra-farmer variability. Note that in this parsimonious formulation, the primary driver of yield differences is pest management ($P_{i,t}$, $e_{i,t}$). This focus on the pesticide-biodiversity relationship is a deliberate simplification, and its limitations are discussed further in the Discussion section. Furthermore, let us stress that the model does not include an exogenous driver for long-term yield growth, a choice that aligns with empirical observations of yield stagnation in Europe over the last few decades [154, 155].

3.2.2 Goods market

After harvest, farmers sell their grain at a central market where the price fluctuates according to supply and demand. The total grain supply $Y_t = \sum_i Y_{i,t}$ is the sum of the quantities produced by each individual farmer.[7] Demand D, on the other hand, is an external factor assumed constant in the model, consistent with the only weak fluctuations observed (over the past 30 years) and forecasted in Europe [156]. In its simplest form we write

$$p_{\text{m},t} = p_{\text{m},t-1}\left(1 + \alpha\frac{D - Y_t}{D}\right) \tag{3.3}$$

[7] We shall henceforth systematically use the notation $A_t = \sum_i A_{i,t}$.

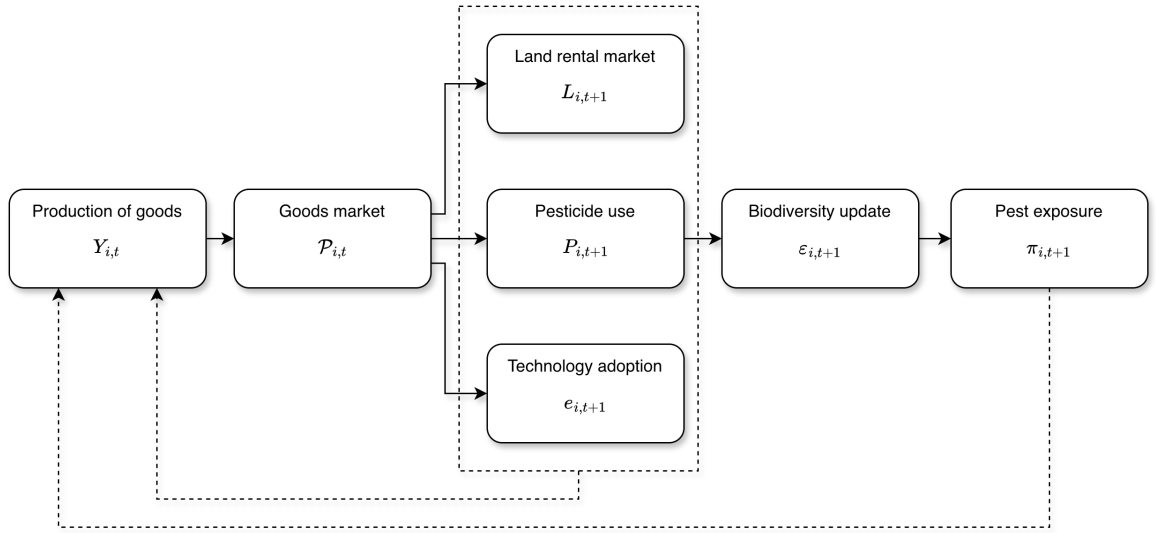


Figure 3.1 Workflow of the model (see Section 3.2). Solid arrows represent direct influences, while dashed arrows indicate feedback loops affecting future production outcomes.

for the price adjustment mechanism, where α reflects market frictions determining the speed at which the price adjusts to imbalances between supply and demand. Farmers' individual profit $\mathcal{P}_{i,t}$ is then given by

$$\mathcal{P}_{i,t} = p_{\mathrm{m},t} Y_{i,t} - C_{i,t} + \frac{L_{i,t}}{L_t} \mathcal{S}, \tag{3.4}$$

where production costs $C_{i,t}$ write

$$C_{i,t} = L_{i,t} \left(p_{\mathrm{p}} P_{i,t} + C_{\mathrm{o}} \right) + (L_{i,t})^b C_{\mathrm{no}}, \tag{3.5}$$

and where C_{o} and C_{no} are operational and non-operational expenses respectively. Operational costs encompass all expenses directly tied to producing grain per hectare, like fertilizer, seeds and fuel expenses (excluding pesticide costs). We assume these costs to be equal for all farmers. Pesticide application costs are factored in separately with $p_{\mathrm{p}} P_{i,t}$, where p_{p} denotes the price of pesticide. Non-operational costs include fixed expenses such as land rental fees, depreciation, and wages. These costs generally scale sub-linearly with the amount of land ($b < 1$), reflecting economies of scale. Larger farms have lower average costs per unit because they can spread fixed costs over more units, benefit from bulk purchasing, and achieve other efficiencies [157, 158]. Finally, the model incorporates direct payment of subsidies $\mathcal{S}$ proportional to the amount of land utilized by each farmer, in line with the Common Agricultural Policy (CAP) over the past three decades [159].

3.2.3 Technology adoption

Farmers strategically allocate a fraction η of their profits to adopt advanced technologies that improve pesticide application efficiency. Examples of these technologies include drones for real-time monitoring of crop health, and predictive models from decision support systems to enhance

pest control strategies [160]. In our model, we assume that these technological advancements contribute to reduced pesticide use by minimizing overspraying, which subsequently benefits biodiversity. However, it is important to acknowledge that newer technologies could also lead to increased ecological harm. For instance, more powerful pesticides might target a wider range of species, potentially offering no net benefit for biodiversity. A discussion exploring this hypothesis is presented in Appendix 3.6.3.

In line with the Evolutionary ABMs literature [161], we assume that the success of farmers' investments in technology adoption follows a Bernoulli trial, indicating that each attempt has a random chance of success. The probability of success $\mathbb{P}^e_{i,t}$ depends on the amount invested and the effectiveness in translating investment into successful innovations program ($\mathcal{P}_{\text{ref}}$) as

$$\mathbb{P}^e_{i,t} = 1 - \exp\left(-\frac{\eta \mathcal{P}_{i,t}}{\mathcal{P}_{\text{ref}}}\right). \tag{3.6}$$

If the investment of farmer i at time t is successful, the farmer's pesticide application efficiency level $e_{i,t}$ is increased by a random value $\upsilon_{i,t}$ as

$$e_{i,t+1} = e_{i,t} + \upsilon_{i,t}, \tag{3.7}$$

where $\upsilon_{i,t}$ is drawn from a uniform distribution within a predefined range $[0, \upsilon_{\max}]$.

3.2.4 Land rental market

Then, farmers strategically adjust their rented land based on their yearly economic performance.[8] The land rental market is described as a centralized market similar to that of Balman *et al.* [162]. Farmers release and acquire land based on the difference between realized returns[9] and opportunity costs r_{ref}, which correspond to the loss in returns of other investments that could have been made instead.

If actual returns on investment $r_{i,t}$ are lower than r_{ref}, farmers terminate some of their rental contracts to release the following quantity of land:

$$L^-_{i,t} = \frac{\beta}{1 + \frac{r_{\text{ref}}}{r_{\text{ref}} - r_{i,t}}} L_{i,t}, \tag{3.8}$$

where β measures the maximum amount of released land per year. Farmer i's available land for farming at the next period is then updated as

$$L_{i,t+1} = L_{i,t} - L^-_{i,t}. \tag{3.9}$$

When the leftover land is less than 0.1 hectares, the farmer terminates all rental contracts and leaves the market, thereby not participating in the next year's production. Note that we do not allow for any farmer entries, in line with strong empirical evidence that the number of farms in the EU has been in decline for a long time — the vast majority of which were small farms of less than 5 hectares [163]. We do not allow for exits from large farms either.

[8] Note that the model assumes an annual adjustment to land tenure. This simplification is suitable for describing the effects of slow, persistent economic pressure on farm viability, which is our focus. A more complex model incorporating multi-year leases would be more appropriate, and indeed necessary, if the primary goal were to analyze the effects of large-scale economic shocks.

[9] Here the realized return on investment is computed as $r_{i,t} = \frac{(1-\eta)\mathcal{P}_{i,t}}{C_{i,t}}$.

Conversely, if opportunity costs are lower than realized returns, the farmer is incentivized to sign new rental contracts. The amount of new prospective rented land is

$$\tilde{L}^+_{i,t} = \frac{\beta}{1 + \frac{r_{\text{ref}}}{r_{i,t} - r_{\text{ref}}}} L_{i,t}. \tag{3.10}$$

However, the actual new land acquisition should not exceed the total amount of land available for rent, computed as the sum of the leftover from the previous period and the land released by all agents

$$L_{i,t+1} = L_{i,t} + L^+_{i,t}, \quad \text{where} \quad L^+_{i,t} = \tilde{L}^+_{i,t} \min\left(1, \frac{\tilde{L}^+_t}{L^{\text{leftover}}_{t-1} + L^-_t}\right). \tag{3.11}$$

Leftover land also needs to be updated as $L^{\text{leftover}}_t = L^{\text{leftover}}_{t-1} + L^-_t - L^+_t$.

3.2.5 Pesticide use

Remaining active farmers adjust their pesticide use according to past trends influencing their performance, rather than by strict economic optimization. Indeed, existing literature shows that pesticide adoption is largely influenced by a variety of behavioral factors [164]. For simplicity, our model assumes that farmers update their pesticide use to meet an evolving yield target. This approach aligns with findings in agricultural economics that suggest farmers often prioritize specific yield targets as measures of success and viability, especially under uncertain conditions [165]. Therefore, farmers update their pesticide use according to the following behavioral rule:

$$P_{i,t+1} = P_{i,t}\left(1 + \gamma \frac{\tilde{y}_{i,t} - y_{i,t}}{y_{i,t}}\right), \tag{3.12}$$

where γ is the speed of adjustment and $\tilde{y}_{i,t}$ is the yield target (see below). This approach takes into account the lack of complete information regarding both pest exposure levels and the efficiency of the technologies employed. The yield target $\tilde{y}_{i,t}$ evolves according to market price fluctuations:

$$\tilde{y}_{i,t+1} = \tilde{y}_{i,t}\left(1 + \lambda \frac{p_{\text{m},t} - p_{\text{m},t-1}}{p_{\text{m},t}}\right). \tag{3.13}$$

This equation reflects the willingness of farmers to decrease or increase their production target according to market price: when the market price has been decreasing (resp. increasing), farmers might lower (resp. increase) their yield target to reduce pesticide related costs. Although this can sound like strong simplification of the farmers' decision-making process, it is commonly employed in ABMs as a plausible heuristic of production target setting by economic agents [139, 166].

3.2.6 Biodiversity update

Finally, the actions of farmers influence biodiversity, described by the rescaled bird population $\varepsilon_t = M_t/M_0$, via a logistic equation in accordance with the existing literature [118, 145, 146, 167]:

$$\varepsilon_{t+1} = \varepsilon_t + r_\varepsilon \left(1 - \frac{\varepsilon_t}{K_t}\right)\varepsilon_t, \tag{3.14}$$

where r_ε is the intrinsic growth rate of the bird population, and K_t is a measure of the carrying capacity [168]. K_t depends on the average pesticide use $\bar{P}_t$ and average farm size $\bar{L}_t$ as defined in the following equation:[10]

$$K_t = \mu \frac{\bar{L}_0}{\bar{L}_t} + (1-\mu)\frac{\bar{P}_0}{\bar{P}_t}, \tag{3.15}$$

where μ reflects their relative importance. The updated ecological conditions influence the pesticide-free typical yield loss due to pests π_t via:

$$\pi_{t+1} = \pi_0 \left(\frac{\varepsilon_0}{\varepsilon_{t+1}}\right)^a, \tag{3.16}$$

where the exponent a determines the extent of biodiversity's impact on pest exposure and, consequently, on crop yields [169] (see Appendix 3.6.2 for further discussion).

3.3 Real data and numerical simulations

3.3.1 Data sourcing

The data for calibrating and initializing the model are sourced from various databases, all containing information relevant to the French agricultural sector. To characterize biodiversity, we use the common farmland bird index, which monitors the abundance of 34 farmland bird species across Europe [170]. Data on the agricultural sector's structure are derived from the Food and Agriculture Organization (FAO)'s "Structural Data from Agricultural Censuses" [171], from which we extracted the data specifically for France. This dataset is compiled through decennial monitoring of UN countries' agricultural censuses and includes detailed information on the size and number of agricultural holdings. Due to the lack of individual farmer data, agronomic information related to wheat production is sourced from the European Farm Accountancy Data Network (FADN) [152]. This pan-European database provides detailed, standardized statistics at the member state level, allowing us to source French-specific data for average wheat yield and pesticide use. Finally, the wheat producer price index is used to track annual changes in selling prices for farmers. This index is constructed using price data in standardized local currency [172] (from FAO) on an annual basis.

3.3.2 Calibration

Model parameters are categorized into three groups (see Table 3.1): (i) those directly inferred from data and literature, henceforth called *measured* parameters (M), (ii) those set by hand to ensure consistent dynamics, namely *estimated* parameters (E), and (iii) those obtained through calibration to reproduce trends during the 1990-2021 period, or *calibrated* parameters (C) (see Fig. 3.2). The main trends within the agricultural landscape are biodiversity degradation (Fig. 3.2a), decline in average pesticide use due to technological innovation depicted (Fig. 3.2b), and land consolidation (Figs. 3.2e-g).

Although derived from existing data, the values of the parameters in the M category are influenced by model assumptions and simplifications. For example, some quantities—such as

[10] Note that $\bar{P}_t$ is computed as a weighted average over farm sizes, in line with the usual reporting methods [152].

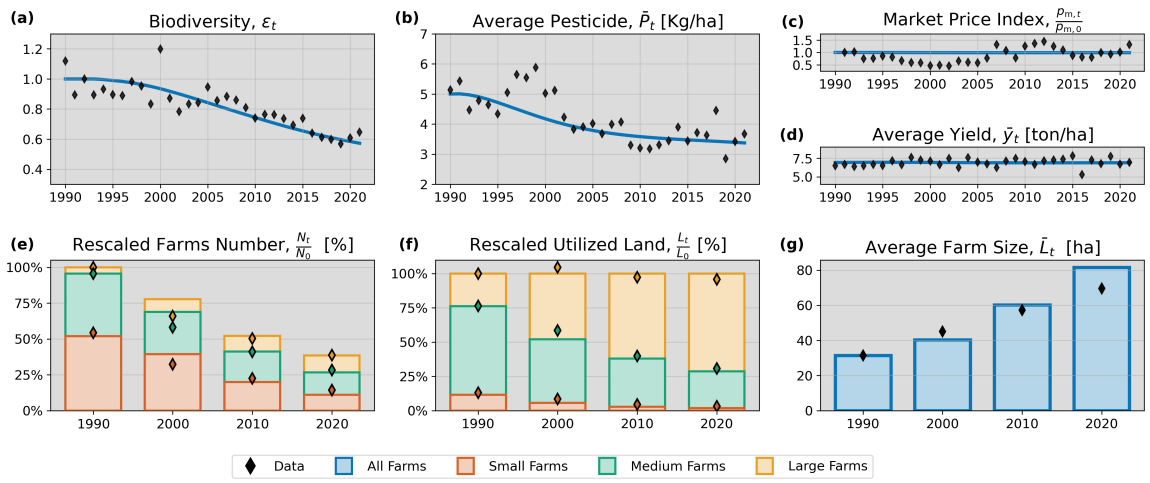


Figure 3.2 Calibration of the model: diamonds represent real data, while blue lines and colored bars display the calibration results. (a) Biodiversity degradation (EU common farmland bird index [170]). (b) Decline in average pesticide use (FADN [152]). (c) Market price index (FAO [172]). (d) Average yield (FADN [152]). (e-g) Land consolidation illustrated with FAO data [171] in terms of (e) total number of farmers, (f) total utilized land for different farm sizes (small farms: less than 20 ha, medium farms: 20-100 ha, large farms: more than 100 ha), and (g) average farm size.

non-operating costs, operating costs, and pesticide prices—fluctuate over time, but are assumed constant and equal to representative values over the 1990-2021 period.

Parameters in the E category are set to reasonable values that ensure consistency between the data and the model's functional forms. For example, the ecological parameter μ in Eq. 3.15 is set to reproduce the biodiversity curve using Eq. 3.14 with historical values of average pesticide use and farm size.[11] Similarly, the value of a (Eq. 3.16) was derived using biodiversity interpolated values, assuming a pest exposure value of 0.3 in 1990 and 0.4 in 2021 [173]. On the economic side, P_{ref} is computed by inverting Eq. 3.2 using average values from 1990 data and $\bar{e}_0 = 1$, while r_{ref} and D are based on the equilibrium hypothesis (see *Initialization* below).

Parameters in the C category are primarily related to technology adoption and behavioral aspects of the model. Realistic values for these parameters are not directly available due to the high-level description of the model, and they cannot be estimated as they depend intrinsically on the model's dynamic realization. Therefore, we opted for calibrating these parameters to ensure the model replicates well the major trends observed in the reference data from 1990 to 2021. The calibration was done through least-squares minimization, with additional methodological details and sensitivity analysis provided in the Supplementary Materials 3.6.1. The results are given in Table3.1 and Fig. 3.2.

[11] Given the noisy nature of the data, we use a rolling average as a more stable proxy of these trends.

Section	Notation	Description	Value	Group	Source
Initialization	N_0	Number of farms	300000	M	[171]
	L_0	Total agricultural land [ha]	10e6	M	[171]
	$\bar{P}_0$	Average pesticide use [kg · ha^{-1}year^{-1}]	5	M	[152]
	$\bar{y}_0$	Average yield [ton · ha^{-1}year^{-1}]	7	M	[152]
	π_0	Potential pest damage [year^{-1}]	0.3	M	[173]
	r_0	Average return on investment [year^{-1}]	0.05	M	[152]
	D	Demand [ton · year^{-1}]	7e7	E	
Ecological factors	r_ε	Intrinsic growth rate [year^{-1}]	0.1	M	[167]
	μ	Carrying capacity weights	0.9	E	
	a	Pest-biodiversity nonlinearity	0.5	E	
Production factors	$y_{\max}$	Maximum yield [ton · ha^{-1}year^{-1}]	8.5	M	[174]
	P_{ref}	Reference pesticide [kg · ha^{-1}year^{-1}]	10	E	
	std(ξ)	Production noise	0.05	M	[175]
Other economic factors	α	Price frictions	0.08	C	
	p_{p}	Pesticide price [€ · kg^{-1}]	10	M	[176]
	C_{O}	Operating costs [€ · ha^{-1}year^{-1}]	500	M	[177]
	C_{NO}	Non-operating costs [€ · ha^{-1}year^{-1}]	600	M	[177]
	b	Economy of scale	0.9	M	[157]
	$\mathcal{S}$	Total subsidies budget [€ · year^{-1}]	5e9	M	[178]
Technology adoption	η	Profit share for technology	0.15	C	
	$\mathcal{P}_{\text{ref}}$	Reference profit for technology [€ · year^{-1}]	1000	C	
	$\upsilon_{\max}$	Maximum efficiency gain [year^{-1}]	0.1	C	
Behavioural factors	β	Land adjustment speed [year^{-1}]	0.45	C	
	r_{ref}	Reference return on investment [year^{-1}]	0.05	E	
	γ	Pesticide adjustment speed	2	C	
	λ	Yield target adjustment speed	0.2	C	

Table 3.1 Parameters of the model. We indicate their units, value, estimation method, and source (see Section 3.3.2).

3.3.3 Initialization

Having set the parameters, the model can now be initialized. On the economic side, the initial number of farmers is determined to approximate the number engaged in fieldcrop farming in 1990, see Table 3.1. The distribution of their land holdings is derived from the FAO's "Structural Data from Agricultural Censuses" dataset for 1990. For agronomic information related to wheat production, we use average values from the FADN dataset. Each farmer is assigned an initial pesticide use and yield as follows:

$$\begin{aligned} P_{i,0} &= \bar{P}_0(1+\zeta_i) \\ y_{i,0} &= \bar{y}_0(1+\psi_i) \end{aligned} \qquad \text{where} \qquad \zeta_i, \psi_i \in \mathcal{N}(0, 0.1) \tag{3.17}$$

with $\mathcal{N}(0, 0.1)$ a Gaussian distribution with zero mean and a standard deviation of 0.1. Further assuming an initial pest exposure of 30% (see above) [173], we calculate the initial efficiency rate and total costs using Eqs 3.2 and 3.5, respectively. The initial market price is set to reflect an average return on investment equal to the opportunity cost, ensuring a competitive agricultural sector at the beginning of the period. Finally, the initial demand is set equal to the total initial production, simulating a market close to equilibrium.

3.3.4 Simulation

With all parameters set and variables initialised, various scenarios can be explored through extensive numerical simulations. For each scenario, we conduct 10 simulations with different random seeds. The results presented are Monte Carlo averages, with their relative standard errors omitted due to their negligible values (below the line width). It is important to note that we do not account for global fluctuations in either ecological or economic aspects, so the relative differences between simulations are solely due to farmer-to-farmer variability. Given the large number of farmers, this variability averages out when examining macro trends.

Instead of relying on a single indicator, we shall propose a stratified analysis to examine each variable's role through its interactions with others, providing a more comprehensive understanding of the dynamics of the model.

3.4 Results

We begin by examining a baseline scenario without additional policy interventions. Our model predicts a decline in biodiversity by 2075 of 10% compared to 2021, and a concerning 55% decline compared to 1990 levels. While these values should be considered as approximate given the nature of our analysis, the significant drop underscores the urgent need for policy changes to protect and, when possible, restore biodiversity. To address this challenge, we explore two potential policy options: (i) reducing pesticide use and (ii) implementing subsidies for small farmers. Our analysis shows that both approaches positively impact overall biodiversity, albeit with some caveats. The most effective strategy appears to be a combined approach that leverages the strengths of both policies.

3.4.1 Baseline scenario

The business-as-usual predictions of our model are represented by the solid blue lines in Fig. 3.3. In this baseline scenario, the ongoing biodiversity degradation process (Fig. 3.3a) proceeds in two distinct phases. In the short term (2022-2050), biodiversity drops to 42% of its 1990 levels. However, in the latter part of the simulation (2050-2075), we observe a slight recovery to eventually reach 45%.

The initial decline is primarily driven by intensified land consolidation. Although pesticide use (Fig. 3.3d) decays over time due to increased efficiency (Fig. 3.3h), the positive effect of such decay on biodiversity is offset by the increase of average farm size (Fig. 3.3c). The land consolidation, where the number of farms continuously decreases (Fig. 3.3f) with smaller farms being absorbed by larger ones, is driven by the following mechanism. Since the market price remains relatively constant (Fig. 3.3b), farmers must compensate for the increase in pest exposure, due to biodiversity loss (Eq. 3.16), by enhancing efficiency to maintain their marginal profit. However, investments in technology adoption depend on current profitability (Eq. 3.6), favoring larger farmers with greater margins due to economies of scale. Over time, small struggling farms terminate rental contracts, sacrificing further economies of scale and profitability, leading to sector abandonment and further biodiversity decline.

In the long term, the number of farmers stabilizes as most farms reach a size sufficient to secure a return on investment greater than the opportunity cost (Fig. 3.3g). Consequently, in this phase, the continued reduction in pesticide use does explain the slight recovery of biodiversity.

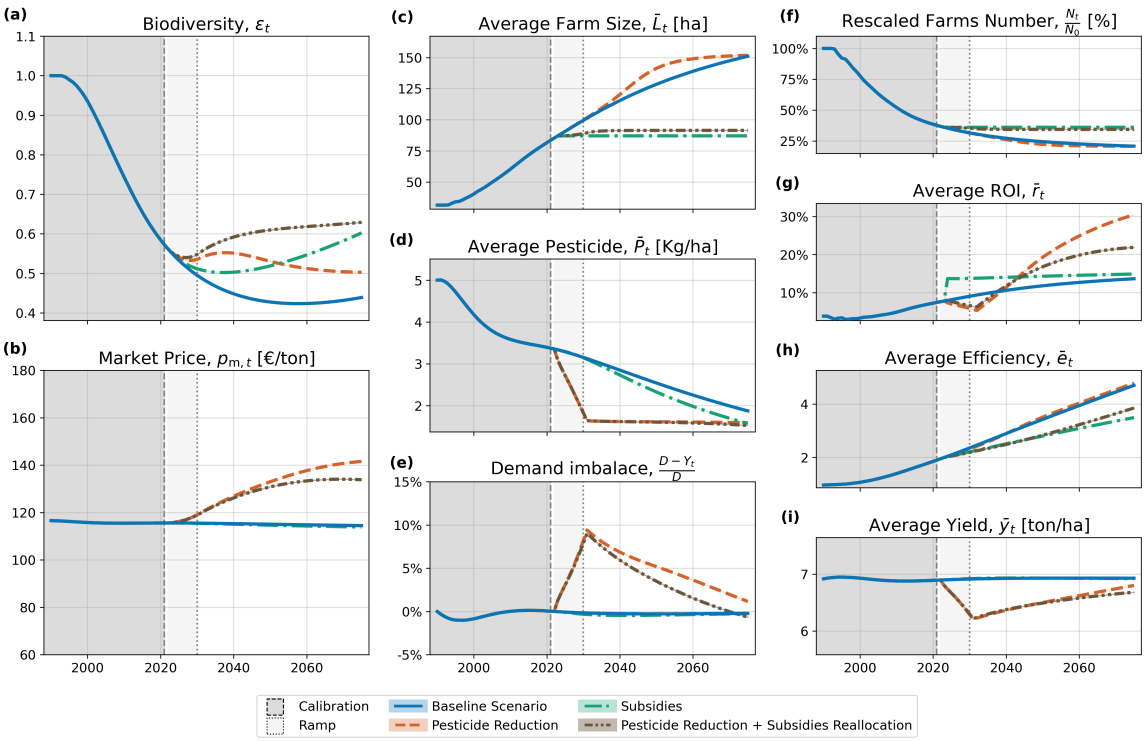


Figure 3.3 Numerical simulations. The gray-shaded area indicates the calibration period (1990-2021). In the baseline scenario (solid blue lines), biodiversity continues to decline due to intensified land consolidation. The pesticide reduction scenario (dashed orange line) shows initial biodiversity recovery, followed by a decline caused by intensified land consolidation due to reduced yields. The light-gray-shaded area marks the 2022-2030 ramp to halving pesticide. The subsidy program favoring small farmers (dash-dotted green line) effectively halts land consolidation, leading to improved biodiversity outcomes. The combined approach of pesticide reduction with subsidies for small farmers (dash-dot-dotted brown line) appears as the most promising solution for biodiversity conservation by mitigating the negative effects of land consolidation while benefiting from pesticide reduction.

While the exact timing of this stabilization should not be taken too seriously, it seems reasonable when considering that European farmers face international competition from countries where the average farm size (and thus their capacity to exploit economies of scale) reaches hundreds of hectares [171]. Therefore, this market pressure on small farmers, which has already driven land consolidation and ecological degradation over the last 30 years, may represent a serious threat to biodiversity in the coming decades [147].

Lastly, it is noteworthy that, as mentioned above, the market price remains nearly unchanged because total production remains aligned with demand (Fig. 3.3e). This equilibrium is achieved by maintaining yield levels (Fig. 3.3i) equivalent to the period 1990-2021, indicating that average efficiency gains offset the effects of increased pest exposure.

3.4.2 Pesticide reduction

Although the decay rate is indeed slowing down, the forecasted biodiversity decline in the baseline scenario remains undesirable from a conservation perspective. Indeed, biodiversity is critical for ecosystem functioning and supporting essential services such as water provision and air purification, vital for societal well-being [179, 180], though these aspects are not the focus of this study. One widely discussed policy proposal to enhance biodiversity is reducing pesticide usage [181–183]. Various methods can be thought of, such as pesticide taxes [182] or incentives for organic farming [183]. Our analysis focuses on a straightforward approach: mandating a gradual reduction in pesticide use by farmers. Specifically, we model a policy requiring farmers to halve their pesticide usage linearly over 2022 to 2030 the period,[12] in line with the European Union considerations [181].

The outcomes of the pesticide reduction policy are illustrated as orange dashed lines in Fig. 3.3. In the beginning, biodiversity recovers rapidly (Fig. 3.3a) due to the immediate effect of reduced pesticide use (Fig. 3.3d). However, this initial boost is quickly followed by a strong decline. Indeed, reduced pesticide use leads to an estimated 10% decrease in crop yield (Fig. 3.3i), consistent with existing literature [184]. Consequently, the reduced yield results in a significant drop in return on investment for farms of all sizes (Fig. 3.3g). Smaller farms, already operating with narrow profit margins, are particularly affected and tend to exit the farming sector even faster. This accelerates land consolidation, as evidenced by a decrease in the number of farmers (Fig. 3.3f) and an increase in average farm size compared to the baseline scenario (Fig. 3.3c). Ultimately, exacerbated land consolidation neutralizes the positive impacts of pesticide reduction, resulting in a net decrease in biodiversity that falls below 2021 levels.

Finally, we observe an increase in market price which can be attributed to an underproduction regime (Fig. 3.3e) resulting from decreased yields (Fig. 3.3i) without corresponding expansion in cultivated land. However, and perhaps surprisingly, such increase in price is not sufficient to outweigh the profit degradation due to yield loss, resulting on average in a lower ROI (Fig. 3.3g). This can be explained by the influence of international competition, which is factored in here as friction in the price dynamics ($\alpha < 1$ in Eq. 3.3). Indeed, in a global market, one expects that local decreases in crop yield are offset by higher production levels in other countries not subject to the same pesticide reduction policies.

While the magnitude of the indirect economic pressure on small farmers exerted by pesticide reduction policies may vary depending on region-specific properties, we believe these effects can be significant. This highlights the need for more integrated model and policy frameworks [185, 186] that consider the interplay between pesticide use, land consolidation, and the economic viability of small farming systems.

3.4.3 Subsidies

As argued above, land consolidation significantly influences biodiversity dynamics. Therefore, it is logical to consider a policy involving subsidies that favors small farmers to maintain a diverse landscape. To this end, we introduce a subsidy program in the form of a direct payment to all

[12] This is achieved via the following equation:

$$P_{i,t+1} = \min\left\{P_{i,2021} \min\left[\max\left(\frac{t+1-2021}{2030-2021}, 0\right), 1\right], P_{i,t}\left(1+\gamma\frac{\tilde{y}_{i,t}-y_{i,t}}{y_{i,t}}\right)\right\}$$

.

farmers (in addition to the existing subsidies per ha), providing a 200-euro coupon regardless of farm size.[13] This policy inherently benefits small farmers due to the marginal increase in profit it provides.

The results of this policy are shown in Fig. 3.3 as green dash-dotted lines. The number of farmers (Fig. 3.3f) rapidly stabilizes after the application of the new policy, as does the average farm size (Fig. 3.3c). Consequently, biodiversity degradation slows down compared to the baseline scenario to eventually increase (Fig. 3.3a). In addition, biodiversity restoration positively affects pesticide use. As pest exposure decreases accordingly to Eq. 3.16, the amount of pesticide required to achieve the same yield also decreases (Figs. 3.3d and i). Finally, the reduction in pesticide use is reflected in slightly lower prices (Fig. 3.3b), due to the slow adjustment behavior of farmers, which results in a phase of overproduction.

The results of this section highlight the critical role of favoring small farmers in halting land consolidation and enhancing biodiversity.

3.4.4 Combined policy: Pesticide reduction and subsidies reallocation

Thus far, we have demonstrated that biodiversity decreases under a business-as-usual scenario. The pesticide policy alone is ineffective in improving the situation due to its associated impact on land consolidation. Conversely, a subsidy policy favoring small farmers tends to mitigate land consolidation.

Regarding policy makers motivations and constraints, on one hand, they may seek to reduce pesticide use regardless of biodiversity benefits given the well-documented negative impact of pesticide use on human health [187]. On the other hand, they may be reluctant to add new subsidies to the already existing ones due to funding constraints. Therefore, we explore the consequences of a coordinated policy that targets (i) pesticide reduction (through the same mechanism as before), while (ii) reallocating a fraction of existing subsidies from a per-hectare basis to a per-farmer basis.[14] The results of this combined policy, assuming a reallocation of 0.3% of existing subsidies, are reported in Fig. 3.3 (dash-dot-dotted brown line). This reallocation choice corresponds to a new subsidy of 65 euros per farmer and a negligible different in subsidy per hectare (see Figs 3.4a-b).

The positive impacts of both policies pesticide reduction and targeted subsidies are successfully combined. Biodiversity rapidly increases due to pesticide reduction (Fig. 3.3a), and, unlike with the pesticide reduction policy alone, such increase is stabilized by the action of the subsidies. Indeed, the number of farmers (Fig. 3.3f) and the average farm size (Fig. 3.3c) stabilize. We also observe that market prices benefit from this increase in biodiversity (Fig. 3.3b). Indeed, due to biodiversity recovery, lower pesticide use is required to achieve the same yield targets (Eq. 3.2), reducing the duration and magnitude of the underproduction phase (Fig. 3.3e). This leads to an overall price level lower than under the pesticide reduction policy alone, thereby benefiting society as a whole.

As stated above, the results of Fig. 3.3 are given for a reallocation fraction of 0.3% of pre-existing subsidies. One may wonder how varying this reallocation fraction affects the overall outcomes. In Fig. 3.4, we report results at the end of the period (year 2075) for different

[13] This modifies Eq. 3.4 by introducing a constant term. Note that the value $\mathcal{S}_{\mathrm{P}} = 200€$ was chosen arbitrarily for illustrative purposes. As shown in Fig. 3.5a, this amount is well within the saturation regime where the policy's maximum effect is achieved; a smaller subsidy is actually sufficient to obtain the same result.

[14] This is achieved by modifying Eq. 3.4 as $\mathcal{P}_{i,t} = p_{\mathrm{m},t} Y_{i,t} - C_{i,t} + \frac{L_{i,t}}{L_t}(1-\theta)\mathcal{S} + \frac{1}{N_t}\theta\mathcal{S}$.

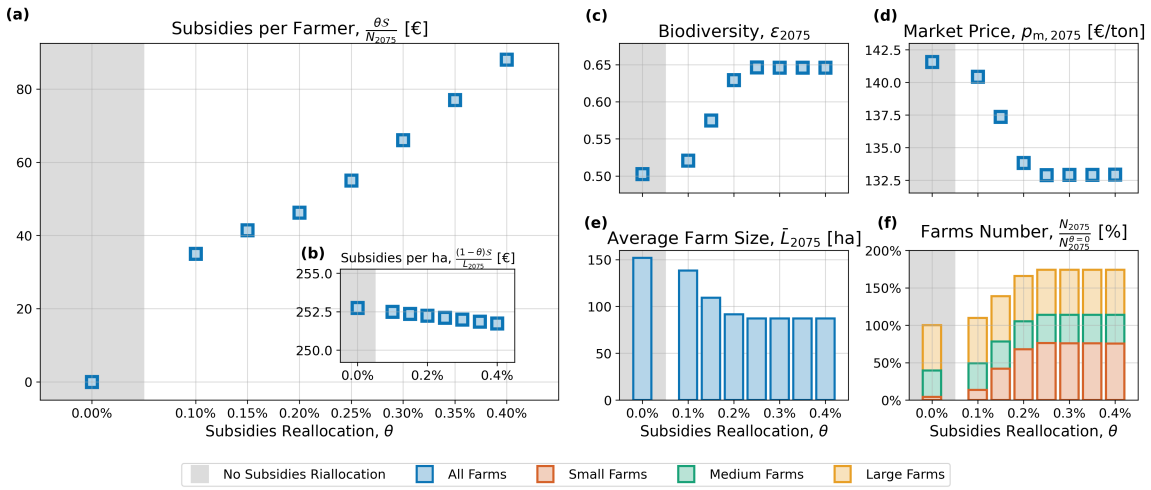


Figure 3.4 Impact of the combined policy in 2075 for different levels of subsidies reallocation. (a) Subsidies per farmer as function of the percentage of subsidies reallocation. (b) Subsidies per hectare negligible decrease. (c) Biodiversity improves significantly with increased subsidies reallocation as the average farm size (e) decreases, indicating a reduction in land consolidation. However a plateau is reached when the numbers of farmers (f) is no longer affected by a further increase in subsidies. (d) The market price decreases slightly with higher subsidies reallocation, as a consequence of biodiversity recovery, ultimately benefiting societal well-being.

reallocation fractions. When the reallocation fraction is too small, the positive effects are limited, with biodiversity showing only a slight improvement over the pesticide reduction policy alone (Fig. 3.4c). However, increasing this fraction by a few basis points leads to a strong increase in overall benefits, as highlighted by higher levels of biodiversity and lower prices (Fig. 3.4d). Increasing further the reallocation fractions is not necessary, indeed benefits saturate as the distribution of farm sizes is no longer affected (Figs 3.4e-f).[15]

While the evaluation of the effects of the subsidy reallocation may not be quantitatively accurate and requires more robust exploration, we believe that the identification of possible feedback loops from biodiversity recovery to societal well-being, as described here, is crucial in halting the ongoing environmental degradation. Indeed, as advocated by an increasing number of researchers, the environmental challenges we face require an analysis that goes beyond first-order economic effects [188]. To this end, minimal models like ours are useful tools for establishing a qualitative phenomenology of such complex phenomena by identifying basic mechanisms and potentially important, yet hidden, positive feedback loops.

3.5 Discussion

Using the French agricultural landscape as a case study, we developed a parsimonious, integrated bio-economic model grounded in historical data. Our approach distinguishes itself

[15] Recall that we have not allowed for entry of new farmers in this version of the model.

by introducing explicit micro-foundations that capture the interactions between economic dynamics and ecological processes, thereby offering insights into both past and potential future trajectories of biodiversity loss, pesticide use, and land consolidation. The model serves as a policy-evaluation tool designed to assess the ecological and economic outcomes of alternative intervention strategies, consistent with the emerging literature on coupled human–natural systems [145, 146, 189] and bio-economic modeling [118, 121, 190, 191].

3.5.1 Main findings and mechanisms

A defining feature of our framework is its explicit representation of feedback loops between bird population dynamics—used as a proxy for biodiversity—and the economic decision-making of individual farmers. Under the business-as-usual scenario, the model predicts a continued and pronounced decline in biodiversity, driven primarily by ongoing land consolidation. This mechanism is fundamentally economic: persistent market pressures favor farms that can exploit economies of scale, making smaller, less-capitalized farms increasingly uncompetitive [157, 192]. As these smaller farms exit the sector, their land is absorbed into larger operations, resulting in landscape homogenization and the loss of semi-natural habitats essential for biodiversity [147, 193–195].

This underlying economic reality reveals both the strengths and weaknesses of isolated policy interventions. On one hand, a policy of pesticide reduction alone delivers a significant and immediate ecological benefit, rapidly boosting biodiversity by reducing chemical pressures [89, 196, 197]. However, this short-term gain comes at a high economic cost: the resulting decline in crop yields and profitability disproportionately harms smaller farms, accelerating the very consolidation process that drives habitat loss [198]. In effect, the policy's initial ecological success is paradoxically undermined by the economic instability it creates.

Conversely, a policy of targeted subsidies for small farmers proves highly effective at addressing the economic root of the problem. Its primary strength lies in halting the consolidation process, thereby preserving the existing network of semi-natural habitats embedded in the agricultural landscape [199, 200]. This structural stability is sufficient to allow for a gradual, long-term biodiversity recovery, supported by ongoing technological improvements and lower pest pressures [201, 202]. However, this approach is fundamentally defensive: it prevents further degradation but does not by itself trigger the rapid ecological improvements observed under pesticide reduction. Note that the mechanism considered here is based on habitat preservation, rather than active restoration, which would likely entail longer ecological adjustment times than those captured by our model. Nonetheless, restoration could represent an additional policy avenue worthy of exploration in future work [203].

Given the trade-offs inherent in these isolated approaches, the most effective outcome arises from a combined policy[16]. This integrated strategy synthesizes the strengths of both interventions while mitigating their respective weaknesses. The pesticide reduction mandate provides a strong, immediate catalyst for ecological recovery, while targeted subsidies create the necessary economic condition to sustain it. By shielding small farms from the financial stress of transition, this dual approach breaks the reinforcing loop between economic consolidation and ecological decline, leading to a rapid and sustained improvement in biodiversity.

[16]The idea that the most effective policies consist in combining policy instruments that are complementary (*e.g.*, duo of subsidies and restrictions) was recently discussed in [204].

3.5.2 Policy implications in the current French context

These findings extend beyond theoretical implications, speaking directly to the ongoing tensions that characterize contemporary agricultural policy in France and across the European Union. The widespread farmer protests of recent years, often directed against environmental regulations, exemplify the perceived incompatibility between economic viability and ecological ambition [205–207].

Our model offers a quantitative interpretation of this structural conflict. The pesticide reduction alone scenario (Fig. 3.3) mirrors the situation frequently reported by farmers: a well-intentioned environmental policy that, by neglecting underlying economic constraints, threatens the financial sustainability of farm operations. Recent developments in French agricultural policy—such as the postponement of pesticide-reduction targets under the *loi Duplomb* [208, 209], the temporary re-authorization of neonicotinoids [210], and the withdrawal of the *Pacte de la haie* (Hedgerow Pact) [211]—can thus be interpreted as political reactions to the socio-economic infeasibility of imposing ecological objectives without corresponding economic safeguards.

However, our results demonstrate that this conflict is not structurally inevitable. The combined policy scenario outlines a feasible pathway for reconciling environmental and economic objectives, showing that meaningful biodiversity recovery can be achieved when ecological regulations are complemented by targeted financial instruments. In particular, providing income support to small and medium-sized farms buffers the short-term economic costs of pesticide reduction, allowing these farms to remain competitive while maintaining more heterogeneous and biodiversity-supportive landscapes [212, 213].

Importantly, the model indicates that such outcomes can be realized with only a modest reallocation of existing agricultural subsidies (approximately 0.3% of the total budget). This finding suggests that a politically and fiscally realistic compromise is within reach—one that aligns with the growing consensus in environmental economics that effective sustainability transitions require the coordinated use of complementary policy instruments rather than reliance on isolated regulatory mandates [214, 215].

3.5.3 Limitations and future directions

While our minimal model provides valuable insights, it is essential to note that our results are qualitative and should not be interpreted as precise quantitative forecasts. The model's parsimony, which is its strength for isolating key mechanisms, also entails necessary simplifications. The policy recommendations drawn from this model should therefore be viewed as heuristic and verified through more detailed extensions.

First, the model's scope could be expanded to better capture the diversity of agricultural systems. Our focus on arable crops omits important farming systems—such as permanent crops and livestock—that exhibit distinct decision-making structures and ecological impacts [216, 217]. Similarly, our agronomic calibration focuses on wheat, assuming relatively stable yields and static input costs. While this simplification isolates the role of pesticides and land consolidation, it omits factors such as mechanization, labor, and other agronomic inputs-such as fertilizer and irrigation-, all of which influence farm competitiveness [218, 219]. Future research should investigate how these omitted variables interact with policy to shape farm structure and biodiversity outcomes.

Second, introducing spatial heterogeneity is a clear priority. Our national-level framework does not capture the fine-scale spatial patterns that underpin habitat connectivity and ecological

resilience [220, 221]. This limitation explains why biodiversity decline in our baseline is almost entirely attributed to land consolidation. A spatially explicit model would allow for more realistic representations of restoration processes, ecological time lags, and spillover effects [2, 222, 223], as well as interactions between regional land-use choices and biodiversity recovery.

Finally, future work should deepen the behavioral realism of farmer decision-making. Our model assumes price-driven heuristic rules for farmers' decision making, yet empirical evidence indicates that real-world decisions are influenced by risk aversion, social norms, and path dependence [126, 130, 165, 224]. Incorporating these behavioral dimensions would improve the capacity of the model to capture inertia and heterogeneity in responses to policy. Moreover, embedding the agricultural sector within broader macroeconomic and trade dynamics would enable a richer analysis of feedbacks between domestic ecological policy and global competitiveness, a key frontier in bioeconomic modeling [4, 225, 226].

In sum, this work contributes to the growing field of integrated ecological–economic modeling by demonstrating how simple yet mechanistically grounded frameworks can shed light the structural linkages between agricultural intensification, market forces, and biodiversity decline. Building on these foundations through spatial, behavioral, and macroeconomic extensions will be crucial for developing policy strategies that are not only ecologically sound but also economically and politically durable.

3.6 Supplementary materials

3.6.1 Calibration procedure and sensitivity analysis

In order to fine-tune the model with historical data, we employed a simple sampling-based approach. The hypothesized ranges for each calibration parameter are detailed in Table 3.2. To comprehensively explore this parameter space, we generated 4096 sample points using a Sobol sequence [227]. For each parameter combination, we ran 10 Monte Carlo simulations, and computed the sum of squared differences between simulated and observed data. To ensure an equal number of data points in the different observational time series, we interpolated linearly the structural data (farmer count, land utilization, farm size), consistent with the observed linear trends. Table 3.2 displays the results. The corresponding R-squared R^2 and adjusted R-squared $\bar{R}^2$ [228] values demonstrate that the model effectively captures the observed dynamics in real data.

	Description	Sampling range	Optimal
α	Price frictions	[0.01, 0.1]	0.08
λ	Yield target adjustment speed	[0.1, 0.5]	0.2
γ	Pesticide adjustment speed	[1.0, 3.5]	3.0
β	Land adjustment speed	[0.4, 0.5]	0.45
η	Profit share for technology	[0.05, 0.5]	0.15
$\mathcal{P}_{\text{ref}}$	Reference profit for technology	[150, 1500]	1000.0
$\nu_{\max}$	Maximum efficiency gain	[0.05, 0.5]	0.10
$\overline{\Delta e}$	Average efficiency gain		0.025
R^2	R-squared		0.719
$\bar{R}^2$	Adjusted R-squared		0.716

Table 3.2 Results of model calibration. The resulting average efficiency gain per year across all farmers $\overline{\Delta e}$ is not a parameter; it is computed from the resulting time series of each simulation.

To assess the model's sensitivity to parameter variations, each calibrated parameter was independently perturbed by ±50%. The resulting impacts on the three key variables, ε_t, $\bar{P}_t$, and $\bar{L}_t$, are illustrated in Fig. 3.5. Our analysis reveals that the land adjustment speed parameter, β, exerts the most significant influence on the model's dynamics, as evidenced by the wide range of variation observed. This substantial influence underscores the critical role of land consolidation phenomena, which are heavily dependent on the value of β. In contrast, the parameters related to technology ($\nu_{\max}$, $\mathcal{P}_{\text{ref}}$, and η) are particularly relevant in determining pesticide adoption rates, while exhibiting a limited impact on biodiversity. This limited impact can be attributed to the high value of μ, which effectively limits the impact of pesticide use on biodiversity evolution. Finally, the adjustment speeds (α, λ, and γ) exhibit less variability, suggesting that they have a relatively minor impact on the system's dynamics. This observed robustness in the model's results, highlighting the minimal impact of specific behavioral details, addresses one of the primary criticisms often leveled against agent-based models [137].

3.6.2 Biodiversity influence on yield

Although it is widely recognized that higher levels of biodiversity contribute to natural pest control and thereby enhance crop productivity, the extent of this effect remains a topic of debate [148–151]. In this section, we examine the consequences of diminishing the impact of biodiversity on crop yield by altering the parameter a in Eq. 3.16. Specifically, by decreasing a, we decrease the dependency of yield on biodiversity, making pest exposure less reliant on it. To evaluate the impact of varying a and compare it to the baseline results, we adjusted the parameter η, which represents the profit share devoted to

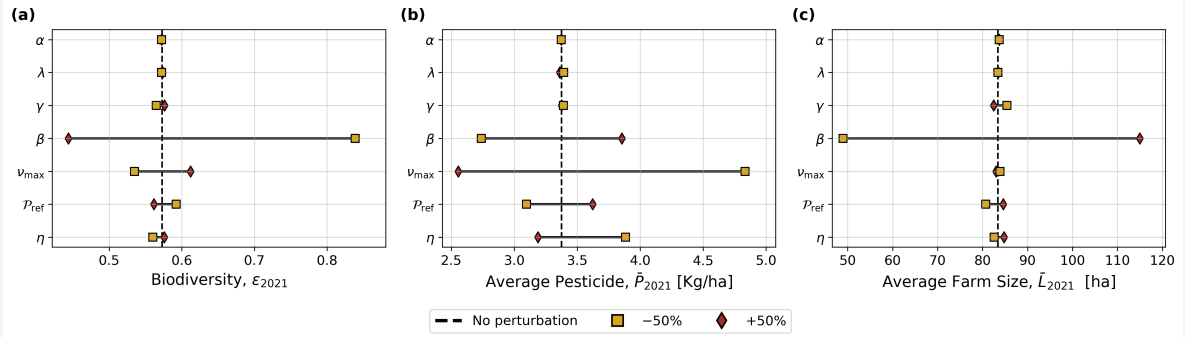


Figure 3.5 Sensitivity analysis for the calibrated parameters (see Table 3.1). This figure shows the variation in three main variables ε_t, $\bar{P}_t$ and $\bar{L}_t$ in the year 2020 when the values in Table 3.1 are independently perturbed by ±50%. As expected, the parameter β, which determines the land speed update, exerts the most significant influence on the dynamics across all variables.

technological improvements. This adjustment reflects the reduced need for pest management investment when pest exposure is lessened. The results are presented in Fig 3.6, in particular for with $a = 0$.

The overall decline in biodiversity remains consistent with the scenario where $a = 0.5$, but the rate of decline is moderated in the absence of the feedback loop. With decreased pest exposure, there is less focus on research and development efforts and a reduced allocation of funds (where $\eta = 0.02$). Consequently, farmers experience increased income, which helps mitigating the land consolidation trend.

3.6.3 Technological advances and sustainable farming

To incorporate the impact of technological progress, particularly advancements that may lead to less sustainable farming practices such as the use of more potent pesticides, we modify Eq. 3.15 by including the technological contribution within the weighted average of pesticide effects:

$$K_{t+1} = \mu \frac{\bar{L}_0}{\bar{L}_{t+1}} + (1-\mu) \frac{\sum_{i=1}^{N_0} L_{i,0} P_{i,0}(e_{i,0})^k}{\sum_{i=1}^{N_0} L_{i,0}} \frac{\sum_{i=1}^{N_{t+1}} L_{i,t}}{\sum_{i=1}^{N_{t+1}} L_{i,t+1} P_{i,t+1}(e_{i,t+1})^k}. \tag{3.18}$$

In this modified framework, when $k = 0$, the previous results are retained. However, for $k > 0$, technological advancements contribute to biodiversity decline. The extreme case of $k = 1$ represents a scenario where technological progress offers no biodiversity benefits. To evaluate the impact of varying k and compare it to the baseline results, we re-estimated the parameter μ to fit historical trends. As shown in Fig 3.7, a higher value of k necessitates a lower μ value, indicating a greater influence of pesticide use on biodiversity decline.

Upon examining forecasted biodiversity, it is evident that increasing k correlates with a general decline in biodiversity, consistent with expectations. Notably, this deterioration is not solely attributed to increased pesticide use but is also exacerbated by heightened land consolidation. As detailed in the main text, the loss of biodiversity disproportionately affects small farmers, who find it challenging to compete with the required technology. These findings suggest that policies supporting small farmers while reducing pesticide use are becoming increasingly critical.

These insights highlight the necessity for a nuanced analysis of efficiency in agricultural systems and the role of green technology adoption by farmers in shaping biodiversity outcomes. However, the interplay of technological adoption, land consolidation, and behavioral dynamics requires a sophisticated approach that considers these multiple factors, as elaborated in [121].

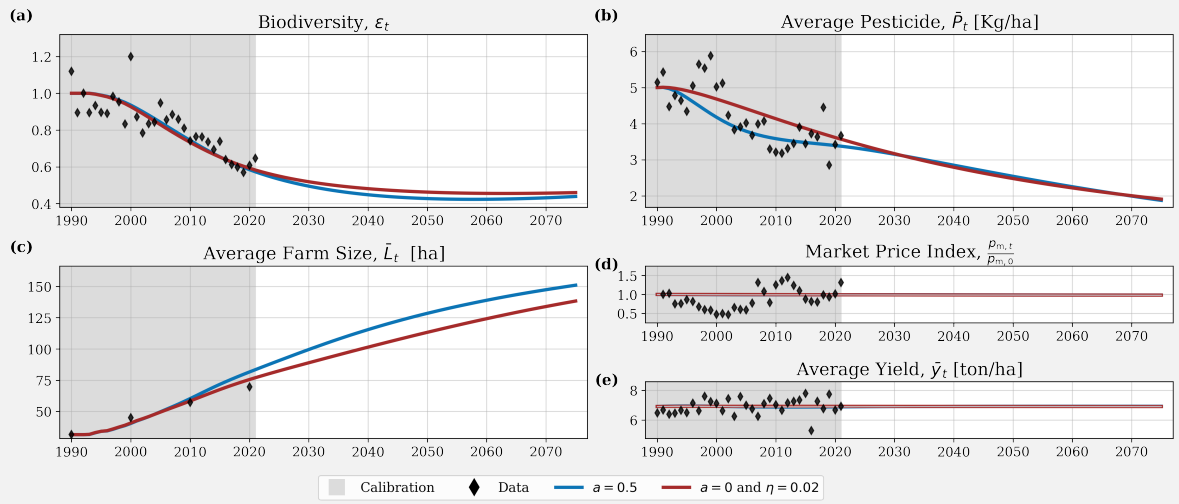


Figure 3.6 Effect of biodiversity on pest exposure and yield. This figure compares model outcomes for two scenarios: (1) the baseline scenario where pest exposure is influenced by biodiversity ($a = 0.5$), and (2) a scenario where pest exposure has no dependency on biodiversity ($a = 0$). The parameter η, controlling the fraction of profit devoted to technology adoption, has been recalibrated to fit historical trends. Results show that reducing the influence of biodiversity on pest control (scenario $a = 0$) leads to reduced land consolidation patterns and thus slows the rate of biodiversity decline. While these results temper the model's conclusions, the overall message remains valid: a policy combining both subsidies and pesticide reduction is necessary to halt biodiversity decline.

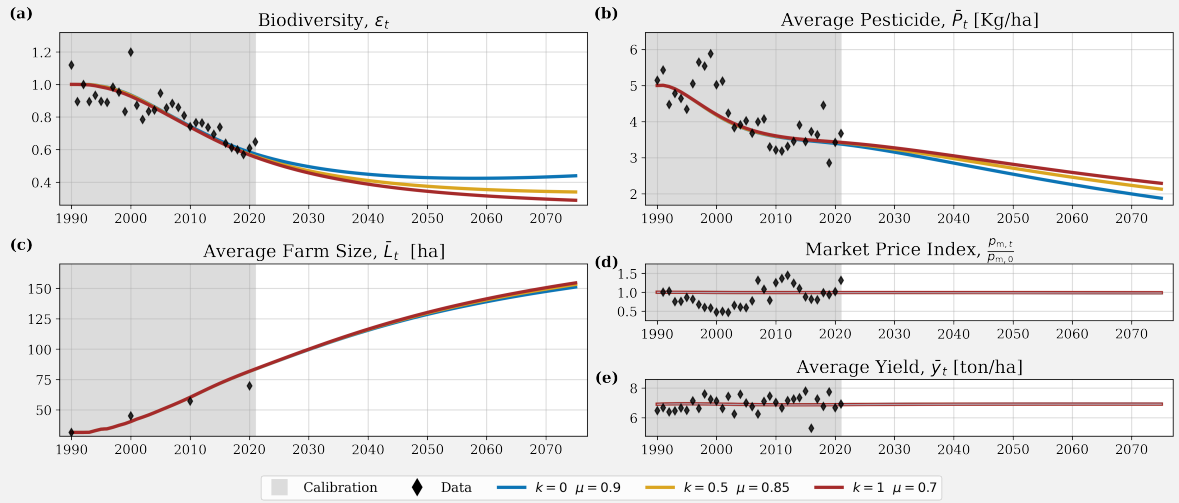


Figure 3.7 Impact of technological advancement on biodiversity decline. This figure illustrates the effects of incorporating technologies that do not contribute to reducing the impact of pesticide use on biodiversity by varying the parameter k. In particular, increasing the parameter k corresponds to neglecting the positive effects of pesticide reduction. The extreme case of $k = 1$ represents a scenario where technological progress offers no biodiversity benefits. For each value of k, we re-estimated the value of μ to fit historical trends. Results show that as k increases, there is a notable acceleration in biodiversity decline. This deterioration is not solely due to increased pesticide use; it is also exacerbated by intensified land consolidation. Indeed, to maintain the same yield, there is an increased reliance on technology, which small farmers often struggle to compete with. This highlights the importance of supporting small farmers while reducing pesticide usage, thereby strengthening the model results.

Key Takeaways

- **A macroscopic bio-economic framework:** We develop an agent-based model incorporating heuristic decision-making grounded in historical data to capture the long-term, macroscopic feedback loops between individual farmer economics and farmland biodiversity.
- **The danger of isolated policies:** Implementing pesticide reductions without economic support accelerates farm consolidation, while subsidies alone fail to reduce chemical pressures, creating severe unintended trade-offs.
- **Synergistic policy design:** A paired approach—mandating pesticide reductions while providing targeted per-farmer subsidies to small operations—effectively breaks the cycle of consolidation and enables rapid biodiversity recovery.

4. An ecological-economic framework for biodiversity and pest management

In the previous chapter, we addressed the problem of farm consolidation and intensification by focusing on the coupled dynamics of farmers' behaviour and ecological responses. However, in the interest of keeping the model simple and transparent, we adopted a spatially implicit framework. While we believe that the results remain qualitatively informative, a spatially explicit representation is a key ingredient for improving our understanding of how biodiversity generates economic value and contributes to the resilience of agricultural systems. For this reason, this chapter presents a model that addresses this gap by developing a spatially explicit ecological economic model that enables us to dissect the complex interplay between landscape structure and pesticide application, and their combined effects on natural enemy populations and farmers' economic returns. In particular, the model investigates how these relationships are modulated by farm size – a crucial aspect frequently overlooked in prior research.

This chapter is structured as follows: we first provide a brief review of the relevant literature, then present the model, and finally discuss the main results and conclusions.

4.1 Literature review

While a wide range of models exists in the literature to describe the interactions between farming activities and biodiversity in an abstract way [88, 102, 106], similar to the model presented in the previous chapter, relatively few provide an explicit representation of a specific ecosystem service and of its contribution to agricultural production. Among such models, pollination is probably the most extensively studied ecosystem service [115, 229, 230]. However, although pollination is essential for fruit and vegetable production, a large share of agricultural land is occupied by arable systems, and in Europe this often means cereal production. For this reason, if the objective is to understand how biodiversity can be preserved and valued across a broader share of farmland, attention must also be given to ecosystem services that are crucial for cereal systems. Among these, pest regulation is particularly important [9, 231, 232].

Pests can generate substantial agronomic and economic damage by reducing crop yields, lowering product quality, and increasing production uncertainty. Historically, natural pest protection—the suppression of pest populations by ecological processes involving predators, parasitoids, pathogens, and other beneficial organisms [231]—provided an important ecosystem service that helped regulate pest outbreaks. However, to further enhance yields and ensure more predictable production, farmers increasingly adopted synthetic pesticides as a complementary

control strategy. While these chemical inputs initially delivered significant protection gains, their extensive and repeated application has directly impacted beneficial insect populations [89, 90]. The unintended consequences of these practices are now becoming increasingly apparent. The reduction in the number of natural enemies of crop pests, coupled with the emergence of pesticide-resistant pest populations, has begun to contribute to a worrying trend of stagnating yields in some agricultural systems [59, 60, 91, 92]. Furthermore, in the face of ongoing climate change, many scientific projections suggest that the vulnerability of these simplified and chemically reliant agricultural systems will likely be exacerbated, potentially leading to further ecological and economic instability if current farming practices persist [9]. This creates a fundamental challenge: how to reconcile effective pest protection with sustainable farm income while restoring the natural enemies that once provided this service.

A substantial body of work has addressed this issue by focusing either on management practices or on pest dynamics. In particular, on the ecological side, many existing models either employ a spatially explicit description while overlooking farm management practices [233] or utilize Lotka-Volterra models for pest control while neglecting landscape configuration [234]. Against this background, our model explicitly integrates both the spatial arrangement of diverse land cover types and the influence of management practices. On the economic side, economic modeling has examined the design and effectiveness of agri-environmental incentives, investigating how payment schemes can be structured to encourage biodiversity-friendly pest management while maintaining profitability [235–237]. However, most of these contributions adopt a highly abstract representation of the distribution and abundance of natural enemies, especially in response to the proposed policies. Neglecting these ecological feedbacks may weaken the analysis, as policy outcomes depend not only on farmers' behavioural responses but also on how ecological communities react over space and time.

More specifically, compared with the limited number of studies that adopt an integrated approach, in the spirit of the framework outlined in the introduction, to study pest management [238, 239], we offer a more mechanistic understanding of these relationships by adopting a parsimonious approach that strategically focuses on the key factors influencing natural enemy abundance. In addition, another distinctive feature of our model is its explicit consideration of farm size heterogeneity. Farms of different scales exhibit distinct landscape configurations [87], management practices [240], and economic objectives [241]. In the European context, larger farms typically feature larger fields [242], fewer semi-natural elements [243], and higher pesticide usage compared to their smaller counterparts. This trend is driven by the pursuit of operational efficiency, which encourages the consolidation of fields and the removal of landscape features such as hedgerows and natural vegetation that can impede large-scale mechanization. At the same time, their capital availability allows them to make more intensive use of chemical inputs, to further increase their economic returns. Consequently, large farms tend to sustain lower levels of biodiversity but achieve higher profits relative to small farms. This relationship is supported both by empirical studies [244–246] and by aggregated European data (see Fig.4.2, left panel). Recognizing and accounting for these differences is therefore crucial for accurately assessing the impacts of agricultural policies.

Accordingly, our study addresses two central questions: (i) Which combinations of policy instruments most effectively halt the decline of natural enemies and other beneficial arthropods across different farm sizes? (ii) Under what spatial and management conditions can such policies be implemented to maintain or enhance economic viability?

4.2 Model and methods

4.2.1 Model overview

We formulate a spatially explicit model that describes the abundance of predatory arthropods and its relationship with farmers' income (Fig. 4.1). The model operates on a discrete spatial representation of the farmland landscape, conceptualized as a square periodic lattice. Each cell within this lattice represents a specific land-cover type, which can be either cropland, hedgerow, or permanent grassland. The spatial arrangement and proportion of these land-cover elements are based on farm size, reflecting the observed tendency for farms of different scales to exhibit distinct landscape characteristics. Indeed, larger farms often feature larger fields and a lower proportion of semi-natural habitat (SNH) than do smaller farms [87, 244–246]. Throughout the study, we use farm size—measured as total utilized agricultural area—as a proxy for economic size, given their strong correlation in our study context (see Supplementary Material for details).

Our model provides a simplified description of flying generalist natural enemies (NE) (*i.e.*, ladybirds) feeding on herbivorous insect pests (*i.e.*, aphids) in annual crop systems (*i.e.*, winter wheat). The dynamics of natural enemy abundance within this spatially defined landscape are modeled using a seasonal logistic growth framework. This ecological component explicitly incorporates the impact of both pesticide application and the landscape on the availability of overwintering sites, food resources, and mortality rates induced by pesticide exposure.

The abundance of predatory arthropods is then used to derive farmers' yield in conjunction with pesticide use. This establishes a direct pathway through which ecological factors influence the economic performance of farming operations. All other economic data required for the calculation of farmers' income, such as crop prices, operational costs, subsidies, and labor input, are incorporated as exogenous variables derived from the European Farm Accountancy Data Network (FADN), providing an empirical basis for the economic simulations.

We then use the model to study how the spatial configuration of the agricultural landscape, in combination with different pesticide use regimes, impacts both the abundance of beneficial predatory arthropods and the resulting economic outcomes for farmers. Specifically, we construct a series of policy scenarios by systematically varying one or more exogenous model parameters—such as pesticide use intensity or landscape composition—representing distinct policy or management interventions (*e.g.*, pesticide reduction programs or landscape diversification schemes). Because these variations are imposed exogenously, and farmers' behavior is not adjusted in response to policy implementation, our analysis does not aim to optimize individual management strategies. Instead, it focuses on exploring how different policies interact and generate varying ecological and economic outcomes across farms of different sizes. In what follows, we provide detailed descriptions of the individual components of the model, including the process of landscape construction, the ecological model of natural enemy dynamics, and the economic model used to assess farmers' income.

4.2.2 Landscape construction

The landscape consists of a two-dimensional lattice (200×200 cells), in which each cell represents an area of 10m $\times$ 10m and can be in one of two states: cropland or SNH. To determine the allocation of each cell, we begin by assuming that the entire landscape is covered with cropland and then assign each cell to a unique field using a Voronoi tessellation, a method widely employed for creating semi-realistic field distributions [247]. For clarity, let us stress that in the

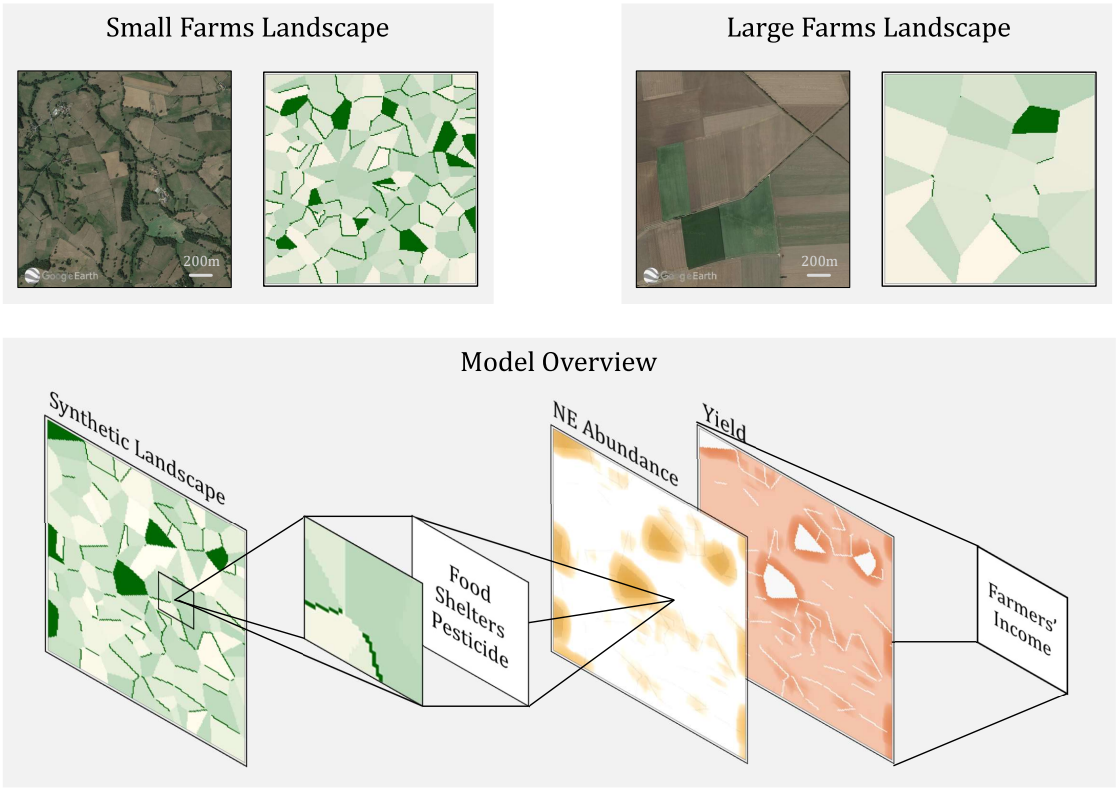


Figure 4.1 Conceptual scheme illustrating the landscape representation and the factors influencing natural enemy (NE) abundance, yield and farmers' income. The top panel shows how our synthetic landscape mimics the characteristics of real agricultural landscapes. Specifically, the left satellite imagery represents a typical small-farm landscape from the South of France near Limoges, while the right imagery depicts a characteristic large-farm landscape from Central Germany near Leipzig. The bottom panel visualizes the process by which we derive natural enemy abundance and farmers' income from a given landscape. As highlighted in the expanded view, the natural enemy (NE) abundance in each individual cell of the landscape grid is determined by considering the conditions within the typical movement range of such arthropods. Specifically, for each cell, we assess the spatial distribution of available food resources, the presence of shelters, and the intensity of pesticide application within that defined movement radius. The combined influence of these factors determines the resulting spatial pattern of NE abundance, visualized in the "NE Abundance" layer, where darker orange signifies higher concentrations. The NE abundance, in conjunction with pesticide use, subsequently influences crop yield, which ultimately contributes to the computation of farmers' income.

following discussion, "cells" always refer to individual "pixels", whereas the larger Voronoi cells that comprise multiple pixels will be referred to as "fields". The pattern generation is

controlled by a parameter describing the desired mean field size (see Supplementary Material for more details).

We then assign SNH by converting some cells into either permanent grassland or hedgerows. A key constraint in the placement of hedgerows is that they are exclusively located along the margins of the previously defined crop fields, reflecting their typical occurrence in real agricultural landscapes. The allocation of grassland and hedgerows is managed by an iterative algorithm. In each iteration, the entire area or a portion of a field (or field margin) is converted into the designated SNH type. This process continues until the total area converted to grassland and hedgerows reaches gA and hA, respectively, where A is the total landscape area, g is the grassland share, and h is the hedgerows share. Although g and h are adjustable parameters, when analyzing landscapes with a specific farm size, we can define them as functions of that size, a relationship strongly supported by existing research and data (see Fig. 4.2 and Supplementary Material for more details).

4.2.3 Natural enemies' abundance

While pest dynamics are only implicit, our model provides an explicit description of the NE lifecycle, distinguishing between summer and winter.

During the summer, NE disperse from their overwintering locations and colonize cereal fields in search for food. The abundance of NE in each grid cell is modeled using logistic growth, incorporating food availability and pesticide-related mortality in the patch and its surroundings:

$$\frac{dN_i}{dt} = rN_i\left(1 - \frac{N_i}{k_i}\right) - N_i m_i \tag{4.1}$$

where r is the reproduction rate, k_i is the carrying capacity, and m_i is an extra-mortality rate due to pesticide use. One unit of time t corresponds to one day during the growing season, which we assume extends for six months.

We define the carrying capacity (k_i) based on the availability of food resources, specifically herbivorous insects, which is influenced by both pesticide use and land cover type. This relationship is expressed by the following equation:

$$k_i = \sum_j \gamma_{ij}\kappa_j \quad \text{where} \quad \kappa_j = \begin{cases} \kappa_{\text{SN}} & \text{if } \tau_j = \text{SN}, \\ \kappa_{\text{C}} \cdot \mathcal{F}\left[\dfrac{\pi_j}{\pi_{\text{ref}}}\right] & \text{if } \tau_j = \text{C}. \end{cases} \tag{4.2}$$

Here, κ_{SN} and κ_{C} represent the maximum predatory arthropod density (number per cell) in the absence of pesticide application for SNH and cropland (C), respectively. The function $\mathcal{F}$ is defined as $\mathcal{F}\left[\frac{x}{y}\right] \equiv \frac{1}{1+\frac{x}{y}}$, and π_j represents the amount of pesticide applied to patch j. In particular, we assume that pesticide application occurs uniformly and exclusively on cropland patches, thereby neglecting potential drift effects into SNH. Finally, γ is a distance-decay function which represents the movement range of NE over a year. Specifically, we employed a Heaviside step function as a computationally efficient approximation of an exponential decay, which is consistent with both theoretical and empirical estimations [233, 248, 249]. We set:

$$\gamma_{i,j} = \begin{cases} 1 & \text{if} \quad d_{i,j} \leq D \\ 0 & \text{if} \quad d_{i,j} > D \end{cases} \tag{4.3}$$

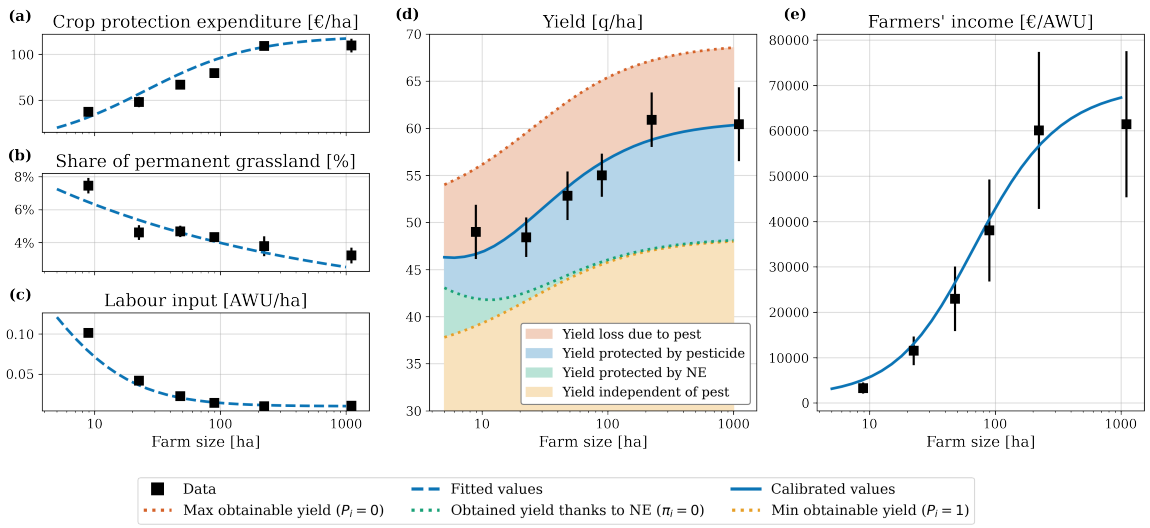


Figure 4.2 This figure illustrates the calibration of our model's parameters using aggregated agricultural data from the European Farm Accountancy Data Network (FADN) for the EU-27 region, averaged over the years 2018-2022 [152]. Black squares represent the weighted average of the observed data across this period, with error bars indicating the standard deviation of year-on-year variation. These data highlight consistent patterns across farm size for different year and regions, including increased reliance on synthetic inputs, a reduced share of grassland, and higher income for large farms relative to small ones. The parameterization process differed based on the variable's dependence on ecological dynamics. For variables independent of these dynamics (examples shown in the left panel), we employed a fitting procedure. Conversely, for variables directly influenced by ecological dynamics (examples in the central and right panels), we utilized a calibration process that minimized a quadratic loss function (further details on the calibration and additional data not displayed here are available in the Supplementary Materials). The central panel, depicting yield, provides a decomposed view: the maximum obtainable yield ($P_i = 0$ in Eq. 4.7), the yield protected by natural enemies ($\pi_i = 0$ in Eq. 4.8), and the minimum obtainable yield ($P_i = 1$ in Eq. 4.7). This disaggregation highlights that smaller farms tend to benefit more significantly from natural pest protection, while larger farms appear to rely predominantly on synthetic inputs for pest protection.

where $d_{i,j}$ represents the distance between cells i and j, and D is the parameter defining the typical annual movement range of natural enemies.

The additional mortality experienced by arthropods in patch i due to pesticide exposure is a function of the total amount of pesticide applied within its movement kernel, γ. Specifically:

$$m_i = \mu_\pi \cdot \mathcal{F}\left[\frac{\pi_{\text{ref}}}{\sum_j \gamma_{ij}\pi_j}\right] \tag{4.4}$$

where $\mu_\pi = (1-q)r$ is the induced mortality rate, and the parameter q modulates the selectivity of the pesticide application in affecting NE or pest population only. A higher q indicates greater selectivity, meaning pesticides have a stronger negative impact on pests relative to their natural

predators, because the effect on the carrying capacity in Eq. 4.2 is more pronounced than the increase in the extra-mortality rate in Eq. 4.4. Conversely, a lower q suggests that the pesticide is less selective, affecting both natural enemies and herbivorous arthropods.

As the season progresses and temperatures begin to drop, NE start to prepare for hibernation, seeking shelters to overwinter. The presence of SNH determines the success of this process [250]. If SNH are not large enough, a portion of the population will die, as implicitly expressed by the equation:

$$N_i(\text{end of winter}) = (1 - s_i)N_i(\text{end of summer}) \tag{4.5}$$

where s_i is the survival rate that depends on the presence of semi-natural habitats:

$$s_i = \mathcal{F}\left[\frac{\text{sn}_{\text{ref}}}{\text{sn}_i}\right] \quad \text{where} \quad \text{sn}_i = \sum_j \gamma_{ij} \cdot \delta(\tau_j = \text{SN}) \tag{4.6}$$

4.2.4 Farmers' economic performance

Given that policy scenarios are specified exogenously in our model, the economic component primarily serves to connect natural enemy abundance with resulting yield and income. The production function employed is a simplified variant of the Mitcherliche-Baul production function, which is commonly referenced in agricultural economics literature [153]. Likewise, the calculation of income effects follows a streamlined version of the economic accounting methodology utilized in FADN reporting [152, 251]. In particular, to compute farmers' yield, we do not consider within-year dynamics but focus on the amount of crop biomass produced annually (y_i), *i.e.*, annual crop yield. In our model, y_i is not represented by a differential equation, as crops are harvested each year and their dynamics do not depend on the previous state. But y_i depends on the amount of pesticide used and the abundance of NE, as represented by the following equation:

$$y_i = \left(y_0 + y_1 \mathcal{F}\left[\frac{L}{L_{\text{ref},y}}\right]\right)(1 - \eta P_i) \tag{4.7}$$

In this equation first contribution represents the maximum potential yield while the second describes the yield loss due to pest exposure. In the first term, y_0 represents the baseline yield achievable in the absence of intensification practices (such as in organic farming [252]) and y_1 represents the increase in yield resulting from the use of fertilizer, which increases with farm size L [253]. In the second term, η represents the maximum loss fraction due to pest damage, and P_i is the pest damage.

To determine pest damage, we consider the impact of pesticide and NE according to:

$$P_i = 1 - \mathcal{F}\left[\frac{\pi_{\text{ref}}}{\pi_i}\right] - \frac{N_i}{\kappa_{\text{C}}} = \mathcal{F}\left[\frac{\pi_i}{\pi_{\text{ref}}}\right] - \frac{N_i}{\kappa_{\text{C}}} \tag{4.8}$$

where N_i represents NE abundance at the end of the summer and π_i depends on farm size according to $\pi_i = \pi_0 \mathcal{F}\left[\frac{L_{\text{ref},\pi}}{L}\right]$. Here, we assume that an increase in either the presence of natural enemies or pesticide application leads to higher yields. It is important to note that, within our framework, the elasticity of substitution cannot be derived analytically, since pesticides and natural enemies are intrinsically interdependent inputs. Changes in pesticide use directly influence natural enemy populations, and the reverse also holds. However, in the Results section, we estimate this elasticity numerically.

Farmers' profit is then given by:

$$\mathcal{P} = pL_{\text{prod}}\bar{y} - C + L\mathcal{S} \tag{4.9}$$

where p is crop price, C operational costs, $\mathcal{S}$ subsidies per hectare, and $L_{\text{prod}} = L - gL - hL$ is the area dedicated to crops. Operational costs increase proportionally to the total land area, including land dedicated to ecological purposes, which requires maintenance:

$$C = (C_0 + \pi)\, L_{\text{prod}} + C_{\text{g}} Lg + C_{\text{h}} Lh \tag{4.10}$$

where C_0 are operational costs per hectare including fuel, fertilizer, and depreciation of machinery; and C_{g} and C_{h} are maintenance costs per hectare for hedgerows and grassland, respectively.

A good proxy for farmers' income, consistent with European institutional practices, can then be computed as the ratio between total profits $\mathcal{P}$ and labor input $\mathcal{L}$ [254]:

$$\mathcal{I} = \frac{\mathcal{P}}{\mathcal{L}} \tag{4.11}$$

where $\mathcal{L}$ decreases with farm size L, reflecting improved management efficiency, and field size S due to the use of larger machinery:

$$\mathcal{L} = L_{\text{prod}} \left(\ell_0 + \ell_1 \mathcal{F}\left[\frac{L_{\text{prod}}}{L_{\text{ref},\mathcal{L}}}\right] \mathcal{F}\left[\frac{S}{S_{\text{ref}}}\right] \right) \tag{4.12}$$

4.2.5 Parameter specification

The model parameters were specified through a combination of data-driven estimation, calibration against observed agricultural performance, and fixed values set to explore different scenarios.

Ecological parameters, such as natural enemy reproduction (r), carrying capacities ($\kappa_{\text{SN}}, \kappa_{\text{C}}$), and dispersal distance (D), were primarily estimated using empirical information and commonly-assigned values found in the literature [115, 238, 255, 256]. However, for some of the parameters for which the literature does not provide a single value, such as pesticide application selectivity (q) or winter survival (sn_{ref}), we adopted reasonable starting values and subsequently performed sensitivity analyses (detailed in the Supplementary Materials) to evaluate their influence on the results, given their inherent context specificity and complexity.

Economic parameters were determined using 2018-2022 EU-27 average data from the European Farm Accountancy Data Network (FADN) [152]. This allowed us to capture trends across farm sizes and countries. Parameters independent of ecological dynamics (as crop prices p, operational costs C_0, subsidies $\mathcal{S}$, and labor input $\mathcal{L}$), were fitted directly to the FADN data. Parameters affecting crop yield ($y_0, y_1, L_{\text{ref},y}, \pi_{\text{ref}}$) were calibrated to reproduce the observed trends in yield, economic outputs, and farmers' income (with some shown in Fig. 4.2 and the complete list of economic outputs available in the Supplementary Materials).

4.2.6 Computational implementation

We conducted extensive numerical simulations to explore various policy scenarios. For each simulation, the abundance of NE was computed over an initial equilibration period of 10 years to ensure the system reached a stable stationary state. NE abundance reported below corresponds

to NE abundance at the end of the summer season, after the equilibration period. Once NE abundance stabilized, we used it to derive all relevant economic variables.

The results presented below are averages across 100 simulations. Relative standard errors were omitted from figures due to their negligible magnitude (smaller than the line width). It is important to note that our analysis did not incorporate stochasticity in either the ecological or economic components of the model; therefore, the minor variations observed between simulations arose solely from the inherent variability among the randomly generated landscape configurations.

4.3 Results

4.3.1 Landscape structure, pesticide use, and natural enemy abundance

We first examine the relationship between natural enemy (NE) abundance, landscape structure, and crop protection expenditure, which serves as an indicator of pesticide use intensity. As expected, increased pesticide use consistently leads to a reduction in NE populations across all landscape scenarios and field sizes examined (Fig. 4.3). This underscores the significant negative impact of pesticides on the decline of predatory arthropod populations [89, 257].

However, the relative effectiveness of different SNH spatial arrangements in supporting NEs is contingent upon the level of crop protection expenditure. This is because two distinct, spatially explicit mechanisms contribute simultaneously to the result. The first is resource provision, whereby SNH positively contributes to the local carrying capacity (k_i) and provides essential overwintering refugia (s_i) locally within an NE's typical movement kernel (γ_{ij}). The second mechanism is pesticide exposure, where the spatial placement of SNH relative to cropland determines the NE's exposure to pesticides and its resulting mortality rate (m_i).

When SNH is fragmented into linear elements like hedgerows, the landscape has a high edge-to-area ratio. This means many SNH cells fall within the typical movement radius (D) of NEs located in adjacent crop cells. This fragmentation maximizes the resource provision mechanism. In practical terms, the numerous, spatially distributed shelters provide consistent NE spillover into crop fields during the growing season (boosting k_i) and also reduce winter mortality by ensuring refugia are accessible within the NE's typical dispersal range (boosting s_i).

By contrast, when SNH is consolidated into fewer, larger grassland patches, it minimize the pesticide exposure mechanism. These patches act as concentrated refuges. Since pesticides are (by assumption) applied only to cropland, NEs within these large grasslands are shielded from direct exposure, which lowers the mortality term (m_i). These refuge zones can then serve as reservoirs for recolonizing adjacent fields. The effectiveness of this, however, decays with distance: if a crop cell is too far from the grassland patch (beyond radius D), it receives little to no NE spillover (see the different crop protection level below).

These contrasting effects explain the pesticide-dependent switch observed in Fig. 4.3. Under low pesticide pressure, the primary limiting factor is overwinter sheltering for a prosperous population, making the widespread, proximate refugia of fragmented hedgerows superior as they boost k_i and s_i across more of the cropland. Under high pesticide pressure, the primary limiting factor is survival. Here, mortality (m_i) near crop fields becomes too high, making the

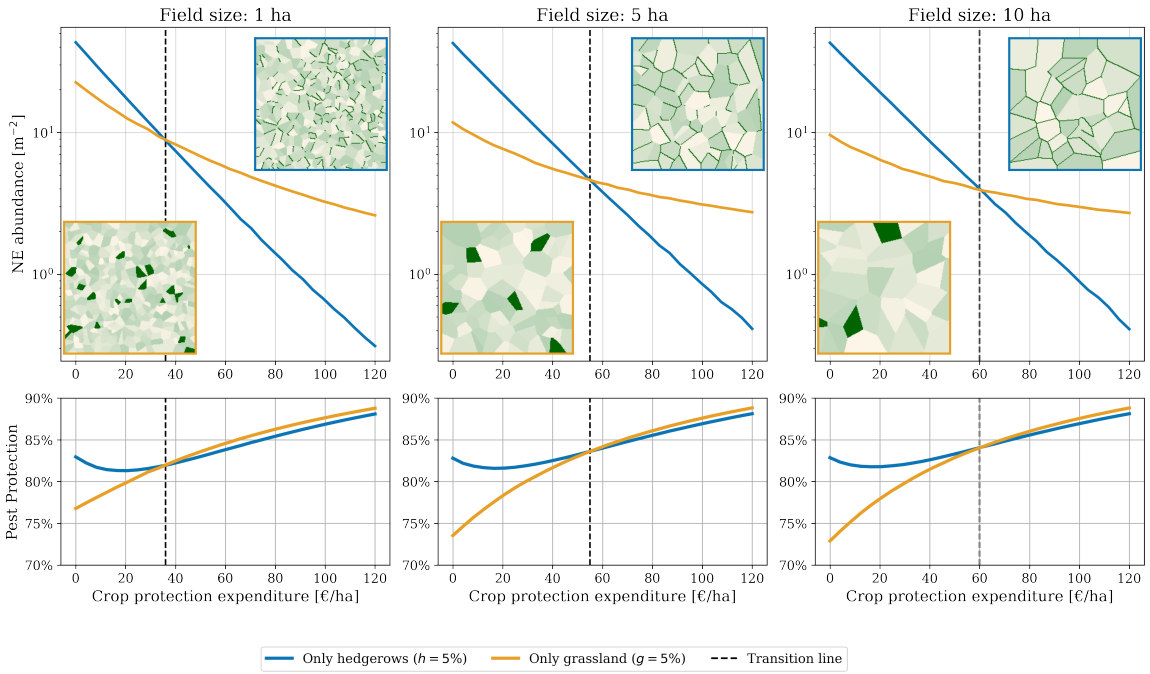


Figure 4.3 Influence of landscape structure and crop protection expenditure on natural enemy (NE) abundance and total pest protection across different field sizes. The top panel illustrates the simulated impact of crop protection expenditure (€/ha), serving as a proxy for pesticide use intensity, on natural enemy abundance (NE abundance [m^{-2}]) across three different field sizes: 1 hectare (ha), 5 ha, and 10 ha. Within each panel, two distinct landscape scenarios are compared: a landscape with 5% coverage of semi-natural habitat (SNH) composed solely of hedgerows (blue line), and a landscape with 5% coverage of SNH composed solely of permanent grassland patches (orange line). Representative spatial configurations of these two SNH types within each field size are depicted as insets within each panel. The figure demonstrate a general trend of decreasing NE abundance with increasing crop protection expenditure across all field sizes and SNH compositions, highlighting the negative impact of pesticide use. However, the relative effectiveness of different SNH compositions in sustaining NE abundance varies depending on both the intensity of crop protection and the average field size. At low levels of crop protection expenditure, landscapes with a higher proportion of hedgerows generally support greater NE abundance. Conversely, at higher levels of crop protection expenditure, landscapes with a higher proportion of permanent grassland tend to maintain relatively higher NE abundance.

large, consolidated grassland patches superior because they provide a refuge zones to sustain an NE reservoir, even if it is more distant.

Average field size shifts this balance. Larger fields inherently increase the average distance from an interior crop cell to the nearest SNH. Because hedgerows are located at field margins, they remain accessible (within radius D) to a larger fraction of the crop cells than a few, large grassland patches. Therefore, as field size increases, hedgerows retain their advantage even under higher pesticide pressure. This pushes the transition point (the vertical dashed line in

Fig. 4.3)—at which grasslands become the more beneficial strategy—toward even higher levels of pesticide expenditure.

The bottom panels of Fig. 4.3 highlight the degree to which natural enemies (NE) and synthetic pesticides act as partially substitutable, yet also antagonistic, inputs in pest control. At zero crop protection expenditure—where pest suppression relies entirely on biological control—the fragmented, hedgerow-dominated landscape (blue line) achieves substantially higher pest protection, measured as $1 - \eta\mathcal{P}$, ($\approx 82\%$), than the grassland-dominated landscape ($\approx 73\%$), directly reflecting its larger NE population (top panels). Interestingly, as pesticide use begins to increase in the hedgerow scenario, total pest protection initially declines. This counterintuitive effect arises because the chemical gain from low pesticide doses fails to offset the rapid, pesticide-induced loss of the highly effective NE population. In such settings, ecological restoration and input reduction can act synergistically (see next section). In contrast, the grassland landscape exhibits a steady increase in pest protection once pesticides are introduced, as its smaller initial NE population entails less biological control to lose. At high pesticide expenditures, chemical control becomes dominant. In this regime, pesticides effectively replace the suppressed NE populations in both landscape types, leading to similar overall protection levels ($\approx 88-89\%$). Note that, within our calibration, the maximum level of pest suppression achieved through chemical control exceeds that attained under purely biological regulation. A detailed discussion comparing these simulated pest suppression efficiencies to empirical findings from the literature is provided in the Discussion section. However, the fact that our model reproduces comparable yield variations across different policy scenarios lends confidence that the resulting input substitutability is consistent with real-world dynamics (see Discussion section).

Finally, field size also plays a crucial role in shaping this substitutability. In landscapes composed of small fields, grasslands and hedgerows tend to function similarly; however, for larger fields, the distinction between these habitat types becomes much more pronounced. This pattern arises from the spillover effects of semi-natural habitats (SNH) into adjacent crops. In agricultural systems with large fields and concentrated landscape features, the effectiveness of natural enemies in replacing pesticides is notably constrained—many areas within the crop interior fall beyond the dispersal range of natural enemies, resulting in minimal spillover from semi-natural refuges. Overall, as illustrated in Fig. 4.3, our results indicate that pesticides and natural enemies are neither perfect substitutes nor independent means of pest control. Their combined efficacy depends strongly on specific context, influenced by the nonlinear dynamics described in Eq. 4.8, the spatial arrangement of semi-natural habitats, and especially the prevailing field size within the landscape. In the following section, we illustrate how this context dependency can inform the development of tailored policy scenarios.

4.3.2 Policy impacts on yield and income across farm sizes

We now examine the potential effects of different policy interventions on NE abundance, crop yield, and farmers' income as a function of farm size, taking into account the structural differences that farm size imposes (large farms typically exhibit higher pesticide use and less SNH than do small farms). Fig 4.4 shows the percentage change in these three key variables under different policy scenarios: no pesticide reduction, a 50% pesticide reduction, and a complete cessation of pesticide use, each combined with either no change in SNH or a 1% increase in either hedgerow or grassland share.

No Pesticide Reduction: In this baseline scenario, adding hedgerows enhances NE abundance



Figure 4.4 Impact of pesticide reduction and semi-natural habitat (SNH) restoration policies on natural enemy (NE) abundance, production, and farmers' income across different farm sizes. The figure displays the percentage change in NE abundance (left column), production (center column), and farmers' income (right column) relative to a baseline scenario under three distinct pesticide reduction levels: no reduction ($\Delta\pi = -0\%$, top row), a 50% reduction ($\Delta\pi = -50\%$, middle row), and a complete cessation of pesticide use ($\Delta\pi = -100\%$, bottom row). Within each row, results are shown for two farm sizes: a small farm (10 ha) and a large farm (1000 ha). For each pesticide reduction level and farm size, three different SNH restoration policies are compared: no change in SNH ($\Delta h = \Delta g = 0$, solid bars), a 1% increase in hedgerow cover ($\Delta h = +0.01, \Delta g = 0$, dashed bars), and a 1% increase in permanent grassland cover ($\Delta h = 0, \Delta g = +0.01$, dotted bars). Without any pesticide reduction, increasing hedgerows leads to a more substantial increase in NE abundance for small farms compared to increasing grasslands, while the opposite is true for large farms. By reducing pesticide reliance, NE abundance increases significantly for both farm sizes, leading to a positive income change for small farms while large farms still suffer from negative income variation. Moreover, hedgerow restoration appears to be the most effective strategy for minimizing income losses under a zero-pesticide regime across all farm sizes.

more for small farms, while adding grasslands is more impactful for large farms. This directly reflects the mechanisms previously discussed. Small farms, already using low levels of pesticides, are in the 'low-pressure' regime where the resource provision (shelter and food) from fragmented hedgerows is the most effective strategy. Conversely, large farms, with their high pesticide use (see Fig. 4.2), are in the 'high-pressure' regime. For them, the exposure avoidance provided by large grassland refuge zones is the more beneficial strategy. Notably, neither SNH increase

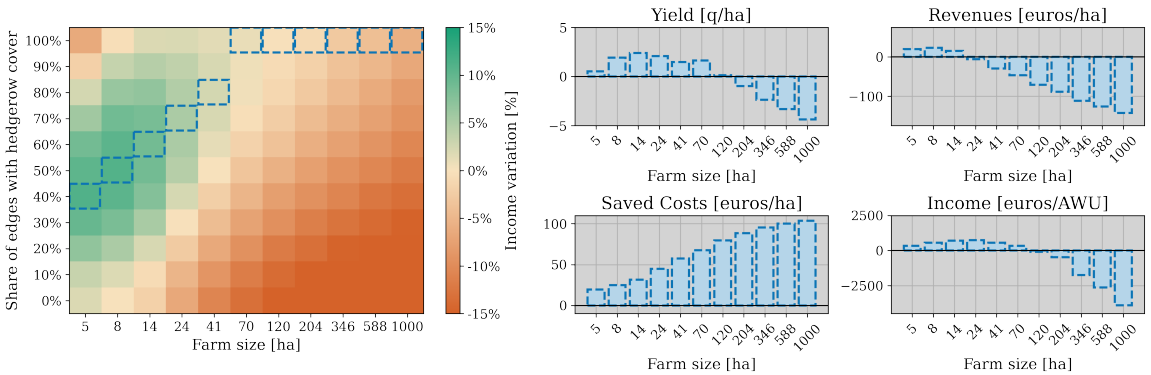


Figure 4.5 Economic impact of transitioning to a zero-pesticide policy combined with varying hedgerow shares across a spectrum of farm sizes. The heatmap on the left illustrates the percentage variation in farmers' income relative to the baseline scenario (current pesticide use and semi-natural habitat levels) as a function of farm size (x-axis, logarithmic scale in hectares) and hedgerow share (y-axis, proportion of total field edges covered by hedgerows). The dashed blue lines highlight regions of maximum income variation, each for a single farm size. The panels on the right provide a more detailed breakdown of the changes in yield (q/ha), revenues (€/ha), saved pesticide costs (€/ha), and income (€/AWU) under the optimal hedgerow share for each farm size. The figure demonstrates that ecological intensification through a zero-pesticide policy and optimized hedgerow restoration can be economically beneficial for small to medium-sized farms. However, for large farms, while pesticide cost savings are substantial, they are insufficient to compensate for the potential revenue losses associated with slightly reduced yields in the absence of synthetic pesticides, highlighting the challenges of directly translating ecological benefits into economic gains at larger agricultural scales.

policy leads to a net yield or income increase for either farm size. In large farms, while increased NE abundance from grassland expansion boosts yield, this does not compensate for the reduced area of arable land, resulting in decreased total production and consequently, lower income. In small farms, although there is a small overall increase in NE abundance from hedgerow restoration leading to a higher yield (due to greater spillover effects than in grasslands), the added management costs associated with habitat restoration outweigh the production gains, leading to a net income decrease.

50% Pesticide Reduction: With a 50% reduction in pesticide use, the patterns of NE abundance remain similar: hedgerow expansion benefits small farms more, and grassland expansion benefits large farms more. This suggests that even at 50% of their baseline, large farms' pesticide use is still high enough to be in the 'high-pressure' regime, where the exposure avoidance from grasslands remains the dominant ecological factor. The income implications, however, diverge. Small farms experience an increase in income under all policy scenarios. This is primarily attributed to the cost savings resulting from reduced pesticide expenditure and the ability of NEs to partially substitute pesticide in the low pressure regime. Indeed, total production decrases in all three scenarios. Among the strategies, maintaining the current SNH levels (no hedgerow or grassland restoration) proves most beneficial for small farmers' income, as

the added management costs of habitat restoration offset the yield benefits as the SNH level can already sustain an enough high enought NEs population. For large farms, none of the considered policies results in a net income increase. Indeed, the enhanced NE abundance does not fully compensate for the reduced pest control from synthetic inputs (low substituitability in the high pressure regime), resulting in lower yields that impact profits more significantly than the saved pesticide costs.

No Pesticide Application: Under a complete cessation of pesticide use, a critical mechanism flip occurs. With chemical inputs removed entirely, the exposure avoidance function of grasslands becomes irrelevant. The entire system becomes limited purely by resource provision (overwintering shelter and spillover into crops). As a result, increasing hedgerows emerges as the most effective strategy to support NE populations and preserve yield for both farm sizes. This highlights the fundamental role of linear, fragmented features when chemical pest control is eliminated. For small farms, production levels even surpass those of the baseline scenario. Here, the yield gains derived from enhanced biological pest protection—enabled by higher NE abundance in the absence of pesticide pressure—offset the slight land loss associated with hedgerow restoration. In contrast, large farms do not experience such benefits: their production remains substantially below baseline levels. Their landscape configuration, characterized by large fields and relatively higher grassland cover, inherently restricts NE spillover into crops and thus limits the capacity to fully replace chemical control with biological regulation. This result raises an important question: can large-field agricultural systems achieve ecological–economic outcomes comparable to small-field systems, or are they intrinsically constrained by their spatial structure?

4.3.3 Economic potential of natural pest protection without pesticides

Building upon the previous finding that hedgerow restoration combined with zero pesticide use can enhance the economic performance of small farmers, we now investigate the potential for large farms to substitute synthetic inputs with natural processes without reducing their income. Specifically, we explore the optimal hedgerow restoration policy required to maximize economic performance under a zero-pesticide regime across the spectrum of farm sizes.

Fig 4.5 illustrates the variation in income resulting from a shift from current practices (current pesticide use and SNH levels) to a zero-pesticide policy combined with varying proportions of hedgerows across different farm sizes. The most substantial positive income variations are evident for small to medium-sized farms, indicating that ecological restoration offers a more economically advantageous pathway than reliance on synthetic inputs at these scales. The combination of increased yield and cost savings (reduced pesticide expenditure minus management costs for increased hedgerows) contributes to an income increase ranging from 5% for 50ha farms to 15% for 5ha farms.

For large farms, while a shift to a zero-pesticide policy with hedgerow restoration does not lead to a net benefit, the relative income decrease remains modest, at approximately -5%. Such limited negative impact is primarily due to the significant cost savings that result from eliminating pesticide use, which partially offset the revenue loss due to lower yields. The latter can be attributed to the increase in NE abundance not fully compensating for the pest control efficacy previously provided by pesticides. This, in turn, is largely because large farms with larger fields inherently have a smaller proportion of edge habitat relative to their total area, limiting the potential for natural pest control to achieve the same level of effectiveness as in landscapes with smaller fields.

4.4 Discussion

The need for a more integrative understanding of pest management in agricultural landscapes stems from the increasing recognition of the ecological costs and sustainability challenges associated with conventional, input intensive farming practices [86, 258]. While the impact of pesticides on biodiversity and ecosystem services is well documented [89, 90], the complex spatial dynamics governing pest and natural enemy interactions, particularly in relation to the configuration of semi-natural habitats, are often overlooked or simplified in existing models. To address this critical gap, our study introduces a novel ecological perspective by employing a parsimonious yet spatially explicit model that links natural pest control to both pesticide application intensity and the spatial arrangement of different land cover types, particularly cropland and SNH. This allows us to provide a more realistic and context-dependent understanding of natural enemy abundance and its potential for pest control across varying farm sizes and policy scenarios.

The insights derived from this spatially explicit modeling approach highlight the importance of considering farm size as a critical factor in the design and implementation of agri-environmental policies aimed at promoting biodiversity and reducing reliance on synthetic inputs. Indeed, the contrasting responses observed in our analysis between small and large farms demonstrates that a one-size-fits-all approach is unlikely to be effective. While our model demonstrates the detrimental impact of conventional pesticide use on predatory arthropod populations, aligning with a substantial body of existing literature, it also shows that the effectiveness of ecological restoration strategies exhibits a strong dependence on farm size and the spatial configuration of SNH.

Specifically, our results indicate that, without any variation in pesticide use, in low-intensity systems—characterized by small farms with a high density of hedgerows and low pesticide use—fragmented SNH may provide the greatest benefit for NE populations. This is because fragmented, linear elements maximize resource provision and spillover by ensuring that overwintering refugia and foraging resources remain within the typical dispersal range of NEs. Conversely, in high-intensity systems associated with large farms, consolidated habitat patches, such as extensive permanent grasslands, are more effective in supporting natural enemies. In these contexts, larger refuges minimize pesticide exposure and mortality, acting as reservoirs from which NEs can recolonize adjacent fields. These findings may help reconcile differing recommendations in the habitat restoration and biodiversity conservation literature: some studies emphasize permanent grasslands as key reservoirs for multiple species and taxa [259, 260], while others prioritize habitat structure, highlighting the role of hedgerows and landscape diversity [261, 262]. Our results suggest that these differences may partly arise from variations in management intensity and field size. By explicitly capturing these interactions, our framework clarifies why the effectiveness of restoration strategies can vary across contexts and provides a conceptual foundation for future empirical and systematic studies examining the coupled effects of agricultural management, landscape configuration, and NE dynamics [109, 263].

In terms of the economic implications of transitioning toward ecological intensification—where natural processes replace synthetic inputs while potentially enhancing farmers' income—our results again show a strong dependence on farm size. Specifically, our model suggests that for small to medium-sized farms, reducing or eliminating pesticide use in combination with targeted hedgerow restoration represents a promising strategy to simultaneously improve farmland biodiversity and economic outcomes.. Hedgerows offer vital shelter for natural enemy

arthropods, potentially increasing yields and reducing the need for costly synthetic inputs.

This finding is consistent with a growing body of literature indicating that the benefits of ecological intensification are most pronounced under low-intensity management regimes [264–266]. In particular, although still limited, evidence suggests that yield gains resulting from enhanced ecosystem service provision—including pest suppression—can offset the economic losses associated with reducing chemical inputs, especially when these inputs are completely removed [267, 268]. Such conditions are more readily achievable on smaller, low-intensity farms than on large-scale operations.

However, despite this economic potential, such a transition is unlikely to occur spontaneously. While it is well documented that immediate economic incentives can boost the adoption of new management approaches, a substantial body of behavioral research demonstrates that financial benefits alone are not sufficient to guarantee widespread uptake [269, 270]. Small farmers often operate with narrow profit margins [241], which makes them particularly vulnerable to potential income losses in the early years of adopting new, ecologically based practices. Furthermore, their limited access to information networks and centralized policy discussions can breed reluctance to adopt unfamiliar strategies [271]. This highlights a crucial role for policymakers in actively facilitating this shift [272].

Nevertheless, in the context of our model, policy changes are assumed to be imposed externally, without explicit representation of farmers' behavioral responses. This highlights the need for future extensions of the model to incorporate aspects of farmer decision-making such as risk aversion [273], access to relevant information [109], labor limitations [274], and the interplay with other sustainable farming initiatives [240]. Integrating these factors would offer a more comprehensive and realistic understanding of the factors influencing adoption, illuminating which policy levers are most effective for realizing the economic potential of ecological intensification shown by our model. Moreover, such an approach could also reveal the emergence of unexpected effects from an economic and ecological point of view when policy interventions are implemented, as recently studied by two of us in [1].

The potential for large farms to achieve similar economic benefits from ecological restoration strategies appears more constrained in our model. The typical characteristics of large-scale agriculture, with a lower proportion of edge habitat, limit the effectiveness of natural pest control. While eliminating pesticide costs offers a significant economic advantage, the yield increases resulting from enhanced natural enemy abundance may not fully compensate for the reduced pest control efficacy previously provided by synthetic inputs. This outcome is consistent with existing literature [275, 276], which documents yield and income reductions following 50% pesticide reductions: for example, Bremmer et al. [275] report a 5% decline in wheat yield for a 180 ha farm in France, a 10% reduction for a 140 ha German farm, and a 7% reduction for a 450 ha Romanian farm under a 50% pesticide ban.

While previous estimations haven't considered any field-level coupled measures, our model allows assessment of impacts when pesticide bans are implemented alongside habitat restoration. Interestingly, our results suggest that large farms might experience a smaller income decrease if a transition to zero pesticide use is paired with hedgerow restoration (approximately −5% compared to −16%) , and a similar income reduction to that observed under a 50% pesticide reduction alone (approximately −5%). These findings emphasize two critical points: first, that synergy between biodiversity restoration measures can substantially affect economic outcomes [277], and second, that field size plays a pivotal role in moderating the benefits of ecological intensification. Indeed, the large field sizes typical of large farms [242] can impede the movement of natural enemies, diminishing the delivery of ecosystem services. Therefore, our

model suggests that biodiversity support schemes should consider incentivizing the maintenance or creation of smaller field sizes, particularly in regions dominated by large-scale agriculture [87]. Moreover, this highlights the potential need to shift from purely individual-farm payments [178] towards more collaborative, landscape-level initiatives that encourage larger farms to support ecological enhancements on smaller neighboring farms [278], potentially fostering a more diverse and resilient agricultural mosaic while addressing concerns about land consolidation.

Our model, while providing valuable insights, exhibits certain limitations that suggest avenues for future refinement. One notable simplification lies in the representation of pest dynamics. By implicitly modeling pest pressure and focusing primarily on natural enemy abundance, we may overlook the feedback loops between pest populations, natural enemy responses, and farmer management decisions. A more explicit incorporation of pest population dynamics, including factors like pest dispersal [279], different growing stages [249], and the development of pesticide resistance [280], could provide a more realistic assessment of the long-term ecological and economic consequences of different policy interventions. Furthermore, the model currently assumes a homogeneous response of natural enemies to landscape features and pesticide exposure. In reality, the arthropod community is diverse, with different taxa exhibiting varying sensitivities and functional roles [222, 281]. Future iterations could benefit from a more species-specific or functional group-based approach to modeling natural enemy abundance and their impact on pest control services.

From an economic perspective, the current model operates on a relatively static landscape structure, with changes in semi-natural habitat and management practices occurring as exogenous discrete shifts. As previously discussed, future work should seek to refine this approach to more accurately reflect the dynamic and evolving nature of decision making in agricultural systems [282]. Moreover, the economic analysis relies on aggregated data from the FADN, which mask some heterogeneity in farm characteristics and market conditions across different regions and farm types within the EU-27 [152]. Incorporating regional specificity and exploring the distributional effects of different policies on various farmer groups would enhance the policy relevance of the model [283, 284]. Addressing these limitations in future research would contribute to a more robust and policy-relevant understanding of the complex relationship between agricultural management practices, landscape structure, and both ecological and economic outcomes.

Finally, it is important to acknowledge that our study did not take into account the potential negative impacts of broader ecosystem degradation driven by external factors such as climate change [9] and invasive species [285]. These factors can only reinforce the need to adopt ecological restoration as a crucial adaptation strategy for all farm sizes, reinforcing the urgency for policymakers to invest in research and provide solid support for such transitions.

Conclusion

In conclusion, our analysis highlights the critical role of both pesticide management and landscape structure in shaping ecological and economic outcomes in agricultural systems, with farm size emerging as a key determinant of the effectiveness of ecological intensification strategies. While reducing pesticide use generally benefits natural enemy populations, the optimal configuration of semi-natural habitats for maximizing these benefits and ensuring economic viability varies significantly between small and large farms. This suggests that a nuanced, scale-dependent approach is necessary for designing effective agri-environmental policies that aim to enhance biodiversity and promote sustainable agriculture across the diverse

European farming landscape.

4.5 Supplementary materials

4.5.1 Landscape generation

Here we describe the algorithm to generate the field pattern and the semi-natural habitat (SNH) distribution over a landscape. The landscape is represented by a two-dimensional lattice of 200×200 cells, where each individual cell represents a $10\,\text{m} \times 10\,\text{m}$ region and can be in one of two states: cropland or SNH. The generation depends on three parameters: the average field size S, the share of hedgerows h, and the share of grassland g.

1. The algorithm starts from a landscape consisting only of cropland. The first step involves the creation of the field pattern distribution using a discrete Voronoi algorithm. From the average field size S, we compute the average number of fields n in our landscape as:

$$n = \left\lfloor \frac{400\text{ha}}{S} \right\rfloor . \tag{4.13}$$

   We then generate n random points within the lattice, which serve as the initial points for the discrete Voronoi tessellation. Specifically, we create a grid for all cells in the landscape and assign each cell to the nearest initial point. Note that for smaller values of n, the variability between different random landscape realizations will be higher compared to larger values of n.

2. Once the field pattern is established, we identify the edge margins between adjacent fields and mark them distinctly in the landscape. Specifically, a single field margin is defined as the ensemble of all edges between two neighboring fields. This is crucial for generating the hedgerow patterns that are not too dispersed in the landscape. After labeling all margins, we iteratively select a field margin. If its area, divided by the total landscape size, is less than h, the entire field margin is converted to a hedgerow. Otherwise, only a contiguous fraction of its area is converted until the total area of hedgerows reaches exactly a share h of the total landscape area. The share of hedgerows is calculated as the total area occupied by hedgerows divided by the total landscape area. Our minimum resolution of 10 m implies that the minimum hedgerow area is 0.01 ha.

3. Following the placement of hedgerows, we proceed with a similar iterative algorithm to place grassland. Here, the units considered for conversion are the individual fields identified in the first step.

While our landscape creation does not depend a priori on the selection of a farm size, as the three parameters described above can be independent, studying realistic agricultural landscapes reveals some consistent characteristics across different farm sizes. Indeed, regions with smaller farm sizes typically exhibit smaller fields, a higher density of hedgerows separating them, and a larger share of permanent grassland. This is because smaller farms, with limited capital, can only afford smaller machinery that does not necessitate large fields for operation. Furthermore, their lower profit margins result in smaller opportunity costs for maintaining existing permanent grassland, and they often benefit from related subsidies. Finally, smaller farmers tend to value the aesthetic appeal and ecological sustainability of their landscape, thus preserving hedgerows.

In contrast, landscapes managed by large farms, benefiting from substantial capital, can acquire large machinery that leads to higher profits. However, larger machinery requires larger fields, often necessitating the removal of hedgerows. Moreover, the opportunity costs of maintaining grassland become too high, leading to the conversion of much of it to productive agricultural area.

These features are strongly evident in data (as shown in Fig. 4.7 and Fig. 4.8) and represent a cross-country pattern. For this reason, the information about farm size alone can be sufficient to characterize all three parameters governing the landscape creation. Specifically:

$$S = S_0 L^a \tag{4.14}$$

$$g = g_0 L^b \tag{4.15}$$

$$h = h_0 L^c \tag{4.16}$$

Notation	Description	Value	Group
Structural parameters			
	Landscape size [ha]	400	
	Landscape resolution (single cell area) [ha]	0.01	
a	Exponent of the farm size-field area relationship	0.4	M
b	Exponent of the farm size-grassland share relationship	-0.2	M
c	Exponent of the farm size-hedgerows share relationship	-0.5	E
S_0	Scale of the farm size-field area relationship	0.4	M
g_0	Scale of the farm size-grassland share relationship	0.1	M
h_0	Scale of the farm size-hedgerows share relationship	0.15	E
Ecological parameters			
r	Growth rate of natural enemies [day^{-1}]	0.01	E
sn_{ref}	Reference semi-natural habitat area for overwintering [ha]	0.5	F
κ_{SN}	Carrying capacity coefficient in semi-natural habitats [ha^{-1}]	5000	E
κ_{C}	Carrying capacity coefficient in cropland [ha^{-1}]	10000	E
π_{ref}	Reference pesticide application rate [$€ \cdot \text{ha}^{-1} \cdot \text{year}^{-1}$]	80	F
q	Selectiveness of pesticide application	0	F
D	Characteristic dispersal distance of natural enemies [$\text{ha} \cdot \text{year}^{-1}$]	0.2	E
Economic parameters			
y_0	Baseline potential yield [$\text{q} \cdot \text{ha}^{-1}$]	51	C
y_1	Potential yield coming from fertilizer use [$\text{q} \cdot \text{ha}^{-1}$]	18	C
$L_{\text{ref},y}$	Reference farm land area for yield scaling [ha]	25	C
η	Maximum yield loss due to pest	0.3	M
π_0	Baseline crop protection expenditure (CPE) [$€ \cdot \text{year}^{-1} \cdot \text{ha}^{-1}$]	120	M
$L_{\text{ref},\pi}$	Reference farm land area for CPE scaling [ha]	25	M
C_0	Operational costs (no CPE but with depreciation) [$€ \cdot \text{year}^{-1} \cdot \text{ha}^{-1}$]	750	M
C_g	Maintenance cost for permanent grassland [$€ \cdot \text{year}^{-1} \cdot \text{ha}^{-1}$]	250	M
C_h	Maintenance cost for hedgerows [$€ \cdot \text{year}^{-1} \cdot \text{ha}^{-1}$]	1000	M
p	Crop price per unit [$€ \cdot \text{q}^{-1}$]	15	M
ℓ_0	Baseline labor input per area [$\text{AWU} \cdot \text{ha}^{-1}$]	0.01	M
ℓ_1	Additional labor input per farm [$\text{AWU} \cdot \text{ha}^{-1}$]	0.6	M
$L_{\text{ref},\mathcal{L}}$	Reference farm land area for labor scaling [ha]	5	M
S_{ref}	Reference field size area for labor scaling [ha]	1	M

Table 4.1 Parameters of the model. We indicate their units, value, and estimation method.

where L is farm size. Here, the parameters for the field-farm area relationship are taken from a recent empirical analysis [242]. The parameters for the g relationship are fitted to data as explained below. While a single estimation for the h relationship is lacking in the literature, we can derive an estimate by observing the historical decrease in hedgerow numbers corresponding to increasing farm sizes [286].

4.5.2 Calibration procedure and parameters value

Model parameters were categorized into four distinct groups (see Table 4.1): (i) *measured* parameters (M), directly fitted from relevant datasets; (ii) *estimated* parameters (E), derived from existing literature; (iii) *calibrated* parameters (C), fine-tuned through a calibration process to ensure model-dependent variables closely match observed data, and (iv) *fixed* parameters (F), set manually to explore alternative scenarios that could not be excluded a priori.

Measured parameters (M) are those whose influence in the model is confined to specific functions for which corresponding data are available. This category primarily includes economic parameters such as

	Description	Sampling range	Optimal
y_0	Baseline potential yield [q · ha^{-1}]	[30, 70]	51
y_1	Potential yield coming from fertilizer use [q · ha^{-1}]	[0, 40]	18
$L_{\text{ref},y}$	Reference farm land area for yield scaling [ha]	[1, 100]	25
R^2	R-squared		0.98
$\bar{R}^2$	Adjusted R-squared		0.97

Table 4.2 Results of model calibration.

crop prices (p), operational costs (C_0), subsidies ($\mathcal{S}$), and labor input ($\mathcal{L}$). These parameters were fitted using EU-27 average values for the 2018-2022 period, obtained from the European Farm Accountancy Data Network (FADN). The fitting procedure involved minimizing the least square error over a reasonable range of values. It is important to note that the objective was not to perfectly replicate the curves but rather to capture the underlying trends relevant to our study. In this regard, all fitted curves adequately represent the empirical data for each parameter (see Fig 4.7).

Estimated parameters (E) were assigned values based on empirical information and commonly reported values found in the literature. This category mainly encompasses ecological parameters. For instance, the carrying capacity of natural enemies (NE) was determined using empirical data on average individual numbers and body mass of natural enemies (NE) [255, 256]. Similarly, information from field-based studies relevant to European cereal systems was used to inform the growth rate of NE r [249]. For the dispersal distance (γ), a plausible range was considered, acknowledging its variability depending on the specific taxa and species.

Parameters in the *calibrated* (C) category are primarily associated with the yield response function, where the ecological model needs to produce realistic yield behavior. These parameters are intrinsically linked to the model's internal dynamics and therefore could not be directly fitted to external data. To align these parameters with observed data, we employed a sampling-based calibration approach. For each parameter, a realistic range of variation was hypothesized, and then a least-squares minimization procedure was performed to find the parameter values that best reproduced the observed trends. The hypothesized ranges for each calibrated parameter are detailed in Table 4.2. Given the high dimensionality of the parameter space, a direct sampling approach would have been computationally prohibitive, requiring over one million model runs for just ten values within each parameter range. To efficiently explore the parameter space, we utilized a Sobol sequence [227], which allows for a more uniform coverage and thus higher precision with fewer computational resources. We generated 4096 unique parameter sets and, for each combination, ran 100 Monte Carlo simulations. Subsequently, we computed the sum of squared differences between the simulated and observed data. Table 4.2 presents the results of this calibration. The corresponding R-squared (R^2) and adjusted R-squared ($\bar{R}^2$) [228] values demonstrate the model's effectiveness in capturing the observed trends in real-world data. For a visual comparison, Fig. 4.8 illustrates the compatibility between the obtained model trends and the empirical data.

Finally, parameters in the *fixed* category (F) are those for which the literature does not provide a single, definitive value. These include reference pesticide application rate (π_{ref}), pesticide application precision (q) and winter survival (sn_{ref}). For these parameters, we established reasonable initial values and subsequently conducted further analysis to assess their influence on the study's conclusions, acknowledging their context-dependent and complex nature.

4.5.3 Rationale for using physical farm size

This section justifies the choice of representing farm size in terms of its physical area (total utilized agricultural area) rather than its economic size.

First, it is important to note that in the European farming sector, and particularly within the field-cropping context of our study, physical and economic size are strongly correlated. As illustrated in Fig. 4.6, this strong correlation demonstrates that total utilized agricultural area is a reliable proxy for a farm's economic scale, meaning the two measures are largely interchangeable for our analytical purposes.

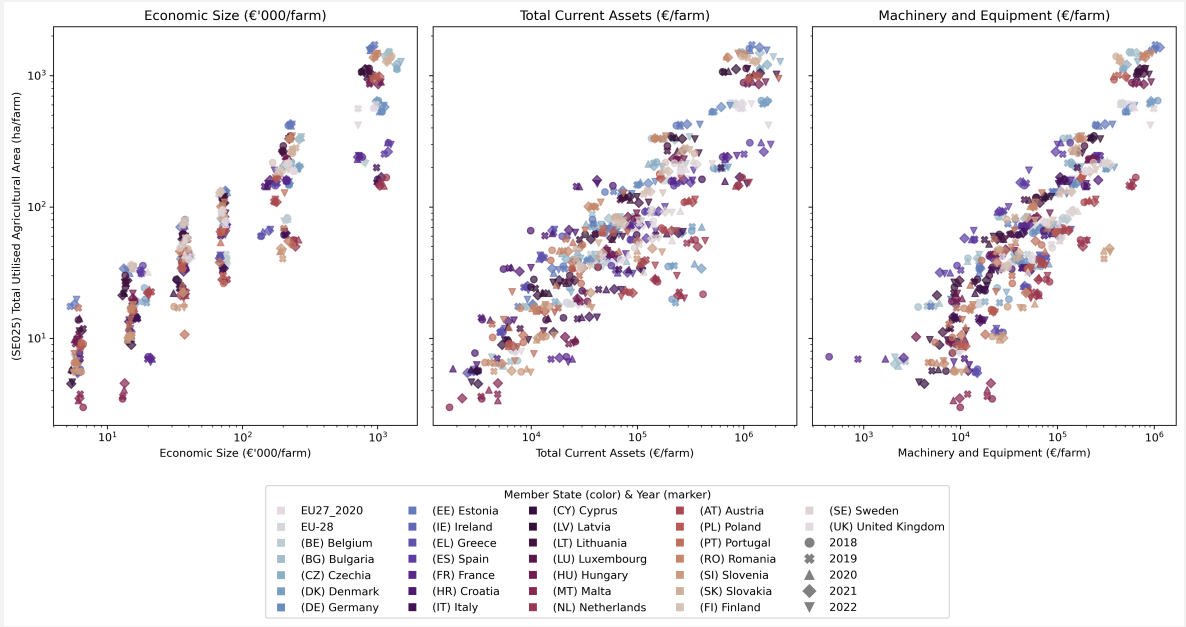


Figure 4.6 Relationship between farm size, assets, and physical land area across European countries (2018–2022). Each panel shows the relationship between Total Utilised Agricultural Area (ha/farm) and three indicators of economic or capital size: (a) Economic Size (€'000 per farm), (b) Total Current Assets (€ per farm), and (c) Machinery and Equipment (€ per farm). Colors represent EU Member States, while marker shapes indicate years. Data points show a strong positive correlation, highlighting the consistent link between physical and economic dimensions of farm size across time and countries.

Our primary rationale for selecting physical size is its direct and intuitive link to landscape simplification, which is a central mechanism in our modeling framework. Physical size is inherently connected to the key spatial elements of our model—such as field consolidation, hedgerow presence, and the spatial configuration of semi-natural habitats. In contrast, while economic size is a vital metric, it is more directly associated with financial and operational dimensions. By focusing on physical farm size, we establish a clearer and more mechanistic connection between the farm's spatial characteristics and the ecological outcomes and biodiversity patterns that our model aims to explain.

4.5.4 Scenario exploration for fixed parameters

For parameters in the *fixed* category (F) we perform further analysis to assess their influence on the study's conclusions, acknowledging their context-dependent and complex nature. We do this by primarily focusing on the ecological consequences of their variation. It is important to note that the following results are obtained after the system has been recalibrated to ensure consistency with the real data description, using the same methodology explained previously.

The role of semi-natural habitat area for overwintering

The parameter sn_{ref} establishes the reference amount of Semi-natural habitat (SNH) required to support the natural enemy (NE) population over winter. Increasing this value has two direct consequences: (i) overwintering becomes increasingly critical in determining the end-of-summer NE abundance, and (ii) the capacity of hedgerows to provide this overwintering service is diminished as they are fragmented within the landscape. Conversely, decreasing this value would lessen the importance of overwintering and enhance the relative contribution of hedgerows.

To observe the impact on our study's conclusions, let us consider Fig. 4.9, where the baseline results (those presented in the main manuscript and depicted in the gray area of the figure) are compared to a scenario where sn_{ref} is doubled, thus $sn_{ref} = 1\,ha$. In this case, the natural enemy protection is less effective compared to the baseline scenario, and the total yield loss due to pests is higher. Regarding ecological variables, increasing grassland cover consistently proves beneficial, as hedgerows alone no longer provide sufficient shelter for the NE population. Consequently, the hedgerow restoration policy does not effectively increase farmers' income when pesticide use is reduced under this altered sn_{ref} value.

The importance of baseline pesticide efficacy in pest control

The parameter π_{ref} defines the baseline efficacy of pesticides in reducing the populations of both natural enemies (NE) and pests, assuming an equal impact on both. Doubling π_{ref} would thus imply a twofold decrease in pesticide effectiveness in killing both groups. Conversely, halving π_{ref} would increase the efficacy of pesticide applications for pest protection.

Considering a scenario where π_{ref} is doubled, leading to less effective pesticides, results in a greater reliance on natural enemies and landscape features for pest control (see Fig. 4.10). Under such conditions, the advantages of enhancing natural enemy populations through semi-natural habitats, such as hedgerows and grassland, become more evident. Specifically, the transition threshold between landscapes favoring hedgerows versus grassland shifts towards higher levels of pesticide use. This indicates that hedgerows become even more crucial for sustaining higher NE population levels during winter when pesticide efficacy is reduced. Consequently, the adoption of more ecologically friendly farming practices becomes more economically favorable for farmers, underscoring the economic value of biodiversity-mediated pest control in a context of less effective chemical interventions.

The differential toxicity of pesticides to pests versus natural enemies

The parameter q quantifies the relative toxicity of pesticides to pests compared to natural enemies. A higher q signifies greater selectivity, where pesticides exert a stronger negative impact on pests than on their natural predators. Conversely, a lower q indicates that pesticides are relatively more harmful to natural enemies.

When the selectivity of pesticides (q) is increased, implying a greater reduction in pest populations relative to natural enemies, the significance of restoring and maintaining hedgerows is amplified. Hedgerows provide essential refuge and resources for natural enemies, enabling them to persist and contribute to pest control. Therefore, even if technological advancements lead to the development of pesticides with higher selectivity, the restoration of SNH and of hedgerows specifically remains a vital strategy for bolstering ecological resilience.

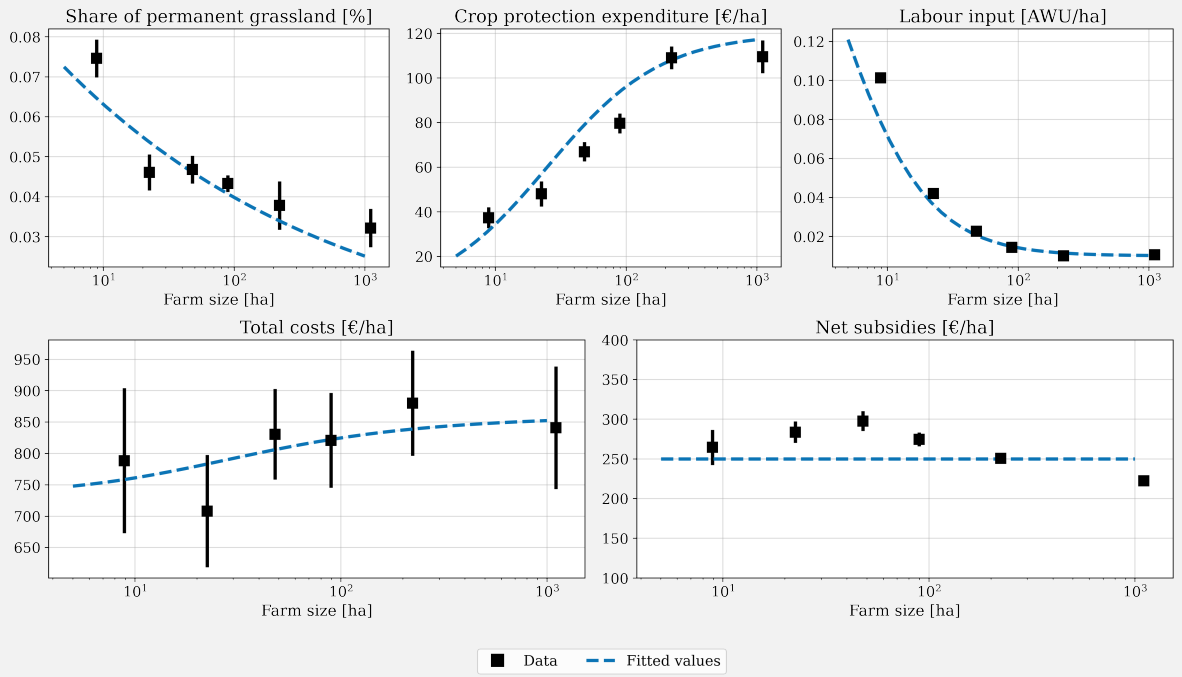


Figure 4.7 Fitted relationships between farm size and key agricultural parameters: share of permanent grassland (%), crop protection expenditure (which is an indicator of pesticide use intensity - €/ha), labor input (Annual Work Units per hectare - AWU/ha), total costs (€/ha), and net subsidies (€/ha). Black squares represent the weighted average of observed data from the European Farm Accountancy Data Network (FADN) [152] for the EU-27 region between 2018 and 2022, with error bars indicating the standard deviation of year-on-year variation. The dashed blue lines illustrate the fitted trends used as exogenous inputs for the subsequent ecological-economic modelling. These fits capture the general tendencies observed in the FADN data, such as the decreasing share of permanent grassland, increasing pesticide use and labor input with increasing farm size. Total costs show a slight positive trend with farm size, while net subsidies appear relatively stable across different farm sizes. These fitted relationships provide a realistic representation of the structural and economic characteristics of European farms of varying scales, forming the basis for simulating the impact of different policy scenarios.

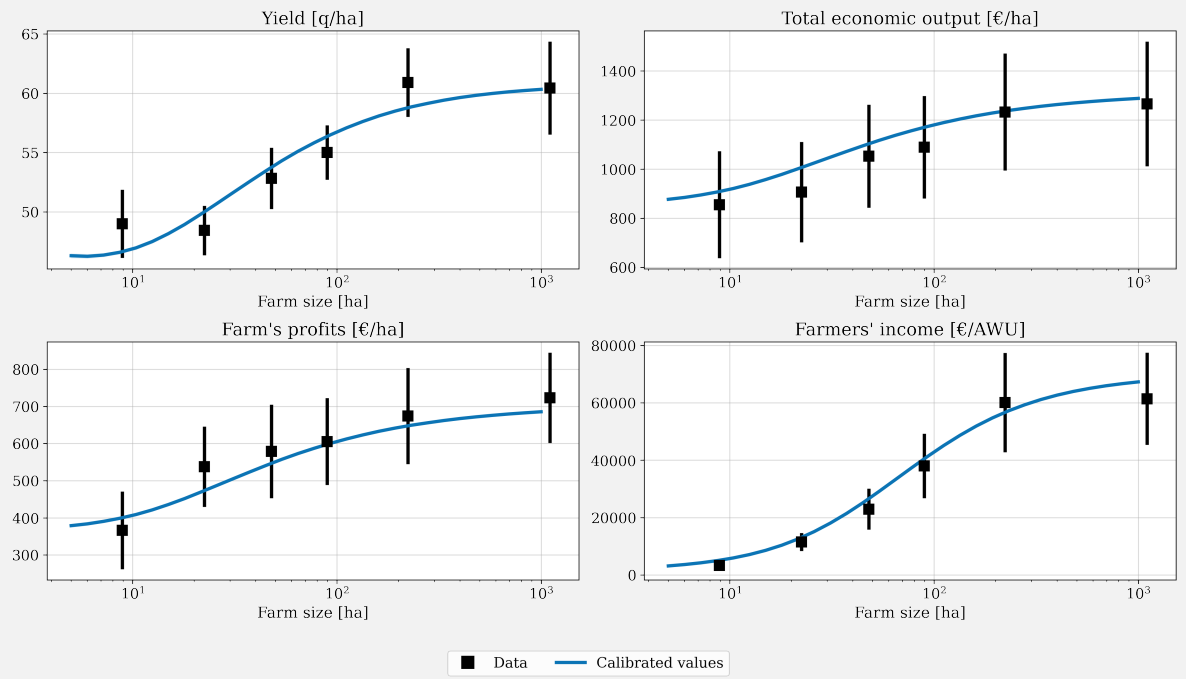


Figure 4.8 Calibrated relationships between farm size and key agricultural output and economic parameters: Yield (q/ha), Total economic output (€/ha), Farm's profits (€/ha), and Farmers' income (€/AWU). Black squares represent the weighted average of observed data from the European Farm Accountancy Data Network (FADN) for the EU-27 region between 1990 and 2021, with error bars indicating the standard deviation. The solid blue lines illustrate the calibrated model outputs, achieved by adjusting *calibrated* parameters (see Table 4.1) to best reproduce the observed trends. These calibrated relationships form a crucial part of the model validation, demonstrating its ability to represent real-world agricultural trends and providing a reliable basis for simulating the impacts of different policy scenarios on farm performance.

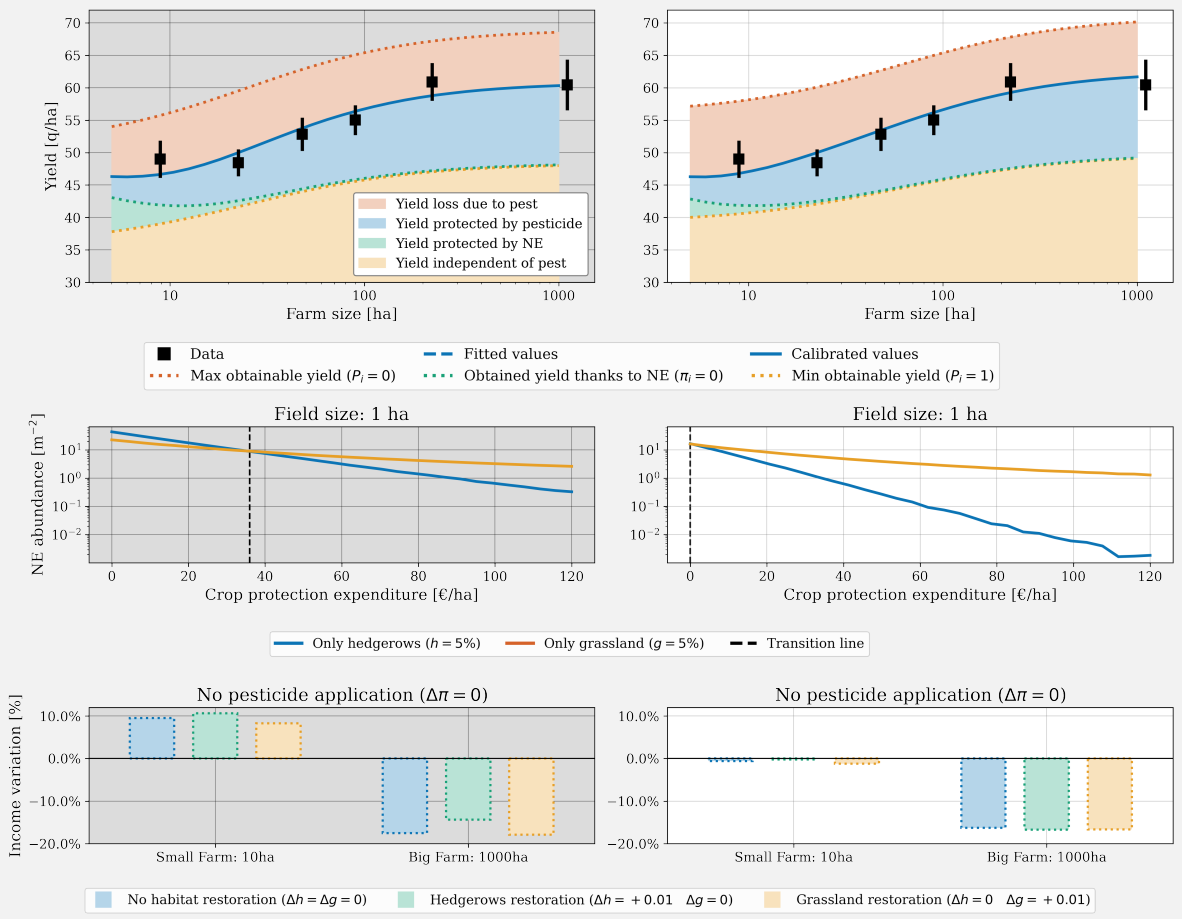


Figure 4.9 The figure illustrates the impacts of doubling the reference semi-natural habitat area required for overwintering natural enemies from $sn_{ref} = 0.5$ ha to $sn_{ref} = 1$ ha. The left panels display the baseline scenario results reported in the manuscript, while the right panels show the outcomes under the modified parameter value. Comparing the left and right columns reveals that a larger reference SNH area generally leads to reduced natural enemy protection and increased overall yield loss compared to the baseline scenario. Under this modified sn_{ref} value, increasing grassland cover consistently proves more beneficial for mitigating these negative effects, as hedgerows alone no longer offer adequate shelter for the NE population. Consequently, policies focused solely on hedgerow restoration are less effective at improving farmers' income when pesticide use is reduced.

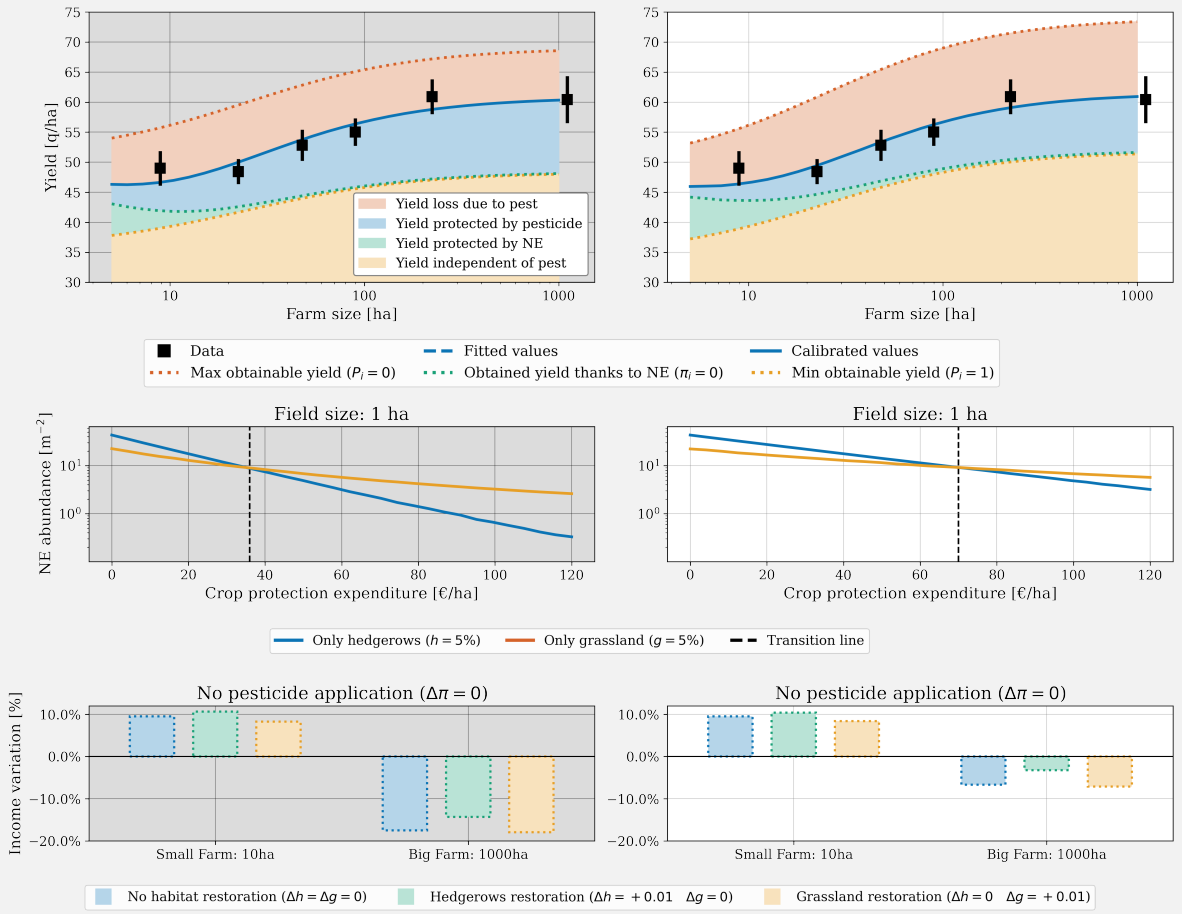


Figure 4.10 Ecological and economic consequences of doubling the baseline pesticide efficacy from $\pi_{\text{ref}} = 80\ € \cdot \text{year}^{-1} \cdot \text{ha}^{-1}$ (left panels) to $\pi_{\text{ref}} = 160\ € \cdot \text{year}^{-1} \cdot \text{ha}^{-1}$ (right panels). The comparison shows that a higher reference pesticide efficacy generally leads to a lower reliance on pesticides for yield protection. In this modified case, the reduced pesticide efficiency results in a larger natural enemy (NE) population. Consequently, providing shelter becomes more important, making hedgerow increases a preferred strategy. Finally, transitioning to a zero-pesticide regime (right column, bottom panel) results in less significant income losses for large farms compared to the baseline π_{ref} (left column, bottom panel) due to the enhanced restoration potential of natural pest control.

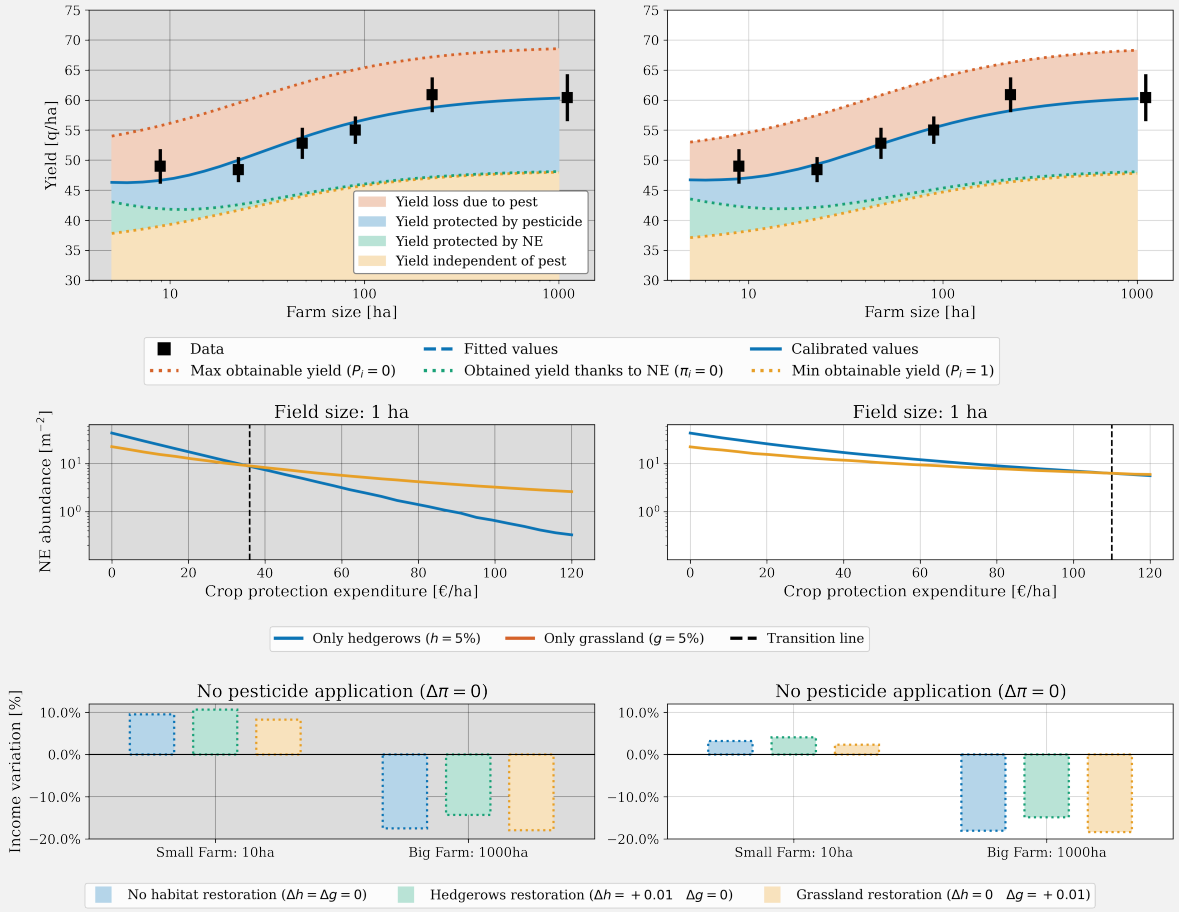


Figure 4.11 This figure illustrates the ecological and economic consequences of choosing the pesticide selectivity q equal to 0.5. The left panels display the baseline scenario results reported in the manuscript, while the right panels show the outcomes under the modified parameter value. Comparing the left and right columns reveals that increased pesticide selectivity enhances the relative importance of hedgerows in supporting NE populations and contributing to yield protection. Under a zero-pesticide regime (bottom row), the benefits of hedgerow restoration for mitigating income losses, particularly for larger farms, become are still very pronounced with higher pesticide selectivity, underscoring the complementary role of selective pesticides and SNH in sustainable pest management.

Key Takeaways

- **A landscape-scale ecological model:** We introduce a spatially explicit framework coupling biodiversity-mediated pest regulation with farmer economics to explore how natural pest control can replace synthetic pesticides across diverse farm sizes and landscape configurations.
- **Context-dependent pest control:** The effectiveness of natural pest control is fundamentally constrained by field size. Large fields inherently limit natural enemy dispersal compared to smaller, fragmented landscapes.
- **Asymmetric economic impacts:** Transitioning to ecological intensification (reducing synthetic pesticide use while restoring semi-natural habitats like hedgerows) yields a 5–15% income increase for small and medium farms, but imposes a modest economic penalty on large-scale operations.
- **Targeted agri-environmental schemes:** One-size-fits-all regulations are ineffective. Environmental policies must be explicitly tailored to local farm sizes and landscape configurations to be both ecologically and economically viable.

Part II

A Brazilian Perspective: The Role of Deforestation

Part II is adapted from Moretti et al. (2026) [3], *Policies for halting deforestation via fragmentation reduction and economic value creation.* Minor modifications have been made to the original texts to align them with the narrative and context of this thesis.

5. Land-use change in the Cerrado and the Soy Republic

Part I situated the mechanics of biodiversity decline within the context of European agricultural systems. In these mature landscapes, the ecological crisis has manifested largely through severe chemical intensification and structural land consolidation rather than outward expansion. Globally, however, the absolute primary driver of biodiversity loss remains outright deforestation and habitat conversion [258]. Because the European landscape is defined by centuries of historical land-use modification and a deeply entrenched socio-technical lock-in, the continent currently exhibits a halt in domestic agricultural frontier expansion—and, in some regions, even a net recovery of forest cover [287]. Consequently, to fully comprehend the global phenomenon of biodiversity decline, our analytical lens must pivot away from geographies where land-use transitions have already run their course. Here we zoom in on the active frontiers where massive land conversion is still occurring.

5.1 The displacement of ecological debt

Although the European agricultural sector provides an essential baseline for domestic food provision, its internal production capacity is supported by external imports (Fig 5.1). The continent's intensive livestock industries and high-protein consumption patterns are structurally dependent on the massive importation of agricultural commodities—most notably soy and beef. To illustrate this scale, the European Union imports over 10 million tons of soybeans and soybean meal annually, alongside hundreds of thousands of tons of beef [288]. These massive commodity flows originate primarily from the Global South; South American nations, particularly Brazil and other Mercosur members, serve as the main producers of European soy imports and account for up to 86% of the EU's imported beef [289].

This dependency is inextricably linked to the spatial displacement of ecological debt [290]. Within environmental economics and land-system science, this phenomenon is conceptualized through the literature on Indirect Land-Use Change (ILUC). The ILUC framework formally demonstrates how market-driven shifts in agricultural demand in one region (*e.g.*, European livestock feed requirements [291] or biofuel mandates [292]) inadvertently trigger land conversion in geographically distant biomes. When mature economies protect their own forests while simultaneously increasing their demand for land-intensive commodities, they inevitably displace the expansionary pressure onto less regulated, highly biodiverse frontiers [293]. In the context of South America, as we will see in Chapter 6, this displacement triggers a cascade effect: the expansion of highly mechanized soy production frequently pushes cattle ranching deeper into pristine ecosystems, accelerating widespread deforestation [294, 295].

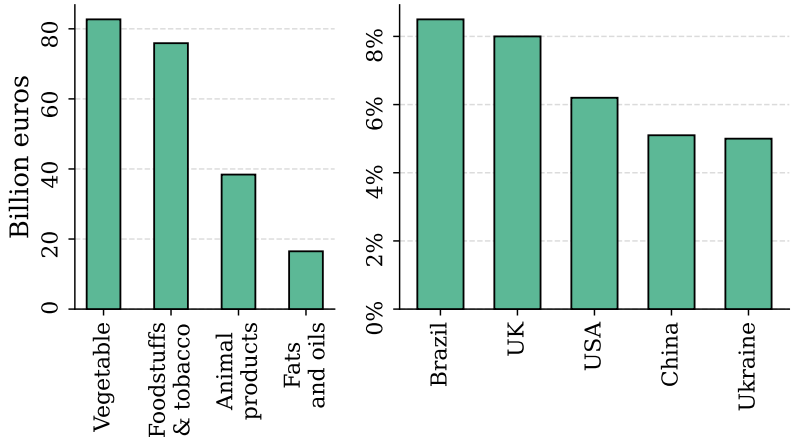


Figure 5.1 Data from [288]. Composition of European Union agricultural imports for 2025, categorized by major product group (billions of euros, left) and top regional distribution by percentage share (right).

Therefore, if we intend to map the systemic drivers of global biodiversity loss and engineer policies to stabilize it, we must pivot to the active frontiers of agricultural expansion. These regions represent primary arenas of contemporary land-use conversion, where the structural demands of commodity markets are actively clashing against hard biological thresholds.

5.2 Brazil: The epicenter of the global agro-export boom

Of the countries of the global south, in the context of this thesis, we focus on the Brazilian case. The Brazilian bio-economic trajectory is defined by a profound, structural paradox. Ecologically, the nation serves as the primary custodian of the Earth's terrestrial biodiversity, harboring massive, irreplaceable carbon sinks and hydrological engines [296, 297]. Economically, however, it has systematically engineered itself to become the undisputed powerhouse of global agricultural expansion (Fig 5.2).

Over the past four decades, Brazil has undergone a radical socio-metabolic transition, evolving from a net food importer into a structural pillar of global commodity trade [298, 299]. Today, the nation operates as a true "Soy Republic" [300] and a dominant pastoral empire [301]. It stands as the world's largest producer and exporter of soybeans [302]—currently commanding over half of total global exports—as well as the world's leading exporter of beef [303]. This absolute dominance in global protein markets is not a spontaneous market anomaly; rather, it is the result of a deliberate, state-sponsored bio-economic project designed to maximize agro-industrial extraction [304].

Historically, the highly acidic, nutrient-poor soils of Brazil's deep interior were considered biophysically unsuitable for intensive, mechanized agriculture. However, catalyzed by strategic state investment and the pioneering agronomic interventions of the Brazilian Agricultural Research Corporation (Embrapa), these natural barriers were systematically dismantled [305]. Through the massive, industrial application of limestone to neutralize soil acidity, combined

with the aggressive genetic adaptation of temperate crops (such as soy) to tropical latitudes, millions of hectares of previously "unproductive" biomes were rapidly integrated into the global supply chain [306, 307].

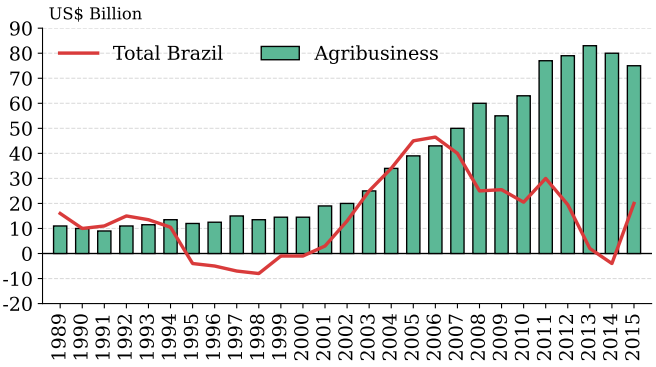


Figure 5.2 Data from [308]. Brazil trade balance evolution.

While this unprecedented agricultural expansion has drawn intense global scrutiny, international conservation efforts have historically suffered from a pronounced "Amazon bias." The Amazon rainforest overwhelmingly dominates public discourse and environmental policy, leading to highly asymmetric governance frameworks [309]. A prominent example is the 2006 Amazon Soy Moratorium (ASM), a zero-deforestation supply chain agreement that successfully decoupled soy production from forest clearing within the Amazon biome [310]. However, because this policy did not extend beyond the rainforest's borders, it inadvertently triggered a spatial displacement of ecological debt [311]. By strictly protecting the Amazon while global commodity demand continued to surge, these asymmetric policies catalyzed a severe "leakage effect," redirecting the aggressive expansion of mechanized agriculture away from the rainforest and into Brazil's less protected, but equally critical, Cerrado biome.

5.3 The Cerrado: The active agricultural frontier

To fully grasp the magnitude of this displaced pressure, one must recognize the profound, yet historically underappreciated, ecological value of the Cerrado [312]. Spanning approximately 200 million hectares (Fig. 5.3), the Cerrado is not a uniform, barren scrubland, but rather a highly complex mosaic of grasslands, savannas, and forest formations. It is formally recognized as the world's most biodiverse savanna, hosting over 4,800 endemic plant and vertebrate species [313]. Beyond its raw biodiversity, the biome functions as the critical hydrological cradle for the South American continent [314]. Characterized by deep, extensive root systems that act as an "upside-down forest," [315] the native vegetation captures and regulates seasonal rainfall, sustaining the base flows of major continental watersheds, including the Amazon, the Paraná-Paraguay, and the São Francisco river basins [316].

Despite its foundational role in maintaining continental environmental stability, this ecological wealth is being systematically dismantled. The Cerrado has become the undisputed primary frontier for the global soy-cattle complex. Driven by telecoupled international demand and domestic infrastructure investments, agro-industrial expansion is rapidly advancing into the biome's northern and eastern frontiers—most notably in the MATOPIBA region (comprising the states of Maranhão, Tocantins, Piauí, and Bahia). Consequently, the Cerrado is experiencing aggressive land-use conversion at a rate that functionally outpaces the Amazon relative to its size, transitioning vast swaths of hyper-diverse ecosystems into simplified monocultures.

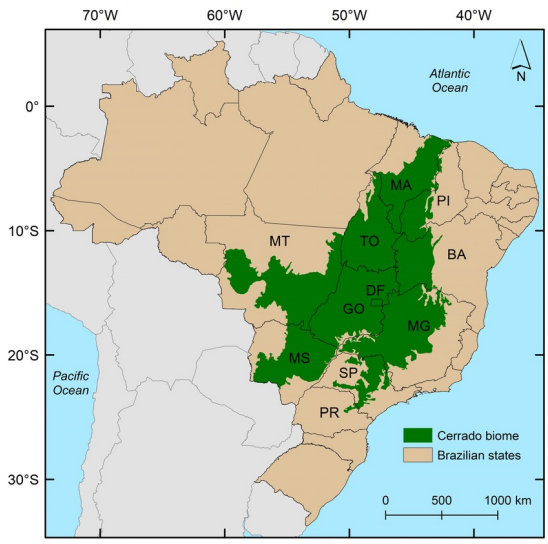


Figure 5.3 Source: [317]. Map of the Cerrado biome and corresponding state boundaries.

The targeting of the Cerrado is not solely a function of agronomic suitability; it is deeply rooted in a structural regulatory gap. The Brazilian environmental governance framework exhibits a profound institutional asymmetry. Under the national Forest Code (*Código Florestal*) [318], private landowners within the Amazon biome are mandated to maintain up to 80% of their properties as native vegetation under the Legal Reserve (*Reserva Legal*) requirement. In stark contrast, within the Cerrado, this conservation mandate drops precipitously to a mere 20% [319].

Coupled with the absence of private-sector supply chain governance, such as the Amazon Soy Moratorium, this legal disparity has effectively codified the Cerrado as a sacrifice zone. It represents a landscape of legally sanctioned, unchecked agricultural intensification. This combination of immense ecological importance, hyper-aggressive commodity expansion, and systemic regulatory vulnerability makes the Cerrado the optimal empirical case study for this thesis. It provides the perfect theater to investigate the collision between macroeconomic expansion and critical biological limits, and to model the socio-economic interventions necessary to stabilize the agricultural frontier.

Key Takeaways

- **Displacement of ecological debt:** Mature agricultural systems (like Europe) achieve domestic stability by outsourcing environmental costs to active frontiers in the Global South through massive commodity imports.
- **Asymmetric policy leakage:** Strict conservation frameworks focused exclusively on the Amazon have inadvertently redirected aggressive agro-industrial expansion into neighboring, unprotected biomes.
- **The Cerrado as a sacrifice zone:** With weak regulatory protections, the biodiverse Cerrado savanna has absorbed this displaced pressure, becoming the epicenter of global agricultural expansion and ecological destruction.

6. A cellular-automata model of landscape transformation

In this chapter, we introduce a modeling framework to (i) understand the dynamics of land use change in relation to agricultural expansion in the Cerrado region, and (ii) evaluate policy instruments to halt deforestation. Specifically, we address two questions: how effective are currently proposed policy instruments? Are the economic benefits derived from these initiatives higher than the costs? We employ a cellular automata bio-economic model at the scale of 25ha and grounded in real data, ensuring our model replicates historical trends in land use (spatially explicit) patterns, fragmentation levels, farm structure (in particular farm size distribution), and productivity evolution. We adopt this integrated bio-economic framework because it is crucial to properly evaluate the economic benefits of nature conservation initiatives.

This chapter is structured as follows. Section 6.1 positions our work within the existing literature. Section 6.2 characterizes the model's structural framework and mathematical formulation, followed by the empirical initialization and numerical calibration details in Section 6.2.9. In Section 6.3, we project land-use trajectories under a baseline "business-as-usual" scenario, highlighting how accelerated deforestation is driven by the displacement of pastureland by expanding cropland. We subsequently evaluate the efficacy and economic viability of two prominent policy mechanisms: a targeted soy moratorium for the Cerrado biome and a payment scheme for forest preservation. Section 6.4 offers concluding remarks.

6.1 Literature review

In regions experiencing rapid agricultural frontier expansion, such as the Brazilian Cerrado, spatially explicit models play a critical role in supporting environmental decision-making [320]. The Cerrado is one of the most threatened biomes globally, experiencing profound historical deforestation driven predominantly by the expansion of agriculture and cattle ranching [312]. In evaluating the systemic impacts of land-use change, Integrated Assessment Models (IAMs) have traditionally served as the foundational analytical paradigm [321–323]. Such macro-scale models are highly adept at mapping the broad climatic consequences of relaxed environmental policies and accelerated forest clearing [324]. However, their top-down architecture fundamentally limits their capacity to resolve the behavioral nuances of individual land managers and the spatial variance in agricultural productivity [325]. Consequently, there is a growing consensus on the need for spatially explicit, high-resolution behavioral models. In the context of the Cerrado, recent literature underscores this imperative, demonstrating that structural constraints—particularly farm-size heterogeneity—must be internalized within the modeling framework to accurately simulate policy compliance and native habitat trajectories [319, 326].

Efforts to mathematically capture farm-level agricultural adaptation have evolved significantly since the 1970s, shifting away from the rigid optimization paradigms exemplified by the early recursive linear programming models of Day and Singh [327]. In response to the need for more realistic representations of human-environment interactions, a rich ecosystem of spatially explicit simulation frameworks has been developed to study land-use change. As detailed in several extensive reviews of this composite literature [328–330], two prominent methodologies stand out among contemporary approaches that prioritize structural and behavioral heterogeneity: Agent-Based Models (ABMs) and Machine Learning (ML). On one hand, ABMs dominate the behavioral modeling sphere, allowing researchers to explicitly simulate how heterogeneous agents—each operating with unique economic constraints, risk profiles, and heuristic behaviors—interact with their environment [331, 332]. On the other hand, a rapid proliferation of ML techniques provides highly accurate, inductive frameworks for mapping spatial land-use transitions without relying on explicit behavioral assumptions [326, 333].

Over the past decades, ABMs have progressed significantly, evolving from relatively abstract theoretical representations used to explore spatial systems [334] to highly complex, empirically grounded models of socio-ecological systems [128, 133, 135]. However, they still present key limitations. Given their inherent computational complexity and heavy reliance on extensive micro-data, ABMs are notoriously difficult to scale up to the biome or national levels—the exact scales essential for capturing macroeconomic shifts [294] and systemic environmental impacts [316]. Notable examples in the literature underscore this scaling limitation. The MP-MAS framework [335], for instance, provided highly detailed insights into the rural economy of Mato Grosso, Brazil; however, its computational and data demands restricted the simulation to a surface area of 15,000 km^2, representing less than 2% of the state. More recently, Ferraro *et al* [133] successfully captured land-use and environmental dynamics in Argentina's Pampas, yet their study was confined to the Pergamino region, covering merely 3,000 km^2. These spatial bottlenecks highlight a critical vulnerability: while ABMs excel at local behavioral accuracy, they cannot easily capture the macro-regional dynamics necessary for biome-wide policy evaluation.

Conversely, Machine Learning (ML) and Artificial Neural Network (ANN) models have proliferated in LULCC forecasting due to their high predictive accuracy and unparalleled capacity to process vast, multi-dimensional geospatial datasets [333]. For instance, approaches utilizing Random Forests or Convolutional Neural Networks have demonstrated exceptional skill in identifying deforestation hotspots and projecting future land-conversion trajectories based on proximity to roads, terrain elevation, and historical clearing patterns [336, 337]. However, these purely data-driven frameworks suffer from a fundamental "black-box" limitation. Because they rely entirely on inductive pattern recognition rather than mechanistic, causal relationships, ML models struggle to perform robust ex-ante policy evaluations [331, 338, 339]. They are inherently constrained by the historical data upon which they are trained. Therefore, they cannot reliably simulate unprecedented structural economic shifts or the complex behavioral shifts that occur when the fundamental rules of the system are altered.

Situated between the computational intractability of large-scale ABMs and the mechanistic opacity of ML models lie Cellular Automata (CA) techniques. By representing the landscape as a grid of interacting spatial units, CA frameworks drive land-cover transitions through localized, rule-based algorithms that account for neighborhood proximities, biophysical suitability, and regional demand [340–343]. This structure offers a highly scalable, spatially explicit architecture capable of simulating complex, emergent patterns—such as the percolation of deforestation [344] or the fragmentation of habitats [117]—without requiring the exhaustive computational overhead of modeling individual agent cognition. Taking inspiration from these scalable spatial mechanics,

we employ a CA bio-economic framework that elegantly anchors complex economic drivers within simple probabilistic transition functions. Rather than simulating exhaustive individual agent cognition, land-use decisions at the parcel level are probabilistically determined by local spatial interactions and expected profitability.

Specifically, our model incorporates two critical features to accurately describe the dynamics of land-use change in response to nature preservation policies in the Cerrado: (i) bio-economic feedbacks and (ii) the evolutionary dynamics of farm-size distribution. Drawing on the flourishing ecological literature regarding the delivery of ecosystem services, we explicitly include two distinct but interacting feedback mechanisms: regional climate stabilization derived from natural vegetation patches [316, 345, 346], and localized ecosystem services such as pollination, pest control, and soil health maintenance [347–350]. The inclusion of these feedbacks is fundamental because the biome's native vegetation acts as a critical hydrological pump that buffers thermal stress and sustains the region's predominantly rainfed agriculture [346, 351]; consequently, the widespread fragmentation of these patches translates into delayed rainy seasons and severe droughts that systemically damage aggregate production [352, 353]. Simultaneously, at the micro-level, the degradation of proximal forest edges deprives farms of vital pollinator habitats, natural pest predators, and soil moisture retention, imposing direct yield penalties [347].

The other crucial element of our model is the inclusion of the evolutionary dynamics of farm-size distribution. We explicitly model the description of farm-size dynamics because distinguishing between legal and illegal deforestation hinges precisely on the proportion of natural land retained within each individual farm holding [319, 326]. Unlike the Amazon biome, where deforestation is predominantly driven by land grabbing on undesignated public lands [354], the Cerrado is already extensively privatized [355]. Consequently, in this biome, land-use conversion is dictated by private owners subject to the Brazilian Forest Code, which mandates retaining a specific fraction of each property as a "Legal Reserve" of native vegetation [319, 356]. Within our framework, the probabilistic fine structure for land clearing is directly tied to whether a holding meets this legal threshold. Consequently, any structural changes in farm boundaries—such as land consolidation or parcel acquisition—alter the property's ratio of natural to agricultural land, immediately shifting the financial risk and legal status of future deforestation.

Ultimately, the key contribution of this integrated bio-economic framework does not reside in introducing a radically novel model structure, but rather in its rigorous systemic reasoning necessary to strip away unnecessary complexity. By tightly calibrating our spatial and economic parameters to replicate historical trends in land-use patterns, fragmentation, and farm size distribution, the model bridges the persistent gap between macroscopic policy goals and micro-level agricultural realities. This empirically grounded approach provides a highly tractable environment for robust ex-ante evaluation. Consequently, it allows us to move beyond abstract simulations to empirically assess the precise behavioral shifts and spatially targeted policy portfolios—such as protecting specific forest edges to block the percolation of deforestation—that are urgently required to halt environmental degradation in the Cerrado. Through this lens, we can rigorously determine not only the spatial effectiveness of proposed policy instruments, but whether the long-term economic benefits derived from these initiatives truly outweigh their structural costs.

6.2 Model and methods

6.2.1 Model overview

We formulate a spatially explicit cellular automata model that describes land-use dynamics and their relationship with both agricultural profitability and ecological integrity in the Brazilian Cerrado. The model operates on a discrete spatial representation of the landscape at a resolution of 25 hectares (500m $\times$ 500m). Each parcel within this lattice is characterized by a stacked set of spatial information layers. The primary biophysical layer defines the land-cover type—specifically natural vegetation, cropland, or pasture. The second fundamental layer maps land ownership, aggregating individual parcels into discrete, privatized farm holdings specializing in either crop or livestock production. Additionally, every productive parcel is further characterized by a dynamic management intensity layer and an ecosystem service provision layer which in conjunction with exogenous technological change, is then used to derive parcel-level agricultural yields and subsequent operational profitability.

These spatial information layers evolve dynamically over time, governed by localized, probabilistic rules rather than top-down macroeconomic equilibrium constraints or exhaustive optimization. Drawing inspiration from agent-based models (ABMs), the underlying decision-making is driven by the expected profit increment evaluated through a boundedly rational expectation framework. However, this logic is executed strictly at the parcel level rather than the agent level, thereby abstracting away complex individual cognitive constraints, such as explicit household budget limits or full-scale utility optimization. Driven by this localized economic calculus, a cell can undergo one of four possible state transitions within any given period: intensification, ownership change, deforestation , or abandonment.

The first possible transition, intensification, alters the management layer by shifting a parcel from conventional to high-intensity production. This binary shift serves as a methodological simplification of the continuous process of capital and input accumulation that occurs in reality. Mechanistically, intensification acts as a localized multiplier for agricultural yields, which translates into higher operational profits. However, it simultaneously degrades the habitat integrity of adjacent natural cells, explicitly establishing a two-way coupling between the biosphere and the agricultural economy.

Operating concurrently, ownership change dynamically reshapes the property boundaries within the simulation. Land transactions occur through a localized market mechanism where a parcel may be acquired by a neighboring farm holding if the prospective buyer demonstrates a sufficiently higher capacity for profit generation. By evaluating these localized profit differentials, this mechanism endogenizes structural farm consolidation, allowing highly efficient operations to absorb adjacent parcels driven by economies of scale. Furthermore, it allows market-driven land-use reallocation, serving as the vehicle for the transition from pasture to mechanized cropland, and vice versa (although the latter occurs less frequently).

The physical expansion of the agricultural frontier is driven by the deforestation mechanism, which directly alters the primary land-cover layer. To accurately mirror the infrastructural and logistical realities of the biome—and in strict agreement with empirical spatial findings—the conversion of natural vegetation into productive land is governed by a spatial adjacency constraint. This ensures that land clearing percolates realistically outward from existing agricultural footprints. The probabilistic decision to clear a parcel is jointly motivated by expected operational revenues and the speculative appreciation of the land as a capital asset.

Crucially, these economic incentives are weighed against direct clearing costs and environmental fines, the latter being structurally linked to the individual farm's compliance with the Legal Reserve requirements mandated by the Brazilian Forest Code. Finally, abandonment acts as the exit mechanism, occurring when a parcel's expected profitability deteriorates sufficiently, leading to its removal from active production.

Ultimately, we utilize this integrated model to simulate how structural land tenure, macroeconomic incentives, and environmental enforcement interact to generate emergent patterns of landscape evolution. In what follows, we provide detailed descriptions of the individual components of the model, including the mathematical details governing agricultural production, the formulation of ecosystem service provision, the economic accounting of farm profitability, and the probabilistic rules dictating spatial land-use transitions.

6.2.2 Production

Parcel-level agricultural yield is driven by three interconnected factors: technological advancement, management intensity, and the provision of ecosystem services. Mathematically, this is defined as:

$$y_{j,t} = y_{\tau_{j,t}}(1 + T_{\tau_{j,t},t})(1 + \alpha_{\tau_{j,t}}\delta_{j,t})(1 + \varepsilon_{j,t}) \tag{6.1}$$

where $\tau_{j,t}$ represents the possible land use types - cropland or pastureland. Within this formulation, y_c and y_p denote the baseline productivities for cropland and pasture. These are assumed to be homogeneous across parcels and are calibrated to the 1995-1996 Brazilian Agricultural Census [357] (more information on initialization and parameters selection in the Supplementary Materials).

Building on this baseline, $T_{\tau_{j,t},t}$ introduces linear, exogenous technological change. We assign a faster growth trajectory to crop production to reflect historical trends in Brazilian total factor productivity (TFP). Specifically, this captures the rapid, state-driven genetic tropicalization of crops like soybean and maize by institutions such as Embrapa, contrasting with the historically slower technological adoption in pastoral systems [306, 358].

At the parcel level, the parameter $\alpha_{\tau_{j,t}}$ scales the productivity gains derived from intensification ($\delta_{j,t} \in \{0, 1\}$). By functioning as a binary proxy for increased capital investment and agrochemical use, this variable structurally approximates the continuous process of yield-gap closure commonly observed as Cerrado producers accumulate capital [359].

Finally, the multiplier $(1 + \varepsilon_{j,t})$, bounded by $\varepsilon_{j,t} \geq 0$, captures the parcel-specific provision of ecosystem services. This specification mechanically aligns with the ecological intensification framework, recognizing natural capital—such as pollination, pest regulation, and microclimate buffering—not merely as a passive environmental externality, but as a functional, localized agricultural input that actively amplifies baseline yields [92, 264].

6.2.3 Ecosystem service provision

The model structurally integrates two scale-dependent ecological feedback mechanisms: regional climate stabilization derived from macro-scale vegetation blocks [345, 351], and localized agroecological benefits such as pollination, pest control, and soil health [347, 348]. While the macro-level mechanism hinges on the total size and fragmentation of the natural matrix across the landscape, the localized mechanism depends on the immediate neighborhood's land use and management intensity. Together, these dynamics define the composite ecosystem service

multiplier for a given parcel:

$$\varepsilon_{j,t} = \lambda_{\tau_{j,t}} \mathrm{HI}_{j,t}^{\mathrm{local}} + \gamma_{\tau_{j,t}} \mathrm{HI}_{t}^{\mathrm{global}} \tag{6.2}$$

Here, λ dictates the parcel's sensitivity to local biotic vectors (such as crop pollinators and natural pest predators), while γ governs its reliance on macro-climatic buffers (such as rainfall regulation). To reflect biological realities, we set $\gamma_c > \gamma_p$ and $\lambda_c > \lambda_p$ to reflect both the heightened vulnerability of rainfed annual crops to systemic shifts in regional rainfall cycles [352] and the strong dependence on localized agroecological services [348, 360].

At the micro-level, the localized habitat integrity surrounding parcel j ($\mathrm{HI}_{j,t}^{\mathrm{local}}$) is computed as the average ecological quality of its immediate neighborhood:

$$\mathrm{HI}_{j,t}^{\mathrm{local}} = \frac{1}{|\partial_j|} \sum_{k \in \partial_j} w_{k,t} \tag{6.3}$$

where ∂_j defines the spatial boundary, and $w_{k,t}$ is a quality weight reflecting the land cover and management intensity of neighbor k. Crucially, this weighting function explicitly penalizes high-intensity management ($\delta_{k,t} = 1$) as well as crop production relative to pasture. This simulates the negative spatial externalities—such as agrochemical drift and soil compaction from heavy machinery—that degrade biodiversity across adjacent property boundaries [88].

At the macro-level, regional habitat integrity ($\mathrm{HI}_{t}^{\mathrm{global}}$) tracks broader ecosystem health, formulated as:

$$\mathrm{HI}_{t}^{\mathrm{global}} = \frac{N_t}{N_0} \exp\left(-\sigma_{\mathrm{patch}} \frac{\mathrm{PD}_t - \mathrm{PD}_0}{\mathrm{PD}_0}\right) \tag{6.4}$$

where the ratio of current (N_t) to baseline (N_0) natural area is modulated by its fragmentation level, measured via patch density—a standard metric in the literature [361, 362]. Here, patch density (PD_t) is defined as the total number of contiguous natural clusters divided by the total natural area. This non-linear dynamic reflects the ecological consensus that regional moisture recycling cascades into a precipitous collapse once advanced structural fragmentation severs the core natural matrix [353, 363].

6.2.4 Costs, revenues, and profitability

All economic accounting within the model is localized at the parcel level. Following foundational theories of land-use change [364] and in the spirit of agro-ecological ABMs [365], parcel-level profitability serves as the primary economic signal driving structural landscape transitions. Here, the operational cost for a given parcel incorporates a baseline conventional cost, which is then dynamically modulated by three interacting mechanisms: intensification premiums, farm-level economies of scale, and localized biophysical suitability. Mathematically, costs are modeled as:

$$C_{j,t} = C_{\tau_{j,t}}^{\mathrm{oc}} (1 + \beta_{\tau_{j,t}} \delta_{j,t}) \left(1 - \frac{\nu_{\tau_{j,t},\max}}{1 + \frac{\nu_{\tau_{j,t},\mathrm{ref}}}{L_{j,t}}}\right) (1 + \xi_{\tau_{j,t}} s_j) \tag{6.5}$$

Here, $C_{\tau_{j,t}}^{\mathrm{oc}}$ represents the baseline operational cost associated with conventional production for the active land use. The parameter β defines the proportional cost penalty incurred by intensified management. This captures the heavy capital requirements—such as elevated spending on advanced agrochemicals, specialized labor, and machinery maintenance—necessary to elevate productivity.

Crucially, the model internalizes structural farm-size heterogeneity through an economies of scale multiplier, in a similar fashion to other existing ABMs [128, 366]. Here, $L_{j,t}$ represents the total area operated by the farm holding parcel j. The parameters $\nu_{\tau,\max}$ (the maximum achievable cost reduction) and $\nu_{\tau,\text{ref}}$ (the rate of realization) dictate how rapidly unit costs fall as the farm expands. We assume substantially larger economies of scale for crop production relative to pasture, directly reflecting the empirical realities of the Brazilian Center-West, where mechanized soy-maize operations rely heavily on extensive land consolidation to remain globally competitive [367, 368].

Finally, s_j acts as a biophysical suitability indicator, with ξ regulating the sensitivity of operating costs to these local conditions. In the Cerrado context, this primarily captures topographical constraints; for instance, steep slopes prohibit the operation of heavy machinery, drastically inflating the costs of mechanized crop production relative to cattle ranching.

Parcel-level revenues are straightforwardly calculated by multiplying the exogenous market price of the respective output ($p_{\tau_{j,t}}$) by the endogenous, bio-economically coupled parcel yield ($y_{j,t}$):

$$R_{j,t} = p_{\tau_{j,t}}\, y_{j,t}. \tag{6.6}$$

Note that commodity prices are assumed to be constant over time to avoid confounding the long-term simulation with short-term, year-on-year fluctuations. This assumption is consistent with empirical observations showing that real soybean prices exhibit no statistically significant trend within our region of interest and temporal horizon (see the Supplementary Materials for an in-depth discussion of this assumption). Consequently, the net operating profit for parcel j at time t—the definitive metric guiding subsequent cellular transition probabilities—is simply:

$$\pi_{j,t} = R_{j,t} - C_{j,t} \tag{6.7}$$

6.2.5 Land market and farm consolidation

Land transactions within the model are catalyzed by localized disparities in profitability. Operating through a decentralized land market, a given parcel j may be sold to a neighboring farm holding j' if the prospective buyer can extract a sufficiently higher economic return from the land. We evaluate this expected profit differential as follows:

$$\Delta\pi_{j,t} = \bar{\pi}_{j',t} - \bar{\pi}_{j,t} - C^{\text{conv}}_{\tau_j \to \tau_{j'}}, \tag{6.8}$$

Here, $\bar{\pi}_{j,t}$ and $\bar{\pi}_{j',t}$ denote the average realized profits, calculated across all productive land, for the owners of parcels j and j', respectively. The term $C^{\text{conv}}_{\tau_j \to \tau_{j'}}$ accounts for the frictional cost of converting the parcel to the buyer's specialized land use. This parameter is particularly crucial in the Cerrado context, where converting pastureland into mechanized cropland requires substantial upfront capital investments for soil correction, liming, and land preparation [369].

When the expected profit differential is positive ($\Delta\pi_{j,t} > 0$), the transaction becomes economically viable. The actual probability of land acquisition is then governed by:

$$\mathbb{P}_{j,t} = 1 - \exp\left(-\frac{\Delta\pi_{j,t}}{\zeta_{\text{acq}}}\right) \tag{6.9}$$

where ζ_{acq} modulates the overall sensitivity of the land market to these profit disparities.

This localized transition rule successfully endogenizes two defining spatial phenomena of the Brazilian agricultural frontier. First, it captures structural farm consolidation, as highly

capitalized, profitable operations systematically absorb adjacent parcels to maximize economies of scale [355]. Second, it drives market-mediated land-use reallocation—most notably, the widespread acquisition and conversion of extensive cattle pastures by mechanized crop producers, a transition that has fundamentally reshaped the Cerrado over the last two decades [359, 370].

6.2.6 Deforestation decision

Consistent with the empirical mechanics of frontier expansion (our analysis using the landscape representation presented in the Supplementary Materials reveals that more than 90% of the deforestation in the state of Goiás between 1995 and 2024 occurred in forest plots adjacent to established agricultural land), the model enforces a strict spatial adjacency constraint for the deforestation of natural plots: deforestation is only permitted when the targeted natural plots are contiguous with the existing productive matrix. This enforces a realistic, contagious percolation pattern that mirrors the infrastructural and logistical dependencies—such as road access and machinery transport—inherent to agricultural encroachment [371].

As with all decision mechanisms in the model, land clearing is probability-driven, evaluated through the expected economic gains of converting a natural cell into productive land. This transition probability is governed by:

$$\mathbb{P}_{j,t} = 1 - \exp\left(-\frac{I^{\text{tot}}_{j,t}}{\zeta_{\text{def}}}\right) \tag{6.10}$$

where ζ_{def} is a sensitivity parameter and $I^{\text{tot}}_{j,t}$ represents the total economic incentive which aggregates both immediate operational returns and broader asset dynamics, net of conversion costs and institutional risks:

$$I^{\text{tot}}_{j,t} = \bar{\pi}_{j,t} + p_{\ell,t} - C^{\text{def}}_{n\to\tau_{j,t}} - f_j \cdot \mathcal{P}_t \tag{6.11}$$

where $\bar{\pi}_{j,t}$ represents the average operational profit over the productive cells of the owner of cell j, $p_{\ell,t}$ is the annualized speculative asset appreciation of the land, $C^{\text{def}}_{n\to\tau_{j,t}}$ represents the direct, annualized clearing and preparation costs[1], and $f_j \cdot \mathcal{P}_t$ denotes the expected legal financial penalty associated with unauthorized or illegal deforestation.

The inclusion of the speculative asset appreciation ($p_{\ell,t}$) captures the potential capital appreciation realized when an unproductive natural plot is integrated into the active agricultural matrix. Empirical evidence from the Cerrado frontier demonstrates that speculative land markets operate alongside direct commodity production as a fundamental, structural driver of landscape clearance [372, 373]. To capture this phenomenon, $p_{\ell,t}$ evolves endogenously within the model as a function of the aggregate macroeconomic performance of the regional agricultural sector ($\tilde{\pi}_t$):

$$p_{\ell,t+1} = p_{\ell,t}\left(1 + \xi_\ell \frac{\tilde{\pi}_t - \tilde{\pi}_{t-1}}{\tilde{\pi}_{t-1}}\right) \tag{6.12}$$

where ξ_ℓ regulates the elasticity of land asset values relative to shifts in sector-wide profitability. This mathematical mechanism seamlessly couples localized, speculative deforestation pressures

[1] To maintain strict temporal alignment with the model's year-on-year operational returns , both the speculative capital appreciation of the land and the upfront deforestation costs are incorporated into the decision framework as annualized values.

with macro-regional commodity cycles. Consequently, it ensures that broader economic booms in agricultural productivity directly translate into increased land capitalization, accelerating the physical expansion of the frontier.

Finally, the expected environmental penalty is derived from the product of the financial fine for deforestation (f_j) and the exogenous probability of enforcement detection ($\mathcal{P}_{j,t}$)[2]. Crucially, this fine structure is dynamically tied to the farm's compliance with the Legal Reserve requirement (ω) mandated by the Brazilian Forest Code [319]. Letting $N_{j,t}$ denote the area of native vegetation remaining within the property holding, the specific fine applied to the farm is determined as:

$$f_j = \begin{cases} f_{\text{aut}} & \text{if } \frac{N_{j,t}}{L_{j,t}} > \omega, \\ f_{\text{ill}} & \text{if } \frac{N_{j,t}}{L_{j,t}} \leq \omega. \end{cases} \tag{6.13}$$

This formulation assumes that even legally compliant farmers (those retaining more vegetation than ω) often bypass complex formal authorization processes, thereby accepting a residual fine risk (f_{aut}). However, this baseline penalty is parameterized to be substantially lower—by an order of magnitude—than the punitive sanctions applied to strictly illegal, non-compliant deforestation (f_{ill}).

6.2.7 Intensification decision

Farmers may transition a parcel from conventional to intensified production systems if the expected economic uplift sufficiently offsets the substantial fixed capital investments required for adoption. Operating via the localized cellular automata rules, the probability of intensification is defined as:

$$\mathbb{P}_{j,t} = 1 - \exp\left(-\frac{\Delta\pi_{j,t}}{\zeta_{\text{int}}}\right) \tag{6.14}$$

To reflect the boundedly rational and myopic horizon of land managers, the potential economic gain from intensification ($\Delta\pi_{j,t}$) accounts exclusively for immediate operational returns, deliberately omitting long-term ecological degradation from the agent's localized decision calculus:

$$\Delta\hat{\pi}_{j,t} = R_{j,t}(1 + \alpha_{\tau_{j,t}}) - C_{j,t}(1 + \beta_{\tau_{j,t}}) - C^{\text{int}}_{\tau_{j,t}} \tag{6.15}$$

where $R_{j,t}$ and $C_{j,t}$ are the revenues and operating costs of parcel j, respectively. The parameters $\alpha_{\tau_{j,t}}$ and $\beta_{\tau_{j,t}}$ map the proportional increases in yield and costs associated with high-input management, while $C^{\text{int}}_{\tau_{j,t}}$ represents the fixed investment barrier required to upgrade the production system.

Importantly, this framework deliberately omits an automatic land-sparing assumption. Because farm-level resource reallocation is not mechanically constrained in our model, localized intensification actively elevates the marginal return to agricultural production, thereby inflating average farm profitability. This heightened profitability directly increases land asset values, which can paradoxically amplify the speculative incentives for further deforestation rather than relieving pressure on the natural matrix. This mechanism closely mirrors the well-documented rebound effect (or Jevons paradox) observed in tropical agricultural frontiers, where technological yield increases frequently catalyze, rather than curb, aggregate expansion [374–376].

[2]For more details on the prescription of this probability of detection, see the Supplementary Materials

6.2.8 Abandonment decision

Finally, the model accounts for the exit of land parcel from active agricultural production through an abandonment mechanism, a widespread phenomenon in the Cerrado [377]. In scenarios where the expected profitability of a parcel deteriorates significantly—mainly due to severe localized ecological degradation in our model—the land is probabilistically abandoned. This transition is governed by:

$$\mathbb{P}_{j,t} = \exp\left(-\frac{\pi_{j,t}}{\zeta_{\text{abn}}}\right) \tag{6.16}$$

6.2.9 Parameter specification and numerical experiments

We selected the state of Goiás as the empirical setting for this modeling exercise. Situated at the historical core of the Brazilian Center-West, Goiás provides an ideal microcosm for this study; over the past three decades, it has undergone profound and well-documented structural transitions, shifting from extensive cattle ranching to a highly capitalized, mechanized hub for global soybean production [373]. Furthermore, focusing the analysis within a single administrative boundary significantly streamlines the data collection required for model initialization and calibration, as it eliminates the need to harmonize different economic datasets and reporting standards across multiple state-level institutions.

The entire landscape of the state, encompassing over 340,000 km^2, is explicitly represented within the model at a spatial resolution of 25 hectares (500m $\times$ 500m). This resolution is deliberately chosen to approximate the scale of an individual agricultural field, providing a realistic spatial unit at which independent, localized management decisions are executed. Furthermore, to streamline the complex array of regional farming systems into the binary crop and pasture representation of the model, we use mechanized soybean and extensive cattle ranching as our strict biophysical and economic reference points. This simplification is empirically justified, as these two commodities overwhelmingly dominate the state's agricultural matrix, accounting for more than 80% of cultivated cropland and 99% of pastoral land use in 2025[3], respectively.

The simulation timeframe spans from 1995 to 2050, partitioned into a historical calibration phase (1995–2024) and a future projection window (2025–2050). Following an initialization phase where the spatial information layers are mapped to the 1995 conditions (as detailed in the Supplementary Materials), the model evolves dynamically using parameters defined to reproduce historical economic trends and spatial land-use patterns. To this end, a rigorous, multi-tiered calibration strategy is adopted that combines direct empirical assignment, literature-derived constraints, and dynamic fitting. First, ecological parameters—such as biophysical degradation and restoration rates, the localized scaling of ecosystem service provision, and the precise yield penalties associated with habitat fragmentation—are anchored using established empirical evidence and widely adopted values from the agroecological literature[4]. Similarly, baseline economic parameters with direct real-world counterparts, including per-hectare clearing costs, fixed intensification investments, and expected yield gains, are explicitly assigned using historical agricultural data. Parameters governing strictly exogenous macroeconomic processes, such as commodity output prices, baseline technological advancement, and institutional

[3] A similar, albeit less pronounced, share is evident in 1995 at the beginning of our analysis.

[4] Exhaustive details regarding parameter choices, calibration mechanics, and specific literature sources are provided in the Supplementary Materials.

enforcement probabilities, are fitted directly to observed time series and historical policy regimes. Finally, the behavioral sensitivity parameters that govern the probabilistic cellular automata transitions—namely land acquisition, deforestation, intensification, and abandonment—are iteratively calibrated. This ensures the model accurately reproduces observed macro-scale land-use trajectories and structural changes in the Cerrado over the calibration period. Note: to maintain temporal consistency across the 1995–2050 simulation horizon, all monetary values are deflated to real 2010 U.S. dollars using historical price indices.

We then explore the emergent dynamics of the system through extensive numerical experiments. Because the spatial transitions are driven by localized probabilistic algorithms, the model is evaluated using a Monte Carlo approach; unless otherwise stated, all reported results reflect the ensemble average across multiple independent simulation runs to ensure statistical robustness. The primary analytical benchmark is the baseline scenario, which represents a business-as-usual (BAU) trajectory generated using the historically calibrated parameter set.

Against this baseline, we introduce three counterfactual policy frameworks that are currently at the center of the conservation debate for the Cerrado biome. Specifically, we simulate the implementation of a targeted agricultural subsidy removal program—a policy-lever penalty mirroring the market exclusion mechanics of the Amazon Soy Moratorium [311]—as well as the introduction of Payments for Environmental Services (PES) aimed at forest preservation [378]. These PES frameworks are evaluated under two distinct structural designs: an untargeted, biome-wide subsidy and a spatially targeted intervention prioritizing critical ecological corridors. Because these policies interact endogenously with the existing bio-economic architecture of the model, they allow for a robust ex-ante evaluation of how structural agricultural dynamics, land markets, and localized profitability respond to targeted conservation interventions.

6.3 Results

Historical calibration and the mechanics of expansion

Before analyzing the long-term future projections, it is crucial to establish the empirical validity of the framework by evaluating its performance during the historical calibration phase (1995–2024). Historically, the Cerrado biome underwent an extensive spatial reorganization, characterized by the persistent retreat of native vegetation as the agricultural frontier advanced. The model successfully captures this macroscopic reality. It faithfully reconstructs the spatial footprint of this expansion, dynamically reallocating land to both extensive pasture and mechanized cropland at rates that align closely with observed historical data (see Fig. 6.1a–d).

Beyond mapping spatial footprints, a valid model must capture the underlying economic drivers of this expansion. Historically, the Brazilian Center-West experienced significant technological advancement [302] and structural land consolidation [373], which substantially increased per-hectare revenues. The simulation proves capable of replicating this intensive margin. It correctly tracks both the historical growth in crop and pasture yields (Fig. 6.1f–g) and the consolidation of large farm ownership (detailed in the Supplementary Materials), resulting in simulated net operating profits by 2025 that reach approximately \$200[5] per hectare for cropland (a three-fold increase relative to 1995) and \$65[6] per hectare for pasture (a two-fold increase), well

[5]All monetary quantities are denominated in real 2010 USD. This approximately corresponds to 1,500 real BRL of 2025.

[6]All monetary quantities are denominated in real 2010 USD. This approximately corresponds to 500

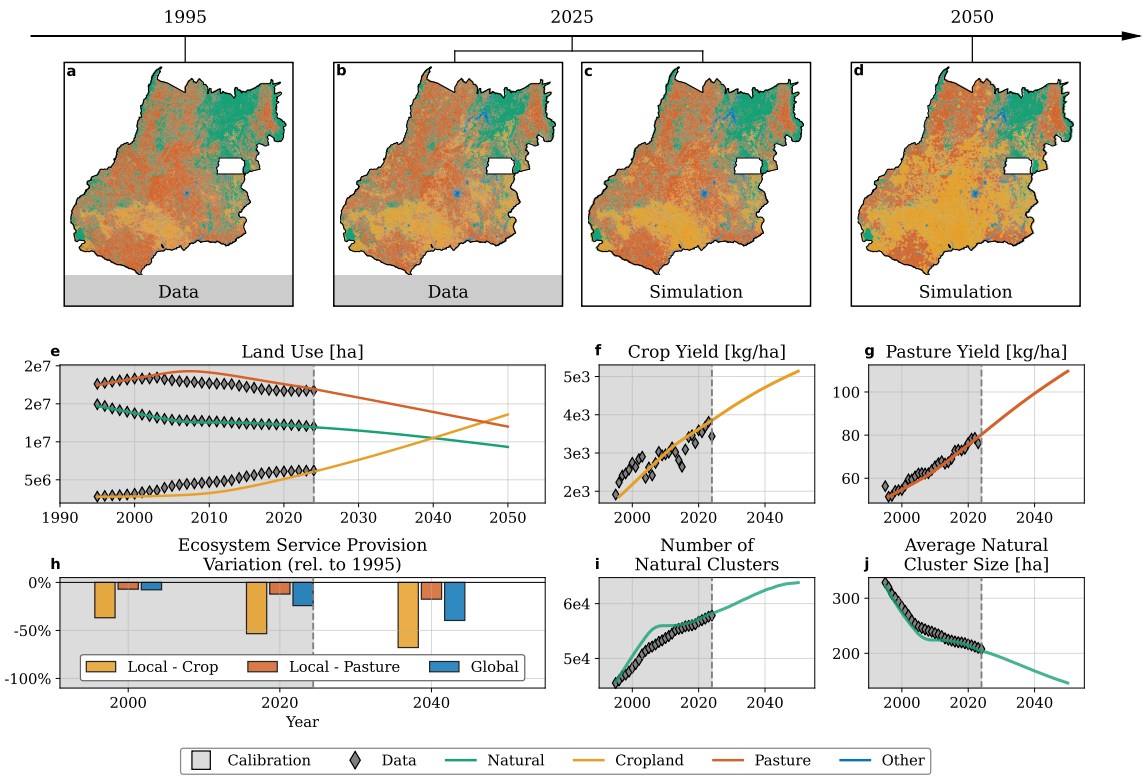


Figure 6.1 Historical calibration (1995–2024) and Business-as-Usual projections (2025–2050) of land-use change and bio-economic dynamics. **(a–d)** Spatial comparison of observed data and model simulations tracking land-use distribution across the biome. The maps illustrate the spatial evolution of areas categorized as Natural, Cropland, Pasture, and Other. Panels (a) and (b) display historical data, while panels (c) and (d) display the simulated spatial configurations for the end of the historical calibration period (2025) and the Business-as-Usual projection (2050), respectively. **(e)** Aggregate macroscopic land-use trajectories (in hectares) from 1995 to 2050, delineating both the historical phase and the subsequent BAU simulation. **(f–g)** Historical growth and projected continuation of Crop and Pasture yields (kg/ha), reflecting the sustained capitalization of the agricultural sector. **(h)** Simulated variation in Ecosystem Service Provision relative to the 1995 baseline, highlighting the structural divergence between the gradual decline of localized services and the severe reduction of global macro-climatic services during the projection phase. **(i–j)** Macroscopic quantification of ecological fragmentation from 1995 to 2050, mechanically captured by the simultaneous rise in the total number of isolated natural clusters and the corresponding sharp decline in their average size.

aligned with reported values [379, 380]. By successfully mirroring these profit spikes, the model validates its core feedback loop: heightened localized productivity inflates expected operational profits and aggregate land asset appreciation (Eq. 6.12), which in turn drives the endogenous probability of further deforestation.

real BRL of 2025.

Furthermore, empirical literature shows that historical expansion was not uniform; it was segmented by intended land use and legal compliance, with pasture often serving as a low-cost speculative vehicle [295, 381]. The model accurately endogenizes these complex, localized incentives. By explicitly stratifying the economic returns of clearing based on conversion costs and the calculated financial risks of environmental fines, the model replicates the real-world dynamic where illegal clearing is penalized while legal clearing remains highly profitable (Fig. 6.2b). Consequently, the simulation successfully reproduces the historical reality: because a reservoir of legally deforestable land remains under the ownership of pasture operators (see Fig. 6.2d,e), the volume of legal clearing potential blunts the impact of strictly enforced anti-deforestation governance (such as the federal policy shifts introduced in 2023–2024).

Finally, it is well documented that this rapid historical intensification came at the cost of ecological degradation [349] which the simulation faithfully recreates. By dynamically tracking the rising total number of isolated natural clusters (Fig. 6.1i) and the corresponding marked decline in average natural patch size (Fig. 6.1j), the model mechanically mirrors the physical fragmentation of the native matrix. Ultimately, this simulated fragmentation, combined with the absolute loss of native land cover, drives an endogenous decline in both localized and global ecosystem services within the model (see Fig. 6.1h). Demonstrating the framework's ecological fidelity, this simulated deterioration translates into a potential crop yield penalty of approximately 6%—a figure that aligns with recent independent empirical estimates [316, 346].

6.3.1 Business-as-usual projections (2025–2050)

Having established the model's accuracy during the historical period, we now project the biome's trajectory through 2050 under a Business-as-Usual (BAU) scenario. Assuming no major changes in global commodity prices or domestic environmental enforcement (because our analysis focuses on the general mechanisms driving structural expansion, we explicitly abstract away from short-term, year-on-year volatility in these variables, providing a comprehensive sensitivity analysis in the Supplementary Materials), the model predicts a clear continuation of historical trends, along with the emergence of new economic and ecological thresholds.

At the macro-scale, the projected land-use trajectories (Fig. 6.1e) show a continuous loss of the remaining natural areas. Similar to the historical phase, native Cerrado vegetation steadily declines as agricultural and pasture lands expand. This physical expansion is matched by ongoing productivity growth; projected pasture yields (Fig. 6.1g) rise alongside crop yields, reflecting continuous investment in the region's agricultural sector over the next three decades. Furthermore, the BAU projections show that the "secondary frontier"—where land initially cleared for pasture is later converted into mechanized cropland—will operate exactly as it did in the past (Fig. 6.2f). The large scale of this delayed conversion highlights a core dynamic in the Cerrado: extensive cattle ranching often serves as a temporary, speculative phase. Once ranchers absorb the initial costs of clearing and soil preparation, highly capitalized crop producers purchase these consolidated lands. Under the BAU scenario, this two-stage succession accelerates, ensuring that the advancing pasture frontier eventually becomes a permanent, intensive agricultural zone by 2050 (Fig. 6.1d).

While these broad patterns of expansion remain consistent, the underlying economic drivers shift gradually. Fig. 6.2a shows that even as the available forest shrinks, clearing rates actually increase over time. This acceleration is driven by the rising profitability of deforestation (Fig. 6.2c). The expected financial returns for land clearing keep growing over time, continuing to encourage both farming expansion and land speculation despite local ecological damage.

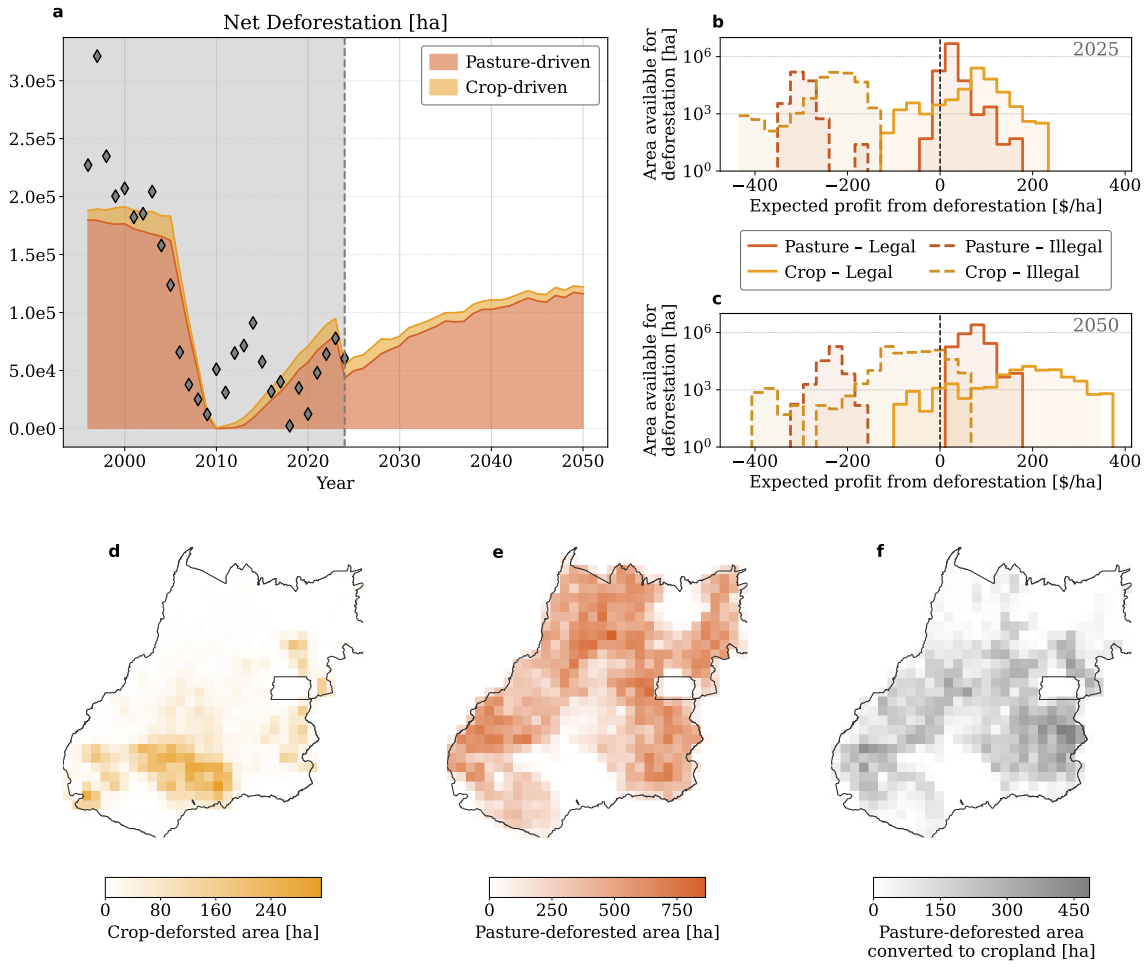


Figure 6.2 Economic drivers and spatial dynamics of historical and projected deforestation. **(a)** Aggregate net deforestation[a] trajectories by proximate driver (2000–2050), highlighting the persistent dominance of pasture expansion and accelerating gross clearing rates toward mid-century. **(b–c)** Expected profitability of deforestation for native parcels, segmented by intended use and legal compliance. While fines keep illegal clearing unprofitable in the 2025 baseline (b), compounding yields and asset appreciation push expected returns for illegal clearing into strictly positive territory by 2050 under BAU (c). **(d–e)** Spatial distribution of cumulative crop- and pasture-driven deforestation. **(f)** Mapping the 2050 "secondary frontier," tracking the subsequent conversion of pasture into mechanized cropland to confirm the biome's two-stage land-use succession.

[a]Net deforestation is defined as the year-on-year difference in natural land. While our model includes an abandonment mechanism, it imperfectly captures the dynamic mosaic of continuous land-use transitions—a localized complexity that also challenges precise empirical classification.

Crucially, in a major change from the historical period, the projected profitability of illegal clearing eventually becomes positive. As rising yields and overall sector profitability drive up land prices, the expected economic gains begin to outweigh the risks of environmental fines

(which we assume remain constant at the historically high level of 2024). This shift turns illegal deforestation from a financial risk into a profitable enterprise, posing a serious threat to future conservation efforts.

By mid-century, this unchecked expansion leads to distinct ecological consequences. We observe a clear divergence in the degradation of ecosystem services: while local services decline gradually—temporarily buffered by the frontier's persistent percolation into native areas, which initially boosts the flow of local services into the expanding agricultural landscape—global macro-climatic services face a substantial reduction. As continuous natural areas are broken apart, regional moisture recycling and climate regulation approach a 50% reduction relative to 1995 in terms of ecosystem services provision. Although these simulated values are approximations, the magnitude of the projected drop, along with the importance of climate regulation for the agricultural sector of Goias [345], highlights the need for behavioral shifts and comprehensive policy portfolios designed to stop environmental degradation. To address this challenge, we explore two policy options currently under discussion: (i) distributing Payments for Environmental Services (PES) to preserve remaining forests, and (ii) revising current agricultural subsidies that inadvertently encourage deforestation.

6.3.2 Policy counterfactuals: Efficacy and bio-economic synergies

To address the ecological degradation projected under the BAU trajectory, we evaluate the ex-ante efficacy of four distinct conservation frameworks. We structure this analysis sequentially, beginning with structurally simple interventions and building toward a synergistic policy portfolio.

The first intervention we simulate is an untargeted, random distribution of Payments for Environmental Services (PES) designed to incentivize forest preservation[7]. As shown in Fig. 6.3a, this baseline approach achieves a modest, albeit functional, reduction in total deforestation relative to the BAU scenario. However, because the subsidies are distributed arbitrarily across the landscape (Fig. 6.3d), the policy fails to prevent the structural percolation of the agricultural frontier into the native matrix. Consequently, it actually results in a slight increase in landscape fragmentation (measured via patch density[8] in Fig. 6.3b) and offers only marginal improvements to agricultural yields (Fig. 6.3c), as the scattered preserved pixels (Fig. 6.3e) fail to generate meaningful ecological buffers.

To correct this structural flaw, we next simulate a spatially targeted PES distribution[9]. Rather than scattering funds arbitrarily, this policy seeks to prevent frontier percolation; by prioritizing highly connected parcels, it actively constructs a physical barrier that seals the frontier and blocks the pathways through which agricultural expansion typically leaks (Fig. 6.3f). This spatial

[7]Specifically, the simulation identifies native parcels at risk of deforestation in 2025—defined by their spatial proximity to active agricultural production—and randomly designates 250,000 hectares as eligible for compensation if preserved. For methodological simplicity and to establish a lower-bound estimate of policy efficiency, the spatial allocation of these eligible plots remains static throughout the 2025–2050 projection period. The baseline subsidy payout is parameterized at $80 per hectare, closely mirroring the financial structures of emerging regional initiatives. Notably, the state of Goiás began implementing a structurally analogous PES framework in 2025 under the *Cerrado em Pé* program.

[8]Patch density is defined as the total number of contiguous natural clusters divided by the total natural area.

[9]Under this targeted framework, eligible parcels are selected from the initial pool of deforestable plots by prioritizing natural pixels that possess the highest number of adjacent forested neighbors. In cases where parcels share an identical number of forest neighbors, the final selection is randomized.

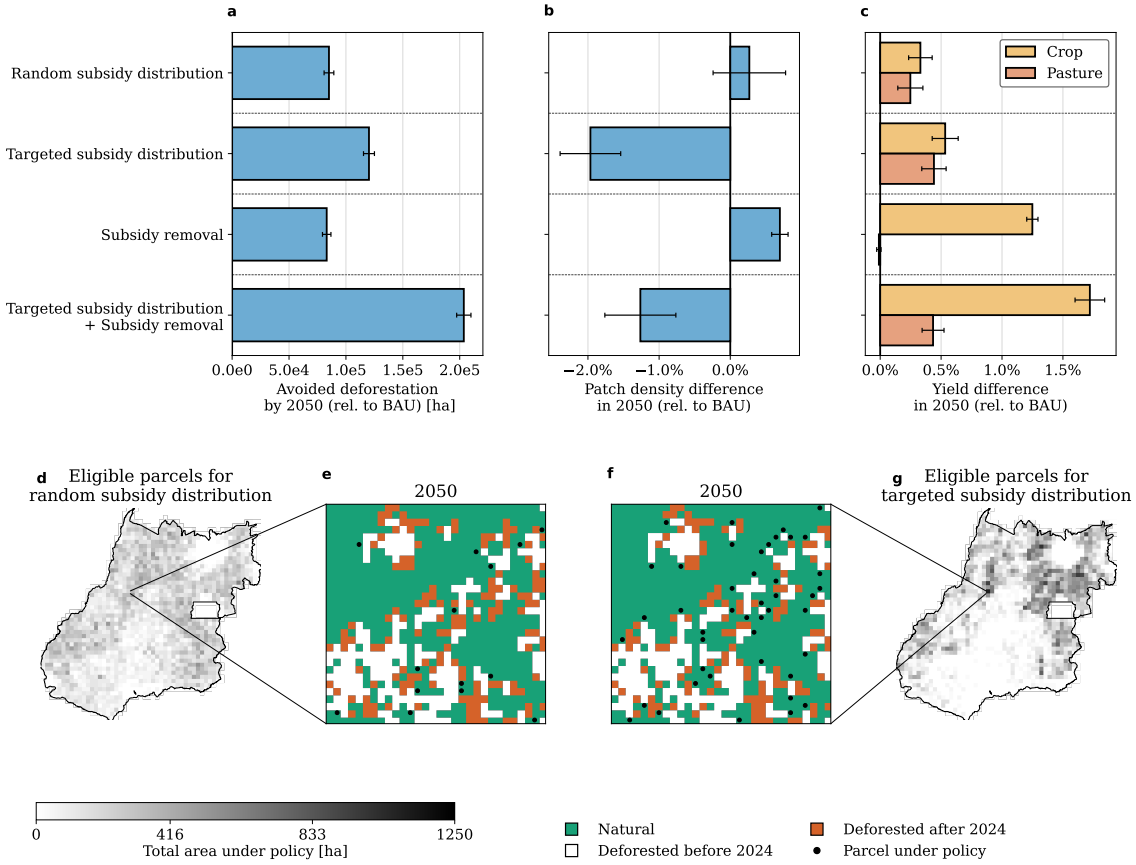


Figure 6.3 Ex-ante evaluation of conservation policy counterfactuals and bio-economic synergies (2025–2050). **(a)** Absolute volume of avoided deforestation (in hectares) relative to the Business-as-Usual (BAU) baseline for four simulated interventions: random PES distribution, spatially targeted PES distribution, post-2024 agricultural subsidy removal, and a synergistic combined portfolio. **(b)** Impact on landscape fragmentation, measured as the percentage difference in patch density relative to BAU. Targeted distributions successfully minimize fragmentation by preventing frontier percolation, whereas random allocation and standalone subsidy removal result in increased patch density. **(c)** Endogenous yield improvements for mechanized crop and pasture systems relative to BAU. The combined policy maximizes these systemic yield increases by optimizing the structural preservation of localized ecosystem services alongside constraints on horizontal expansion. **(d, g)** Biome-scale spatial allocation of eligible conservation parcels under the random (d) and spatially targeted (g) subsidy frameworks. **(e, f)** Localized spatial dynamics in 2050 illustrating the percolation mechanism. Panel (e) demonstrates how the expanding agricultural frontier bypasses isolated, randomly distributed protected parcels (black dots). Conversely, panel (f) shows how targeting highly sensible parcels actively constructs physical barriers, sealing the frontier and preserving contiguous blocks of native vegetation.

targeting drives substantially improved conservation outcomes, increasing the total volume of avoided deforestation by 1.5× compared to the random allocation (Fig. 6.3a). Furthermore, by successfully preserving contiguous blocks of vegetation, the targeted policy drastically reduces patch density and landscape fragmentation (Fig. 6.3b). This structural preservation is vital because it maintains the flow of micro-climate regulation, which in turn generates higher endogenous yield improvements for both mechanized crop and pasture systems relative to the untargeted baseline (Fig. 6.3c).

While targeted subsidies are effective at preserving the native matrix, implementing them at the biome scale requires substantial financial resources. To theoretically fund this conservation effort—and to simultaneously dismantle the economic incentives driving frontier expansion—we simulate a third policy: the targeted removal of existing agricultural subsidies. Mirroring the mechanics of a zero-deforestation supply chain agreement (such as a "Soy Moratorium"), this intervention actively penalizes new land clearing by stripping domestic agricultural subsidies from any crop parcel deforested after the baseline year of 2024[10]. As a standalone measure, this penalty works reasonably well, achieving avoided deforestation levels comparable to the random PES distribution (Fig. 6.3a). Interestingly, by constraining easy horizontal expansion, it forces localized capitalization, resulting in a substantial boost to crop yields (Fig. 6.3c), even though it still leaves the remaining natural matrix highly fragmented (Fig. 6.3b).

Finally, we evaluate a comprehensive policy portfolio that combines both the targeted PES distribution and the post-2024 subsidy removal. This combined approach leverages the unique strengths of both mechanisms: the moratorium-style penalty generates the spatial constraints (and theoretical fiscal savings) necessary to halt aggressive agricultural sprawl, while the targeted subsidies actively preserve the vital ecological corridors. As demonstrated across all metrics, this synergy delivers the optimal bio-economic outcome. It achieves the highest absolute volume of avoided deforestation (Fig. 6.3a) and maximizes the systemic yield increase—approaching an additional 1.5% for crops and 0.5% for pasture relative to the BAU baseline (Fig. 6.3c).

6.3.3 Policy optimization: Maximizing bio-economic efficiency

Having established the structural superiority of the combined policy portfolio, we next seek to optimize its design. A viable conservation framework must be not only ecologically effective but also fiscally efficient. To determine this optimal balance, we perform a sensitivity analysis on the combined policy (targeted subsidies implemented on top of post-2024 subsidy removal). We systematically vary two core parameters: the financial intensity of the program (the targeted subsidy payout per hectare) and its spatial footprint (the total eligible area for conservation).

The macroscopic cost-efficiency of these configurations is mapped in Fig. 6.4a, which calculates the ultimate "cost of avoided deforestation" (total allocated budget divided by the net hectares of preserved forest). The heatmap reveals a distinct optimal configuration.

[10]Implementing this policy framework requires several simplifying assumptions. First, we assume all mechanized crop operations utilize the primary form of domestic agricultural subsidy (subsidized interest rates for capital investment). Second, we assume this financial support is distributed uniformly across all crop parcels, parameterized at $80 per hectare (approximately 600 BRL of 2025). The policy scope strictly applies to parcels classified as natural vegetation in the 2024 baseline. Mechanically, this $80/ha penalty is explicitly factored into both the expected revenue of deforestation (Eq. 6.11 and the profit differentials in land market transactions (Eq. 6.8). If an agent proceeds with clearing a post-2024 natural parcel despite the penalty, the baseline operational costs for that specific plot are permanently increased by $80/ha to reflect the loss of subsidized credit (Eq. 6.7).

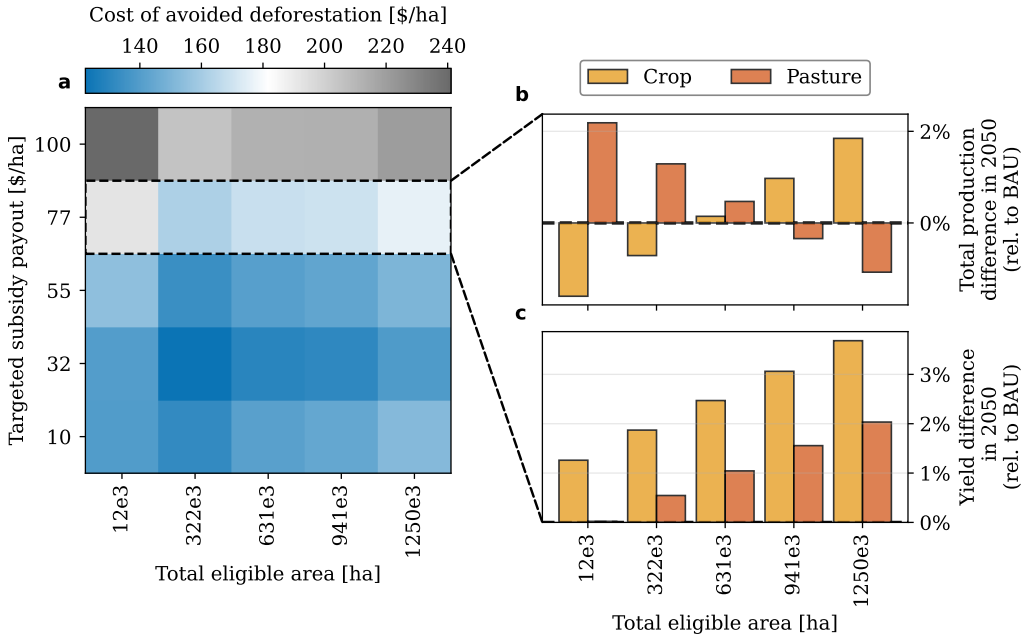


Figure 6.4 Optimization of the combined conservation policy across financial and spatial dimensions. **(a)** Macroscopic cost-efficiency heatmap, calculating the ultimate cost of avoided deforestation across varying targeted subsidy payouts and total eligible conservation areas. The parameter space reveals a distinct efficiency frontier at intermediate financial intensities (the \$32/ha tier), minimizing the cost per preserved hectare before the inclusion of less strategic land inherently drives marginal costs upward. **(b–c)** Structural trade-offs and bio-economic dividends of expanding the physical conservation network, holding the subsidy payout fixed close to the current baseline ($\approx$ 80\$/ha). Panel (c) tracks endogenous yield improvements relative to the Business-as-Usual (BAU) scenario, demonstrating monotonically increasing ecological dividends for both sectors as larger contiguous areas are preserved. Panel (b) isolates the resulting shifts in aggregate production. While smaller conservation footprints initially penalize total crop production due to the subsidy removal policy (Soy moratorium like), expanding the network to its maximum extent generates yield boosts (seen in panel c) that overcompensate for the loss of expansible land, ultimately driving total crop production above BAU levels at the costs of pasture.

Unsurprisingly, setting the subsidy payout too high (*e.g.*, \$100/ha) results in fiscal inefficiency, driving the cost of avoided deforestation to nearly \$200 per hectare. Conversely, intermediate payout levels—specifically around the \$35/ha threshold—achieve optimal financial leverage, minimizing the cost per preserved hectare across the entire spectrum of spatial footprints.

By fixing the subsidy payout, we can isolate the bio-economic effects of physically expanding the conservation network (the total eligible area). Initially, expanding the network increases cost-efficiency, as incorporating a critical mass of geographically localized patches is necessary to generate meaningful ecological barriers. However, this efficiency does not scale indefinitely. Because the spatial targeting mechanism first prioritizes the parcels most critical for preventing

percolation, expanding the program beyond a certain threshold forces the inclusion of less strategic land. Consequently, the marginal cost per effectively preserved hectare begins to rise once the network expands beyond these vital core corridors. According to our model, this dynamic establishes an optimal program size of approximately 300,000 hectares.

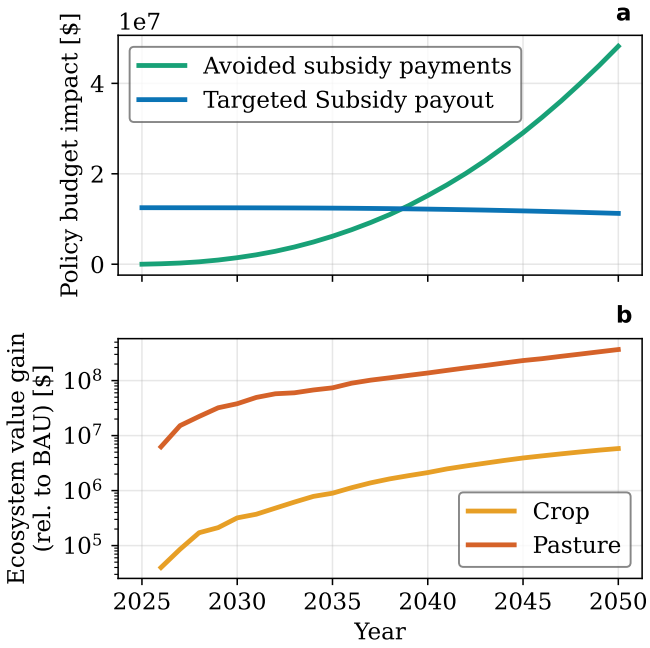


Figure 6.5 Fiscal dynamics and monetized ecological dividends of the optimized conservation policy. **(a)** Annual policy budget impact. Compounding savings from targeted subsidy removal offset the stable conservation payout costs by the late 2030s, generating a net public surplus. **(b)** Economic value of preserved ecosystem services relative to BAU (logarithmic scale). Preserving native corridors maintains localized ecological buffers, translating directly into protected, compounding revenue for both crop and pasture sectors.

To contextualize the impact of this optimal footprint, we must analyze the complex structural trade-offs it imposes on aggregate agricultural production (Fig. 6.4b–c). At smaller conservation footprints, spatial restrictions disproportionately penalize crop producers; total crop production falls relative to BAU. Meanwhile, pasture—serving as a more flexible, low-cost frontier—temporarily absorbs the remaining available land, driven in part by the paired subsidy removal policy that heavily targets mechanized crops. However, a distinct structural shift occurs as the conservation network continues to expand. The ecological benefits of preserving the native matrix become pronounced enough to overcompensate for the loss of expansible land. Total crop production rebounds and ultimately surpasses BAU levels, driven entirely by ecologically intensified yields rather than areal expansion. Notably, the model identifies an equilibrium threshold—a "sweet spot"—where both crop and pasture production simultaneously experience net increases. If the conservation network is expanded further past this point, land constraints tighten and total pasture production ultimately falls behind BAU levels.

Crucially, this optimal production equilibrium is structurally dependent on the simultaneous implementation of the subsidy removal policy. The yield improvements generated by the preserved ecosystem increase the underlying profitability of crop production. Without an accompanying penalty mechanism, such heightened profitability would inevitably incentivize agricultural operators to encroach further upon pristine native areas, exploiting the superior yields generated by local ecosystem services (Eq. 6.12). As established under the BAU scenario (Fig. 6.2c), the expected financial returns of clearing land eventually turn positive even when accounting for the penalties of illegal deforestation. Therefore, relying exclusively on targeted subsidies would fail to prevent highly capitalized producers from exploiting their inflated margins. The paired subsidy removal is strictly necessary to constrain this expansion and

prevent the conservation network from inadvertently inducing further frontier encroachment.

6.3.4 Fiscal feasibility and the monetization of ecological dividends

To establish the long-term viability of the optimized conservation portfolio, we must analyze its temporal fiscal dynamics and its broader economic impact on the agricultural sector. A primary criticism of large-scale Payments for Environmental Services (PES) is the enduring burden they place on public budgets. However, by explicitly coupling the targeted PES network with the post-2024 subsidy removal, the model projects a highly sustainable, self-funding financial trajectory.

Fig. 6.5a tracks the annual policy budget impact over the projection window. The direct fiscal cost of the targeted conservation network—represented by the annual subsidy payout—remains highly stable at approximately $10 million per year. Conversely, the policy's penalty mechanism generates compounding fiscal savings. By legally stripping existing domestic agricultural subsidies from any parcel deforested after 2024, the state avoids substantial future payouts. As the simulation progresses and the theoretical frontier attempts to expand, these avoided subsidy payments grow exponentially. By the late 2030s, the annual savings completely offset the cost of the PES payouts, pushing the policy past its fiscal break-even point. By 2050, the avoided payments reach approximately $50 million annually, transforming the conservation framework from a perceived fiscal liability into a net surplus for the public budget.

Beyond generating direct public savings, this policy portfolio produces compounding economic value for the private agricultural sector itself. Fig. 6.5b explicitly quantifies the monetized ecosystem value gain relative to the BAU baseline. This metric captures the direct financial dividends of the policy portfolio established in the previous section. By preserving contiguous native vegetation, the policy sustains environmental services—such as micro-climate regulation, soil moisture retention, and pest control—that organically buffer and boost agricultural yields.

Because these ecological buffers increase agricultural yield on existing farmland, their preservation translates directly into protected agricultural revenue. Over the projection period, the economic value of these ecological services grows exponentially for both agricultural matrices. For the extensive pasture sector, the monetized value of these preserved ecosystem services eclipses $100 million annually by mid-century. Similarly, the mechanized crop sector realizes compounding financial benefits that gets close to $10 million per year.

6.4 Discussion

6.4.1 Systemic evaluation of frontier dynamics

The Brazilian Cerrado stands at a critical juncture, representing one of the most intense frontiers of global agricultural expansion. The central challenge lies in reconciling the profound economic drivers of this expansion—characterized by highly capitalized, large-scale commodity production [306]—with the urgent need to halt the structural degradation of the biome's native matrix [316, 382]. As our historical analysis demonstrates, the unchecked advance of the agricultural frontier not only fragments vital ecological corridors but systematically reduces ecosystem services provisions, such as micro-climate regulation and moisture recycling, upon which long-term agricultural resilience depends.

To address this fundamental tension, this study introduced a novel spatially explicit bio-economic framework. The value of this integrated approach lies in its ability to strip away unnecessary complexity while retaining strict empirical grounding. Because the spatial and economic parameters were tightly calibrated to historical land-use patterns, fragmentation, and farm size distributions (1995–2024), the framework successfully bridged the gap between macroscopic policy goals and micro-level agricultural realities. Rather than relying on the macro-level abstraction of IAMs or getting bogged down in the micro-complexity of full-size ABMs, this empirically grounded approach provides a highly tractable environment to assess the exact behavioral shifts and spatially targeted policy portfolios urgently required to halt environmental degradation.

Through this analytical lens, we demonstrated that the persistent advance of the agricultural frontier is fundamentally driven by a highly capitalized, two-stage land-use succession. Initially, extensive cattle pasture serves as a low-cost, speculative vehicle to clear land and establish spatial footprints, which is subsequently consolidated and converted into highly mechanized cropland. This two-stage dynamic of indirect land-use change and frontier capitalization is well documented in the empirical literature [311, 373, 383], where pasture expansion frequently paves the way for intensive soy production by minimizing the opportunity costs of initial clearing.

Projecting these dynamics under a Business-as-Usual (BAU) scenario reveals a concerning structural threshold. As agricultural capitalization compounds and regional infrastructure improves, the expected financial returns from land clearing begin to systematically outweigh the parameterized financial risks of environmental fines. Consequently, illegal deforestation transitions from a penalized risk to a strictly profitable enterprise. It is precisely this threshold that necessitates intervention. Our framework allows us to rigorously determine not only the spatial effectiveness of proposed policy instruments—such as payment for forest preservation—but whether the long-term, monetized economic benefits derived from these conservation initiatives truly outweigh their structural costs.

6.4.2 The structural necessity of spatial targeting

Evaluating these ex-ante interventions reveals that the spatial configuration of conservation policies is just as critical as the financial incentives driving them. In highly dynamic agricultural frontiers, achieving environmental stability fundamentally requires actively sealing the geographic pathways of encroachment. Untargeted approaches—such as spatially arbitrary Payments for Environmental Services (PES)—fail to achieve this constraint. When conservation funds are scattered randomly across a landscape, they leave the broader topological connectivity of the expansible land matrix intact. Consequently, driven by the path of least economic resistance, the agricultural frontier simply flows around these isolated protected patches. This phenomenon mirrors a percolation process: the advancing agricultural matrix exploits unprotected gaps, resulting in continued structural fragmentation and edge-effect degradation rather than genuine ecological preservation [117, 384, 385].

Spatial targeting directly resolves this vulnerability by transforming conservation from a passive financial subsidy into an active structural defense. By deliberately anchoring interventions to highly sensitive native parcels, targeted policies act to sever the pathways of agricultural expansion. This strategic allocation constructs physical, localized barriers that block frontier percolation. Crucially, this geometric constraint is essential for preventing the "leakage" effect—a common policy failure where deforestation is not halted, but merely displaced to adjacent, less protected pixels [386].

Ultimately, prioritizing these critical spatial nodes does more than just arrest horizontal land-use conversion. It is the only effective methodology to preserve the contiguous ecological corridors necessary for the biome's survival. Maintaining these unbroken tracts of native vegetation is vital to sustaining the macro-climatic regulation, moisture recycling, and localized agroecological services that underpin long-term agricultural resilience.

6.4.3 Structuring a synergistic policy portfolio

Optimal conservation outcomes are strictly dependent on a synergistic policy portfolio. By anchoring PES eligibility in highly exposed native parcels, the state can actively construct physical ecological barriers that prevent frontier percolation. Maintaining these contiguous corridors is critical; preserving the structural integrity of tropical and savanna ecosystems sustains the hydrological cycles, pest control, and localized climate regulation that organically buffer and boost adjacent agricultural yields [312, 316].

Crucially, however, our simulation reveals a dangerous bio-economic feedback loop: the preservation of these ecosystem services generates endogenous yield improvements, which inadvertently inflate the profitability of mechanized crop production. If left unchecked, agricultural operators would exploit these inflated margins, utilizing their increased profits to encroach further into pristine areas to capture even higher localized ecosystem benefits.

Therefore, to prevent the conservation network from inadvertently inducing its own frontier expansion, the targeted subsidy distribution must be paired with a strict penalty mechanism. Specifically, the targeted removal of domestic agricultural subsidies for any land deforested post-2024 strips away the cheap capital necessary for this secondary encroachment. By legally and financially constraining highly capitalized operators, this paired approach ensures that the yield improvements generated by conservation drive localized intensification rather than horizontal expansion.

6.4.4 Maximizing bio-economic efficiency and fiscal sustainability

Our optimization analysis reveals that a precisely calibrated conservation network fundamentally redefines the traditional zero-sum trade-off between ecological preservation and agricultural output. While expanding the protected area initially imposes a spatial penalty on agricultural producers by constraining the expansible frontier, this limitation is superseded by emergent ecological feedbacks. Upon reaching a critical programmatic footprint, the localized yield dividends generated by the preserved ecosystems systematically overcompensate for the opportunity cost of lost expansible land.

This dynamic reveals a critical structural synergy within the landscape. As the conservation network expands to its optimal programmatic footprint, it reaches a bio-economic "sweet spot" where the localized yield improvements generated by the preserved ecosystems overcompensate for spatial restrictions across both primary sectors. At this threshold, rather than facing displacement, both total crop production and pasture output simultaneously surpass their Business-as-Usual (BAU) levels through endogenous ecological intensification. This finding quantitatively corroborates the emerging ecological consensus: when governed by robust spatial constraints and the active integration of ecosystem services, commodity agriculture and conservation can co-exist to drive absolute, multi-sector productivity gains without necessitating further deforestation [387–389].

Furthermore, this paired policy framework guarantees long-term fiscal viability. By structurally linking conservation payouts to the punitive removal of agricultural subsidies on newly cleared land, the policy establishes a self-financing mechanism. Over the projection horizon, the compounding public savings derived from these avoided subsidies progressively eclipse the direct operational costs of the targeted PES network. Consequently, the conservation apparatus transcends its initial financial burden, transforming into a net fiscal surplus for the public budget by mid-century.

6.4.5 Methodological limitations and future research

While this framework provides a robust macroscopic mechanism for evaluating bio-economic policies, the findings must be interpreted within the context of several structural simplifications and methodological limitations. A transparent acknowledgement of these boundaries is necessary to guide future empirical extensions.

First, the model operates under simplified assumptions regarding macro-economic volatility. Exogenous factors such as global commodity prices and domestic inflation are smoothed over the projection period. In reality, the Brazilian agricultural sector is highly sensitive to international trade dynamics and exchange rate fluctuations [382]. Future iterations of the model should incorporate realistic price time-series to determine how short-term commodity dynamics could temporarily impact the penalty structures of the optimized policy portfolio.

Second, the behavioral mechanics of the simulated agents rely on a framework of relatively perfect information regarding policy parameters. The simulation assumes that agricultural operators accurately price in the expected cost of environmental fines and the loss of subsidized credit. In practice, land-use decisions in frontier regions are frequently influenced by systemic institutional friction, varying levels of localized enforcement, and speculative land-grabbing behaviors that may not strictly adhere to our simplifications.

Third, the ecological feedbacks embedded within the model represent necessary approximations of highly complex, non-linear Earth system dynamics. While the translation of patch density and natural cluster size into ecosystem service provision aligns with current empirical estimates, the model simplifies the temporal lag of ecological degradation and recovery. The localized yield penalties associated with the loss of micro-climate regulation may be subject to abrupt ecological tipping points that are difficult to parameterize. Future research should prioritize integrating more granular eco-hydrological models to refine the bounds of these localized yield dividends.

Ultimately, given these methodological boundaries, the outcomes of this bio-economic framework should not be interpreted as strictly deterministic forecasts of future land-use trajectories or precise fiscal audits. Rather, the model's true heuristic value lies in its capacity to isolate structural vulnerabilities and evaluate the relative efficacy of interacting policy mechanisms. Policymakers and researchers should utilize these results as a virtual laboratory to understand directional trends—specifically, identifying the dangerous tipping points where compounding agricultural capitalization overrides environmental penalties, and mapping the necessary synergistic conditions under which conservation can successfully drive economic value creation. By illuminating the underlying systemic mechanics that govern frontier expansion, this framework provides a robust, empirically grounded compass for designing integrated policy portfolios that structurally align agricultural economic incentives with long-term ecological preservation.

6.4.6 Conclusion

This study deployed a spatially explicit, historically calibrated bio-economic framework that demonstrates that deforestation in the Brazilian Cerrado is driven by a highly capitalized, two-stage land-use succession—from extensive pasture to mechanized cropland—that systematically overrides existing environmental penalties under Business-as-Usual conditions. Through rigorous ex-ante simulation, we found that standalone conservation mechanisms are structurally insufficient to arrest this trajectory; untargeted Payments for Environmental Services (PES) fail to prevent frontier percolation, while isolated subsidy removals cannot construct the contiguous ecological barriers necessary to sustain localized micro-climate regulation. Instead, halting environmental degradation requires a strictly synergistic policy portfolio that anchors PES eligibility in highly exposed native corridors while simultaneously removing agricultural subsidies for newly deforested land. This paired approach successfully seals the agricultural frontier, displaces low-yield pasture, drives localized crop intensification, and proves fiscally self-sustaining over the long term. Acknowledging that this framework inherently simplifies exogenous macro-economic shocks and institutional frictions, we strongly encourage future research to build upon these mechanics by integrating stochastic price volatility and dynamic institutional behaviors. However, even with these abstractions, the model functions as a highly effective heuristic compass. By isolating the structural thresholds where agricultural capitalization overpowers environmental policy, it provides actionable, empirically grounded insights into the precise behavioral shifts required to transform the Cerrado from a speculative frontier into a landscape of sustainable, high-yield conservation.

6.5 Supplementary materials

6.5.1 Detailed initialization procedure

To establish a robust empirical baseline for the simulation, the model's spatial and economic initial conditions are strictly calibrated to the year 1995. The initialization procedure follows a four-step spatial layering process: land cover classification, infrastructure masking, public conservation zoning, and the probabilistic allocation of private landholdings.

First, we retrieve the spatially explicit 1995 land cover and land use map from the MapBiomas dataset (Collection 10.0) at a uniform grid resolution of 500m × 500m. To align the empirical data with the operational mechanics of our bio-economic framework, the highly granular MapBiomas classifications are aggregated into four macro-categories: *Natural*, *Cropland*, *Pastureland*, and *Other* (which includes urban infrastructure, mining, and water bodies). The exact mapping of these reclassifications is detailed in Table 6.1.

Second, we apply a forward-looking infrastructure mask. Because our framework models agricultural dynamics but lacks an endogenous mechanism for urban or industrial expansion, we must prevent agricultural agents from claiming land that is destined for non-agricultural development. To resolve this, we extract the spatial footprint of the *Other* category from the 2024 MapBiomas dataset and overlay it onto the initial 1995 map. This permanently removes future urban and mining zones from the available pool of expansible agricultural land.

Third, we delineate strictly protected public lands. We import the spatial boundaries of established conservation units and indigenous territories from ICMBio [390]. Parcels falling within these boundaries are designated as public land; they cannot be acquired by private agricultural agents and are permanently restricted from undergoing any land-use change throughout the simulation window.

Finally, the remaining expansible and already-cleared land must be divided into discrete properties managed by agricultural agents. To establish a realistic baseline of farm sizes, we utilize the empirical farm size distribution for the Cerrado region provided by the 1995 Brazilian Institute of Geography and Statistics (IBGE) Agricultural Census [357]. Because the census provides aggregate distributions rather than spatially explicit property boundaries, we spatially allocate these landholdings using a probabilistic centroid approach. We first seed property centroids across the available private landscape. Subsequently, adjacent parcels are iteratively assigned to these centroids based on a Gaussian probability distribution, ensuring that parcels closer to a centroid have a higher likelihood of assimilation. This procedural generation produces spatially contiguous, pseudo-realistic property boundaries that reflect the same statistical properties of the empirical IBGE farm size distribution.

Description	Code ID	Assigned Category
Forest	1, 3, 4, 5, 6, 49	Natural
Herbaceous and Shrubby Vegetation	10, 11, 12, 32, 29, 50	Natural
Beach, Dune and Sand Spot	23	Natural
Forest Plantation	9	Natural
Temporary Crop	18, 19, 39, 20, 40, 62, 41	Cropland
Perennial Crop	36, 46, 47, 35, 48	Cropland
Pasture	15	Pastureland
Mosaic of Uses	21	Pastureland
Water	26, 33	Natural
Urban Area	24	Other
Mining	30	Other
Other non-Vegetated Areas	25	Other
Aquaculture	31	Other
Not Observed	27	Other

Table 6.1 MapBiomas Land Cover Classification aggregated into Natural, Cropland, Pastureland, and Other macro-categories.

6.5.2 Exogenous inputs: Commodity price dynamics and enforcement probability

To isolate the structural bio-economic mechanisms driving frontier expansion, our framework simplifies certain macroeconomic and institutional variables into exogenous inputs. Two of the most critical structural assumptions concern the dynamics of agricultural commodity prices and the perceived probability of environmental enforcement.

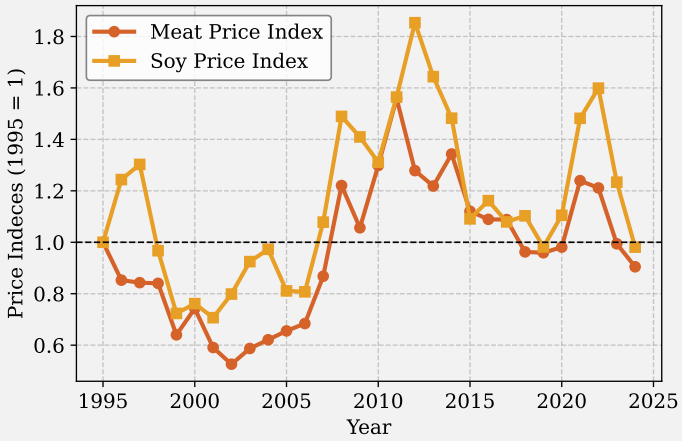


Figure 6.6 Historical agricultural price indices (normalized to be 1 in 1995) used to calculate the time-averaged commodity values for the simulation. Note: the underlying prices are denominated in real 2010 USD as for all the other monetary quantities in this study.

Regarding price dynamics, Fig. 6.6 illustrates the historical volatility of both meat and soy price indices over the past three decades. Despite these significant short-term fluctuations, the time series lacks a definitive long-term directional trend, with both indices effectively exhibiting mean-reverting behavior across the 30-year window. Anchored by this observation, the model intentionally applies a constant, time-averaged price for both crop and pasture commodities across the historical and projection periods. While stabilizing prices is admittedly a strong assumption that abstracts away transient macroeconomic shocks, it is an empirically defensible simplification given the data's ultimate trajectory. By holding prices constant, we effectively filter out high-frequency market noise, ensuring that the simulated land-use transitions are driven strictly by the structural variables under investigation: endogenous yield improvements, spatial constraints, and policy interventions.

Parameterizing the perceived risk of environmental fines presented a more complex empirical challenge. Currently, there is no comprehensive historical dataset detailing either the subjective risk perceived by agricultural operators or the objective ratio of prosecuted versus total illegal deforestation specifically for the Cerrado biome over a long horizon. Consequently, we constructed a proxy timeline of enforcement probability. We established an upper bound using available enforcement data from the neighboring Amazon biome (represented by the grey markers in Fig. 6.7), drawing on the empirical work provided by [391]. Indeed, the Cerrado has historically been subject to less rigorous environmental supervision and lower federal prioritization than the Amazon [383, 392].

Using this empirical estimation as an upper bound, we systematically scaled the baseline probabilities downward (represented by the solid blue trajectory) to accurately reflect the Cerrado's specific institutional reality. In particular, to capture the temporal evolution of enforcement over the 1995–2024 calibration window, we dynamically modulated this scaled probability to mirror the well-documented political and technological cycles of Brazilian environmental governance. As illustrated by the plotted trajectory in Fig. 6.7, the sharp escalation in enforcement probability between 2005 and 2010 reflects a period of unprecedented structural deterrence. This era was characterized by the deployment of the DETER real-time satellite monitoring system by the National Institute for Space Research (INPE), which exponentially increased the state's capacity to detect rapid land-clearing [393]. Coupled with the rollout of integrated federal action plans (initially the PPCDAm for the Amazon, followed by the PPCerrado), this technological leap allowed field agencies like IBAMA to execute rapid-response operations, fundamentally elevating the perceived risk of illegal deforestation for agricultural operators.

Conversely, the subsequent plateau and gradual decline in the enforcement trajectory capture later phases of institutional friction and deregulation. Emerging towards the end of the initial Lula administrations, a more permissive environmental political orientation began to take shape. A critical

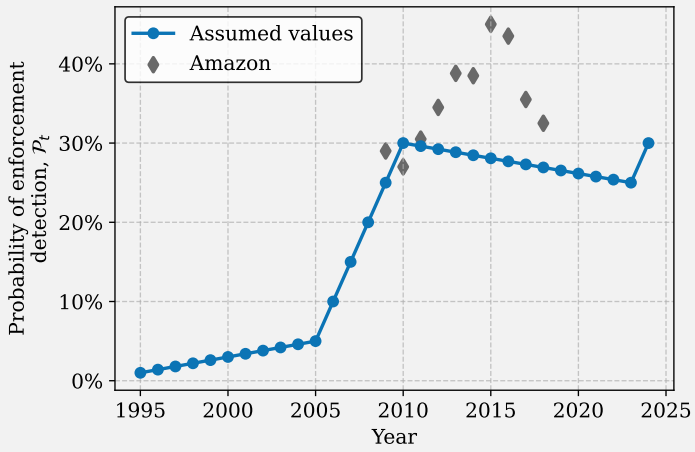


Figure 6.7 Estimated historical evolution of enforcement probability (solid line), scaled downward from Amazonian baselines (grey markers) and calibrated to reflect political and technological cycles.

milestone in this shift was the controversial revision of the Brazilian Forest Code [391]. This legislative overhaul generated widespread expectations of amnesty for past illegal clearing, which temporarily stalled federal enforcement momentum. This downward trajectory subsequently accelerated under the successive administrations of Michel Temer and Jair Bolsonaro. The continuous decline observed throughout the late 2010s and early 2020s directly parameterizes a period of severe institutional dismantling. During this phase, drastic budget reductions for environmental agencies, the deliberate weakening of localized inspection protocols, and permissive political rhetoric effectively minimized the operational risk of illegal agricultural expansion. Finally, the sharp upward correction at the end of the calibration window reflects the return of the Lula administration in 2023, which marked a renewed federal commitment to restoring stringent environmental enforcement protocols.

6.5.3 Parameterization

To ensure the bio-economic framework accurately replicates the structural drivers of land-use change, the model's parameters are calibrated to reflect the fundamental agronomic, economic, and institutional realities of the state of Goiás. Rather than attempting to capture high-frequency, localized data fluctuations, our parameterization strategy focuses on establishing the correct relative magnitudes that drive long-term agent behavior. All final parameter values utilized in the simulations are summarized in Table 6.3. Where possible, baseline values are derived directly from empirical datasets and regional census data; otherwise, structural parameters are grounded in established agricultural economics and landscape ecology literature.

Baseline yield decomposition: To accurately anchor the model to historical realities, the initial 1995 agricultural yields are derived from the IBGE Agricultural Census [357]. However, because our model employs endogenous yields, these values must be mathematically decomposed into three distinct, interacting components: ecological feedbacks, technological advancement, and endogenous intensification.

Ecological feedback and integrity thresholds: Regarding ecological parameters, calibrating local and global integrity thresholds requires necessary structural assumptions, given the highly simplified nature of the framework's eco-hydrological feedbacks. While there is no single report quantifying the importance

of local versus global ecosystem services in isolation, we set the value of λ_c as 0.15, reflecting the modest but significant average yield premium generated by wild pollinator visitation in Brazilian soybean fields [394–396]. In contrast, λ_p is set at 0.05, capturing the lower dependence of tropical cattle herds on localized biodiversity related services. Furthermore, we set γ_c as 0.35 and γ_p as 0.15 (Eq. 6.2), formalizing the empirical evidence that annual crops exhibit a higher vulnerability to macro-regional precipitation anomalies and shortened rainy seasons than the structurally resilient, deep-rooted tropical grasses typical of local pastures [397, 398].

As for the computation of the two contributions, $\mathrm{HI}_{j,t}^{\mathrm{local}}$ and $\mathrm{HI}_{t}^{\mathrm{global}}$, the local ecological contribution (Eq. 6.3) is determined by a spatial weighting function applied to the surrounding landscape matrix:

$$w_{k,t} = \begin{cases} 1 & \text{if } \tau_{k,t} = n, \\ 0.75 & \text{if } \tau_{k,t} = p \text{ and } \delta_{k,t} = 0, \\ 0.5 & \text{if } \tau_{k,t} = p \text{ and } \delta_{k,t} = 1, \\ 0.25 & \text{if } \tau_{k,t} = c \text{ and } \delta_{k,t} = 0, \\ 0 & \text{if } \tau_{k,t} = c \text{ and } \delta_{k,t} = 1. \end{cases} \tag{6.17}$$

where the values are inferred from general studies about the importance of local disturbance on local biodiversity, serving the biggest role in pollination and pest control. Native vegetation ($\tau = n$) provides the baseline maximum ecological functionality. Low-intensity pastures ($\tau = p, \delta = 0$) offer partial permeability for biodiversity, which decreases as intensification ($\delta = 1$) introduces higher stocking rates. Croplands are penalized more heavily ($\tau = c$), with high-intensity conventional cropland ($\delta = 1$) acting as an absolute ecological sink ($w = 0$) due to the severe externalities of pesticide drift and heavily simplified habitat structures on native biotic vectors [399, 400].

This localized calculation is then balanced against the global ecological contribution, which evaluates the aggregate integrity of the regional biome. By parameterizing the scale σ_{patch} at 0.2, the global ecosystem contribution incorporates well documented macro-scale landscape tipping points observed during regional Cerrado aridification trends [401–404]. To ensure these theoretical spatial penalties accurately reflect reality, we validated the resulting net 1995 ecological yields against independent empirical estimates documented in the broader agronomic literature [345].

Exogenous technological advancement: Parameterizing exogenous technological advancement presents a well-documented empirical challenge, specifically in isolating pure productivity gains from mere increases in synthetic inputs. To resolve this, we establish two theoretical boundaries. First, we utilize Total Factor Productivity (TFP) studies for the region as an upper bound, which generally report a year-on-year increase of approximately 2% [358]. Indeed, utilizing this aggregate TFP figure directly would overestimate exogenous progress; because TFP metrics inherently capture systemic landscape improvements—such as structural land consolidation, economies of scale, and localized capital intensification—applying this full rate would result in double-counting the dynamics our bio-economic framework already generates endogenously.

Conversely, specialized agronomic studies focusing on agrochemical efficiency and genetic yield-gap closures provide a rigorous lower bound [405]. Because their methodology strictly isolates the biological response of crops to specific synthetic inputs under controlled conditions, these estimates structurally exclude the broader operational efficiencies, machinery upgrades, and macroscopic management adaptations that drive real-world frontier expansion. To balance these extremes, our framework adopts an intermediate exogenous growth rate. Furthermore, we deliberately assign a steeper technological growth trajectory to mechanized crops than to extensive pasture, thereby reflecting the historical concentration of institutional research and capital investment in the export-driven soybean sector.

Endogenous intensification: Endogenous intensification requires a different abstraction, as the model simplifies a continuous agronomic evolution into a discrete system upgrade. To parameterize this, we apply distinct yield and cost multipliers. Crucially, the intensification cost multipliers (β_C, β_P) are kept structurally lower than their corresponding yield multipliers. This mathematical relationship guarantees

that the transition to intensified practices delivers higher return on investment, even while substantial upfront investment constraints prevent immediate, universal adoption.

Operational and land conversion costs: Economic cost parameters are calibrated to reflect the specific capital requirements of distinct agricultural systems based on regional datasets and technical reports. Baseline annual operating costs for crops, as well as the justification for the intensification cost multipliers, are derived from historical CONAB data for the Rio Verde locality, utilizing the earliest available figures from 1997 [406]. Operational costs for pasture are sourced from the ABIEC beef report [407]. For land clearing, the annualized cost of converting native vegetation directly to mechanized cropland is parameterized at \$150/ha, while conversion to pasture is set at \$100/ha, based on agricultural development reports [408]. Finally, the cost of secondary conversion from established pasture to cropland is deduced by the authors as a structurally discounted value, accounting for the initial clearing and partial soil preparation already absorbed during the first transition.

Land valuation and price elasticity: Finally, baseline 1995 land prices are extracted from historical literature, differentiated by crop and pastureland, and annualized using a weighted average by land use [409]. In conjunction with established economic literature, these historical land valuations also inform the calibration of the model's land-price elasticity parameter.

6.5.4 Computational calibration of behavioral parameters

In contrast to the agronomic and economic variables derived directly from empirical datasets, parameters governing agent behavioral responses—such as profit sensitivities and land-use transition probabilities—lack direct, measurable real-world counterparts. Consequently, these parameters must be computationally calibrated to ensure that the simulated macro-dynamics accurately replicate historical land-use trajectories. This calibration procedure is executed against the historical timelines illustrated in Fig. 6.1.

To align our simulation results with observed empirical data, we implemented a highly structured, sampling-based calibration framework. We first established theoretically plausible boundaries for each behavioral parameter, as detailed in Table 6.2. Given the high dimensionality of the parameter space, a traditional grid-search approach would have been computationally intractable, requiring over one million model runs merely to test ten discrete values per parameter. To efficiently map this space, we employed a quasi-random Sobol sequence [227], which guarantees a more uniform exploration of the parameter landscape and yields higher precision with fewer computational resources. Using this method, we generated more than 1000 unique parameter configurations, executing 10 Monte Carlo simulations for each combination to adequately account for stochastic variability.

The optimal parameter set was primarily identified through a least-squares minimization procedure, which calculated the sum of squared differences between the simulated land-use transitions and the historical empirical trends. However, to ensure the robustness of the framework, this algorithmic optimization was complemented by rigorous manual fine-tuning where the match with empirical data on the 2017 distribution of land ownership obtained from the IBGE Agricultural Census [410] (Fig. 6.8) was also checked—due to constraints in the temporal granularity of the data, this could not be incorporated into the R^2 computation. This qualitative oversight was critical to verify that the model was fundamentally "well-behaved"—meaning the selected parameters did not just numerically overfit the aggregate historical curve, but genuinely produced structurally stable and logically sound micro-economic decisions at the individual agent level.

The final selected parameter values resulting from this hybrid calibration approach are presented in Table 6.2. The model's high fidelity in capturing historical frontier dynamics is quantitatively validated by the resulting R-squared (R^2) and adjusted R-squared ($\bar{R}^2$) [228] metrics. Furthermore, Fig. 6.1 provides a visual confirmation, illustrating the strong temporal and spatial compatibility between the calibrated model outputs and the observed empirical data.

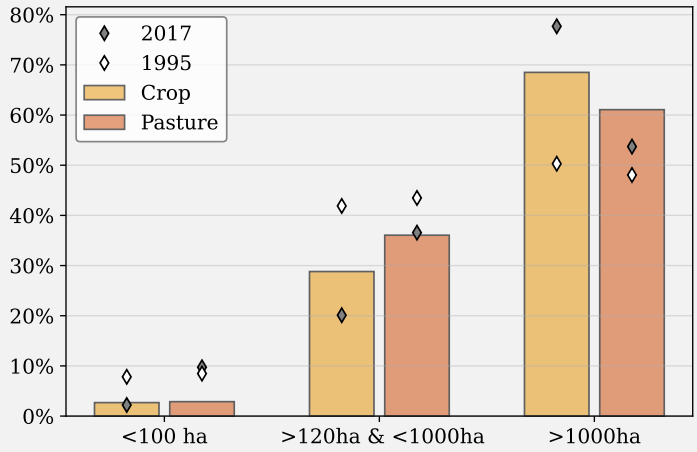


Figure 6.8 Comparison of simulated land ownership distributions for the crop and pasture sectors against empirical IBGE Agricultural Census benchmarks (1995 and 2017). Although the model does not exhibit a perfect point-by-point numerical match across all size classes, the simulated structural dynamics consistently move in the same direction as the empirical data, accurately capturing the macro-regional trajectory of land consolidation into large-scale holdings (> 1000 ha).

	Description	Sampling range	Optimal
γ_{def}	Profit sensitivity for stochastic deforestation	[100, 10000]	2500
γ_{int}	Profit sensitivity for stochastic intensification	[100, 10000]	2500
γ_{owner}	Profit sensitivity for owner competition	[10, 1000]	150
γ_{abandon}	Profit sensitivity for land abandonment	[0, 10]	1
R^2	R-squared		0.96
$\bar{R}^2$	Adjusted R-squared		0.94

Table 6.2 Results of model calibration.

6.5.5 Sensitivity analysis

To evaluate the robustness of our bio-economic framework and identify the structural parameters that most strongly govern long-term system dynamics, we conducted a localized sensitivity analysis. Specifically, we systematically perturbed selected key parameters by increasing their selected baseline values by exactly 5%. For each test, we isolated the effect of the targeted parameter while holding all other variables strictly constant.

We then quantified the impact of these isolated shocks by calculating the relative difference in core response variables projected for the end of the simulation window in 2050, compared against the standard baseline trajectory. The results of this perturbation analysis are visualized in Fig. 6.9. This approach allows us to establish the relative elasticity of the model's outcomes—specifically total natural area, average crop and pasture profits, and global ecosystem integrity—in response to marginal shifts in underlying agronomic, economic, or institutional assumptions.

As illustrated in Fig. 6.9, the system's macro-dynamics are overwhelmingly governed by the core economic determinants of agricultural profitability. Marginal increases in primary revenue drivers—namely baseline yields (y_c, y_p), commodity prices (p_c, p_p), and intensification multipliers (α_c, α_p)—act as the strongest catalysts for frontier expansion. These upward shocks consistently translate into significant

declines in both total natural area and global ecosystem integrity, as agents are financially incentivized to accelerate land clearing.

Conversely, parameters that increase the financial friction of land acquisition and management exert a strong protective effect. Increases in baseline operational costs ($C_{oc,c}$, $C_{oc,p}$), the direct costs of clearing native vegetation for pasture ($C_{n\to p}^{def}$), and institutional deterrents like the fine for unauthorized deforestation (f_{aut}) effectively act as brakes on the agricultural frontier, leading to relative gains in natural area retention and ecosystem recovery.

Crucially, the analysis reveals that the model is highly inelastic to changes in secondary parameters, such as economies of scale ($v_{c,\max}$, $v_{p,\max}$), specific habitat quality weights ($w_{c,int}$, $w_{p,conv}$), and stochastic decision sensitivities (ζ_{def}, ζ_{int}). This inelasticity is a strong indicator of structural robustness; it confirms that the simulated frontier dynamics are fundamentally anchored by the basic cost-revenue dichotomy of land clearance, rather than being overly sensitive to localized agent heterogeneity or minor calibration assumptions.

Notation	Description	Value
Yields and Economic Baselines		
y_c	Baseline crop yield (soy) [kg · ha^{-1} · year^{-1}]	1300
y_p	Baseline pasture yield (live weight gain) [kg · ha^{-1} · year^{-1}]	45
p_c	Commodity price (soy) [\$ · kg^{-1}]	0.24
p_p	Commodity price (live weight) [\$ · kg^{-1}]	2.3
C_c^{oc}	Annual operating costs (crop) [\$ · ha^{-1} · year^{-1}]	420
C_p^{oc}	Annual operating costs (pasture) [\$ · ha^{-1} · year^{-1}]	70
ξ_c	Slope cost factor (crop) [−]	1
Intensification and Technological Growth		
α_c	Intensification yield multiplier (crop) [−]	2
α_p	Intensification yield multiplier (pasture) [−]	2
β_c	Intensification cost factor (crop) [−]	1.8
β_P	Intensification cost factor (pasture) [−]	1.9
$T_{c,t}$	Annual technological growth rate (crop) [year^{-1}]	0.2/30
$T_{p,t}$	Annual technological growth rate (pasture) [year^{-1}]	0.1/30
$\nu_{c,\max}$	Maximum economy of scale reduction (crop) [−]	0.15
$\nu_{c,\text{ref}}$	Reference scale size (crop) [ha]	10
$\nu_{p,\max}$	Maximum economy of scale reduction (pasture) [−]	0.05
$\nu_{p,\text{ref}}$	Reference scale size (pasture) [ha]	10
Capital Investment and Transition Costs		
C_c^{int}	Upfront intensification investment (crop) [\$ · ha^{-1}]	150
C_p^{int}	Upfront intensification investment (pasture) [\$ · ha^{-1}]	90
$C_{n\to c}^{\text{def}}$	Annualized conversion cost: Natural to Crop [\$ · ha^{-1}]	150
$C_{n\to p}^{\text{def}}$	Annualized conversion cost: Natural to Pasture [\$ · ha^{-1}]	100
$C_{p\to c}^{\text{conv}}$	Annualized conversion cost: Pasture to Crop [\$ · ha^{-1}]	75
$C_{c\to p}^{\text{conv}}$	Annualized conversion cost: Crop to Pasture [\$ · ha^{-1}]	10
$p_{\ell,0}$	Annualized initial land appreciation value [\$ · ha^{-1}]	100
μ	Rigidity factor for land price adjustments [−]	0.5
Institutional Policies and Behavioral Sensitivity		
ω	Legal reserve requirement [−]	0.2
f_{aut}	Fine for deforestation without authorization [\$ · ha^{-1}]	350
f_{ill}	Fine for strictly illegal deforestation [\$ · ha^{-1}]	1000
ζ_{def}	Profit sensitivity for stochastic deforestation [−]	2500
ζ_{int}	Profit sensitivity for stochastic intensification [−]	2500
ζ_{acq}	Profit sensitivity for owner competition [−]	150
ζ_{abn}	Profit sensitivity for land abandonment [−]	1
Ecological Feedbacks and Degradation		
$w_{c,\text{conv}}$	Natural integrity (conventional crop) [−]	0.25
$w_{c,\text{int}}$	Natural integrity (intensified crop) [−]	0.0
$w_{p,\text{conv}}$	Natural integrity (conventional pasture) [−]	0.75
$w_{p,\text{int}}$	Natural integrity (intensified pasture) [−]	0.5
∂	Kernel size for local ecosystem integrity [cells]	5
λ_c	Local ecosystem integrity weight (crop) [−]	0.15
γ_c	Global ecosystem integrity weight (crop) [−]	0.35
λ_p	Local ecosystem integrity weight (pasture) [−]	0.05
γ_p	Global ecosystem integrity weight (pasture) [−]	0.1
σ_{patch}	Scale patch density [−]	0.2

Table 6.3 Parameters of the bio-economic model for the Cerrado region, detailing units and calibrated baseline values updated to match the sensitivity analysis charts.

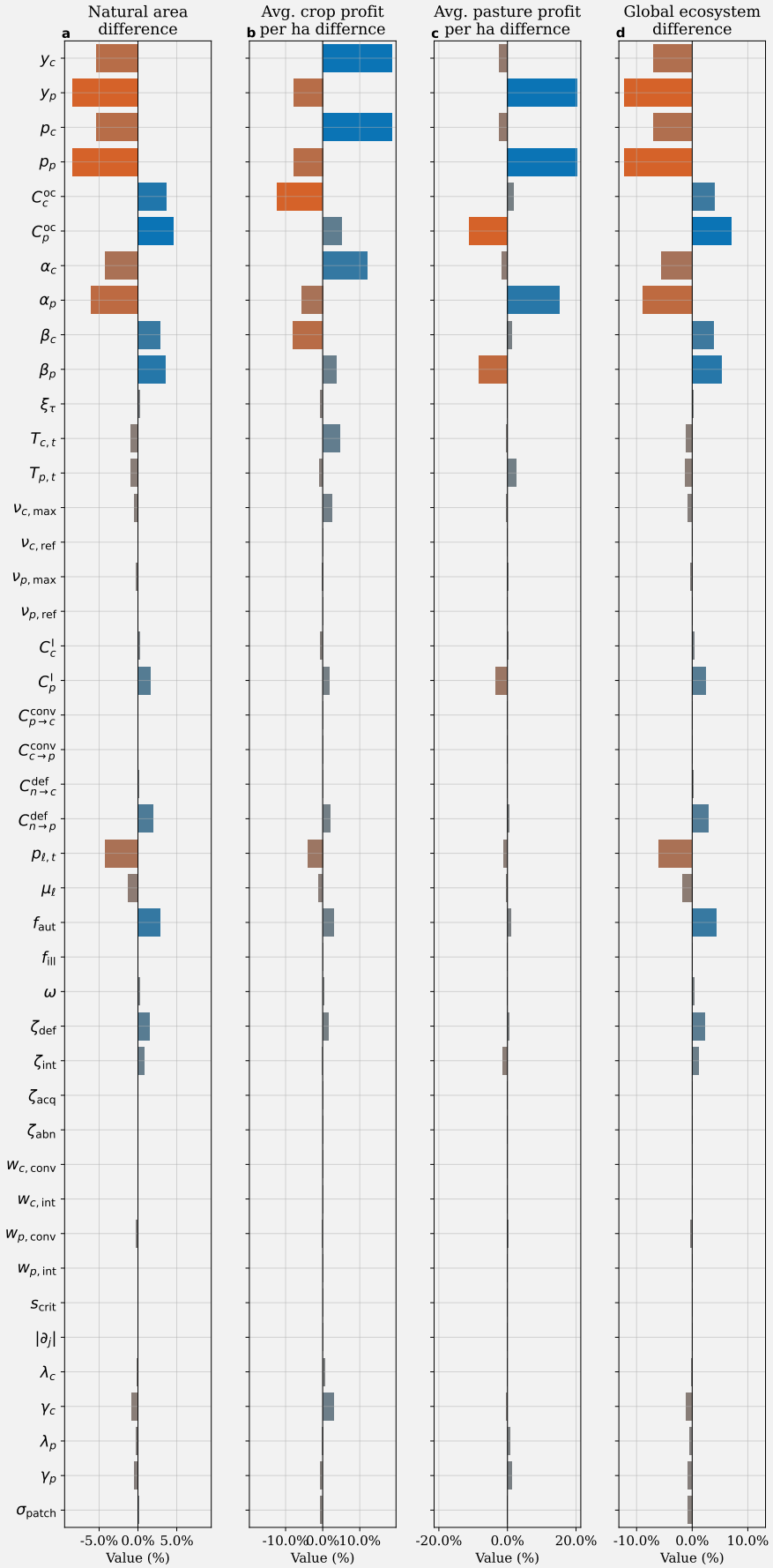


Figure 6.9 Relative difference in primary response variables projected for 2050, resulting from an isolated 5% increase in selected baseline parameter values.

Key Takeaways

- **A spatially explicit frontier model:** By calibrating a dynamic cellular automata model to historical land-use data (1995–2024), this framework serves as a virtual laboratory to formally evaluate the spatial percolation of deforestation driven by capitalized commodity producers.
- **The necessity of spatial targeting and paired mechanisms:** Standalone conservation policies fail to seal the frontier. Success requires leveraging the spatially explicit nature of our framework to strategically target positive incentives (Payments for Ecosystem Services) in critical ecological corridors, closely coupled with negative constraints (removing subsidies on newly cleared land).
- **A net bio-economic surplus:** Optimized conservation does not inherently sacrifice agricultural output. The localized yield improvements generated by preserved ecosystems overcompensate for the protected land area, while public savings from removed subsidies ensure fiscal sustainability.

Part III

A Global Perspective: The Role of Food Demand

Part III is adapted from Moretti et al. (2025) [4], *A global systems perspective on food demand, deforestation and agricultural sustainability*. Minor modifications have been made to the original texts to align them with the narrative and context of this thesis.

7. Ecological limits, resilience, and societal vulnerability

In the previous chapters, we examined the specific cases of Europe and Brazil in order to understand how current trends may shape future agricultural production and ecological resilience. In doing so, however, we deliberately left aside the role of demand and its feedbacks. The main reason is that, in an increasingly interconnected world, trade enables commodities to circulate across regions, so that food demand is determined less by local conditions than by broader global patterns. From this perspective, excluding demand from a regional analysis was justified. At the same time, demand cannot be ignored altogether, since prices—and thus the economic incentives driving intensification, expansion, or deforestation—emerge from the interaction between supply and demand. In this chapter, we therefore shift the focus to the global scale and examine the relationship between food production and ecological degradation from a systemic perspective. More specifically, we ask whether continued increases in agricultural productivity can be sufficient to meet rising food demand, driven by population growth and global economic development, while preserving ecosystems.

7.1 Societal collapse discussion

Agriculture has long been a central determinant of societal trajectories [411, 412]. By increasing food availability, it has supported population growth, urbanization, and the emergence of more complex social and political institutions [413]. Yet this productive role has always carried an inherent fragility: when demographic expansion and institutional complexity outpace the capacity of agricultural and ecological systems to sustain them, the same processes that once enabled growth can become sources of instability.

This tension has been discussed in relation to a number of historical cases. Mid-Holocene societies in Europe [414], the Maya civilization [415], and episodes of crisis in imperial China [416, 417] have all been interpreted through frameworks that emphasize the interaction between environmental stress, agricultural constraints, demographic pressure, and institutional fragility. These examples do not imply a simple or deterministic link between environmental degradation and societal decline. Rather, they suggest that agriculture occupies a pivotal position in social resilience, and that disruptions to food production can amplify pre-existing political, economic, and demographic tensions.

Comparable concerns have re-emerged in the context of the contemporary global food system. As discussed in the Introduction chapter, agriculture has expanded and intensified under the combined pressure of rising demand and strong profit incentives [418]. Although this transformation has supported major gains in food production, it has also entailed substantial ecological costs. The increasing reliance on synthetic fertilizers, pesticides, irrigation, and monocultures

has contributed to soil degradation, biodiversity loss, and water contamination [419, 420]. At the same time, a large share of the Earth's land surface is already devoted to agriculture [421], while intensive practices continue to degrade soils in many regions [422]. These developments have revived a broader question: can continued social and economic expansion remain compatible with the biophysical conditions on which food production depends? This question has been most explicitly articulated in the literature on *Limits to Growth* [423].

7.2 The *limits to growth* discussion

The idea that human societies may encounter ecological limits has been examined across a wide range of disciplines, including history, archaeology, anthropology, environmental research, and ecological economics [424–426]. Within this literature, the Malthusian intuition that any society faces environmental constraints on its long-run expansion has remained highly influential [427, 428]. Meadows and colleagues' *Limits to Growth* [429] gave this intuition a systems-theoretic formulation by exploring the implications of continued population and industrial growth in a finite world. Their contribution shifted attention from isolated resource shortages to the broader dynamics through which economic and demographic growth may eventually conflict with ecological constraints.

Although the original *Limits to Growth* framework was widely criticized, the questions it raised have remained central and have been revisited repeatedly [430]. Subsequent work by Diamond [431, 432] and Turchin [413, 433], among others, enriched this debate by emphasizing the interactions between environmental stress, political organization, demographic change, and social conflict. This line of inquiry has also inspired a growing body of formal modelling work on deforestation [434], economic inequality [426], and climate change [435] as possible drivers of systemic instability.

Despite its relevance, this literature also has important limitations. In particular, several contributions place too much explanatory weight on population growth alone, whereas land conversion and deforestation are also strongly mediated by agricultural profitability, trade, technological change, and other economic forces [436]. Moreover, analyses centered on a single driver often overlook the ecological feedbacks through which environmental degradation feeds back into agricultural productivity and social vulnerability. These limitations point to the need for a broader framework that retains the systemic ambition of the limits-to-growth tradition while incorporating the economic mechanisms that shape human pressure on ecosystems.

7.3 Economic incentives behind ecological dynamics

An ecological perspective is essential for understanding the scale of the problem, but it does not by itself explain why environmentally damaging trajectories persist. Deforestation, land conversion, and agricultural intensification are not autonomous processes. They emerge from decisions taken within specific economic and institutional contexts. Farmers respond to prices, expected profits, input costs, and policy incentives, while consumers' demand evolves with population growth, income growth, and dietary change. As incomes rise, food demand tends to increase not only in quantity but also in composition, often with a higher share of animal products and other resource-intensive goods [437, 438].

This economic dimension is central because it shows that ecological degradation is mediated

by individual decisions operating within imperfect incentive structures. Forests are converted because agricultural land becomes profitable. Chemical inputs are adopted because they increase expected yields or reduce production risks. Livestock systems expand because changing diets create profitable markets for meat and dairy products. Environmental degradation is therefore not simply the result of ecological ignorance; it is also the consequence of economic systems that reward expansion while only imperfectly accounting for long-term environmental costs.

For this reason, a more pragmatic approach to global systemic sustainability requires moving beyond generalized narratives of collapse and toward an explicit analysis of the mechanisms linking demand, production, land use, and ecological degradation. The key issue is not only whether current trajectories are unsustainable, but under what conditions they can be altered. This requires understanding how supply-side measures, such as productivity improvements or more sustainable farming practices, interact with demand growth and with the incentives that shape land-use decisions. Without such an integrated perspective, one risks either overstating the capacity of technological progress to alleviate environmental pressure or invoking ecological limits without identifying the mechanisms through which they may be avoided.

7.4 Our contribution

In the next chapter, we address a central question in the debate on food-system sustainability: can continued increases in agricultural productivity, together with the adoption of more sustainable farming practices—such as organic and conservation agriculture, reductions in chemical inputs, or lower livestock densities—be sufficient to meet rising food demand while preserving ecosystems [439, 440]? Or does avoiding the transgression of more critical environmental thresholds require a more fundamental transformation of demand, particularly through dietary change and coordinated, system-wide policy interventions?

To investigate this question, we develop a stylized but calibrated modelling framework that links food demand, crop and livestock production, deforestation, and agricultural sustainability within a single dynamic system. The model is deliberately parsimonious: rather than reproducing the full complexity of the global food system, it isolates the core feedbacks through which economic drivers and ecological constraints shape long-run outcomes. At the same time, it remains empirically grounded through calibration to observed long-run trends in population, income, yields, inputs, and land use. This combination of abstraction and empirical discipline allows us to move beyond purely theoretical discussions of collapse and toward a more operational analysis of the trade-offs, limits, and policy options involved in reconciling food provision with ecological integrity.

Key Takeaways

- **The resilience paradox:** While the relentless expansion of agriculture has historically sustained human population growth, it now generates systemic ecological pressures that threaten the long-run resilience of the global food system.
- **Integrating limits and incentives:** Reconciling global food security with planetary boundaries requires understanding how macro-economic consumption trends clash with absolute biophysical thresholds.

8. A stylized, spatially explicit model of global food demand and production

In the previous chapter, we introduced the challenges associated with feeding a growing and increasingly affluent population in the 21st century, and we outlined the type of systemic analysis required to address the question of whether continued increases in agricultural productivity can meet rising food demand—driven by population growth and global economic development—while preserving ecosystems. To examine this issue, we begin with a review of the existing literature and modelling approaches. We then present our model and discuss the main results. Finally, we conclude.

8.1 Literature review

The literature tackling the problem of reconciling food demand with the ecological constraint of preserving nature spans empirical, scenario-based, and theoretical approaches. While global integrated assessment models (IAMs) such as GLOBIOM [441], IMAGE [442], and MAgPIE [443] have illuminated the possible consequences of alternative technology, land use, and diet scenarios for GHG emissions, biodiversity, and food security; yet, their complexity and extensive parameterization can make it difficult to parse out causal mechanisms and feedback loops, or to transparently compare policy levers on a conceptual level.

For this reason, a substantial body of literature has approached the same problem from a more systemic and theoretical perspective. The objective of these contributions is not to reproduce reality in all its complexity, but rather to identify the key mechanisms operating behind observed dynamics and to develop a clearer intuition about the structure of the problem. In this sense, theoretical models should be understood less as direct mimics of reality than as tools that render complex socio-ecological processes more intelligible. Beyond the literature on societal collapse discussed in the previous chapter, several modelling exercises have pursued this goal with different emphases. In particular, dynamic and system-analytic models have provided key insights into food system tipping points, feedback loops between agricultural intensification and land expansion, and the implications of self-reinforcing land degradation [365, 444–446]. Land use and food system theories drawing on non-linear dynamics, spatially explicit frameworks, and ecosystem service feedback loops have highlighted the risks of unintended consequences and compensatory effects across spatial and management scales [447–449]. Notably, archetype-based and stylized models have clarified how yield gains can sometimes induce additional land clearing ("rebound" or Jevons effects) rather than sparing nature, depending on feedback loops

among value chains, governance, and behavioral factors [450–452]. Complementing this are explorations of "land sparing" versus "land sharing" paradigms, which have underlined the limitations of both simplistic intensification and extensive conservation solutions in isolation [453, 454].

Building on this theoretical tradition, our study contributes by combining several of these ingredients into a parsimonious framework calibrated to reproduce global trends. Many existing models focus on specific dimensions of the problem, but lack an integrated structure that can be confronted with real-world data in a systematic way. Where calibration has been attempted, it has often taken the form of reproducing stylized facts, in the spirit of agent-based modelling, as for example in the recent contribution by Bologna et al. [455]. By calibrating our model to historical trends, we aim both to ensure that it captures the main feedbacks required to describe global dynamics from a systemic perspective and to enable a more realistic assessment of baseline trajectories, as well as an exploration of plausible supply- and demand-side alternatives. We argue that combining a parsimonious stylized model with trend-based calibration can substantially enrich the discussion and help bridge the gap between highly abstract theoretical models and more empirically detailed frameworks such as IAMs.

In terms of modelling choices, we draw inspiration from dynamical-systems descriptions of human–nature interactions for the core representation of intensification and deforestation dynamics. In particular, the work of Lafuite et al. [189] has been an important source of inspiration. However, while that model offers valuable insights into possible biodiversity trajectories, it remains spatially implicit, which limits its ability to capture heterogeneity and emergent properties in coupled socio-ecological systems. To incorporate an explicit spatial dimension, we also build on the approach developed in [140], where land-use types are stochastic and their propensities to change depend on imbalances between production and demand. This spatially explicit representation of ecological services allows us to investigate "policy mixes" and the synergies or trade-offs that may emerge from their interaction—issues that remain underexplored in the literature, yet are highly relevant for real-world sustainability transitions [456, 457].

Within this framework, we directly address whether supply-side productivity gains can meet future food demand while protecting global ecosystems, or whether coordinated policy interventions that also target consumption patterns are necessary to achieve long-term sustainability. By highlighting the dynamic and cross-scale feedbacks underlying both successful and unsuccessful management strategies, our analysis contributes to a growing and more theoretically grounded understanding of the pathways—and potential pitfalls—toward a sustainable food future.

8.2 Model

8.2.1 Model overview

We have developed a spatially explicit, discrete-time model that dynamically links the growth in food demand to agricultural production, land conversion among primary land-cover types — namely cropland, pasture, and natural land — and crucially incorporates feedback loops from natural ecosystem integrity (Fig. 8.1). The model landscape is represented as a square grid where each cell's land-cover class changes over time, allowing us to track both spatial configuration and aggregate stocks of land-use types. This enables robust quantification of processes such as deforestation, natural regeneration, and degradation pressure as they unfold

over time.

The drivers of food demand are exogenous time series that combine projected population growth, changes in per-capita income, and a parameter reflecting dietary preference for meat. This framework is flexible enough to accommodate demand-side policy interventions, such as shifts to lower-meat diets, by perturbing these demand trajectories.

Agricultural production in our model is governed by both land area and the intensity of management. Cropland yields respond to chemical intensification and mechanization while livestock output depends on available pasture area and on an adjustable livestock-density variable. If, at any time step, aggregate production fails to meet demand, the system responds first by intensifying production (for example, by increasing mechanization and chemical inputs, or livestock density). Persistent shortfalls inevitably trigger the conversion of natural land to cropland or pasture, resulting in deforestation and loss of critical habitat.

Central to the model is the ecosystem integrity index, a composite indicator reflecting both soil health and biodiversity. This index decreases with intensified mechanization and chemical use but recovers through periods of natural restoration. The integrity trajectories follow exponential decay and recovery processes, each with a characteristic time scale. Importantly, ecosystem integrity feeds back into agricultural yields, while overexploitation undermines future productivity, thereby creating self-limiting dynamics. In addition, the remaining intact vegetation modulates the pace of ecosystem degradation and restoration at the landscape level through the provision of vital ecosystem services, such as water filtration, climate stability, and biodiversity storage.

The model incorporates a sustainable alternative to conventional farming through the inclusion of organic management. The choice to focus on organic systems is motivated by their clear institutional definition and the availability of consistent global datasets on organically managed land [458, 459]. In the model, the transition to organic farming is treated as an exogenous process—that is, the share of organic land is calibrated to empirical data and provided as an input rather than emerging endogenously from the system's dynamics. Organic management is characterized by the absence of synthetic chemical inputs and stricter limits on livestock density, thereby reducing pressure on ecosystems, albeit often at the cost of short-term yield reductions. The model explores the implications of policy-driven increases in organic adoption and broader reductions in chemical input use, assessing their combined effects on production and ecosystem integrity.

Our framework is capable of contrasting a business-as-usual development trajectory with a suite of alternative policy scenarios, where changes are implemented as constraints or shifts to key model parameters. These include limiting livestock density, restricting deforestation, reducing chemical inputs, and implementing demand-side interventions. This architecture allows us to systematically assess the synergies and trade-offs inherent in: (i) supply-side sustainability measures, (ii) combinations of supply- and demand-side interventions, and (iii) the overall scale of consumption habit transformation needed to achieve a transition onto ecologically sustainable pathways for global land use and food production.

8.2.2 Demand: Economic and population growth

Population (N_t) and per-capita income (I_t) are specified as exogenous drivers that change throught time t. Income determines both the total caloric requirement and the composition of human diets. Total caloric demand is modeled using a logarithmic (Engel-type) relationship [460] :

$$D_t = (a + b \log I_t) N_t, \tag{8.1}$$

where D_t is total caloric demand, and a and b are positive parameters. The logarithmic form is widely used in empirical studies of food demand because it captures the diminishing marginal increase of total caloric intake with rising income [461].

Demand for animal products is modeled as a power-law function of income:

$$D_{\mathrm{m},t} = c\, I_t^d\, N_t, \tag{8.2}$$

with $c, d > 0$, where d represents the income elasticity of meat demand. Power-law (or constant-elasticity) functions are commonly adopted in agricultural economics to represent the empirically observed sublinear increase in meat and high-value food consumption with income[462, 463].

The demand for crops directly consumed by humans is the residual once the caloric contribution of meat is subtracted:

$$D_{\mathrm{c},t}^{\mathrm{food}} = D_t - D_{\mathrm{m},t}. \tag{8.3}$$

Then, total crop demand in the system comprises both food and feed uses:

$$D_{\mathrm{c},t} = D_{\mathrm{c},t}^{\mathrm{food}} + D_{\mathrm{c},t}^{\mathrm{feed}}, \tag{8.4}$$

where $D_{\mathrm{c},t}^{\mathrm{feed}}$ is the requirement of the livestock sector for feed inputs (see Section 8.2.3). To mimic real-world adaptive demand responses, the model incorporates a feedback mechanism in which consumption is partially suppressed if prior output falls short of demand—analogous to price feedback in markets:

$$D_{\mathrm{m},t} \leftarrow \frac{D_{\mathrm{m},t}}{\omega_{\mathrm{m}}} \left[1 - \alpha_{\mathrm{m}} \frac{D_{\mathrm{m},t-1} - Q_{\mathrm{m},t-1}}{D_{\mathrm{m},t-1}}\right], \tag{8.5}$$

$$D_{\mathrm{c},t}^{\mathrm{food}} \leftarrow \frac{D_{\mathrm{c},t}^{\mathrm{food}}}{\omega_{\mathrm{c}}} \left[1 - \alpha_{\mathrm{c}} \frac{D_{\mathrm{c},t-1} - Q_{\mathrm{c},t-1}}{D_{\mathrm{c},t-1}}\right], \tag{8.6}$$

where $Q_{\mathrm{m},t-1}$ and $Q_{\mathrm{c},t-1}$ denote last period's meat and crop output, respectively, and ω_{m}, $\omega_{\mathrm{c}}^{\mathrm{food}}$ are normalization constants. The notation $\leftarrow$ indicates that the exogenously determined demand at time t is endogenously adjusted in response to supply shortfalls in $t-1$. Lastly, normalizing by ω_{m} and ω_{c} ensures appropriate scaling of global demand within our stylized representation of the Earth system, while preserving the overall trend – see Appendix 8.6.1 for further details.

8.2.3 Production: Crop and livestock systems

Our model incorporates both conventional and organic production systems, which together determine the total outputs of crops and livestock at each time step:

$$Q_{\mathrm{c},t} = q_{\mathrm{c},t} + q_{c,t}^{\mathrm{o}} \qquad Q_{\mathrm{m},t} = q_{\mathrm{m},t} + q_{m,t}^{\mathrm{o}}, \tag{8.7}$$

where $q_{\cdot,t}$ and $q_{\cdot,t}^{\mathrm{o}}$ denote conventional and organic outputs respectively. The share of land under organic management increases exogenously, while both systems are managed by adaptive rules simulating a representative farmer who adjusts input intensities in response to changing economic and environmental conditions.

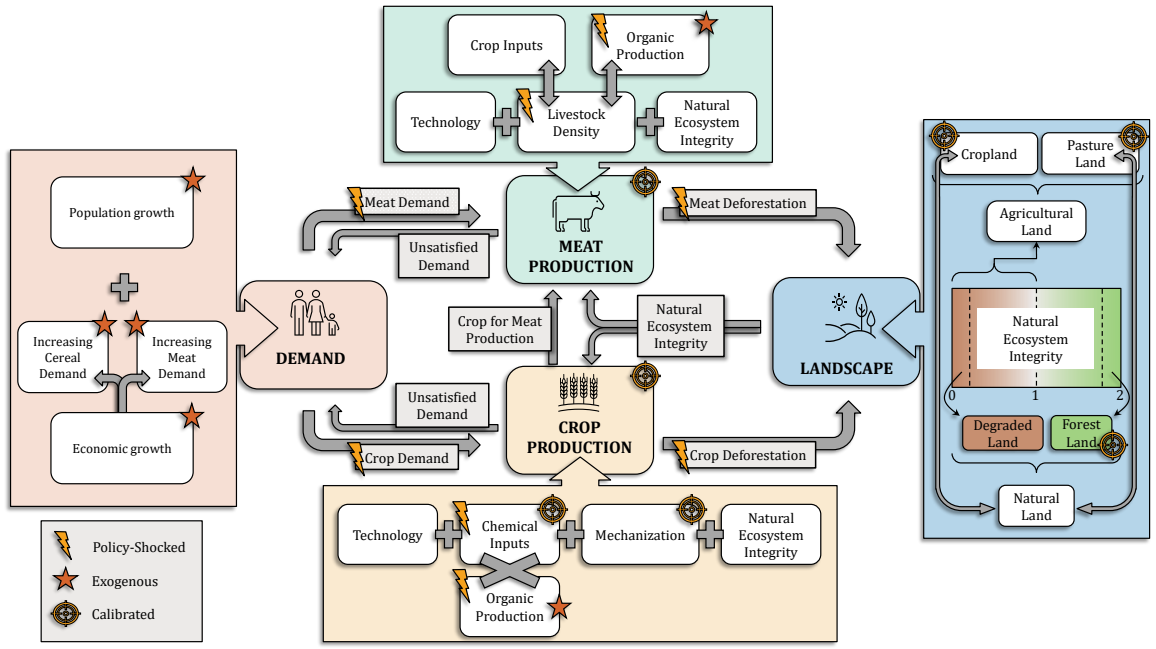


Figure 8.1 Schematic overview of the our dynamic simulation model organized into four main sections: the left panel introduces the demand drivers; the top and bottom panels detail the production and ecological feedback processes; and the right panel summarizes the resulting landscape structure and transitions. Specifically, the left panel shows how external drivers—specifically, population and economic growth (marked with stars for exogenous variables)—jointly determine increases in both cereal and meat demand. Central panels illustrate how these demand trajectories feed into crop and meat production systems, which are influenced by intensification variables such as technology advancement, chemical inputs, mechanization, livestock density, and the adoption of organic production (with targets indicating calibrated variables and lightning bolts indicating policy-shocked variables). Meat and crop production outcomes depend on and feedback to the integrity of natural ecosystems (a synthetic measure of local biodiversity and soil health, see Section 8.2.4), with low integrity reducing yields and increasing future land needs. The model tracks unsatisfied demand for both crops and meat, which triggers further land conversion—expanding either cropland or pasture at the expense of natural land and semi-natural vegetation. The right panel details landscape structure and transitions among key land categories: cropland, pastureland, natural land, forest, and semi-natural vegetation. Feedback loops connect ecosystem integrity not only to landscape structure, but also to production system performance, thus enabling the model to capture cross-scale dynamics and the effects of multiple policy levers.

For conventional crop production, total yield ($q_{c,t}$) is modeled as a multiplicative function of cultivated area ($A_{c,t}$), technological level (T_t), chemical inputs ($\Phi_{c,t} \geq 1$), mechanization ($M_{c,t} \geq 1$), and the condition of the natural ecosystem ($0 < \bar{\varepsilon}_{c,t} \leq 1$):

$$q_{c,t} = A_{c,t}(1 + T_t)(\Phi_{c,t})^k (M_{c,t})^f (\bar{\varepsilon}_{c,t})^{1-k-f} \tag{8.8}$$

The exponents $k < 1$ and $f < 1$ determine the sensitivities of yield to chemical and mechanical intensification, while $\bar{\varepsilon}_{c,t}$ captures the impact of average ecosystem integrity on conventional cropland.

This multiplicative function follows the long tradition of agricultural production modeling (*e.g.*, Cobb–Douglas and Mitscherlich-type functions, see [153]), which assume proportional rather than additive contributions of inputs. Including chemical inputs and mechanization reflects historical evidence that these were the dominant drivers of yield growth during the Green Revolution [464, 465]. In contrast, T_t is modeled as an efficiency shifter that increases the productivity of inputs without proportionally raising environmental degradation—for instance, through innovations in precision agriculture or improved crop varieties (see Eq. 8.20). This follows the common interpretation of technology as a residual factor capturing yield gains not directly attributable to input intensification [466, 467].

Total organic crop yield, which forgo chemical inputs, is given by:

$$q^{\mathrm{o}}_{c,t} = A_{c,t}(1 + T_t)(M_{c,t})^f(\bar{\varepsilon}^{\mathrm{o}}_{c,t})^{1-k-f} \tag{8.9}$$

where $\bar{\varepsilon}^{\mathrm{o}}_{c,t}$ is averaged only over organic cropland. Since $\Phi_{c,t} \geq 1$, organic yields are typically lower than those from conventional management.

Conventional meat production follows a similar structure, with intensification achieved through increased livestock density ($\Lambda_{m,t}$):

$$q_{m,t} = A_{m,t}(1 + T_t)(\Lambda_{m,t})^h(\bar{\varepsilon}_{m,t})^{1-h} \tag{8.10}$$

where $A_{m,t}$ is pasture area, $\Lambda_{m,t}$ is livestock density, and h modulates sensitivity to ecosystem integrity. Under organic livestock management, livestock densities are restricted, and yields are determined as:

$$q^{\mathrm{o}}_{m,t} = A_{m,t}(1 + T_t)(\min\{\Lambda_{\max}, \Lambda_{m,t}\})^h(\bar{\varepsilon}^{\mathrm{o}}_{m,t})^{1-h}. \tag{8.11}$$

Planned meat output generates a demand for crop-derived feed, which is passed to the crop module as:

$$D^{\mathrm{feed}}_{c,t} = r\left(q_{m,t} + q^{\mathrm{o}}_{m,t}\right) \tag{8.12}$$

where r is the crop-to-meat feed conversion factor. If total crop production is insufficient to meet both food and feed demands, livestock production is scaled back accordingly:

$$Q_{m,t} \leftarrow Q_{m,t} \min\left(1, \frac{Q_{c,t}}{D^{\mathrm{food}}_{c,t} + D^{\mathrm{feed}}_{c,t}}\right) \tag{8.13}$$

This minimization ensures that meat output does not exceed the level achievable with available crop resources after accounting for both direct human consumption and animal feed requirements. The symbol $\leftarrow$ indicates that this constraint applies within the same time period, *i.e.*, livestock are assumed to rely on crop production from the current period. While this represents a simplification—real systems include storage and trade—introducing such mechanisms would substantially increase model complexity.

Input intensities (mechanization, chemical use, livestock density) are updated dynamically for both organic and conventional systems as if managed by a representative farmer who adjusts input intensities to reduce gaps between demand and output in each period. This assumption is consistent with standard adjustment-cost frameworks in agricultural economics and ecological-economic modeling [365, 468].

Formally, adjustment follows a proportional correction rule:

$$M_t = M_{t-1} + \beta M_{t-1} \left(\frac{D_{c,t} - Q_{c,t-1}}{D_{c,t}} \right) \tag{8.14}$$

$$\Phi_t = \Phi_{t-1} + \delta \Phi_{t-1} \left(\frac{D_{c,t} - Q_{c,t-1}}{D_{c,t}} \right) \tag{8.15}$$

$$\Lambda_t = \Lambda_{t-1} + \gamma \Lambda_{t-1} \left(\frac{D_{m,t} - Q_{m,t-1}}{D_{m,t}} \right) \tag{8.16}$$

where β, δ, and γ set the speed of adaptive intensification. Technology advances exogenously via logistic growth, aligning with standard practice in stylized food–environment models [189]:

$$T_t = T_{t-1} + \nu T_{t-1} \left(1 - \frac{T_{t-1}}{T_{max}} \right) \tag{8.17}$$

where ν and T_{max} respectively determine the rate and the upper bound of technological advance.

8.2.4 Landscape and natural ecosystem integrity

The simulated landscape is represented as a 100×100 grid[1], where each cell is designated as cropland, pasture, or natural land, providing a stylized analogue of real-world land use (Fig. 8.2). The initial allocation reflects global 1960 conditions; over time, land transitions between states as economic and environmental pressures change.

Natural land may be converted to agriculture if production consistently falls short of demand, whereas underutilized or low-productivity agricultural plots can be abandoned and gradually restored through natural processes. In addition to these demand-driven adjustments, the model incorporates a baseline rate of land expansion and contraction to capture natural turnover in the agricultural sector. This reflects the reality that some farmers exit or enter farming independently of production shortfalls or market conditions, due to personal, institutional, or contextual factors [469, 470]. Specifically, the rates of expansion ($\varphi^+_{\cdot,t}$) and contraction ($\varphi^-_{\cdot,t}$) of agricultural land are modeled as:

$$\varphi^+_{\cdot,t} = \varphi \left\lfloor 1 + \zeta^+_{\cdot} \left(\frac{D_{\cdot,t} - Q_{\cdot,t-1}}{D_{\cdot,t}} \right) \right\rfloor \tag{8.18}$$

$$\varphi^-_{\cdot,t} = \varphi \left\lfloor 1 + \zeta^-_{\cdot} \left(\frac{Q_{\cdot,t-1} - D_{\cdot,t}}{D_{\cdot,t}} \right) \right\rfloor \tag{8.19}$$

Here, $\varphi^+\cdot$ and $\varphi^-\cdot$ represent baseline expansion and contraction rates, while $\zeta^+\cdot$ and $\zeta^-\cdot$ scale the response to unmet demand or excess production. The notation $\cdot$ is a placeholder for the relevant land type (crop or pasture).

Sites prioritized for conversion to agriculture are those with highest ecosystem integrity (thus promising higher yields), while marginal, less productive plots tend to be abandoned first, consistent with empirical patterns of agricultural abandonment in more degraded areas [382, 471].

[1]This system size was chosen to be sufficiently large to smooth out effects of random initialization, while remaining computationally tractable. Results remain consistent when varying grid size, since no variable explicitly depends on system dimensions.

Each site is assigned a natural ecosystem integrity index (ε), which serves as a synthetic indicator quantifying both above-ground and below-ground ecosystem conditions. Specifically, ε reflects the multi-dimensional state of ecosystem health, including biodiversity as well as soil health attributes. This approach draws on established ecological frameworks [472–474], where ecosystem integrity is understood as the capacity of an ecosystem to maintain its characteristic structure, composition, and functional processes in the face of human disturbance. In our model, natural sites have ε values between 0 and 2, reflecting a gradient from degraded to pristine conditions, whereas agricultural plots are constrained between 0 and 1. Conversion from high-integrity natural to agricultural land causes a sharp drop in ε, representing rapid loss of habitat complexity [475]. In contrast, restoration or abandonment of agriculture allows for gradual recovery, with sites retaining their existing ε and accumulating integrity over time. For analytical purposes, we refer to cells with $\varepsilon > 1.9$ as forest and those with $\varepsilon < 0.1$ as degraded—these labels facilitate interpretation but do not alter the underlying dynamics.

Ecosystem integrity in each cell ($\varepsilon_{i,t}$) is updated at every time step using exponential decay, a standard approach in stylized ecological models [476, 477]. This formulation captures both degradation from agricultural use and natural restoration when land is left fallow. Exponential decay is widely used to represent gradual ecosystem degradation due to sustained pressures, while logistic-style recovery functions mimic the diminishing returns of restoration as ecosystems approach their maximum integrity [478]. Let τ_i denote the land-use type of cell i—m for pasture, c for cropland, and n for natural land—and let E_t represent the system-wide provision of ecosystem services at time t (see 8.21). The update rule is:

$$\varepsilon_{i,t} = \begin{cases} \varepsilon_{i,t-1}\left[1 - \theta_{i,\mathrm{m}}\dfrac{\Lambda_t}{E_t}\right] & \text{if } \tau_i = \mathrm{m} \\ \varepsilon_{i,t-1}\left[1 - \theta_{i,\mathrm{c}}\dfrac{M_t + \Phi_t}{E_t}\right] & \text{if } \tau_i = \mathrm{c} \\ \varepsilon_{i,t-1}\left[1 - \theta_{i,\mathrm{n}}E_t\left(1 - \dfrac{\varepsilon_{i,t-1}}{\varepsilon_{\max}}\right)\right] & \text{if } \tau_i = \mathrm{n} \end{cases} \tag{8.20}$$

Here, Λ_t, M_t, and Φ_t are the intensities of livestock density, mechanization, and chemical inputs, respectively. The parameters $\theta_{i,\mathrm{m}}$, $\theta_{i,\mathrm{c}}$, and $\theta_{i,\mathrm{n}}$ determine the rates of degradation (for agricultural land) or restoration (for natural land), modulated by overall system intensification and the supply of ecosystem services. $\varepsilon_{\max}$ represents the maximum possible ecosystem integrity.

Ecosystem service supply is captured by a non-linear function of the area and integrity of natural patches in the landscape, drawing on empirical evidence for sublinear (concave) scaling [478, 479]:

$$E_t = \left(\frac{\sum_{i \in N} \varepsilon_{i,t}}{\sum_{i \in N} \varepsilon_{i,0}}\right)^p \tag{8.21}$$

where N stands for all natural cells and $p < 1$ ensures diminishing returns as the natural area increases.

8.2.5 Parameter specification and numerical experiments

The model parameters were determined by combining data-driven estimation, calibration against observed agricultural trends, and fixed assignments based on commonly-used values found in the literature (Fig. 8.3). Most ecological parameters, including the average degradation

and restoration rates ($\theta_{i,\cdot}$), and the ecosystem service exponent (n), were primarily set using empirical data or well-established values from previous studies. The same approach was used for the power exponents in the production functions. For these parameters, a more detailed discussion of choice, context specificity, and inherent complexity is provided in the Appendix.

Of the remaining parameters, those with influence limited to exogenous variables were fitted directly to corresponding empirical data (*e.g.*, demand parameters and the rates of sustainable and organic production adoption). Those that depended on the dynamic realization of the system were calibrated to reproduce observed land use and input trends, particularly using the 1960–2022 FAO data [171].

We explored our model through extensive numerical simulations. Unless stated otherwise, results are presented as averages over 500 simulation runs, and standard errors are not shown in the figures as their magnitude was found to be negligible (smaller than line width). It should be noted that the model does not include stochasticity in the production functions; thus, the observed variation among simulations arises solely from the randomly generated landscape configurations, the stochasticity of restoration and degradation rates, and the random nature of the cells targeted for land-use change.

We evaluated a business-as-usual trajectory alongside a suite of alternative policy scenarios. The baseline scenario was produced by running the model up to the year 2100 with the parameter values listed in Table 1 of the Appendix, while the policy scenarios targeted modifications in the form of constraints or adjusted model parameters. Unless otherwise noted (as in Fig. 8.6), all parameter variations in these scenarios represent a 10% increase or decrease relative to the corresponding calibrated baseline value. For scenarios involving changes in demand, we implemented a 10% reduction with respect to the additional demand attributed to projected population and income growth between 2022 and 2100. To maintain consistency and comparability between scenarios, every simulation was initialized with all natural ecosystem integrity values set to their maximum value for both natural and agricultural land, and assumed that all land not allocated to agriculture is classified as forest, and thereby excluding the presence of semi-natural vegetation. Although this initial condition may not fully reflect levels of natural degradation in 1960, it is reasonable given that the global expansion of intensive agricultural practices has occurred mainly in recent decades. Moreover, because our primary focus is on outcomes relative to the baseline scenario, this assumption does not substantially affect our overall conclusions. Further information on the initialization procedure can be found in the Appendix.

8.3 Results

The business-as-usual scenario provides a reference trajectory under current trends in population, consumption habits, and land management practices. This scenario serves as a baseline against which the effectiveness and trade-offs of alternative policy interventions can be assessed.

8.3.1 Business-as-usual scenario

The business-as-usual scenario highlights a persistent transformation of the landscape, primarily driven by increasing demand for food and livestock products (see Fig. 8.4). As agricultural activity intensifies and expands, natural and semi-natural ecosystems are progressively converted or degraded (see Fig. 8.4a and Fig. 8.4d). Indeed, the expansion of agricultural land directly

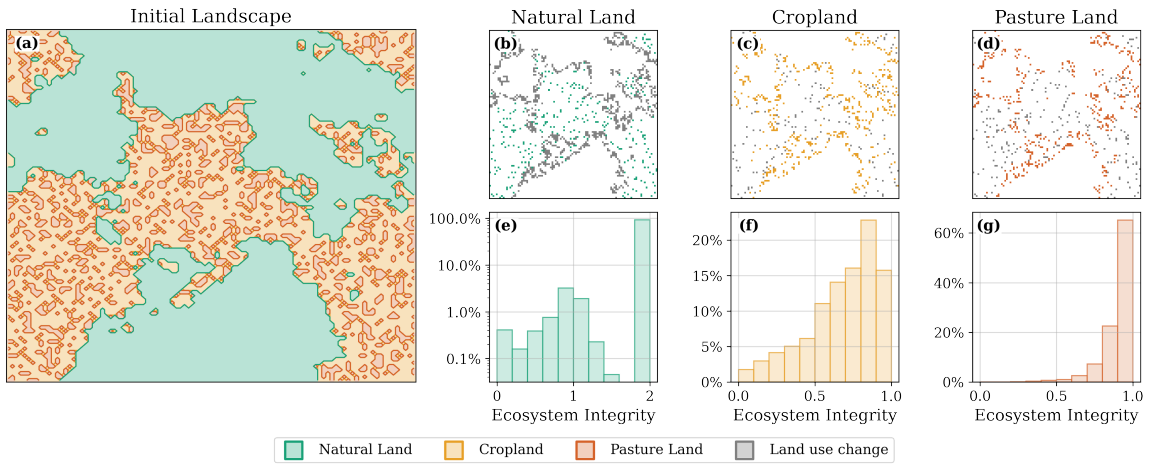


Figure 8.2 Spatial patterns of the initial landscape and subsequent land-use changes. Panel (a) shows the initial arrangement of natural land (green), cropland (yellow), and pastureland (brown), capturing the mosaic structure at the start of the simulation. Panels (b) to (d) illustrate land-use transitions by 2100: green marks new natural land arising from abandonment and restoration, yellow corresponds to recent cropland expansion, brown highlights pastureland conversion, and gray indicates cells that switched from natural land, cropland or pasture land land-use types, respectively, to another over the simulation period. As agriculture expands, cropland and pasture increasingly encroach upon forest edges, concentrating in more fertile zones and leaving behind scattered, less productive patches that begin natural restoration. Panels (e) to (g) present histograms of the final distribution of ecosystem integrity for natural land, cropland, and pastureland, respectively. These distributions reveal pronounced degradation in croplands due to continued intensification via mechanization and chemical inputs. Simultaneously, abandoned sites emerge in the natural land distribution, showing early signs of ecological recovery, although these seminatural patches remain well below the ecosystem integrity threshold necessary to qualify as forest ($\varepsilon_{i,t} > 1.9$, see Eq. 8.20).

reduces both the area and overall integrity of natural habitats, resulting in a notable decline in forest land and average ecosystem health within each land use category.

This transformation is particularly evident in the case of cropland (see Fig. 8.4b and Fig. 8.4e). Here, both land consumption and ecological degradation reach their highest levels, largely as a consequence of the high degree of intensification and mechanization required to meet rising food demands. A substantial proportion ($\approx$ 40% in recent years) of these crops is allocated to livestock feed, and thus the ecological footprint of crop expansion is strongly tied to meat production and associated changes in dietary habits.

Pastureland dynamics further illustrate the complex feedback mechanisms in the system. While advances in technology and animal husbandry—such as vaccines and growth hormones—have enabled higher livestock densities and contributed to a recent decline in the area under pasture, our model projects that this trend will ultimately reverse. As technological improvements plateau and can no longer keep pace with rapidly rising demand for meat, the pressure for additional pasture expansion resurfaces.

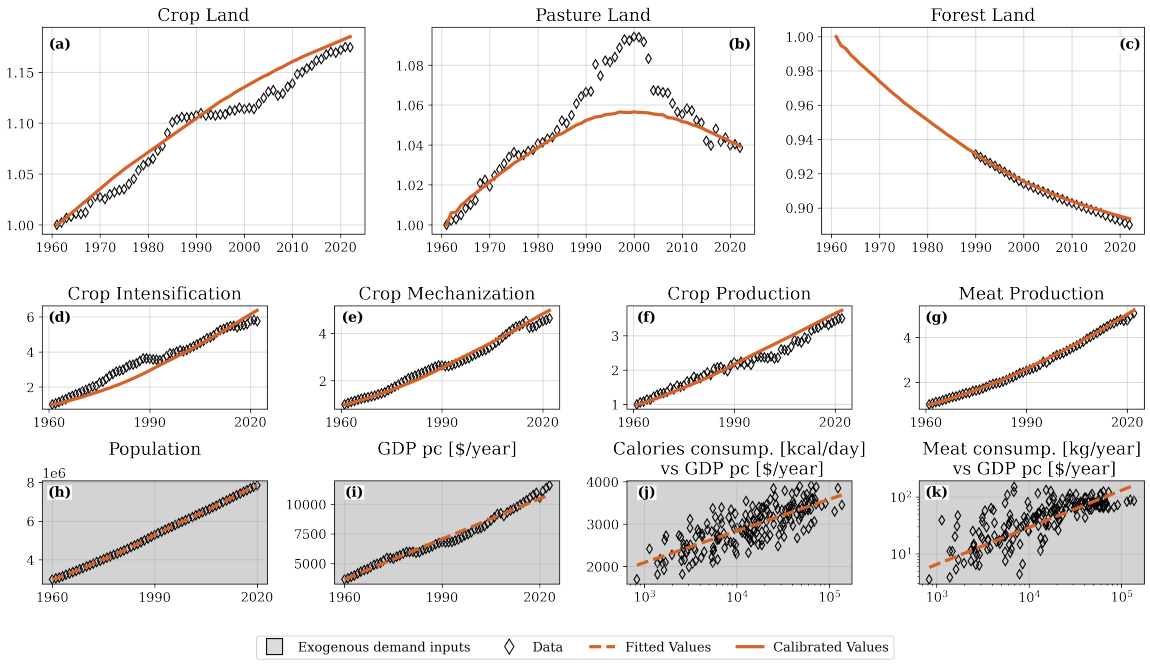


Figure 8.3 Model calibration against major historical trends in agricultural, land use, and socioeconomic indicators. Each panel displays the model's simulated results (solid orange lines, normalized to 1 in 1960 to emphasize rates of change) and historical observations from 1960 to 2022 (black diamonds; data from FAO [171, 480]). The model parameters were calibrated to reproduce empirical trends, and all curves represent averages over 500 Monte Carlo simulations. In particular, the model closely captures key historical patterns, in particular sustained increases in agricultural production and yield, driven by a significant expansion in total demand for both crop and animal products. It also reproduces the peak and subsequent decline in the rate of pasture land expansion, which results from land use efficiency gains as intensification has offset some demand growth. Stable or rising trends in production inputs, such as fertilizer use and mechanization, are also well represented. Gray-shaded panels indicate exogenous input variables (*e.g.*, population, per capita income): here, dashed orange lines represent fitted values matched directly to observed data, which are then used as fixed, absolute model inputs.

Taken together, these trends accelerate the fragmentation of remaining high-integrity habitats and the spread of degraded patches across the landscape. As demonstrated by spatial analyses (Fig. 8.2), contiguous forest edges are eroded, creating a more fragmented matrix of land uses, while marginal agricultural areas are often abandoned in favor of clearing more productive forested sites. This mosaic of change not only undermines biodiversity but also weakens the ecosystem services that support long-term agricultural productivity.

Collectively, these findings underscore that, without targeted interventions, current trajectories reinforce a self-perpetuating cycle of ecological decline and agricultural expansion. Under this business-as-usual scenario, we observe reduced landscape resilience, increasing dependence on intensification solutions. The baseline scenario therefore highlights the urgent

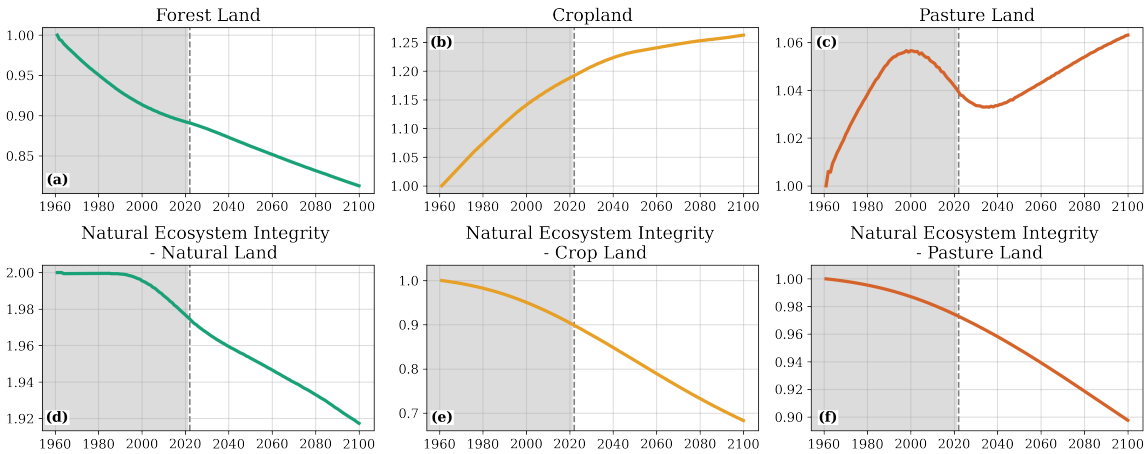


Figure 8.4 Land use and ecosystem integrity trajectories under the business-as-usual scenario. Top panels (a–c) show the temporal trends of the various land-use types: panel (a) tracks the ongoing decline in forest area, panel (b) captures the steady expansion of cropland, and panel (c) traces changes in pastureland. The gray-shaded background indicates the historical period, with projected dynamics shown to the right of the dashed vertical line. Pastureland area initially decreases due to advances in technology and more efficient animal husbandry, which allow for higher livestock densities. However, as technological improvements plateau and can no longer match the rising demand for meat, our model anticipates a renewed expansion of pasture area in the future. Bottom panels (d–f) depict temporal changes in the mean ecosystem integrity index for natural land (d), cropland (e), and pastureland (f). These plots reveal the rapid and sustained degradation of ecosystems associated with agricultural expansion and the ongoing loss of ecological integrity across all land types. Of particular interest is the fact that declines in natural ecosystem integrity lag behind the decrease in forest area; this is because deforestation initially diminishes the supply of ecosystem services vital for maintaining ecosystem stability (see Eq. 8.21). As these services decline, the degradation of agricultural land accelerates (see Eq. 8.20), leading to land abandonment and a reduction in the average natural ecosystems integrity.

need to explore alternative policy actions.

8.3.2 Effects of single policy measures

We next assess the effects of implementing individual policy interventions, each focused on a specific lever within the food and land system. The complete set of considered scenarios is presented in Fig. 8.5, with corresponding parameter details provided in the Appendix. This analysis not only evaluates the direct impact of each measure but also reveals how compensatory system responses can undercut their effectiveness, producing trade-offs or unintended outcomes.

Fig. 8.5a maps single-policy scenarios in a space defined by forest land area variation and degraded land variation, both calculated relative to the baseline. These two metrics were selected to capture the dual dimensions of land system change: forest land variation reflects shifts in the extent of intact natural habitats (landscape-scale expansion or protection), while

degraded land variation quantifies changes in ecosystem integrity within managed areas due to intensification or restoration efforts. By presenting results in this way, we can compare policies that limit expansion (horizontal direction) with those that primarily aim to improve land already in production (vertical direction), clearly illustrating system-wide trade-offs.

The analysis reveals considerable variability in policy outcomes, much of which stems from compensatory dynamics—where gains in one area trigger pressures elsewhere. For example, supply-side measures such as reducing chemical inputs or expanding organic crop production are effective at lowering land degradation, but typically cause declines in forest area. This is because reduced yields on existing farmland (from chemical restrictions or organic conversion) require compensatory expansion, driving new deforestation and landscape fragmentation to maintain overall production levels. Similarly, implementing deforestation bans for crop or meat production often leads to increased land degradation, because production pressures shift onto existing agricultural land, resulting in more intensive management. Over time, such intensification can diminish yields and degrade ecosystem integrity, which may ultimately drive further land expansion and limit the effectiveness of deforestation policies.

Conversely, demand-focused interventions—particularly reductions in crop or meat consumption—deliver more comprehensive positive outcomes, as they simultaneously relieve pressure for both intensification and expansion. Policies that reduce meat consumption result in the largest gains for forest area and the most pronounced reductions in degraded land. This is because a substantial share of cropland is devoted to growing feed for livestock, and thus plant-based diets reduce both direct and indirect land pressures

8.3.3 Synergies and trade-offs in policy portfolios

We then turn to the analysis of policy combinations addressing multiple drivers at once, exploring how different mixes of interventions impact ecosystem integrity. Figures 8.5b, 8.5c, 8.7 and 8.6 summarize these results, allowing direct comparison of policy portfolios.

An initial finding, visible in Fig. 8.5b, is that policies often regarded as highly sustainable—namely, widespread adoption of organic crop production (eliminating chemical inputs) and reduced livestock intensification (for improved animal welfare)—consistently result in a declining forest land area, regardless of whether they are combined with moderate reductions (10%) in crop and meat demand.

The underlying mechanisms behind this result differ between crop and meat systems. For organic crop production, the primary constraint is related to the strong diminishing returns ($k = 0.2$ in Eq. 8.8 and Eq. 8.9) from chemical inputs. It is important to note that our model represents organic farming as a strict exogenous constraint on input substitutions, abstracting away from more complex agroecological practices that could mitigate these yield losses. Moderate chemical use can maintain relatively high yields, but if chemical inputs are eliminated entirely, yield losses grow disproportionately and become very difficult to offset. Most farmers are unable to fully compensate for these losses through additional intensification or mechanization, as the required extra effort would be prohibitive—leading the system to expand cultivation into natural areas to maintain production targets.

The dynamics differ for organic meat production. Here, shifting to organic practices does not generate the same drastic loss of productivity per unit area because industrial animal production is less constrained by input intensification—modern techniques like vertical livestock integration (as seen recently in China [481, 482]) support continued output growth. Consequently, organic meat policy mixes exert only modest negative effects on forest land. However, if livestock

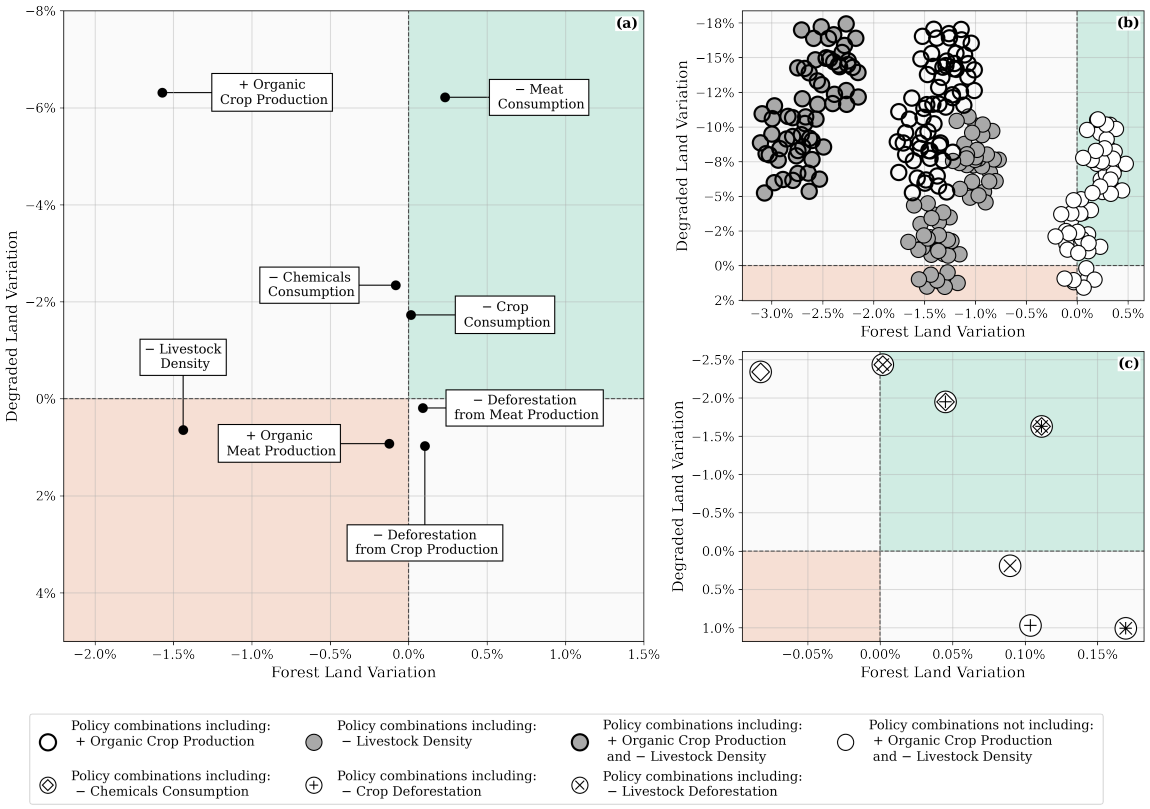


Figure 8.5 Impact of individual and combined policy interventions on forest and degraded area variation. Variations in forest area (horizontal axis) and degraded area (vertical axis) are shown as percentage changes with respect to the baseline scenario. Points in the upper-right green quadrant indicate policy strategies that succeed in both expanding forest area and reducing degraded land, while those in the lower-left quadrant are detrimental on all grounds. Panel (a) shows the effects of individual (single) policy interventions, each marked by a labeled point. Only the reduction in meat consumption achieves positive outcomes on both axes, illustrating that most single interventions are insufficient due to persistent compensatory dynamics within the system. Panel (b) reports outcomes for policy mixes that specifically include increased organic crop production and decreased livestock density—two interventions often viewed as hallmarks of sustainability. Here, each point represents a different mix with other measures. The results demonstrate that these strategies, even when paired with moderate reductions (10%) in crop and meat demand, consistently fail to halt forest loss, often resulting in further declines in forest land area. Panel (c) highlights selected policy mixes containing key interventions, such as chemical use reduction or restrictions on "crop and livestock-driven" deforestation, with distinct symbols denoting which measures are included. This panel shows that policy mixes combining interventions that target both intensification and expansion (*i.e.*, orthogonal strategies) are situated in the green quadrant, signifying that integrated approaches are most effective at overcoming compensatory effects.

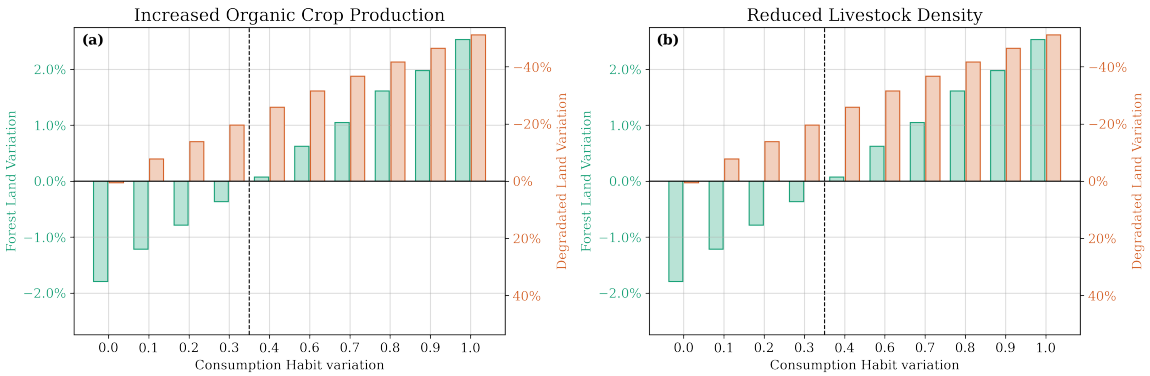


Figure 8.6 Effect of demand reductions on forest and degraded land areas under enhanced organic crop production and reduced livestock density policies. Each panel shows the percentage change in forest land (green, left axis) and degraded land (orange, right axis) compared to the baseline, across scenarios with progressive demand reductions. In particular, the x-axis represents increasing reductions in projected crop and meat demand by 2100, where 0 means no change from business-as-usual and 1 means no demand increase after 2022. The results demonstrate that only when demand reductions surpass roughly 40% do both forest expansion and significant decreases in degraded land occur.

production is broadly de-intensified without such adaptive capacity, the pressure to maintain meat supply quickly translates into greater expansion of pasture or feed crops, significantly amplifying deforestation.

While some past studies have stopped at these findings [454]—concluding that sustainable production is unfeasible—our model enables quantification of the scale of demand reduction necessary to reverse these negative trends. As shown in Fig. 8.6, only scenarios with at least a 40% reduction in projected crop and meat demand by 2100 achieve net gains in forest cover and notable reductions in degraded land when either an increase of organic crop production or a reduction in livestock density is promoted. This highlights the scale of lifestyle and societal change required for promoting animal welfare and eliminating chemical use.

Focusing next on policy mixes that exclude organic crop expansion and livestock intensity reduction, the analysis reveals that combining interventions yield more favorable outcomes than isolated policies. As demonstrated in Fig. 8.5c, mixes incorporating at least two different policies outperform single interventions. When policies target both degradation (*e.g.*, reduced chemical use) and deforestation (*e.g.*, conversion controls) together, their effects reinforce one another and mitigate compensatory expansion or intensification. Furthermore, these policies can initiate a positive feedback loop: by halting deforestation, ecosystem service provision is enhanced, and when combined with reduced intensification, this leads to improved natural ecosystem integrity. As ecosystem health recovers, agricultural yields are boosted, which in turn reduces the need for future land expansion.

Examining the highest-performing mixes (Fig. 8.7), we see that the top portfolios for reducing degradation mainly involve a combination of reduction in chemical inputs alongside decrease in crop and meat consumption—pointing again to the necessity of shifting dietary

habits. Conversely, the best-performing portfolios for forest preservation include deforestation restrictions and meat demand reduction, while measures aimed solely at reducing chemicals or crop demand are less central—since they contribute minimally to curbing deforestation, especially that driven by livestock.

Ultimately, only a single portfolio achieves top-tier outcomes for both forest recovery and land degradation, combining deforestation limiting measures, intensification limits, and reductions in both meat and crop consumption. While additional trade-offs may exist beyond the scope of this study, these results highlight that well-designed policy portfolios aligning both supply- and landscape-level actions—with a strong emphasis on demand reduction—are essential for achieving "win-win" gains and real progress toward sustainability.

8.4 Discussion

8.4.1 Beyond the supply-side: Systemic barriers to sustainability

Our results highlight important limits to achieving a sustainable food system through supply-side reforms alone, echoing findings across the literature on land use, agricultural intensification, and food system sustainability [456, 483, 484]. Measures such as reducing chemical inputs and adopting more animal-friendly or organic production systems provide meaningful improvements at the farm scale—ranging from reductions in local pollution to gains in animal welfare and soil health [439, 485]. These changes are valuable in themselves, and often come with additional social benefits, including positive impact on human health and responsiveness to consumer demand for more sustainable food options.

However, our model suggests that when per-hectare productivity is deliberately limited—whether by banning chemical inputs or reducing livestock density—the system tends to compensate by converting additional natural or semi-natural land to agriculture. This compensatory expansion can reduce or even offset the environmental benefits achieved on existing farmland, and in some cases may exacerbate pressures such as deforestation, landscape fragmentation, and ecosystem degradation, consistent with previous observations about indirect land-use change [451, 486]. Even when multiple supply-side measures are combined, our analysis indicates that their cumulative impacts alone are unlikely to halt forest loss or secure broad-based ecosystem integrity.

Let us stress that these findings do not imply that supply-side reforms are undesirable; rather, they highlight the need to complement them with demand-side transformations and broader systemic changes if the goal is to achieve consistent sustainability.

8.4.2 Structural need for demand reductions

A second, and more profound, implication of our findings is that only strong demand-side interventions are capable of delivering transformative change. Substantial reductions in total food—especially meat—consumption relieve system-wide pressure by cutting both the intensification and expansion drivers simultaneously. This is consistent with a growing body of research indicating that dietary shifts toward reduced animal-source foods (*i.e.*, more plant-based diets) are critical to staying within planetary boundaries and achieving global climate, biodiversity, and public health targets [438, 487, 488].

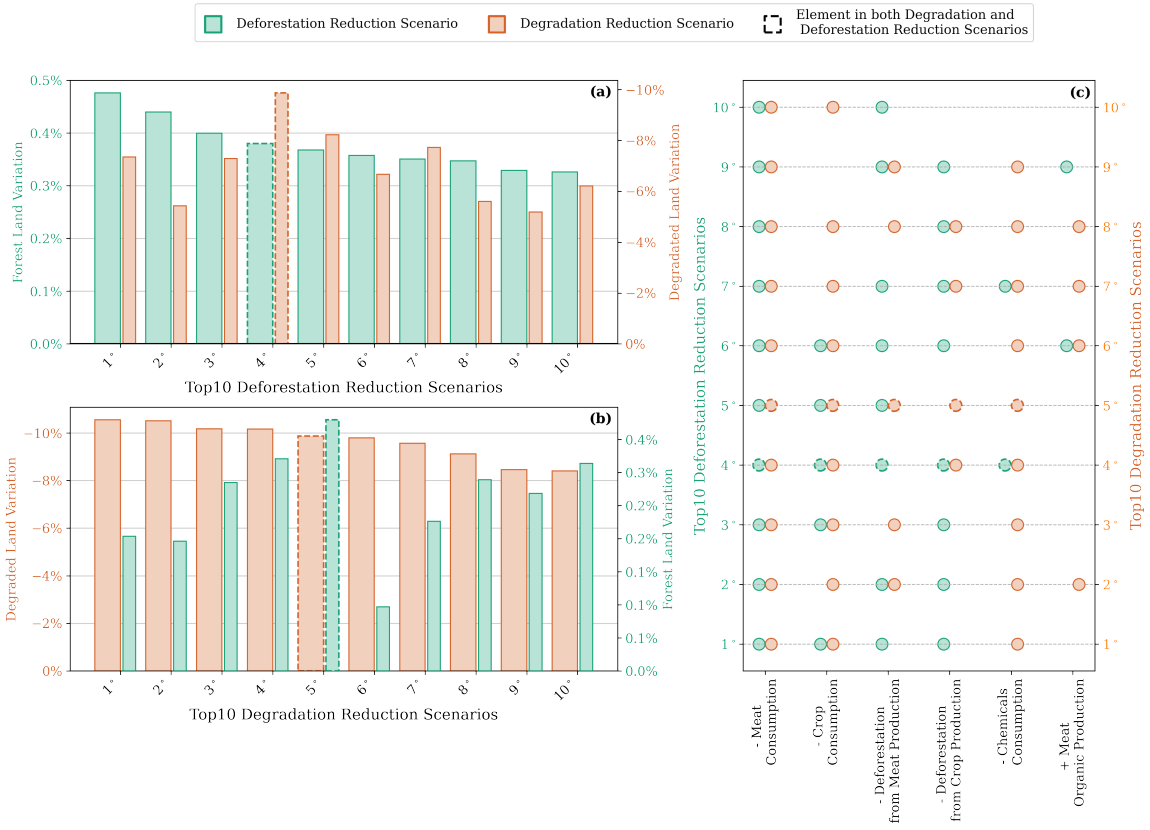


Figure 8.7 Comparative effectiveness of top-performing policy mixes for reducing deforestation and land degradation. Panels (a) and (b) display, for each of the ten best policy combinations, the relative variation in forest land and degraded land areas as a percentage change from the baseline scenario. Policy mixes are ranked separately by their success in reducing deforestation (a) and degradation (b). Dashed bars indicate policy mixes that appear among the top performers for both objectives together. Panel (c) details the intervention composition of each policy mix. Each row represents a ranked policy mix (from most to least effective; top to bottom), and each circle indicates the inclusion of specific interventions for the corresponding scenario (green for deforestation-focused, orange for degradation-focused). Despite some overlap, the policy measures most effective at reducing deforestation are not always the same as those best at lowering land degradation. Only a policy portfolio achieves high performance in both dimensions, highlighting the importance—and challenge—of integrated strategies capable of delivering simultaneous gains for forest conservation and reduced agricultural ecosystem degradation.

Our quantitative analysis provides a concrete threshold: unless roughly 40% of projected excess demand for crops and meat is curbed by 2100, even the most ambitious supply-side or reforestation interventions are unlikely to reverse deforestation or halt land degradation (see also [489]). Crucially, demand modification is not only more effective at limiting land use changes but also makes it easier for other sustainability policies (like reduced chemical use or organic expansion) to succeed—a synergy recognized in other modeling exercises and global

sustainability assessments [457].

8.4.3 Integrated approaches and systemic solutions

Despite the importance of demand-side measures, our results do not dismiss the value of integrated, multi-faceted policy mixes. Rather, they demonstrate that combinations of carefully designed interventions—addressing both production and consumption—yield the most robust improvements for both forest and degraded land areas variation. Such an integrative approach directly mitigates compensatory effects, wherein policies addressing one part of the system inadvertently shift environmental pressures elsewhere unless implemented holistically [447, 451, 490]. For instance, coupling landscape-level deforestation controls with intensity reduction measures (*e.g.*, limits on chemical inputs) can prevent rebound effects and increase overall ecosystem integrity [1, 491].

It is worth noting, however, that many popular narratives around sustainable intensification or organic conversion tend to overemphasize the benefits of any single intervention, without sufficient attention to the cross-scale feedbacks and compensatory land dynamics illuminated by both our results and other studies [492, 493]. A successful transition to a food system that maintains ecosystem integrity and food security together will likely require not just technical or agronomic innovation, but deep societal, economic, and behavioral changes [456].

8.4.4 Limitations and unaccounted aspects

While we believe our study advances the understanding of systemic trade-offs and leverage points in the pursuit of sustainable food and land systems, it is important to acknowledge several limitations that may influence the interpretation and applicability of our findings—both in terms of modeling assumptions and the practicalities of real-world policy implementation.

Our framework adopts a stylized, spatially explicit global representation. This abstraction allows us to distill essential system dynamics and identify general insights on policy interactions, while avoiding the computational and data demands of fully resolving geographic, ecological, and socio-economic heterogeneity. But, local variations—shaped by climate variability, land tenure, market integration, and governance [447, 451, 494]—are not explicitly represented. However, these features could be incorporated in future extensions through nested multi-scale models or spatially explicit downscaling approaches, enabling more context-sensitive analyses [495].

Similarly, our land conversion and abandonment rules respond primarily to aggregate supply-demand imbalances. This simplification abstracts from mediating effects such as access to infrastructure, transaction costs, or governance quality. While this allows transparent exploration of system-wide drivers, future model iterations could incorporate heterogeneous decision-making rules or probabilistic entry/exit dynamics to capture local socio-institutional variation [492].

Crop and livestock production modules rely on generic functional forms calibrated to global data. While sufficient for identifying broad trends, these formulations omit local adaptation, site-specific constraints (*e.g.*, soil degradation, pests, water stress), and stochastic variability in yields. Likewise, our management systems currently exclude agroecological or diversified strategies, focusing instead on conventional and organic monocultural systems. Future work could integrate heterogeneity in production technologies, mixed-cropping systems, or resilience-enhancing practices to more realistically capture the spectrum of sustainable management

options [496].

The socio-political dimension of policy implementation is currently represented exogenously, assuming instantaneous and uniform enactment. While this simplification enables clear analysis of policy potential, it neglects real-world constraints such as political resistance, institutional capacity, stakeholder engagement, and uneven enforcement [2, 497]. Incorporating adaptive policy implementation, delays, and compliance heterogeneity would allow more realistic assessment of feasible outcomes and the robustness of interventions.

Our model does not differentiate actors in the food system, and therefore omits social and equity dimensions. While this enables focus on aggregate system-level trade-offs, it excludes potential distributional consequences such as food insecurity, livelihood impacts, or shifts in nutrition. Future extensions could integrate agent-based or household-level modules to explore these outcomes under alternative policy scenarios [498, 499].

Climate-related risks and long-term ecological processes are simplified. Feedbacks from extreme events, biodiversity loss, tipping points, and delayed ecosystem recovery are not dynamically represented. This choice was made to retain tractability for global simulations while highlighting general mechanisms. Future work could include stochastic climate shocks, ecological inertia, and recovery lags to capture more realistic ecological dynamics [500–502].

Behavioral and demographic dynamics are also exogenous. Food demand does not adapt through social learning, policy feedback, or price-mediated behavior, and population changes and migration are not modeled. These processes are known to shape long-term land-use trajectories [449, 503]. Incorporating endogenous behavioral adaptation and demographic dynamics would allow more robust exploration of feasible pathways and potential rebound effects [504, 505].

Finally, as with all global modeling efforts, results are subject to parameter uncertainty, data limitations, and simplifications of real-world complexity. Our stylized approach enables identification of core system-level interactions and policy synergies, but should be interpreted as generating hypotheses rather than prescriptive solutions. Future work should prioritize multi-scale, participatory, and transdisciplinary models that incorporate climate risk, social equity, behavioral feedbacks, and realistic policy processes, providing the basis for actionable, locally calibrated insights [504, 506].

8.5 Conclusion

The results of this study highlight the urgent need for a paradigm shift in how we address food system sustainability. Technological and agronomic improvements, while necessary, are insufficient in isolation to meet the challenges posed by rising global food demand and intensifying environmental pressures. Our systemic approach reveals that only integrated strategies—combining ambitious dietary changes with reformed agricultural practices and strengthened landscape conservation—can reconcile the competing demands of productivity, ecosystem integrity, and social equity.

Our research supports the growing consensus in the literature that demand-side interventions must be placed at the center of sustainability and climate agendas [438, 507]. Avoiding counterproductive trade-offs requires a holistic, system-based approach that aligns policies across supply, demand, and governance. At the same time, future progress depends on robust efforts to tailor and implement these solutions to diverse regional, cultural, and socio-economic contexts, as well as on building public support for transformative change.

Going forward, further refinement of integrated models like ours is needed. In particular, future research should focus on incorporating more explicit representations of climate impact, equity dimensions, market and policy dynamics, and the complex processes underlying behavior and dietary shifts. Advancing multi-scale, participatory, and interdisciplinary modeling will be crucial to develop actionable roadmaps for policymakers and stakeholders.

8.6 Supplementary materials

8.6.1 Initialization

The system initialization proceeds as follows:

- The model employs a 100×100 grid to represent the landscape, initially allocating 50% of the area to forest land. This proportion reflects estimates for the year 1960 based on FAO data [171]. To spatially distribute this fraction, a fractal field with a characteristic correlation length ξ is generated. Previous research suggests that fractal patterns realistically capture empirical land use distributions [508, 509]. The value for ξ, chosen to produce a visually realistic arrangement, is reported in Table 8.1. After allocating forested cells, the remaining landscape is randomly assigned to pasture (35%) and cropland (15%).
- Next, each cell receives specific degradation and restoration rates. These are assigned using the concept of lifespan, which aligns well with the properties of exponential distributions. This approach has been motivated by soil science literature, where the exponential lifetime of soil layers is tied to degradation and erosion processes [510]. Following results this stream of research, each parameter $\theta_{i,\cdot}$ is sampled as:
$$\theta_{i,\cdot} = \frac{1}{\mathcal{N}(\mu_{\cdot}, \sigma_{\cdot})},$$
where $\cdot$ stands for natural (n), pasture (m), or cropland (c), and $\mathcal{N}$ denotes a lognormal distribution. The adoption of a lognormal distribution ensures the statistical characteristics of the rates are consistent with those reported by Evans et al. [510].
- Initial real demand for both crops and meat is computed following Eq. 8.1 and Eq. 8.2. To translate this demand into the model's internal units, we normalize by assigning constants $\omega_{\cdot}$ such that the initial yield for both livestock and crops is set to $q_{\cdot,0} = 1$. Assuming that at the starting point total production matches demand, we have $Q_{\mathrm{c},0} = 1500 = D_{\mathrm{c},0}$ and $Q_{\mathrm{m},0} = 3500 = D_{\mathrm{m},0}$. Since this step only rescales the reference point, the overall system dynamics are unaffected.
- Intensification factors are then initialized to have $q_{\cdot,0} = 1$ in the initial year, which requires livestock density, mechanization, chemical input intensity, and average ecosystem integrity to all be set to one at initialization. In contrast, we assign the initial technology level a small value ($T_0 = 0.001$), reflecting the limited state of agricultural innovation prior to the Green Revolution. While this may result in yields slightly above one, the difference is negligible for trend analysis.
- With all state variables initialized, the model is ready to proceed with the simulation.

8.6.2 Calibration procedure and parameter values

Model parameters were categorized into four distinct groups (see Table 8.1): (i) *measured* parameters (M), which are directly fitted from empirical datasets; (ii) *estimated* parameters (E), sourced from values reported in the literature; (iii) *calibrated* parameters (C), which are adjusted during model calibration to achieve the best agreement between simulated and observed data; and (iv) *fixed* parameters (F), which are manually specified due to the lack of real-world analogs or because of model simplifications.

Measured parameters (M) are defined as those whose values are determined using empirical data corresponding directly to the model functions they influence. This group mainly encompasses parameters governing demand and the initial state of the landscape, where reliable datasets are readily available. Parameter values were estimated by fitting model outputs to observed data from FAO[171, 480], using a least squares minimization approach to ensure alignment with real-world patterns. It should be emphasized that the aim of this calibration was not to achieve exact reproduction of the full distribution of empirical curves, but rather to capture the essential trends relevant to the aims of this study. Within this context, all fitted functions yield a robust agreement with the empirical data, adequately representing the characteristic patterns for each parameter considered (see Fig. 8.3).

Estimated parameters (E) were assigned values drawn from empirical studies and widely reported literature benchmarks. This category chiefly includes ecological parameters such as rates of degradation

Section	Notation	Description	Value	Group
Landscape Initialization		Grid size	100x100	F
		Natural land share	50%	M
		Cropland share	15%	M
		Pasture land share	35%	M
	ξ	Landscape fragmentation	10	F
	μ_c	Crop degradation distribution shift	1	E
	μ_m	Pasture degradation distribution shift	1	E
	σ_c	Crop degradation distribution scale	10000	E
	σ_m	Pasture degradation distribution scale	5000	E
	μ_n	Nature restoration distribution shift	1	E
	σ_n	Pasture degradation distribution scale	1000	E
Demand	a	Calories demand calculation [kcal $\cdot$ year^{-1} $\cdot$ per capita]	-138.2	M
	b	Calories demand calculation [kcal $\cdot$ \$$^{-1}$ $\cdot$ per capita]	744.4	M
	c	Baseline demand for animal products [Kg $\cdot$ year^{-1} $\cdot$ per capita]	210	M
	r	Conversion demand for animal products to calories [kcal $\cdot$ Kg^{-1}]	3000	E
	d	Income elasticity of meat demand	0.65	M
	α_m	Feedback strength for meat demand	0.5	C
	α_c	Feedback strength for crop demand	0.1	C
Production	k	Yield elasticity to chemical inputs	0.2	E
	f	Yield elasticity to mechanization	0.5	E
	h	Sensitivity of meat yield to intensification	0.95	E
	Λ_{max}	Maximum livestock density (organic)	3	E
	β	Speed of mechanization adjustment	0.95	C
	δ	Speed of chemical input adjustment	1.1	C
	γ	Speed of livestock density adjustment	0.95	C
	ν	Technological progress rate	0.1	E
	T_{max}	Technological ceiling	0.2	E
Landscape dynamics	φ	Baseline land expansion rate (crop/pasture)	3e-4	C
	ζ_c^+	Expansion rate (cropland)	130	C
	ζ_m^+	Expansion rate (pasture land)	500	C
	ζ_c^-	Contraction rate (cropland)	120	C
	ζ_m^-	Contraction rate (pasture land)	500	C
	ε_{max}	Maximum natural ecosystem integrity	2	F
	p	Diminishing return for ecosystem service	0.25	E

Table 8.1 Parameters of the model. Group codes can be: measured (M), estimated (E), calibrated (C), or fixed (F).

and restoration, for which precise values are not directly measurable within the model context. As described in Section 8.6.1, these rates were informed by global analyses and meta-analyses covering soil degradation and forest recovery dynamics[510–512]. For parameters associated with the yield function, values were chosen based on extensive agricultural economics and ecological economics literature[153, 513, 514]. While reported values do vary between studies and there is no universal consensus—often due to differences in scale, crop types, or methodological approaches—our selections are consistent with established ranges. Importantly, the chosen parameter values are supported by the model's ability to reproduce historical patterns of yield growth observed in real-world data, lending further confidence to

their plausibility within the framework of this study.

Parameters classified as *calibrated* (C) are primarily associated with the model's adjustment and feedback mechanisms. These parameters cannot be directly inferred from empirical data as they are fundamentally linked to internal model behavior—that is, they govern logical or process-based linkages for which data are sparse or context-specific. Accordingly, they were tuned manually to best reproduce the broad patterns present in observed system dynamics, using an iterative, trial-and-error approach. The goal here, as elsewhere, was not to exactly fit every empirical curve but to recapitulate the essential dynamic behavior pertinent to our research questions. This calibration approach ensures the model captures the relevant system variability while maintaining enough flexibility to allow exploration of alternative scenarios within the stylized earth system structure.

Key Takeaways

- **A global planetary boundary model:** We construct a stylized, discrete-time model linking global population and economic growth to agricultural production, land conversion, and natural ecosystem integrity, contrasting business-as-usual trajectories against alternative policy portfolios.
- **The limits of supply-side optimism:** Technological improvements and sustainable intensification are necessary at the farm level, but they are structurally insufficient to halt global ecological degradation when aggregate food demand continues to rise.
- **The structural necessity of dietary shifts:** Only robust demand-side interventions—specifically reducing global meat consumption—can simultaneously relieve the dual pressures of agricultural expansion and intensification.
- **Integrated systemic solutions:** A sustainable planetary future cannot be achieved through isolated levers. It requires a holistic policy portfolio that actively coordinates supply-side conservation constraints with transformative demand-side reductions to prevent rebound effects.

Conclusion and Perspectives

9. Conclusion and perspectives

9.1 Conclusion

The ongoing collapse of global biodiversity represents a systemic, multi-dimensional crisis that is inextricably tied to the economic incentives and structural evolution of agricultural landscapes. Moving beyond the terminal metric of the "Sixth Mass Extinction," this thesis has sought to deconstruct the erosion of functional, taxonomic, and genetic diversity by tracing it back to its fundamental driver: the global food system's escape from historical biophysical constraints through intensive capitalization and spatial expansion. The central ambition of this work was to shed light on the complex, non-linear feedback loops between individual farmer decision-making, landscape architecture, and global ecological stability.

To navigate the sheer complexity of these socio-ecological interactions, I adopted a multi-scale approach—from the local field boundaries of European farms to the active deforestation frontiers of the Brazilian Cerrado, and ultimately to the global dynamics of food demand. Rather than relying on a single monolithic architecture, the common methodological thread of this research was the progressive evolution of stylized, data-driven models. By bridging theoretical econophysics, complexity science, and applied ecology, these models stripped away unnecessary complexity to reveal fundamental causal mechanisms.

9.1.1 Part I: The European context

Previous knowledge: Within the European agricultural landscape, the prevailing scientific and political consensus acknowledges that high-input farming and landscape homogenization are primary drivers of biodiversity loss. Consequently, current policy frameworks (such as aspects of the Common Agricultural Policy) frequently attempt to curb this decline through top-down, isolated environmental regulations, such as blanket targets for pesticide reduction or fixed ecological focus areas. Furthermore, traditional agro-economic models evaluating these policies often treat farms as static, spatially homogeneous entities operated by perfectly rational actors. As a result, this standard approach fails to adequately capture the deep structural socio-economic frictions—specifically, the relentless economic pressure for land consolidation—and often ignores the precise spatial ecology governing how natural enemies interact with crop pests across different field geometries.

Contribution of this work: Moving beyond standard economic assumptions, this research conceptualizes the European agricultural sector as a complex adaptive system. By first deploying a spatially implicit Agent-Based Model (ABM), this work provides a critical structural critique of isolated environmental mandates. It demonstrates that when policies like mandated pesticide reductions are applied without corresponding economic safeguards, they compress the already thin profit margins of smaller farmers. This triggers an unintended feedback loop: smallholders

exit the market, their land is absorbed by highly capitalized operations, and the landscape is further homogenized. Acknowledging the limitations of a simple spatially explicit indicator for biodiversity levels and ecosystem service provision, the analysis then delves into the precise ecological mechanisms of natural pest control. By advancing to a spatially explicit framework, this second study quantitatively maps the biophysical limits of the agroecological transition. It demonstrates that replacing synthetic inputs with natural pest control is highly sensitive to the spatial arrangement of semi-natural habitats (SNH) and field size. The fundamental contribution here is establishing that ecological intensification is economically viable for small-to-medium farms, but faces a hard, structural spatial constraint in large-scale consolidated operations due to the limited dispersal range of natural enemies.

9.1.2 Part II: The Brazilian Cerrado

Previous knowledge: The Brazilian Cerrado represents one of the most active and contested agricultural frontiers on the planet, buckling under the expansion of highly capitalized commodity production (primarily soy and cattle). In both academic literature and practical governance, the discourse around mitigating this deforestation is heavily fragmented. Interventions are typically analyzed and debated in isolation—weighing the merits of supply-chain embargoes (like the Soy Moratorium) against purely financial mechanisms like Payments for Environmental Services (PES). Current spatial models often struggle to capture the non-linear, infectious nature of how agribusiness physically expands and encroaches upon virgin ecosystems, leaving policymakers to rely on piecemeal, linear projections of land-use change.

Contribution of this work: This research reframes the expansion of the agricultural frontier not as a linear progression, but as a spatial percolation process driven by localized economic incentives. Employing a spatially explicit cellular automata model, this work formally evaluates the spatial dynamics of deforestation. The defining contribution is conceptual proof that standalone conservation policies are fundamentally insufficient to halt systemic degradation. The model demonstrates that singular interventions are easily bypassed by the spatial fluidity of agricultural capital. To arrest this, the thesis establishes the strict necessity of a synergistic policy portfolio. By strategically coupling negative economic constraints (the removal of agricultural subsidies on newly cleared land to create spatial friction) with targeted positive incentives (PES to maintain critical ecological corridors), the model optimizes the landscape architecture. Ultimately, this work shifts the paradigm from a zero-sum conflict to a quantified synergy, proving that when policies are spatially and economically coupled, halting deforestation actually generates a net bio-economic surplus.

9.1.3 Part III: The global scale

Previous knowledge: At the global scale, the debate on reconciling food security with planetary boundaries is heavily dominated by supply-side optimism. The prevailing narrative—often framed as "sustainable intensification" or the "land sparing vs. land sharing" debate—assumes that if technological advancements can increase yield efficiency, the total land footprint required for agriculture will naturally contract. While the literature increasingly acknowledges the environmental burden of shifting global diets, standard macroeconomic models frequently fail to dynamically couple these consumption patterns with the absolute, physical limits of spatial expansion, leading to policies that heavily subsidize agricultural efficiency while treating aggregate demand as an exogenous, unstoppable force.

Contribution of this work: Scaling the bio-economic analysis to the global level, this thesis directly challenges the structural viability of supply-side optimism. By showing the limited effects of supply-side technological improvements, the primary contribution of this section is qualitatively demonstrating the structural necessity of demand-side interventions. It demonstrates that technological innovation and localized conservation are necessary but entirely insufficient conditions for global ecological stability. Unless the underlying aggregate demand for resource-intensive commodities (specifically animal-based proteins) is actively reduced, the global food system will continue to expand beyond its biophysical limits.

9.2 Perspectives

While the stylized frameworks developed in this thesis successfully isolate critical bio-economic feedback loops, the abstraction required to maintain computational tractability and conceptual clarity inevitably introduces structural limitations. A rigorous scientific endeavor must not only synthesize its contributions but also confront its boundaries. A deep perspective analysis of this thesis reveals several theoretical and methodological caveats that set the starting point for future research.

9.2.1 The limits of behavioral and cognitive simplifications

The models presented herein rely heavily on boundedly rational, heuristic decision-making rules driven primarily by expected profitability and price signals. While this approach effectively captures the macro-level inertia of agricultural markets and avoids the paralyzing complexity of fully parameterized cognitive models, it inherently strips away the rich socio-cultural dimensions of farmer behavior. Real-world agricultural transitions are rarely dictated by profit maximization alone. They are heavily mediated by risk aversion, deeply ingrained social norms, peer-to-peer knowledge networks, and historical path dependencies [130, 165, 224]. By omitting the friction generated by these psychosocial factors, the models may underestimate the time lags associated with policy adoption or the resistance to ecological intensification [126]. The assumption that farmers will seamlessly shift to sustainable practices once an economic threshold is met ignores the reality that transitioning to agroecology requires a fundamental restructuring of systemic knowledge and labor allocation, not just capital reallocation. To bridge this gap, future research must incorporate insights from empirical behavioral experiments, grounding these stylized models in the complex psychosocial realities of farmer decision-making.

9.2.2 Ecological homogeneity and simplified biophysical dynamics

A second critical weakness lies in the homogeneous representation of ecological variables. In both the European pest-management model and the Cerrado deforestation model, biodiversity and ecosystem services are aggregated into standardized indices or functional proxies (*e.g.*, a generic "natural enemy" abundance or a generalized "habitat integrity" score). This functional aggregation masks the deep complexity of multi-trophic interactions [197, 234] and the specific sensitivities of diverse taxa. For instance, the implicit modeling of pest dynamics completely bypasses evolutionary realities such as the rapid development of pesticide resistance [280], which is currently a primary driver of yield stagnation. Furthermore, the framework operates within a relatively stable biophysical envelope, omitting stochastic extreme climate events, disease

outbreaks, and the non-linear tipping points associated with severe localized climate change. By not explicitly modeling these compounding shocks, the projected long-term economic returns of "business-as-usual" scenarios may be significantly overestimated, masking a significant existential threat to highly capitalized, simplified agro-ecosystems.

9.2.3 The absence of global trade feedbacks

While the thesis explores multiple scales, the scales themselves remain somewhat insulated within their respective models. The regional analyses (Europe and Brazil) treat global demand and market prices as largely exogenous or simply responsive parameters. Consequently, the models fail to capture the complex dynamics of global trade leakage—the displacement of ecological debt across borders. If a stringent pesticide reduction policy is implemented in Europe, or a strict deforestation moratorium is enforced in the Cerrado, the resulting supply contractions will inevitably trigger price spikes in global commodity markets. Without a fully coupled macroeconomic trade module, the current research cannot quantify how these price signals might incentivize compensatory deforestation in unprotected biomes (*e.g.*, the Gran Chaco or the African savannas). This perspective limits the ability to evaluate the true net-global impact of regional conservation policies [4, 225, 226]. While acknowledging that a fully closed global economy model masks important regional trade feedbacks—such as the leakage of agricultural emissions across borders—this abstraction provides a necessary baseline to evaluate the purely biophysical boundaries of the Earth system before incorporating geopolitical market distortions.

9.2.4 The omission of alternative farming paradigms

A further limitation of the current work is the implicit framing of agricultural production around conventional, highly capitalized systems. Throughout the models, interventions are largely evaluated as adjustments or constraints applied to this baseline—such as mandated pesticide reductions, taxation, or the preservation of semi-natural habitats within standard monocultures. Consequently, the thesis does not explicitly model a transition toward fundamentally different agricultural paradigms, such as certified organic agriculture, complex agroforestry systems, or permaculture [216, 217]. These alternative systems possess vastly different cost structures, labor requirements, yield dynamics, and price premiums that cannot be accurately represented by simply tweaking the parameters of a conventional farming model [458]. By omitting these structural alternatives, the analysis may overlook viable transition pathways that entirely sidestep the economic traps of conventional intensification. However, we have recently begun to address this specific gap; with the help of a master's thesis student, we have started modeling the transition dynamics and economic viability of organic farming within the European context. While this ongoing work has yielded promising preliminary insights, it is included in the appendix (see Appendix A) as the research remains in its preliminary stages.

9.2.5 The omission of distributional impacts

Finally, the analytical focus on aggregate bio-economic efficiency and overall farm viability obscures profound distributional consequences. By analyzing systemic trade-offs at the level of total production, land area, or average sector profitability, the models are blind to the localized impacts on food insecurity, rural poverty, and social equity [498, 499]. For instance, while

the global model suggests that dietary shifts and reduced agricultural demand are structural necessities for biosphere preservation, it does not assess how the economic contraction of the agricultural sector would impact the livelihoods of millions of smallholder farmers in developing nations. Similarly, the Cerrado model optimizes for maximum bio-economic efficiency and fiscal sustainability but does not differentiate between the socio-economic vulnerabilities of capitalized agribusinesses versus traditional, indigenous, or marginalized rural communities.

9.3 Final remarks

The historical trajectory of human civilization has been defined by our ability to continually engineer our way out of localized ecological limits, a "success story" underwritten by the massive application of synthetic inputs and the continuous expansion of the agricultural frontier. However, this thesis demonstrates that we have reached the planetary boundaries of this paradigm. The continuous degradation of biodiversity is no longer an externalized environmental cost; it is an apex systemic risk actively cannibalizing the economic foundations of global agriculture.

Reconciling human socio-economic development with the Earth's biophysical limits is the defining challenge of our era. As the models developed in this work illustrate, there are no panaceas or isolated technological fixes. True agricultural sustainability requires a sophisticated, spatially targeted, and policy-layered approach that simultaneously addresses the micro-economic realities of the individual farmer and the macro-structural pressures of global consumption. By continually refining our modeling frameworks to embrace the deep complexities and interconnectedness of these systems, we can transition from merely documenting the ongoing collapse toward actively engineering a resilient and equitable biosphere.

Appendix

This appendix presents preliminary research currently being developed in collaboration with Lucas Selva and Michael Benzaquen.

A. Externality costs of agricultural production and the organic alternative

A.1 Introduction

Throughout the preceding chapters, this thesis has primarily investigated the structural role of agricultural expansion and consolidation in driving biodiversity decline. In this chapter, we broaden our analytical horizon to encompass a wider spectrum of biophysical pollution vectors. Methodologically, we also transition toward a classical environmental economics paradigm, explicitly focusing on the monetization of these environmental impacts. Originating from foundational theories of welfare economics, the concept of pricing externalities addresses inherent market failures: when the true social and ecological costs of production are not reflected in commodity prices, they must be quantified to design optimal regulatory mechanisms. The agricultural sector in France exemplifies this structural failure, generating massive environmental externalities. Because these damages are entirely decoupled from traditional market pricing, their financial and ecological burdens are absorbed by public infrastructure, local health systems, and future generations, rather than by the emitting economic agents. Within the European context, the primary channels of this uninternalized degradation are robustly documented [515, 516]: the toxic contamination and eutrophication of aquatic ecosystems via diffuse nitrate and pesticide runoff [517, 518]; the emission of potent greenhouse gases (GHGs) inextricably linked to intensive livestock operations and synthetic fertilizers [519]; and the atmospheric release of ammonia, a primary precursor to fine particulate matter responsible for severe epidemiological health crises [520].

To fully grasp the economic magnitude of these market failures, it is necessary to explicitly define the biophysical mechanisms underlying these three primary externalities. First, diffuse water pollution occurs when surplus nitrates from synthetic fertilizers and chemical pesticide residues leach into regional groundwater and river networks. This ecological degradation forces downstream municipalities to shoulder massive water purification costs to guarantee potable supplies, an expense entirely absent from the market price of the agricultural output [521]. Second, the sector is a profound emitter of potent greenhouse gases—specifically methane (CH_4) from enteric fermentation in ruminant livestock and nitrous oxide (N_2O) from intensive soil management. These localized emissions drive long-term global climate forcing, imposing severe, cumulative socio-economic damages on future generations [501]. Finally, the volatilization of ammonia (NH_3), heavily linked to manure management and nitrogenous fertilizers, reacts in the lower atmosphere to form secondary fine particulate matter (PM2.5). The resulting deterioration of regional air quality precipitates severe respiratory and cardiovascular pathologies, effectively transferring the hidden cost of intensive farming directly onto the public health infrastructure [522].

Although these externalities are widely recognised, their spatial distribution remains insufficiently documented. Most available valuations are produced at the national scale, which is appropriate for macroeconomic appraisal but less informative for regional policy design. This limitation is particularly important in agriculture because pollution pressures depend strongly on the territorial concentration of livestock, the intensity of chemical input use, land availability, and production specialisation. Identical national targets may therefore generate very different environmental returns depending on where action occurs.

A regional perspective is needed for two reasons. First, spatial heterogeneity is central to policy efficiency: diffuse pollution control is generally more effective when instruments are differentiated according to local pressures and abatement opportunities rather than imposed uniformly across space [523]. Second, the regional distribution of externality costs is essential for evaluating alternative transition pathways toward less input-intensive farming systems, including organic agriculture. The relevance of organic farming in this context does not lie in the claim that it is environmentally superior under every metric, but in the broad empirical finding that it tends to reduce pesticide use, improve biodiversity outcomes, and lower several pressures per unit of land, even though some trade-offs remain when impacts are assessed per unit of output rather than per hectare [524–526].

This chapter addresses this gap by developing a transparent spatial downscaling framework that allocates established national-level externality costs to the 13 metropolitan French regions. Rather than reconstructing a highly granular biophysical model of regional emissions, this approach provides a first-order, policy-relevant accounting baseline utilizing harmonized public data. We deploy a parsimonious allocation rule driven by observable proxies for livestock density and crop-input intensity, ensuring both internal consistency and reproducibility. This strategy not only preserves aggregate national totals while exposing stark spatial asymmetries, but also allows us to evaluate alternative pathways for achieving organic land-use targets—ultimately demonstrating that the geographic configuration of the transition is as critical as the aggregate target itself.

The remainder of the chapter is structured as follows: Section A.3 presents the valuation perimeter and the downscaling methodology. Section A.4 analyzes the spatial distribution of costs and the organic transition scenarios. Section A.5 evaluates the limitations of the modeling approach, and Section A.6 concludes.

A.2 The paradigm and trajectory of organic farming in Europe

Organic farming represents a fundamental paradigm shift in agricultural production, prioritizing ecological processes, closed nutrient cycles, and landscape biodiversity over the application of external synthetic inputs. At its core, organic agriculture is explicitly designed to internalize and mitigate the severe environmental externalities generated by conventional farming. It achieves this by strictly prohibiting the use of synthetic pesticides, herbicides, and mineral fertilizers, relying instead on integrated ecosystem management practices such as complex crop rotations, cover cropping, mechanical weeding, and the application of organic soil amendments [527, 528]. By re-coupling agricultural outputs with local biophysical carrying capacities, organic systems aim to reconcile economic production with long-term ecological resilience.

The environmental co-benefits of this agro-ecological approach are substantial and well-

documented. Empirical meta-analyses demonstrate that organic systems support significantly greater farmland biodiversity, yielding a roughly 34% increase in species richness [529] alongside vastly higher abundances of critical soil fauna, such as nematodes and earthworms [530]. Organic soil management systematically builds soil organic matter, resulting in 10–20% higher carbon stocks [531]. Furthermore, the elimination of synthetic chemical inputs drastically lowers the risk of diffuse water pollution and toxic runoff; pesticide residues are rarely quantifiable in organic food, whereas over half of conventional samples contain detectable traces [532]. From a climate perspective, mixed organic farming emits less methane and nitrous oxide per hectare due to lower nitrogen applications and more extensive grazing [533], though the inherent reduction in yields means that emissions per unit of product can sometimes remain comparable to conventional systems.

Driven by growing consumer awareness of these environmental benefits, the organic sector in the European Union has experienced rapid commercial and spatial expansion. Generating €45 billion in sales in 2022, the EU is now the second-largest organic market globally [534]. This economic viability is underpinned by a combination of consumer price premiums and public subsidies, which offset the higher labor demands and lower yields associated with organic practices. Between 2012 and 2020, the share of the EU-27's Utilised Agricultural Area (UAA) certified as organic rose from approximately 5.7% to 9.1%. However, this spatial uptake remains highly heterogeneous. Adoption is heavily clustered in mountainous and extensive pastoral zones—driving national shares to roughly 26% in Austria, 22% in Estonia, and 20% in Sweden—while intensive arable plains in Eastern Europe and Iberia frequently remain below 10%. Production structures also mirror this geographic divide: Mediterranean nations dedicate higher shares to permanent crops, whereas northern and central European organic land is predominantly allocated to arable crops and pasture, heavily supporting ruminant livestock (cattle, sheep, and goats) over intensive monogastric sectors like pigs and poultry.

Recognizing organic agriculture's proven capacity to deliver critical ecosystem services, the EU has positioned the sector at the center of its environmental governance. Most notably, the Farm to Fork Strategy established a legally binding policy target to reach "at least 25% of the EU's agricultural land under organic farming by 2030" [535]. To incentivize this massive structural transition, the EU injected €12 billion in specific Common Agricultural Policy (CAP) funding between 2014 and 2022, with an additional €14.7 billion earmarked for the 2023–2027 period [536].

Despite this unprecedented financial commitment, achieving the 25% target requires the historical uptake rate to double. More critically, the current policy framework operates through broad, flat-rate expansion mandates that lack robust spatial targeting. As demonstrated by the sector's uneven development, the environmental returns on organic conversion are highly context-dependent. Transitioning a hectare of intensively farmed, chemically dependent arable land vastly greater marginal ecosystem gains than formally certifying a hectare of already-extensive mountain pasture. This profound structural heterogeneity suggests that uniformly expanding organic area is both economically and ecologically sub-optimal. Building on this premise, the subsequent sections of this analysis will leverage spatial, structural, and environmental disparities to evaluate how targeted agri-environmental policies can optimize the net externality benefits of organic farming expansion.

A.3 Methodology

To operationalize our spatial downscaling framework, we select metropolitan France among European countries as our primary empirical case study. Establishing robust baseline estimates for agricultural externality costs is a challenge, as such macroeconomic valuations are rarely centralized in international repositories. Instead, acquiring these parameters necessitates a rigorous synthesis of highly specific sectoral reports, environmental audits, and institutional grey literature, which are almost exclusively published in the local language (see Table A.1). We therefore chose France to deliberately leverage the native linguistic expertise of one of the co-authors (Lucas), enabling a comprehensive and accurate extraction of these critical economic parameters from French governmental archives.

The analysis focuses on five externality categories for which national-scale estimates can be constructed from official emission inventories and existing valuation studies: water pollution, CO_2, CH_4, N_2O, and NH_3. This selection does not exhaust the environmental footprint of French agriculture, but it captures the main damage categories for which monetisation is sufficiently documented to support policy-oriented comparison [537–539]. The logic of the exercise is sequential. We first establish a set of national annual costs. We then split each cost between crop and livestock activities according to its dominant causal origin. Finally, we allocate these sectoral components across regions using activity proxies that are observable at a harmonised territorial scale. The resulting regional values should therefore be interpreted as an accounting-based spatial distribution of national damages rather than as direct observations of region-specific measured impacts.

Table A.1 Primary datasets and valuation parameters used in the analysis.

Variable	Source	Year
GHG emission quantities	CITEPA, Rapport Secten [540]	2023
NH_3 emission quantities	CITEPA, Rapport Secten [540]	2023
Social cost of CO_2-eq	Quinet report [539]	2025
Social cost of NH_3	Marcus and Simon [538]	2015
Water pollution cost	Bommelaer and Devaux [537]	2011
Livestock Units (LSU) by region	Eurostat, agricultural census / farm structure statistics [541]	2023
Pesticide & fertiliser proxy by farm type	FSDN Public Database Standard Results [542]	2025
Utilised Agricultural Area (UAA) by region	Eurostat, farm structure statistics [541]	2023
Organic area trajectories	Agence Bio regional historical series [543]	2008–2025

The national baseline combines official physical emission data with literature-based or policy-based monetary values. Climate damages are monetised using the French reference value of climate action of 256 €/tCO_2-eq, following the updated Quinet report [539]. This value is a public appraisal benchmark aligned with long-run decarbonisation objectives rather than a direct observation of market carbon prices, which makes it appropriate for socio-economic evaluation. Agricultural emissions of CO_2, CH_4, and N_2O are taken from the CITEPA Secten inventory for 2023 [540]. NH_3 damages are valued at 759 €/tNH_3, reflecting the health costs

associated with the secondary formation of particulate matter, especially $PM_{2.5}$, and following French environmental-economic work on nitrogen and phytosanitary externalities [538]. For diffuse water pollution, we use the central estimate of 1 815 M€/year based on Bommelaer and Devaux [537]. Retaining this estimate allows the spatial exercise to remain comparable with earlier French work, even if the underlying benchmark should be interpreted cautiously in light of inflation and regulatory change.

A direct regional valuation of agricultural externalities would ideally rely on region-specific emissions, local environmental fate, exposure pathways, and damage functions. In practice, such a full bottom-up reconstruction is not available in a homogeneous format across all relevant pollutants and regions. The chapter therefore adopts a downscaling strategy. This choice is justified by three considerations. First, the national totals are grounded in official inventories and published valuation studies, so it is preferable to preserve those totals and make the spatial allocation explicit rather than to create partially inconsistent regional estimates. Second, a proxy-based method remains transparent and replicable with publicly available data. Third, the purpose of the exercise is comparative: identifying where pollution costs are most concentrated, not claiming exact local causal attribution.

Before introducing space, each externality is decomposed into a crop component and a livestock component. This step is necessary because the drivers of pollution differ structurally across production systems. Methane is overwhelmingly associated with livestock; most direct agricultural CO_2 emissions are linked to fuel use and input-dependent crop activities; N_2O and NH_3 have mixed origins through manure handling, stocking density, and fertilisation; and water pollution depends on both synthetic inputs and livestock-related nitrogen surpluses [538, 540]. This distinction serves two methodological purposes. It avoids allocating all damages through a single activity proxy, which would mechanically bias the spatial distribution, and it makes the scenario analysis more policy-relevant because the environmental return to organic conversion is unlikely to be identical in livestock-dense and crop-intensive systems.

Let $E_0^{(i)}$ denote the aggregate national social cost for a given externality i. We define $C_0^{(i)}$ and $L_0^{(i)}$ as the respective proportional shares attributable to crop cultivation and livestock rearing, such that:

$$C_0^{(i)} + L_0^{(i)} = 1. \tag{A.1}$$

The resulting attribution shares, alongside their institutional sources, are detailed in Table A.2. This structural apportionment is driven by causal mechanisms extracted from primary datasets, ensuring full alignment with both academic literature [544, 545] and official reporting frameworks such as CITEPA and FSDN. Notably, water pollution remains the most challenging category to explicitly allocate, as both synthetic pesticide applications and nitrogen leaching jointly drive aquatic damages. Therefore, the designated 54%–46% crop-livestock split serves as an accounting heuristic based on national input usage rather than a direct biophysical quantification of localized hydrological loads. This approximation is theoretically necessary to preserve methodological coherence between the specific nature of each pollutant and the activity proxies utilized for regional allocation.

The spatial downscaling is executed across the 13 metropolitan NUTS-1 regions of France. This administrative scale offers an optimal compromise between policy relevance and empirical tractability: it is sufficiently disaggregated to expose macroscopic geographic heterogeneities, yet remains fully compatible with harmonized datasets from Eurostat and the FSDN. To distribute the sector-specific national costs across these regions, we deploy two distinct activity proxies.

For livestock-driven externalities—specifically CH_4, NH_3, and the relevant fraction of N_2O—

Table A.2 National agricultural externality costs and crop–livestock attribution. Monetary values are expressed in M€/year. GHG damages are valued at 256 €/tCO_2-eq [539]; NH_3 damages are valued at 759 €/t [538].

Ext.	Adverse effect	Total (M€)	Crop (%)	Livest. (%)	Source
Water	Water pollution	1 815	54	46	[537]
CO_2	Greenhouse gas	2 918	99	1	[540]
CH_4	Greenhouse gas	10 372	0	100	[540]
N_2O	Greenhouse gas	5 382	87	13	[540]
NH_3	Fine particles	368	61	39	[538]
Total		20 855			

we utilize Livestock Units (LSU). As a standardized metric of animal populations, LSU serves as a robust and direct biophysical proxy for localized livestock intensity.

Conversely, allocating crop-driven externalities requires a more pragmatic approach due to the absence of harmonized, region-level data detailing cropping intensity. To bridge this data gap, we construct a composite Pesticide and Fertiliser (P&F) index derived from FSDN standard results, mirroring the methodological framework established by the European Commission for agri-environmental indicators related to farming intensity [546]. This index leverages expenditure-based indicators (euros spent on agrochemicals, derived from [152]) to establish the relative intensity of conventional input use across regions. We explicitly acknowledge the limitations of this financial proxy: monetary outlays do not perfectly correlate with biophysical toxicity or precise nutrient leaching, nor does the index capture other mechanized externalities such as fossil fuel consumption from tillage. Nevertheless, this compounded P&F index provides a transparent, internally consistent, and publicly reproducible heuristic for crop intensity. The theoretical implications of this central simplifying assumption are critically evaluated in Section A.5.

For each region $k = 1, \ldots, 13$, we define

$$\omega_k^{\mathrm{LSU}} = \frac{\mathrm{LSU}_k}{\sum_l \mathrm{LSU}_l}, \qquad \omega_k^{P\&F} = \frac{(P\&F)_k}{\sum_l (P\&F)_l}. \tag{A.2}$$

Regional externality costs are then allocated as

$$E_k^{(i)} = E_0^{(i)} \left[L_0^{(i)} \cdot \omega_k^{\mathrm{LSU}} + C_0^{(i)} \cdot \omega_k^{P\&F} \right]. \tag{A.3}$$

By construction,

$$\sum_k E_k^{(i)} = E_0^{(i)} \qquad \forall i, \tag{A.4}$$

which guarantees consistency between the regional distribution and the national benchmark. Total regional externality costs are then defined as

$$E_k = \sum_i E_k^{(i)}, \tag{A.5}$$

and to compare regions of different agricultural size we also compute a land-normalised measure,

$$\frac{E_k}{\mathrm{UAA}_k}, \tag{A.6}$$

where UAA_k is the Utilised Agricultural Area of region k. This normalisation is essential because absolute costs and cost intensities answer different questions: absolute costs identify where the largest aggregate burdens are generated, whereas per-hectare values capture the pressure exerted by local farming systems relative to land area.

The second part of the this work shifts from a static diagnostic framework to a prospective policy simulation, evaluating how alternative spatial configurations of organic conversion alter the regional distribution and aggregate volume of environmental externalities. To construct a meaningful scenario analysis, we discard the mathematically convenient but ecologically flawed assumption that organic conversion yields uniform environmental returns across all landscapes. Instead, the mitigation impact of an expanding organic share is modeled as a function of the pre-existing baseline intensity of the local conventional farming system.

This formulation reflects a core principle of environmental economics: the marginal social and ecological benefits of transitioning to an agro-ecological paradigm are non-linear and context-dependent. Converting a low-input conventional hectare that already operates near ecological equilibrium will inherently generate negligible marginal environmental gains compared to dismantling or converting a highly input-intensive or heavily stocked conventional hotspot.

To formalize this geographic and structural heterogeneity, let $\Delta O_{k,s}$ represent the incremental increase in the organic land-use share (measured as a percentage point deviation from the 2025 baseline year) within region k under policy scenario s. We construct localized, area-normalized intensity thresholds for both production sectors. For livestock-driven systems, regional intensity is defined as the localized stocking density:

$$x_k^L = \frac{\text{LSU}_k}{\text{UAA}_k}, \tag{A.7}$$

where LSU_k is quantified in livestock units and UAA_k is the utilized agricultural area. For cropping systems, agrochemical intensity is analogously normalized as:

$$x_k^C = \frac{(P\&F)_k}{\text{UAA}_k}, \tag{A.8}$$

where $(P\&F)_k$ represents the regional composite proxy for chemical expenditures.

We model the dynamic reduction of localized externality costs through a non-linear, asymptotic framework. For livestock-mediated externalities, the updated post-conversion cost is formulated as:

$$E_{k,s}^{(i)} = E_k^{(i)} \left[1 - 2I_l^{(i)} \frac{1}{1 + \frac{\langle x^L \rangle}{x_k^L - 0.4}} \Delta O_{k,s} \right] \qquad \text{if } x_k^L > 0.4, \tag{A.9}$$

whereas the environmental damage function is assumed to be structurally unresponsive to formal organic certification ($E_{k,s}^{(i)} = E_k^{(i)}$) whenever regional stocking densities fall below the extensive threshold ($x_k^L \leq 0.4$).

For crop-mediated externality categories, the updated post-conversion cost follows an analogous non-linear discount function:

$$E_{k,s}^{(i)} = E_k^{(i)} \left[1 - 2I_c^{(i)} \frac{1}{1 + \frac{\langle x^C \rangle}{x_k^C}} \Delta O_{k,s} \right]. \tag{A.10}$$

Within these structural equations, the parameters $I_l^{(i)}$ and $I_c^{(i)}$ represent the maximum theoretical impact-reduction coefficients documented in the agronomic literature for each specific externality i, while $\langle x^L \rangle$ and $\langle x^C \rangle$ represent the arithmetic national means of the respective intensity indices.

The mathematical rationale for this specific non-linear structure lies in the sigmoidal scaling factor, which embeds a multi-stage logic. In regions where local intensity significantly exceeds the national average ($x_k > \langle x \rangle$), the ratio $\frac{\langle x \rangle}{x_k}$ shrinks toward zero, driving the scalar fraction toward its upper bound and capturing the high societal returns of converting highly concentrated conventional systems. Conversely, as regional intensity drops below the national average ($x_k < \langle x \rangle$), the scaling factor drops rapidly, ensuring that the model heavily discounts the mitigation potential of organic conversion in territories that are already structurally extensive. Finally, the introduction of the 0.4 LSU/ha threshold represents a strict biophysical constraint boundary; below this level, pastoral systems naturally conform to extensive carrying capacities, meaning that shifting their administrative status to "certified organic" does not alter their physical emission profile and renders the marginal benefit of the policy subsidy close to zero.

To operationalize our prospective analysis, we must formalize the regional trajectory of the organic land share, denoted as $\Delta O_{k,s}$, under distinct structural pathways.

First, we establish a business-as-usual benchmark by computing a baseline scenario. This is achieved via a linear extrapolation of historical regional organic area trajectories utilizing data from Agence Bio (2008–2025) [543]. The primary objective of this extrapolation is not to generate a structural or behavioral forecast of the organic market, but rather to establish a transparent, empirical benchmark that quantifies the inherent inertia of current trends. This benchmark serves to isolate the exact "policy effort gap" required to achieve the mandate set by the European Commission's Farm to Fork Strategy: ensuring that at least 25% of the utilized agricultural area is under organic management by 2030 [535]. Because the baseline trajectory falls structurally short of this 25% threshold at the national level (as demonstrated in Supplementary Materials), it defines a residual policy gap that must be absorbed.

By calculating the precise deficit between the projected 2025 regional shares and the normative 2030 target, we formulate three distinct counterfactual allocation rules to distribute the remaining organic land. In Scenario 1 (Uniform Allocation), the additional organic area required to close the national policy gap is distributed evenly across all NUTS-1 regions, imposing a flat, geographically blind regulatory expansion mandate regardless of localized agro-ecological or economic baseline conditions. In Scenario 2 (Proportional Growth), the residual required area is allocated proportionally according to recent regional conversion dynamics. Under this rule, regions that have demonstrated strong historical momentum and pre-existing institutional capacity for organic farming absorb a larger share of the remaining policy target. In Scenario 3 (Optimised Allocation), the required conversion hectares are strategically directed to the specific regions and agricultural production typologies (crops or livestock) that exhibit the highest baseline pollution intensities. This constitutes an optimization framework in the restricted, accounting sense of our model: it actively minimizes total social costs by prioritizing the conversion of the most high-cost conventional hectares, using the spatial intensity indicators developed in the study.

A.4 Results

A.4.1 National-level cost structure

The aggregate uninternalized cost of French agricultural externalities is estimated at approximately 20.8 billion euros annually. To contextualize this staggering macroeconomic baseline, this hidden societal liability is more than double the total annual subsidies allocated to French farmers through the Common Agricultural Policy (roughly 9 billion euros). This scale reveals a profound structural market failure, wherein a massive proportion of conventional agricultural production costs is externalized onto public health systems and environmental infrastructure.

Fig. A.1 illustrates the distribution of these costs across pollutant vectors and production sectors. The cost architecture is overwhelmingly dictated by climate-forcing damages. Biogenic methane (CH_4) alone constitutes exactly 50% of the total societal burden, while nitrous oxide (N_2O) contributes 26% and carbon dioxide (CO_2) accounts for 14%. Consequently, the environmental liability of French agriculture is fundamentally driven by livestock biology and nutrient cycle management rather than direct fossil-fuel combustion.

While water contamination and atmospheric ammonia (NH_3) represent smaller proportional shares—at 9% and 2% respectively—they maintain elevated policy relevance. Unlike globally mixed greenhouse gases, chemical runoff and fine particulate precursors directly manifest as localized environmental degradation and acute regional public health crises.

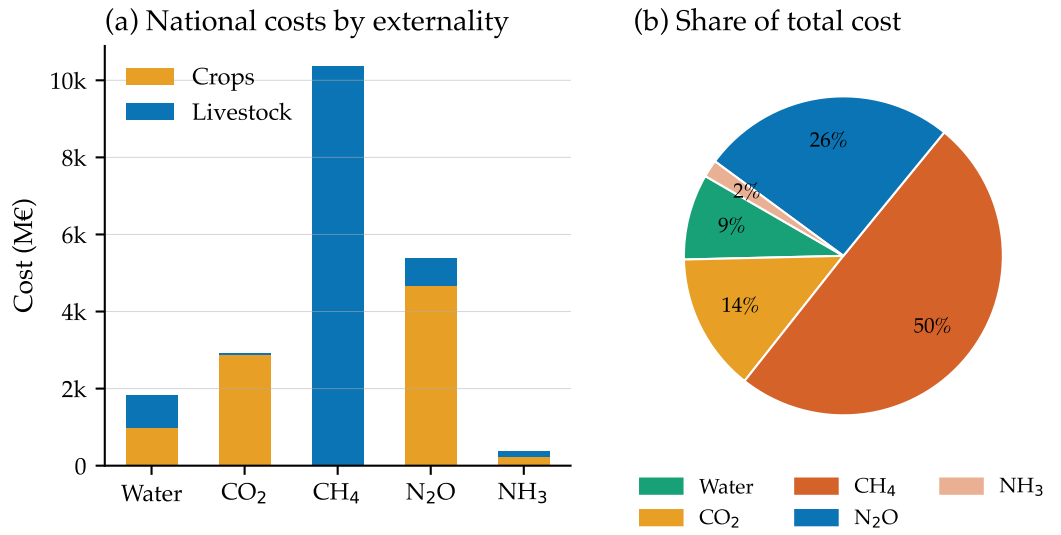


Figure A.1 National agricultural externality costs. *Left*: Absolute cost contributions (M€) separated by crops (yellow) and livestock (blue). *Right*: The proportional share of each pollutant relative to the total 20.8 billion euro national burden, heavily dominated by methane (50%).

Crucially, this baseline must be understood as a policy-oriented appraisal rather than a purely physical emissions inventory. Because the social value of carbon adopted here is explicitly calibrated to long-term global abatement targets (256 €/tCO_2-eq), climate-related categories

are heavily weighted by construction. This underscores that the dominance of CH_4 and N_2O is a joint function of physical material flows and a stringent societal valuation paradigm.

A.4.2 Regional distribution and typology of damages

Moving beyond national aggregates, Fig. A.2 maps the spatial distribution of these externality costs. The data reveals a stark concentration of environmental burdens in a select few territories.

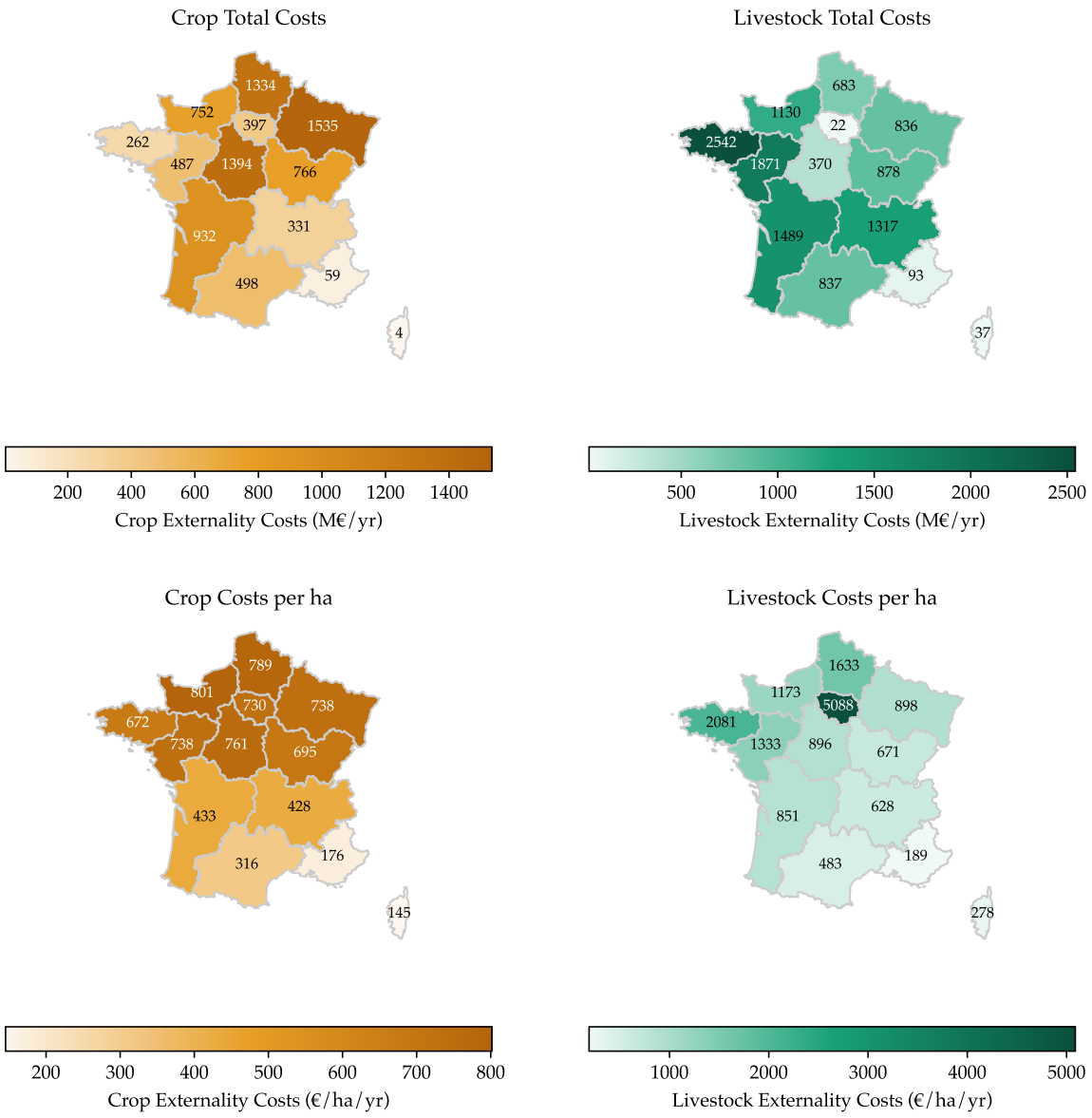


Figure A.2 Spatial distribution of externality costs across French regions. The mapping delineates the geographic polarization between high crop-driven externalities (left) and high livestock-driven externalities (right), highlighting peak concentrations in specific territorial systems.

When decomposing these regional totals into pollutant-specific components (Fig. A.3), two

distinct environmental profiles emerge. In Bretagne (BRE), which exhibits the highest aggregate cost nearing 2,750 M€, damages are overwhelmingly driven by CH_4. This is the expected signature of land-scarce, highly intensive livestock systems where enteric fermentation and manure processes dominate. Conversely, regions like Hauts-de-France (HDF) and Grand Est (GES) rank high due to the scale and intensity of arable production, exhibiting a more diversified cost structure driven by CO_2, N_2O, and water pollution.

Comparing absolute costs to per-hectare densities adds a critical analytical layer. Regions with vast agricultural sectors naturally dominate absolute totals. However, when normalized by utilized agricultural area (UAA), regions combining dense livestock populations with constrained land areas (*e.g.*, Bretagne) exhibit drastically amplified per-hectare pressures. This distinction dictates policy approaches: absolute totals matter for efficiently reducing the national aggregate burden, whereas per-hectare intensities are vital for addressing local ecological stress and territorial acceptability.

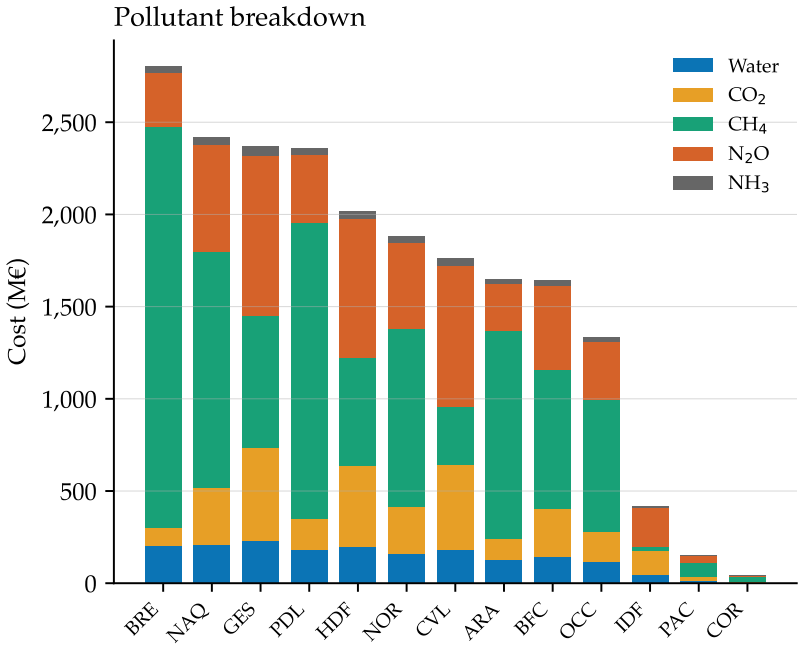


Figure A.3 Decomposition of regional externality costs. The stacked bars illustrate the pollutant-specific composition for each region, revealing the stark contrast between methane-dominated western regions (*e.g.*, BRE) and diversified, arable-heavy regions (*e.g.*, GES).

A.4.3 Scenario analysis: The imperative of spatial targeting

Given that the baseline extrapolation of historical organic-area trends structurally fails to meet the 25% European target by 2030, a clear policy gap exists. The central analytical question is therefore not just *how much* land must convert, but *where* that conversion should be targeted to maximize social welfare. Fig. A.4 evaluates three allocation rules for bridging this gap.

The scenario modeling yields three critical insights:

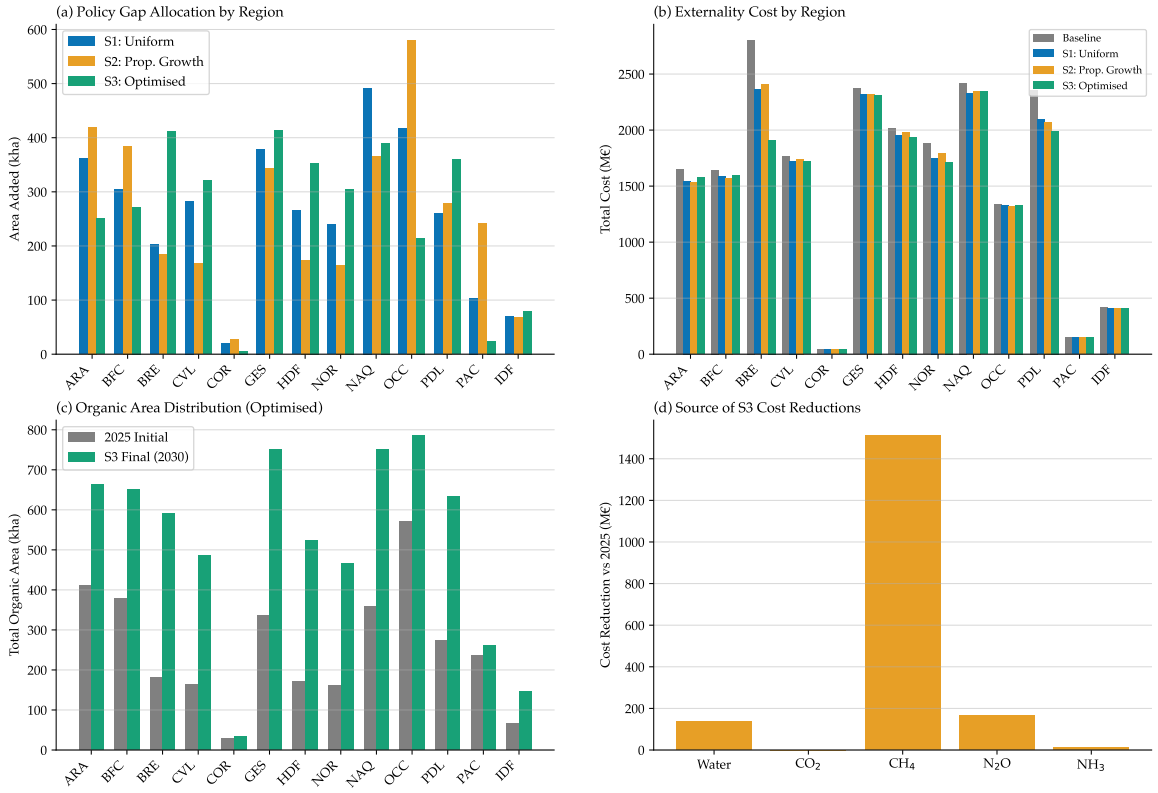


Figure A.4 Scenario comparison for closing the organic transition policy gap. *(a)* Area added per region under uniform (S1), proportional (S2), and optimized (S3) rules. *(b)* Aggregate externality costs remaining. *(c)* The resulting optimized organic area distribution. *(d)* The vast majority of cost reductions in the optimized scenario stem from mitigating methane, exceeding 1400 M€.

First, uniform expansion (Scenario 1) is environmentally inefficient. Distributing the required conversion area evenly across regions satisfies headline acreage targets but ignores the profound heterogeneity in conventional pollution intensity. Consequently, transition budgets are wasted on low-impact hectares, yielding limited environmental returns.

Second, relying on historical momentum (Scenario 2) offers negligible improvement. While politically plausible, scaling up pre-existing regional dynamics fails to target pollution hotspots. Historical organic growth is driven by market demand and advisory networks, which rarely overlap with the geographies suffering the highest social damages.

Third, targeted conversion (Scenario 3) delivers structural welfare gains. By explicitly directing the organic mandate toward regions and production typologies with the highest baseline pollution intensities, the aggregate social cost is minimized. As shown in Fig. A.4d, prioritizing these high-cost conventional hectares unlocks massive reductions, particularly in methane (yielding over 1,400 M€ in cost reductions) and nitrous oxide.

Ultimately, these scenarios reveal a potential conflict between territorial cohesion and environmental efficiency. The regions historically leading the organic transition are not necessarily those generating the highest damages. Therefore, achieving genuine environmental

mitigation requires moving beyond geographically blind acreage targets toward spatially targeted, intensity-driven policy instruments.

A.5 Discussion and limitations

The framework presented in this chapter serves as a structured first approximation. While its explicit assumptions provide analytical transparency, they inherently delimit the scope of the conclusions.

Our spatial downscaling relies on activity proxies (Livestock Units and expenditure-based input indices) rather than localized biophysical models. While this preserves consistency with national reporting totals, it assumes uniform average externality weights across regions for a given production type. This simplification is more defensible for GHG emissions than for diffuse water pollution, which is highly sensitive to unobserved local soil typologies, hydrology, and crop rotations. Furthermore, utilizing financial expenditures to proxy crop-input intensity effectively captures economic dependence, but it imperfectly translates to the physical toxicity of specific pesticide mixes or actual nutrient leaching rates.

Additionally, the underlying valuation benchmarks—particularly for water pollution—rely on legacy econometric estimates. Inflation, evolving drinking-water treatment technologies, and shifting regulatory standards inevitably alter the present-day magnitude of these damages. Therefore, our regional distribution should be interpreted as a spatial decomposition of a canonical baseline rather than a continuously updated toxicological inventory.

Finally, the valuation perimeter itself is structurally incomplete. By omitting difficult-to-monetize impacts such as biodiversity collapse, soil degradation, antimicrobial resistance, and localized odor nuisances, the calculated 20.8 billion euro aggregate remains a strict lower bound. Nonetheless, by operating within these defined parameters, the spatial methodology successfully demonstrates that the geographic geometry of organic transition policies is just as critical as the aggregate acreage targets they seek to achieve.

A.6 Conclusion

This chapter develops a transparent method to regionalise the externality costs of agricultural pollution in metropolitan France. Starting from national cost benchmarks and combining them with observable proxies of crop-input intensity and livestock concentration, it produces a first-order map of the geography of agricultural environmental damages.

Three results are especially important. First, the aggregate cost of the selected externalities is very large, exceeding 20 855 M€/year under the retained valuation framework. Second, this burden is highly uneven across regions: western livestock-intensive regions dominate total and per-hectare costs, while northern arable regions stand out for crop-driven externalities. Third, the scenario analysis shows that reaching an aggregate organic-area target is not enough to guarantee efficient environmental outcomes. The spatial allocation of conversion is crucial.

The chapter therefore supports a broader policy conclusion: in the presence of strong regional heterogeneity, uniform transition mandates are unlikely to be welfare-maximising. Even a relatively simple targeting rule can generate substantially larger environmental gains than spatially blind expansion. Future work should build on this framework by coupling

regional economic data with more explicit biophysical and hydrological models so as to move from proxy-based downscaling toward more causal regional damage estimation.

A.7 Supplementary materials

This appendix reports the numerical parameters used in the downscaling and scenario analyses. Table A.3 summarises the baseline national externality costs and the impact-scaling parameters used to model the maximum cost reduction associated with organic conversion.

Table A.3 Baseline national externality costs (E_0) and organic impact scaling factors (I_c, I_l).

Externality Category	E_0 Crop (M€)	E_0 Live (M€)	I_c	I_l
Water Pollution	980.1	834.9	0.5	0.5
CO_2 Emissions	2876.7	41.7	0.0	0.0
CH_4 Emissions	0.0	10371.8	0.0	1.0
N_2O Emissions	4670.0	712.2	0.2	0.2
NH_3 Emissions	224.0	144.0	0.2	0.2

Table A.4 reports the regional dataset used in the spatial allocation step.

Table A.4 Official NUTS-1 Regional Agricultural Data (Eurostat 2023 & FADN). The P&F Index represents the aggregated pesticide and fertiliser expenditure scaled by farm size.

Region	**Acronym**	**UAA (kha)**	**LSU (kLSU)**	**P&F Index**
Île-de-France	IDF	548.3	36.0	55015
Centre-Val de Loire	CVL	2243.7	594.6	193139
Bourgogne-Franche-Comté	BFC	2413.3	1410.5	106192
Normandie	NOR	1902.3	1815.2	104224
Hauts-de-France	HDF	2109.4	1096.3	184779
Grand Est	GES	3008.8	1342.0	212609
Pays de la Loire	PDL	2063.1	3005.3	67472
Bretagne	BRE	1610.5	4082.5	36236
Nouvelle-Aquitaine	NAQ	3900.2	2391.8	129062
Occitanie	OCC	3309.1	1344.7	68954
Auvergne-Rhône-Alpes	ARA	2871.0	2115.0	45920
Provence-Alpes-Côte d'Azur	PAC	825.6	148.7	8183
Corse	COR	161.7	58.9	605

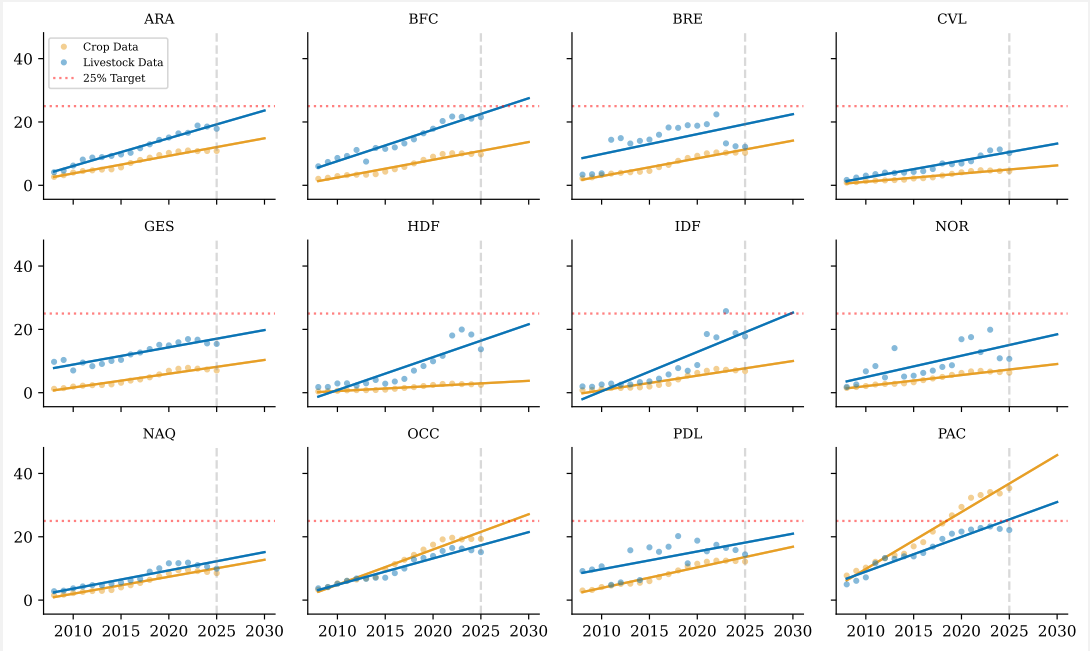


Figure A.5 Historical regional trajectories of organic farming (2008–2025) and linear extrapolation to 2030. The red dotted line indicates the 25% target.

References

[1] E. Moretti and M. Benzaquen, "Mitigating farmland biodiversity loss: A bio-economic model of land consolidation and pesticide use," *Royal Society Open Science*, vol. 12, no. 12, 2025.

[2] E. Moretti, M. Loreau, and M. Benzaquen, "Farm size matters: A spatially explicit ecological-economic framework for biodiversity and pest management," *Journal of Environmental Management*, vol. 396, p. 128 111, 2025.

[3] E. Moretti, J. V. S. Marcolin, M. Coronese, F. Lamperti, A. Roventini, and M. Benzaquen, "Policies for halting deforestation via fragmentation reduction and economic value creation," Working paper, Jun. 2026.

[4] E. Moretti, M. Loreau, and M. Benzaquen, "A global systems perspective on food demand, deforestation and agricultural sustainability," *arXiv preprint arXiv:2510.14720*, 2025.

[5] B. Jarvis, "The insect apocalypse is here," *The New York Times Magazine*, Nov. 2018. [Online]. Available: https://www.nytimes.com/2018/11/27/magazine/the-insect-apocalypse-is-here.html.

[6] A. P. Møller, "Parallel declines in abundance of insects and insectivorous birds in denmark over 22 years," *Ecology and evolution*, vol. 9, no. 11, pp. 6581–6587, 2019.

[7] C. A. Hallmann et al., "More than 75 percent decline over 27 years in total flying insect biomass in protected areas," *PloS one*, vol. 12, no. 10, e0185809, 2017.

[8] S. G. Potts, J. C. Biesmeijer, C. Kremen, P. Neumann, O. Schweiger, and W. E. Kunin, "Global pollinator declines: Trends, impacts and drivers," *Trends in ecology & evolution*, vol. 25, no. 6, pp. 345–353, 2010.

[9] C. A. Deutsch et al., "Increase in crop losses to insect pests in a warming climate," *Science*, vol. 361, no. 6405, pp. 916–919, 2018.

[10] T. D. Schowalter, *Insect ecology: an ecosystem approach*. Academic press, 2022.

[11] G. Ceballos, P. R. Ehrlich, A. D. Barnosky, A. García, R. M. Pringle, and T. M. Palmer, "Accelerated modern human–induced species losses: Entering the sixth mass extinction," *Science advances*, vol. 1, no. 5, e1400253, 2015.

[12] G. Ceballos and P. R. Ehrlich, "The misunderstood sixth mass extinction," *Science*, vol. 360, no. 6393, pp. 1080–1081, 2018.

[13] H. Ritchie. "The long-run decline of the world's wild mammals." Data sources: Barnosky (2008); Smil (2011); Bar-On et al. (2018). Accessed: 2026-05-22. [Online]. Available: https://ourworldindata.org/biodiversity?insight=wild-mammals-have-declined-by-85-since-the-rise-of-humans#key-insights.

[14] A. D. Barnosky, "Megafauna biomass tradeoff as a driver of quaternary and future extinctions," *Proceedings of the National Academy of Sciences*, vol. 105, no. supplement_1, pp. 11 543–11 548, 2008.

[15] V. Smil, "Harvesting the biosphere: The human impact," *Population and development review*, vol. 37, no. 4, pp. 613–636, 2011.

[16] Y. M. Bar-On, R. Phillips, and R. Milo, "The biomass distribution on earth," *Proceedings of the National Academy of Sciences*, vol. 115, no. 25, pp. 6506–6511, 2018.

[17] H. Ritchie. "Distribution of mammals on earth." Data sources: Bar-On et al. (2018). Accessed: 2026-05-22. [Online]. Available: https://ourworldindata.org/biodiversity?insight=wild-mammals-make-up-only-a-few-percent-of-the-worlds-mammals#key-insights.

[18] H. Ritchie. "Global living planet index." Accessed: 2026-05-22. [Online]. Available: https://ourworldindata.org/biodiversity?insight=on-average-there-has-been-a-large-decline-across-tens-of-thousands-of-wildlife-populations-since-1970#key-insights.

[19] B. Collen, J. Loh, S. Whitmee, L. McRAE, R. Amin, and J. E. Baillie, "Monitoring change in vertebrate abundance: The living planet index," *Conservation Biology*, vol. 23, no. 2, pp. 317–327, 2009.

[20] M. Puurtinen, M. Elo, and J. S. Kotiaho, "The living planet index does not measure abundance," *Nature*, vol. 601, no. 7894, E14–E15, 2022.

[21] S. H. Butchart et al., "Measuring trends in extinction risk: A review of two decades of development and application of the red list index," *Philosophical Transactions of the Royal Society B: Biological Sciences*, vol. 380, no. 1917, 2025.

[22] A. D. Barnosky et al., "Has the earth's sixth mass extinction already arrived?" *Nature*, vol. 471, no. 7336, pp. 51–57, 2011.

[23] R. H. Cowie, P. Bouchet, and B. Fontaine, "The sixth mass extinction: Fact, fiction or speculation?" *Biological Reviews*, vol. 97, no. 2, pp. 640–663, 2022.

[24] P. M. Hull, S. A. Darroch, and D. H. Erwin, "Rarity in mass extinctions and the future of ecosystems," *Nature*, vol. 528, no. 7582, pp. 345–351, 2015.

[25] S. Díaz and Y. Malhi, "Biodiversity: Concepts, patterns, trends, and perspectives," *Annual Review of Environment and Resources*, vol. 47, no. 1, pp. 31–63, 2022.

[26] M. Dornelas et al., "Assemblage time series reveal biodiversity change but not systematic loss," *Science*, vol. 344, no. 6181, pp. 296–299, 2014.

[27] H. Hillebrand and B. Matthiessen, "Biodiversity in a complex world: Consolidation and progress in functional biodiversity research," *Ecology letters*, vol. 12, no. 12, pp. 1405–1419, 2009.

[28] D. U. Hooper et al., "Effects of biodiversity on ecosystem functioning: A consensus of current knowledge," *Ecological monographs*, vol. 75, no. 1, pp. 3–35, 2005.

[29] C. R. Biggs et al., "Does functional redundancy affect ecological stability and resilience? a review and meta-analysis," *Ecosphere*, vol. 11, no. 7, e03184, 2020.

[30] C. P. Carmona et al., "Erosion of global functional diversity across the tree of life," *Science advances*, vol. 7, no. 13, eabf2675, 2021.

[31] A. R. Hughes, B. D. Inouye, M. T. Johnson, N. Underwood, and M. Vellend, "Ecological consequences of genetic diversity," *Ecology letters*, vol. 11, no. 6, pp. 609–623, 2008.

[32] M. Exposito-Alonso et al., "Genetic diversity loss in the anthropocene," *Science*, vol. 377, no. 6613, pp. 1431–1435, 2022.

[33] R. Frankham, "Genetics and extinction," *Biological conservation*, vol. 126, no. 2, pp. 131–140, 2005.

[34] S. L. Pimm et al., "The biodiversity of species and their rates of extinction, distribution, and protection," *science*, vol. 344, no. 6187, p. 1 246 752, 2014.

[35] A. Valiente-Banuet et al., "Beyond species loss: The extinction of ecological interactions in a changing world," *Functional ecology*, vol. 29, no. 3, pp. 299–307, 2015.

[36] D. M. Leigh, A. P. Hendry, E. Vázquez-Domínguez, and V. L. Friesen, "Estimated six per cent loss of genetic variation in wild populations since the industrial revolution," *Evolutionary applications*, vol. 12, no. 8, pp. 1505–1512, 2019.

[37] F. Bocchi, A. Bokulich, L. C. Brache, G. Grand-Pierre, and A. Watkins, "Are we in a sixth mass extinction? the challenges of answering and value of asking," *The British Journal for the Philosophy of Science*, vol. 76, no. 4, pp. 977–1010, 2025.

[38] L. Linke and C. F. Clements, "A sixth mass extinction? how linguistic uncertainty shapes our understanding of the biodiversity crisis," *Ecology and Evolution*, vol. 14, no. 12, e70653, 2024.

[39] H. Ritchie. "The size of world population over the long run." Accessed: 2026-05-22. [Online]. Available: https://ourworldindata.org/population-growth?insight=the-world-population-has-increased-rapidly-over-the-last-few-centuries#key-insights.

[40] A. D. Barnosky, P. L. Koch, R. S. Feranec, S. L. Wing, and A. B. Shabel, "Assessing the causes of late pleistocene extinctions on the continents," *science*, vol. 306, no. 5693, pp. 70–75, 2004.

[41] F. A. Smith, R. E. Elliott Smith, S. K. Lyons, and J. L. Payne, "Body size downgrading of mammals over the late quaternary," *Science*, vol. 360, no. 6386, pp. 310–313, 2018.

[42] J. O. Kaplan, K. M. Krumhardt, and N. Zimmermann, "The prehistoric and preindustrial deforestation of europe," *Quaternary science reviews*, vol. 28, no. 27-28, pp. 3016–3034, 2009.

[43] N. L. Boivin et al., "Ecological consequences of human niche construction: Examining long-term anthropogenic shaping of global species distributions," *Proceedings of the National Academy of Sciences*, vol. 113, no. 23, pp. 6388–6396, 2016.

[44] T. Malthus, "An essay on the principle of population," in *British Politics and the Environment in the Long Nineteenth Century*, Routledge, 2023, pp. 77–84.

[45] Q. Ashraf and O. Galor, "Dynamics and stagnation in the malthusian epoch," *American Economic Review*, vol. 101, no. 5, pp. 2003–2041, 2011.

[46] E. A. Wrigley, "Energy and the english industrial revolution," *Philosophical Transactions of the Royal Society A: Mathematical, Physical and Engineering Sciences*, vol. 371, no. 1986, 2013.

[47] W. Steffen, W. Broadgate, L. Deutsch, O. Gaffney, and C. Ludwig, "The trajectory of the anthropocene: The great acceleration," *The anthropocene review*, vol. 2, no. 1, pp. 81–98, 2015.

[48] J. W. Erisman, M. A. Sutton, J. Galloway, Z. Klimont, and W. Winiwarter, "How a century of ammonia synthesis changed the world," *Nature geoscience*, vol. 1, no. 10, pp. 636–639, 2008.

[49] P. L. Pingali, "Green revolution: Impacts, limits, and the path ahead," *Proceedings of the national academy of sciences*, vol. 109, no. 31, pp. 12 302–12 308, 2012.

[50] R. York and J. A. McGee, "Understanding the jevons paradox," *Environmental Sociology*, vol. 2, no. 1, pp. 77–87, 2016.

[51] R. M. Ewers, J. P. Scharlemann, A. Balmford, and R. E. Green, "Do increases in agricultural yield spare land for nature?" *Global Change Biology*, vol. 15, no. 7, pp. 1716–1726, 2009.

[52] D. Byerlee, J. Stevenson, and N. Villoria, "Does intensification slow crop land expansion or encourage deforestation?" *Global food security*, vol. 3, no. 2, pp. 92–98, 2014.

[53] R. Cowan and P. Gunby, "Sprayed to death: Path dependence, lock-in and pest control strategies," *The Economic Journal*, vol. 106, no. 436, pp. 521–542, May 1996, ISSN: 0013-0133. DOI: 10.2307/2235561. eprint: https://academic.oup.com/ej/article-pdf/106/436/521/27041419/ej0521.pdf. [Online]. Available: https://doi.org/10.2307/2235561.

[54] G. Orjuela-Ramirez, J. C. Zuluaga, C. Gonzalez, and J. Mockshell, "Lock-in and power in agrifood systems: A literature review and analytical framework," *Agroecology and Sustainable Food Systems*, pp. 1–22, 2025.

[55] S. Naeem, D. E. Bunker, A. Hector, M. Loreau, and C. Perrings, *Biodiversity, ecosystem functioning, and human wellbeing: an ecological and economic perspective*. OUP Oxford, 2009.

[56] B. J. Cardinale et al., "Biodiversity loss and its impact on humanity," *Nature*, vol. 486, no. 7401, pp. 59–67, 2012.

[57] M. Dainese et al., "A global synthesis reveals biodiversity-mediated benefits for crop production," *Science advances*, vol. 5, no. 10, eaax0121, 2019.

[58] C. Folke, R. Biggs, A. V. Norström, B. Reyers, and J. Rockström, "Social-ecological resilience and biosphere-based sustainability science," *Ecology and society*, vol. 21, no. 3, 2016.

[59] N. Brisson, P. Gate, D. Gouache, G. Charmet, F.-X. Oury, and F. Huard, "Why are wheat yields stagnating in europe? a comprehensive data analysis for france," *Field crops research*, vol. 119, no. 1, pp. 201–212, 2010.

[60] D. K. Ray, N. Ramankutty, N. D. Mueller, P. C. West, and J. A. Foley, "Recent patterns of crop yield growth and stagnation," *Nature communications*, vol. 3, no. 1, p. 1293, 2012.

[61] X. Wei et al., "Is yield increase sufficient to achieve food security in china?" *PloS one*, vol. 10, no. 2, e0116430, 2015.

[62] C. S. Ferreira, S. Seifollahi-Aghmiuni, G. Destouni, N. Ghajarnia, and Z. Kalantari, "Soil degradation in the european mediterranean region: Processes, status and consequences," *Science of the Total Environment*, vol. 805, p. 150 106, 2022.

[63] S. G. Potts et al., "Safeguarding pollinators and their values to human well-being," *Nature*, vol. 540, no. 7632, pp. 220–229, 2016.

[64] E. G. Frank, "The economic impacts of ecosystem disruptions: Costs from substituting biological pest control," *Science*, vol. 385, no. 6713, eadg0344, 2024.

[65] E. Frank and A. Sudarshan, "The social costs of keystone species collapse: Evidence from the decline of vultures in india," *American Economic Review*, vol. 114, no. 10, pp. 3007–3040, 2024.

[66] M. R. Springborn, J. A. Weill, K. R. Lips, R. Ibáñez, and A. Ghosh, "Amphibian collapses increased malaria incidence in central america," *Environmental Research Letters*, vol. 17, no. 10, p. 104 012, 2022.

[67] J. R. Rohr et al., "Emerging human infectious diseases and the links to global food production," *Nature sustainability*, vol. 2, no. 6, pp. 445–456, 2019.

[68] S. Díaz et al., "Pervasive human-driven decline of life on earth points to the need for transformative change," *Science*, vol. 366, no. 6471, eaax3100, 2019.

[69] E. C. Ellis and Z. Mehrabi, "Half earth: Promises, pitfalls, and prospects of dedicating half of earth's land to conservation," *Current Opinion in Environmental Sustainability*, vol. 38, pp. 22–30, 2019.

[70] Z. Mehrabi, E. C. Ellis, and N. Ramankutty, "The challenge of feeding the world while conserving half the planet," *Nature Sustainability*, vol. 1, no. 8, pp. 409–412, 2018.

[71] E. Neumayer, "Weak versus strong sustainability: Exploring the limits of two opposing paradigms," in *Weak versus strong sustainability*, Edward Elgar Publishing, 2010.

[72] T. M. Lenton, "Environmental tipping points," *Annual review of Environment and Resources*, vol. 38, pp. 1–29, 2013.

[73] W. B. Arthur, "Foundations of complexity economics," *Nature Reviews Physics*, vol. 3, no. 2, pp. 136–145, 2021.

[74] Y. Aruka and A. Kirman, *Economic foundations for social complexity science*. Springer, 2017.

[75] C. L. Spash, "New foundations for ecological economics," *Ecological Economics*, vol. 77, pp. 36–47, 2012.

[76] C. Hamilton, "Foundations of ecological economics," in *Human Ecology, Human Economy*, Routledge, 2020, pp. 35–63.

[77] IPBES, *Summary for policymakers of the global assessment report on biodiversity and ecosystem services*, version summary for policy makers, Nov. 2019. DOI: 10.5281/zenodo.3553579. [Online]. Available: https://doi.org/10.5281/zenodo.3553579.

[78] R. E. A. Almond, M. Grooten, and T. Petersen, "Living planet report 2020 - bending the curve of biodiversity loss," WWF, Gland, Switzerland, Report, 2020.

[79] M. S. Warren et al., "The decline of butterflies in europe: Problems, significance, and possible solutions," *Proceedings of the National Academy of Sciences*, vol. 118, no. 2, e2002551117, 2021.

[80] IUCN, *The iucn red list of threatened species. version 2024-1*, Accessed: 2023-07-14, 2024. [Online]. Available: https://www.iucnredlist.org.

[81] S. J. Ormerod and A. R. Watkinson, "Editors' introduction: Birds and agriculture," *Journal of Applied Ecology*, vol. 37, no. 5, pp. 699–705, 2000. DOI: https://doi.org/10.1046/j.1365-2664.2000.00576.x. eprint: https://besjournals.onlinelibrary.wiley.com/doi/pdf/10.1046/j.1365-2664.2000.00576.x. [Online]. Available: https://besjournals.onlinelibrary.wiley.com/doi/abs/10.1046/j.1365-2664.2000.00576.x.

[82] J. C. Biesmeijer et al., "Parallel declines in pollinators and insect-pollinated plants in britain and the netherlands," *Science*, vol. 313, no. 5785, pp. 351–354, 2006.

[83] R. P. Keller, J. Geist, J. M. Jeschke, and I. Kühn, "Invasive species in europe: Ecology, status, and policy," *Environmental Sciences Europe*, vol. 23, pp. 1–17, 2011.

[84] K. Henle et al., "Identifying and managing the conflicts between agriculture and biodiversity conservation in europe–a review," *Agriculture, ecosystems & environment*, vol. 124, no. 1-2, pp. 60–71, 2008.

[85] N. Dudley and S. Alexander, "Agriculture and biodiversity: A review," *Biodiversity*, vol. 18, no. 2-3, pp. 45–49, 2017.

[86] D. L. Wagner, "Insect declines in the anthropocene," *Annual review of entomology*, vol. 65, no. 1, pp. 457–480, 2020.

[87] Y. Clough, S. Kirchweger, and J. Kantelhardt, "Field sizes and the future of farmland biodiversity in european landscapes," *Conservation Letters*, vol. 13, no. 6, e12752, 2020. DOI: https://doi.org/10.1111/conl.12752. eprint: https://conbio.onlinelibrary.wiley.com/doi/pdf/10.1111/conl.12752. [Online]. Available: https://conbio.onlinelibrary.wiley.com/doi/abs/10.1111/conl.12752.

[88] T. Tscharntke et al., "Landscape moderation of biodiversity patterns and processes-eight hypotheses," *Biological reviews*, vol. 87, no. 3, pp. 661–685, 2012.

[89] F. Geiger et al., "Persistent negative effects of pesticides on biodiversity and biological control potential on european farmland," *Basic and Applied Ecology*, vol. 11, no. 2, pp. 97–105, 2010.

[90] A. Sharma et al., "Worldwide pesticide usage and its impacts on ecosystem," *SN Applied Sciences*, vol. 1, pp. 1–16, 2019.

[91] B. Schauberger, T. Ben-Ari, D. Makowski, T. Kato, H. Kato, and P. Ciais, "Yield trends, variability and stagnation analysis of major crops in france over more than a century," *Scientific reports*, vol. 8, no. 1, p. 16 865, 2018.

[92] R. Bommarco, D. Kleijn, and S. G. Potts, "Ecological intensification: Harnessing ecosystem services for food security," *Trends in ecology & evolution*, vol. 28, no. 4, pp. 230–238, 2013.

[93] S. K. Lowder, J. Skoet, and T. Raney, "The number, size, and distribution of farms, smallholder farms, and family farms worldwide," *World development*, vol. 87, pp. 16–29, 2016.

[94] R. Eastwood, M. Lipton, and A. Newell, "Farm size," *Handbook of agricultural economics*, vol. 4, pp. 3323–3397, 2010.

[95] A. Vitikainen, "An overview of land consolidation in europe," *nordic Journal of Surveying and real Estate research*, vol. 1, no. 1, 2004.

[96] L. Piet, L. Latruffe, C. Le Mouël, and Y. Desjeux, "How do agricultural policies influence farm size inequality? the example of france," *European Review of Agricultural Economics*, vol. 39, no. 1, pp. 5–28, 2012.

[97] J. Loughrey, T. Donnellan, and J. J. Lennon, "The inequality of farmland size in western europe," *Research Papers in Economics*, 2016. [Online]. Available: https://api.semanticscholar.org/CorpusID:133168581.

[98] R. Howarth, "The cap: History and attempts at reform," *Economic Affairs*, vol. 20, no. 2, pp. 4–10, 2000.

[99] A. Giuliani and H. Baron, "The cap (common agricultural policy): A short history of crises and major transformations of european agriculture," in *Forum for Social Economics*, Taylor & Francis, vol. 54, 2025, pp. 68–94.

[100] A.-C. L. Knudsen, *Farmers on welfare: the making of Europe's common agricultural policy*. Cornell University Press, 2011.

[101] G. Pe'er and S. Lakner, "The eu's common agricultural policy could be spent much more efficiently to address challenges for farmers, climate, and biodiversity," *One Earth*, vol. 3, no. 2, pp. 173–175, 2020.

[102] P. Batáry, L. V. Dicks, D. Kleijn, and W. J. Sutherland, "The role of agri-environment schemes in conservation and environmental management," *Conservation Biology*, vol. 29, no. 4, pp. 1006–1016, 2015.

[103] I. Cuadros-Casanova et al., "Opportunities and challenges for common agricultural policy reform to support the european green deal," *Conservation Biology*, vol. 37, no. 3, e14052, 2023.

[104] I. Hodge, J. Hauck, and A. Bonn, "The alignment of agricultural and nature conservation policies in the european union," *Conservation Biology*, vol. 29, no. 4, pp. 996–1005, 2015.

[105] S. Rigal et al., "Farmland practices are driving bird population decline across europe," *Proceedings of the National Academy of Sciences*, vol. 120, no. 21, e2216573120, 2023.

[106] D. Ansell, D. Freudenberger, N. Munro, and P. Gibbons, "The cost-effectiveness of agri-environment schemes for biodiversity conservation: A quantitative review," *Agriculture, Ecosystems & Environment*, vol. 225, pp. 184–191, 2016.

[107] J. A. Vickery, R. E. Feber, and R. J. Fuller, "Arable field margins managed for biodiversity conservation: A review of food resource provision for farmland birds," *Agriculture, ecosystems & environment*, vol. 133, no. 1-2, pp. 1–13, 2009.

[108] D. A. Landis, "Designing agricultural landscapes for biodiversity-based ecosystem services," *Basic and Applied Ecology*, vol. 18, pp. 1–12, 2017.

[109] D. Kleijn, R. Bommarco, T. P. Fijen, L. A. Garibaldi, S. G. Potts, and W. H. Van Der Putten, "Ecological intensification: Bridging the gap between science and practice," *Trends in ecology & evolution*, vol. 34, no. 2, pp. 154–166, 2019.

[110] D. Kleijn and W. J. Sutherland, "How effective are european agri-environment schemes in conserving and promoting biodiversity?" *Journal of applied ecology*, vol. 40, no. 6, pp. 947–969, 2003.

[111] R. J. Burton and G. Schwarz, "Result-oriented agri-environmental schemes in europe and their potential for promoting behavioural change," *Land use policy*, vol. 30, no. 1, pp. 628–641, 2013.

[112] X. B. Lastra-Bravo, C. Hubbard, G. Garrod, and A. Tolón-Becerra, "What drives farmers' participation in eu agri-environmental schemes?: Results from a qualitative meta-analysis," *Environmental Science & Policy*, vol. 54, pp. 1–9, 2015.

[113] R. Chaplin-Kramer, M. E. O'Rourke, E. J. Blitzer, and C. Kremen, "A meta-analysis of crop pest and natural enemy response to landscape complexity," *Ecology letters*, vol. 14, no. 9, pp. 922–932, 2011.

[114] J. M. Woltz, R. Isaacs, and D. A. Landis, "Landscape structure and habitat management differentially influence insect natural enemies in an agricultural landscape," *Agriculture, ecosystems & environment*, vol. 152, pp. 40–49, 2012.

[115] D. Montoya, B. Haegeman, S. Gaba, C. De Mazancourt, and M. Loreau, "Habitat fragmentation and food security in crop pollination systems," *Journal of Ecology*, vol. 109, no. 8, pp. 2991–3006, 2021.

[116] J. F. Brodie et al., "A well-connected earth: The science and conservation of organismal movement," *Science*, vol. 388, no. 6745, eadn2225, 2025.

[117] D. Bengochea Paz, K. Henderson, and M. Loreau, "Habitat percolation transition undermines sustainability in social-ecological agricultural systems," *Ecology Letters*, vol. 25, no. 1, pp. 163–176, 2022.

[118] L. Mouysset, L. Doyen, F. Jiguet, G. Allaire, and F. Leger, "Bio economic modeling for a sustainable management of biodiversity in agricultural lands," *Ecological Economics*, vol. 70, no. 4, pp. 617–626, 2011, ISSN: 0921-8009. DOI: https://doi.org/10.1016/j.ecolecon.2010.12.006. [Online]. Available: https://www.sciencedirect.com/science/article/pii/S092180091000501X.

[119] J. Ahnström, J. Höckert, H. Bergeå, C. Francis, P. Skelton, and L. Hallgren, "Farmers and nature conservation: What is known about attitudes, context factors and actions affecting conservation?" *Renewable agriculture and food systems*, vol. 24, no. 1, pp. 38–47, 2009.

[120] A. Thompson, A. Reimer, and L. Prokopy, "Farmers' views of the environment: The influence of competing attitude frames on landscape conservation efforts," *Agriculture and human values*, vol. 32, pp. 385–399, 2015.

[121] M. Coronese, M. Occelli, F. Lamperti, and A. Roventini, "Agrilove: Agriculture, land-use and technical change in an evolutionary, agent-based model," *SSRN Electronic Journal*, Jan. 2021. DOI: 10.2139/ssrn.3944282.

[122] S. Heckbert, T. Baynes, and A. Reeson, "Agent-based modeling in ecological economics," *Annals of the new York Academy of Sciences*, vol. 1185, no. 1, pp. 39–53, 2010.

[123] R. Greiner, "Motivations and attitudes influence farmers' willingness to participate in biodiversity conservation contracts," *Agricultural Systems*, vol. 137, pp. 154–165, 2015.

[124] A. Bourceret, L. Amblard, and J. Mathias, "Adapting the governance of social–ecological systems to behavioural dynamics: An agent-based model for water quality management using the theory of planned behaviour," *Ecological Economics*, vol. 194, p. 107 338, 2022.

[125] L. An, "Modeling human decisions in coupled human and natural systems: Review of agent-based models," *Ecological modelling*, vol. 229, pp. 25–36, 2012.

[126] F. J. Dessart, J. Barreiro-Hurlé, R. Van Bavel, et al., "Behavioural factors affecting the adoption of sustainable farming practices: A policy-oriented review," *European Review of Agricultural Economics*, vol. 46, no. 3, pp. 417–471, 2019.

[127] R. B. Matthews, N. G. Gilbert, A. Roach, J. G. Polhill, and N. M. Gotts, "Agent-based land-use models: A review of applications," *Landscape Ecology*, vol. 22, pp. 1447–1459, 2007.

[128] D. Kremmydas, I. N. Athanasiadis, and S. Rozakis, "A review of agent based modeling for agricultural policy evaluation," *Agricultural systems*, vol. 164, pp. 95–106, 2018.

[129] D. S. Utomo, B. S. Onggo, and S. Eldridge, "Applications of agent-based modelling and simulation in the agri-food supply chains," *European Journal of Operational Research*, vol. 269, no. 3, pp. 794–805, 2018.

[130] R. Huber et al., "Representation of decision-making in european agricultural agent-based models," *Agricultural systems*, vol. 167, pp. 143–160, 2018.

[131] A. Alonso-Adame, J. Van Meensel, F. Marchand, S. Van Passel, and S. Farahbakhsh, "Sustainability transitions in agri-food systems through the lens of agent-based modeling: A systematic review," *Sustainability Science*, pp. 1–18, 2024.

[132] M. F. Alam, M. McClain, A. Sikka, and S. Pande, "Understanding human–water feedbacks of interventions in agricultural systems with agent based models: A review," *Environmental Research Letters*, vol. 17, no. 10, p. 103 003, 2022.

[133] D. O. Ferraro, F. Ghersa, and R. Castro, "Predicting land use and environmental dynamics in argentina's pampas region: An agent-based modeling approach across varied price and climatic scenarios.," *Ecological Modelling*, vol. 498, p. 110 881, 2024.

[134] J. Groeneveld et al., "Theoretical foundations of human decision-making in agent-based land use models–a review," *Environmental modelling & software*, vol. 87, pp. 39–48, 2017.

[135] K. Happe, K. Kellermann, and A. Balmann, "Agent-based analysis of agricultural policies: An illustration of the agricultural policy simulator agripolis, its adaptation and behavior," *Ecology and society*, vol. 11, no. 1, 2006.

[136] R. Huber, H. Xiong, K. Keller, and R. Finger, "Bridging behavioural factors and standard bio-economic modelling in an agent-based modelling framework," *Journal of Agricultural Economics*, vol. 73, no. 1, pp. 35–63, 2022.

[137] G. Fagiolo, A. Moneta, and P. Windrum, "A critical guide to empirical validation of agent-based models in economics: Methodologies, procedures, and open problems," *Computational Economics*, vol. 30, pp. 195–226, 2007.

[138] J.-P. Bouchaud, *Navigating through economic complexity: Phase diagrams & parameter sloppiness*, 2024. arXiv: 2412.11259 [econ.TH]. [Online]. Available: https://arxiv.org/abs/2412.11259.

[139] S. Gualdi, M. Tarzia, F. Zamponi, and J.-P. Bouchaud, "Tipping points in macroeconomic agent-based models," *Journal of Economic Dynamics and Control*, vol. 50, pp. 29–61, 2015.

[140] D. Bengochea Paz, K. Henderson, and M. Loreau, "Habitat percolation transition undermines sustainability in social-ecological agricultural systems," *Ecology Letters*, vol. 25, no. 1, pp. 163–176, 2022.

[141] B. T. Van Zanten et al., "European agricultural landscapes, common agricultural policy and ecosystem services: A review," *Agronomy for sustainable development*, vol. 34, pp. 309–325, 2014.

[142] D. Kleijn et al., "Mixed biodiversity benefits of agri-environment schemes in five european countries," *Ecology letters*, vol. 9, no. 3, pp. 243–254, 2006.

[143] P. Ciaian, D. Kancs, J. Swinnen, K. V. Herck, and L. Vranken, *Key Issues and Developments in Farmland Rental Markets in EU Member States and Candidate Countries*. Brussels (Belgium): Centre for European Policy Studies (CEPS), 2012, pp. 1–29, ISBN: 978-94-6138-151-4. [Online]. Available: http://www.factormarkets.eu/system/files/FM_WP13%20CEPS%20on%20Key%20Issues%20in%20Farmland%20Rental%20Markets_D14.2_final.pdf.

[144] E. C. of the Regions et al., *Towards an 8th Environment Action Programme – Local and regional dimension*. European Committee of the Regions, 2018. DOI: doi/10.2863/70733.

[145] D. Montoya, B. Haegeman, s. Gaba, C. de Mazancourt, V. Bretagnolle, and M. Loreau, "Trade-offs in the provisioning and stability of ecosystem services in agroecosystems," *Ecological Applications*, vol. 29, no. 2, e01853, 2019. DOI: https://doi.org/10.1002/eap.1853. eprint: https://esajournals.onlinelibrary.wiley.com/doi/pdf/10.1002/eap.1853. [Online]. Available: https://esajournals.onlinelibrary.wiley.com/doi/abs/10.1002/eap.1853.

[146] D. Montoya, B. Haegeman, s. Gaba, C. de Mazancourt, V. Bretagnolle, and M. Loreau, "Habitat fragmentation and food security in crop pollination systems," *Journal of Ecology*, vol. 109, no. 8, pp. 2991–3006, 2021. DOI: https://doi.org/10.1111/1365-2745.13713. eprint: https://besjournals.onlinelibrary.wiley.com/doi/pdf/10.1111/1365-2745.13713. [Online]. Available: https://besjournals.onlinelibrary.wiley.com/doi/abs/10.1111/1365-2745.13713.

[147] Y. Clough, S. Kirchweger, and J. Kantelhardt, "Field sizes and the future of farmland biodiversity in european landscapes," *Conservation Letters*, vol. 13, no. 6, e12752, 2020. DOI: https://doi.org/10.1111/conl.12752. eprint: https://conbio.onlinelibrary.wiley.com/doi/pdf/10.1111/conl.12752. [Online]. Available: https://conbio.onlinelibrary.wiley.com/doi/abs/10.1111/conl.12752.

[148] C. J. Whelan, D. G. Wenny, and R. J. Marquis, "Ecosystem services provided by birds," *Annals of the New York academy of sciences*, vol. 1134, no. 1, pp. 25–60, 2008.

[149] P. Díaz-Siefer, N. Olmos-Moya, F. Fontúrbel, B. Lavandero, R. Pozo, and J. Celis-Diez, "Bird-mediated effects of pest control services on crop productivity: A global synthesis," *Journal of Pest Science*, vol. 95, Mar. 2022. DOI: 10.1007/s10340-021-01438-4.

[150] L. Labuschagne, L. H. Swanepoel, P. J. Taylor, S. R. Belmain, and M. Keith, "Are avian predators effective biological control agents for rodent pest management in agricultural systems?" *Biological Control*, vol. 101, pp. 94–102, 2016.

[151] L. P. Koh, "Birds defend oil palms from herbivorous insects," *Ecological applications*, vol. 18, no. 4, pp. 821–825, 2008.

[152] European Commission, Directorate-General for Agriculture and Rural Development, *Farm accountancy data network public database*, Accessed: 2024-07-10, 2024. [Online]. Available: https://agridata.ec.europa.eu/extensions/FarmEconomyFocus/FADNDatabase.html.

[153] C. B. Moss, *Production Economics*. World Scientific, 2022. DOI: 10.1142/12332. eprint: https://www.worldscientific.com/doi/pdf/10.1142/12332. [Online]. Available: https://www.worldscientific.com/doi/abs/10.1142/12332.

[154] D. K. Ray, N. Ramankutty, N. D. Mueller, P. C. West, and J. A. Foley, "Recent patterns of crop yield growth and stagnation," *Nature communications*, vol. 3, no. 1, p. 1293, 2012.

[155] B. Schauberger, T. Ben-Ari, D. Makowski, T. Kato, H. Kato, and P. Ciais, "Yield trends, variability and stagnation analysis of major crops in france over more than a century," *Scientific reports*, vol. 8, no. 1, p. 16 865, 2018.

[156] A. Tibi et al., "Place des agricultures européennes dans le monde à l'horizon 2050 : Entre enjeux climatiques et défis de la sécurité alimentaire. rapport de synthèse de l'étude," INRAE, France, Rapport de synthèse, 2020, + Annexes, p. 159.

[157] M. Duffy, "Economies of size in production agriculture," *Journal of hunger & environmental nutrition*, vol. 4, pp. 375–392, Jul. 2009. DOI: 10.1080/19320240903321292.

[158] F. Kuhlmann and E. Berg, "The farm as an enterprise–the european perspective," 2002.

[159] OECD, *Evaluation of Agricultural Policy Reforms in the European Union*. 2011, p. 184. DOI: https://doi.org/https://doi.org/10.1787/9789264112124-en. [Online]. Available: https://www.oecd-ilibrary.org/content/publication/9789264112124-en.

[160] J. Xiao et al., "Application method affects pesticide efficiency and effectiveness in wheat fields," *Pest Management Science*, vol. 76, no. 4, pp. 1256–1264, 2020.

[161] G. Dosi, "Technological paradigms and technological trajectories: A suggested interpretation of the determinants and directions of technical change," *Research Policy*, vol. 11, no. 3, pp. 147–162, 1982, ISSN: 0048-7333. DOI: https://doi.org/10.1016/0048-7333(82)90016-6. [Online]. Available: https://www.sciencedirect.com/science/article/pii/0048733382900166.

[162] K. Kellermann, C. Sahrbacher, and A. Balmann, "Land markets in agent based models of structural change," Feb. 2008.

[163] Eurostat, *Farms and farmland in the european union - statistics*, Eurostat Statistics Explained, Accessed: 2025-10-22. Data from the 2020 Agricultural Census., Apr. 2023. [Online]. Available: https://ec.europa.eu/eurostat/statistics-explained/index.php?title=Farms_and_farmland_in_the_European_Union_-_statistics.

[164] E. Meunier, P. Smith, T. Griessinger, and C. Robert, "Understanding changes in reducing pesticide use by farmers: Contribution of the behavioural sciences," *Agricultural Systems*, vol. 214, p. 103 818, 2024.

[165] M. Robert, A. Thomas, and J.-E. Bergez, "Processes of adaptation in farm decision-making models. a review," *Agronomy for sustainable development*, vol. 36, pp. 1–15, 2016.

[166] F. Lamperti, G. Dosi, M. Napoletano, A. Roventini, and A. Sapio, "Faraway, so close: Coupled climate and economic dynamics in an agent-based integrated assessment model," *Ecological Economics*, vol. 150, pp. 315–339, 2018.

[167] L. Mouysset, M. Miglianico, D. Makowski, F. Jiguet, and D. Luc, "Selection of dynamic models for bird populations in farmlands," *Environmental Modeling & Assessment*, vol. 21, Jun. 2016. DOI: 10.1007/s10666-015-9494-y.

[168] A. Dhondt, "Carrying capacity: A confusing concept.," *ACTA OECOL.(OECOL. GEN.).*, vol. 9, no. 4, pp. 337–346, 1988.

[169] B. J. Cardinale, C. T. Harvey, K. Gross, and A. R. Ives, "Biodiversity and biocontrol: Emergent impacts of a multi-enemy assemblage on pest suppression and crop yield in an agroecosystem," *Ecology letters*, vol. 6, no. 9, pp. 857–865, 2003.

[170] E. B. C. Council, R. S. for the Protection of Birds, B. International, and C. S. for Ornithology, *Geographical coverage: Eu=eu-27 (except malta)*, Source provided by European Bird Census Council, Royal Society for the Protection of Birds, BirdLife International, and Czech Society for Ornithology, 2008.

[171] Food and Agriculture Organization of the United Nations (FAO), *Structural data from agricultural censuses*, FAOSTAT database, Accessed on July 10, 2024, Accessed 2024. [Online]. Available: https://www.fao.org/faostat/en/#data/WCAD.

[172] Food and Agriculture Organization of the United Nations (FAO), *Agriculture producer prices and producer price index*, FAOSTAT database, Accessed on July 10, 2024, Accessed 2024. [Online]. Available: https://www.fao.org/faostat/en/#data/PP.

[173] E. Parliament, D.-G. for Parliamentary Research Services, D. Bylemans, B. De Coninck, and W. Keulemans, *Farming without plant protection products – Can we grow without using herbicides, fungicides and insecticides?* Publications Office, 2019. DOI: doi/10.2861/05433.

[174] R. Schils et al., "Cereal yield gaps across europe," *European Journal of Agronomy*, vol. 101, pp. 109–120, 2018.

[175] B. Joernsgaard and S. Halmoe, "Intra-field yield variation over crops and years," *European Journal of Agronomy*, vol. 19, no. 1, pp. 23–33, 2003.

[176] E. Parliament, D.-G. for Parliamentary Research Services, J. Bremmer, M. Manshanden, A. Smit, and J. Jager, *Cost of crop protection measures – A follow-up to the study 'The future of crop protection in Europe' (2021)*. European Parliament, 2021. DOI: doi/10.2861/67868.

[177] E. Commission, "Eu cereal farms report: Based on 2017 fadn data," European Commission, 2017, Accessed: 2024-07-13. [Online]. Available: https://agriculture.ec.europa.eu/system/files/2020-01/fadn-cereal-report-2017_en_0.pdf.

[178] A. Giuliani and H. Baron, "The cap (common agricultural policy): A short history of crises and major transformations of european agriculture," in *Forum for Social Economics*, Taylor & Francis, 2023, pp. 1–27.

[179] R. Haines-Young, M. Potschin, et al., "The links between biodiversity, ecosystem services and human well-being," *Ecosystem Ecology: a new synthesis*, vol. 1, pp. 110–139, 2010.

[180] P. Sandifer, A. Sutton-Grier, and B. Ward, "Exploring connections among nature, biodiversity, ecosystem services, and human health and well-being: Opportunities to enhance health and biodiversity conservation," *Ecosystem services*, vol. 12, pp. 1–15, 2015.

[181] J. Wesseler, "The eu's farm-to-fork strategy: An assessment from the perspective of agricultural economics," *Applied Economic Perspectives and Policy*, vol. 44, no. 4, pp. 1826–1843, 2022.

[182] T. Böcker and R. Finger, "European pesticide tax schemes in comparison: An analysis of experiences and developments," *Sustainability*, vol. 8, no. 4, p. 378, 2016.

[183] M. Stolze, A. Piorr, A. Häring, and S. Dabbert, *Environmental impacts of organic farming in Europe*. Universität Hohenheim, Stuttgart-Hohenheim, 2000.

[184] E. Commission, *Commission response to council decision (eu) 2022/2572 of 19 december 2022*, Accessed: 2023-07-14, 2023. [Online]. Available: https://food.ec.europa.eu/document/download/f9c54e6c-023c-4399-8c24-6c1920efeeba_en?filename=pesticides_sup_comm-response_2022-2572_en.pdf.

[185] N. Möhring et al., "Pathways for advancing pesticide policies," *Nature food*, vol. 1, no. 9, pp. 535–540, 2020.

[186] E. Commission and D.-G. for Environment, *EU biodiversity strategy for 2030 – Bringing nature back into our lives*. Publications Office of the European Union, 2021. DOI: doi/10.2779/677548.

[187] A. Hernández, T. Parrón, A. Tsatsakis, M. Requena, R. Alarcón, and O. López-Guarnido, "Toxic effects of pesticide mixtures at a molecular level: Their relevance to human health," *Toxicology*, vol. 307, pp. 136–145, 2013.

[188] I. Otero et al., "Biodiversity policy beyond economic growth," *Conservation letters*, vol. 13, no. 4, e12713, 2020.

[189] A.-S. Lafuite, G. Denise, and M. Loreau, "Sustainable land-use management under biodiversity lag effects," *Ecological Economics*, vol. 154, pp. 272–281, 2018.

[190] V. Beckers, J. Beckers, M. Vanmaercke, E. Van Hecke, A. Van Rompaey, and N. Dendoncker, "Modelling farm growth and its impact on agricultural land use: A country scale application of an agent-based model," *Land*, vol. 7, no. 3, p. 109, 2018.

[191] L. M. Castro, F. Härtl, S. Ochoa, B. Calvas, L. Izquierdo, and T. Knoke, "Integrated bio-economic models as tools to support land-use decision making: A review of potential and limitations," *Journal of Bioeconomics*, vol. 20, no. 2, pp. 183–211, 2018.

[192] R. Finger and N. El Benni, "Farm income in european agriculture: New perspectives on measurement and implications for policy evaluation," *European Review of Agricultural Economics*, vol. 48, no. 2, pp. 253–265, 2021.

[193] P. Yang et al., "Effects of land consolidation intensity on landscape pattern and biodiversity in paddy ecosystem," *Agriculture, Ecosystems & Environment*, vol. 381, p. 109 458, 2025.

[194] T. Osawa, K. Kohyama, and H. Mitsuhashi, "Trade-off relationship between modern agriculture and biodiversity: Heavy consolidation work has a long-term negative impact on plant species diversity," *Land Use Policy*, vol. 54, pp. 78–84, 2016.

[195] X. Shi et al., "Can landscape level semi-natural habitat compensate for pollinator biodiversity loss due to farmland consolidation?" *Agriculture, Ecosystems & Environment*, vol. 319, p. 107 519, 2021.

[196] R. Finger, K. Schneider, J. Candel, and N. Möhring, "Europe needs better pesticide policies to reduce impacts on biodiversity," *Food Policy*, vol. 125, p. 102 632, 2024.

[197] M. A. Beketov, B. J. Kefford, R. B. Schäfer, and M. Liess, "Pesticides reduce regional biodiversity of stream invertebrates," *Proceedings of the National Academy of Sciences*, vol. 110, no. 27, pp. 11 039–11 043, 2013.

[198] T. Tscharntke, I. Grass, T. C. Wanger, C. Westphal, and P. Batáry, "Restoring biodiversity needs more than reducing pesticides," *Trends in Ecology & Evolution*, vol. 37, no. 2, pp. 115–116, 2022.

[199] S. Lecq, A. Loisel, F. Brischoux, S. J. Mullin, and X. Bonnet, "Importance of ground refuges for the biodiversity in agricultural hedgerows," *Ecological Indicators*, vol. 72, pp. 615–626, 2017.

[200] S. Kratschmer, J. Hauer, J. G. Zaller, A. Dürr, and T. Weninger, "Hedgerow structural diversity is key to promoting biodiversity and ecosystem services: A systematic review of central european studies," *Basic and Applied Ecology*, vol. 78, pp. 28–38, 2024.

[201] H. Li, E. Y. Zeng, and J. You, "Mitigating pesticide pollution in china requires law enforcement, farmer training, and technological innovation," *Environmental toxicology and chemistry*, vol. 33, no. 5, pp. 963–971, 2014.

[202] M. A. Oliver, T. F. Bishop, B. P. Marchant, et al., *Precision agriculture for sustainability and environmental protection*. Routledge Abingdon, UK, 2013, vol. 39.

[203] L. Morandin, R. Long, and C. Kremen, "Pest control and pollination cost–benefit analysis of hedgerow restoration in a simplified agricultural landscape," *Journal of Economic Entomology*, vol. 109, no. 3, pp. 1020–1027, 2016.

[204] A. Stechemesser et al., "Climate policies that achieved major emission reductions: Global evidence from two decades," *Science*, vol. 385, no. 6711, pp. 884–892, 2024.

[205] R. Finger, A. Fabry, M. Kammer, J. Candel, T. Dalhaus, and E. M. Meemken, "Farmer protests in europe 2023–2024," *EuroChoices*, vol. 23, no. 3, pp. 59–63, 2024.

[206] A. Matthews, "Farmer protests and the 2024 european parliament elections," *Intereconomics*, vol. 59, no. 2, pp. 83–87, 2024.

[207] E. Mc Loughlin, "Protesting the future: The evolution of the european farmer," *Anthropology Today*, vol. 40, no. 5, pp. 3–6, 2024.

[208] G. Rivière-Wekstein, "Loi duplomb: Un coup d'arrêt à la profusion des contraintes agricoles," *Paysans & société*, vol. 413, no. 5, pp. 10–13, 2025.

[209] A. Aulagnier, "Loi duplomb et pesticides: Comment la fnsea a imposé ses revendications," *The Conversation France*, 2025.

[210] F. Kinniburgh, "The politics of expertise in assessing alternatives to glyphosate in france," *Environmental Science & Policy*, vol. 145, pp. 60–72, 2023.

[211] C. de MENTHIÈRE, P. Falcone, V. Piveteau, and X. Ory, "La haie, levier de la planification écologique," *Rapport du CGAAER*, vol. 22114, p. 116, 2023.

[212] P. Reidsma et al., "Alternative systems and strategies to improve future sustainability and resilience of farming systems across europe: From adaptation to transformation," *Land Use Policy*, vol. 134, p. 106 881, 2023.

[213] E. Skrimizea et al., "Sustainable agriculture: Recognizing the potential of conflict as a positive driver for transformative change," in *Advances in ecological research*, vol. 63, Elsevier, 2020, pp. 255–311.

[214] C. Turney, A.-G. Ausseil, and L. Broadhurst, "Urgent need for an integrated policy framework for biodiversity loss and climate change," *Nature Ecology & Evolution*, vol. 4, no. 8, pp. 996–996, 2020.

[215] T. K. Gottschalk et al., "Impact of agricultural subsidies on biodiversity at the landscape level," *Landscape Ecology*, vol. 22, no. 5, pp. 643–656, 2007.

[216] C. Bockstaller, L. Guichard, D. Makowski, A. Aveline, P. Girardin, and S. Plantureux, "Agri-environmental indicators to assess cropping and farming systems. a review," *Agronomy for sustainable development*, vol. 28, pp. 139–149, 2008.

[217] T. Gomiero, D. Pimentel, and M. G. Paoletti, "Environmental impact of different agricultural management practices: Conventional vs. organic agriculture," *Critical reviews in plant sciences*, vol. 30, no. 1-2, pp. 95–124, 2011.

[218] E. López-Gunn, B. Mayor, and A. Dumont, "Implications of the modernization of irrigation systems," *Water, agriculture and the environment in Spain: Can we square the circle*, pp. 241–255, 2012.

[219] H. Von Blottnitz, A. Rabl, D. Boiadjiev, T. Taylor, and S. Arnold, "Damage costs of nitrogen fertilizer in europe and their internalization," *Journal of environmental planning and management*, vol. 49, no. 3, pp. 413–433, 2006.

[220] C. A. Correa Ayram, M. E. Mendoza, A. Etter, and D. R. P. Salicrup, "Habitat connectivity in biodiversity conservation: A review of recent studies and applications," *Progress in Physical Geography*, vol. 40, no. 1, pp. 7–37, 2016.

[221] J. M. Holland et al., "Semi-natural habitats support biological control, pollination and soil conservation in europe. a review," *Agronomy for Sustainable Development*, vol. 37, pp. 1–23, 2017.

[222] T. Bradfer-Lawrence et al., "Spillovers and legacies of land management on temperate woodland biodiversity," *Nature Ecology & Evolution*, pp. 1–12, 2025.

[223] X. Chen, Q. Wang, B. Cui, G. Chen, T. Xie, and W. Yang, "Ecological time lags in biodiversity response to habitat changes," *Journal of Environmental Management*, vol. 346, p. 118 965, 2023.

[224] C. Roussy, A. Ridier, and K. Chaib, "Farmers' innovation adoption behaviour: Role of perceptions and preferences," *International Journal of Agricultural Resources, Governance and Ecology*, vol. 13, no. 2, pp. 138–161, 2017.

[225] M. Ramzan and H. Li, "An analytical framework to link factors affecting agricultural trade intensity in the world: Pathways to sustainable agricultural development 2030 agenda: An analytical framework to link factors affecting...: M. ramzan, h. li.," *Environment, Development & Sustainability*, vol. 27, no. 1, 2025.

[226] A. Haniotis, "Global challenges and the eu's shifting agri-trade goalposts," *Studies in Agricultural Economics*, 2025.

[227] I. Sobol, "On the distribution of points in a cube and the approximate evaluation of integrals," *Ussr Computational Mathematics and Mathematical Physics*, vol. 7, pp. 86–112, 1967. [Online]. Available: https://api.semanticscholar.org/CorpusID:122581245.

[228] H. Carver, "Reviewed work: Methods of correlation analysis by mordecai ezekiel," *Journal of the American Statistical Association*, vol. 26, no. 175, pp. 350–353, 1931, ISSN: 01621459, 1537274X. Accessed: Sep. 19, 2024. [Online]. Available: http://www.jstor.org/stable/2277917.

[229] L. Hein, "The economic value of the pollination service, a review across scales," *Open Ecology Journal*, vol. 2, no. 1, pp. 74–82, 2009.

[230] T. D. Breeze, N. Gallai, L. A. Garibaldi, and X. S. Li, "Economic measures of pollination services: Shortcomings and future directions," *Trends in Ecology & Evolution*, vol. 31, no. 12, pp. 927–939, 2016.

[231] D. Dent and R. H. Binks, *Insect pest management*. Cabi, 2020.

[232] E. Oerke and H. Dehne, "Safeguarding production—losses in major crops and the role of crop protection," *Crop Protection*, vol. 23, no. 4, pp. 275–285, 2004, ISSN: 0261-2194. DOI: https://doi.org/10.1016/j.cropro.2003.10.001. [Online]. Available: https://www.sciencedirect.com/science/article/pii/S0261219403002540.

[233] C. Rega et al., "A pan-european model of landscape potential to support natural pest control services," *Ecological Indicators*, vol. 90, pp. 653–664, 2018.

[234] A. Janssen and P. C. van Rijn, "Pesticides do not significantly reduce arthropod pest densities in the presence of natural enemies," *Ecology letters*, vol. 24, no. 9, pp. 2010–2024, 2021.

[235] S. Engel, S. Pagiola, and S. Wunder, "Designing payments for environmental services in theory and practice: An overview of the issues," *Ecological economics*, vol. 65, no. 4, pp. 663–674, 2008.

[236] H. Yan, H. Yang, X. Guo, S. Zhao, and Q. Jiang, "Payments for ecosystem services as an essential approach to improving ecosystem services: A review," *Ecological Economics*, vol. 201, p. 107 591, 2022.

[237] K. Simpson, P. R. Armsworth, M. Dallimer, M. Nthambi, F. P. de Vries, and N. Hanley, "Improving the ecological and economic performance of agri-environment schemes: Payment by modelled results versus payment for actions," *Land Use Policy*, vol. 130, p. 106 688, 2023.

[238] V. Martinet and L. Roques, *An ecological-economic model of land-use decisions, agricultural production and biocontrol. r. soc. open sci. 9: 220169*, 2022.

[239] R. S. Cantrell and C. Cosner, *Spatial ecology via reaction-diffusion equations*. John Wiley & Sons, 2004.

[240] C. Ren et al., "The impact of farm size on agricultural sustainability," *Journal of Cleaner Production*, vol. 220, pp. 357–367, 2019.

[241] Ł. Kryszak, M. Guth, and B. Czyżewski, "Determinants of farm profitability in the eu regions. does farm size matter?" *Agricultural Economics/Zemědělská ekonomika*, vol. 67, no. 3, 2021.

[242] C. Jänicke et al., "Can we estimate farm size from field size? an empirical investigation of the field size to farm size relationship," *Agricultural Systems*, vol. 220, p. 104 088, 2024.

[243] L. T. Hauser, T. Van Der Sluis, and M. Giezen, "The role of farm management characteristics in understanding the spatial distribution of landscape elements: A case study in the netherlands," *Rural Landscapes: Society, Environment, History*, vol. 3, no. 1, pp. 7–7, 2016.

[244] K. Belfrage, J. Björklund, and L. Salomonsson, "Effects of farm size and on-farm landscape heterogeneity on biodiversity—case study of twelve farms in a swedish landscape," *Agroecology and Sustainable Food Systems*, vol. 39, no. 2, pp. 170–188, 2015.

[245] G. Levin, "Farm size and landscape composition in relation to landscape changes in denmark," *Geografisk Tidsskrift-Danish Journal of Geography*, vol. 106, no. 2, pp. 45–59, 2006.

[246] G. Martel, S. Aviron, A. Joannon, E. Lalechère, B. Roche, and H. Boussard, "Impact of farming systems on agricultural landscapes and biodiversity: From plot to farm and landscape scales," *European Journal of Agronomy*, vol. 107, pp. 53–62, 2019.

[247] K. Adamczyk-Chauvat, M. Kassa, K. Kiêu, J. Papaïx, and R. S. Stoica, *Gibbsian t-tessellation model for agricultural landscape characterization*, 2020. arXiv: 2007.16094 [stat.AP]. [Online]. Available: https://arxiv.org/abs/2007.16094.

[248] C. Robinet et al., "A suite of models to support the quantitative assessment of spread in pest risk analysis," 2012.

[249] A. Le Gal, C. Robert, F. Accatino, D. Claessen, and J. Lecomte, "Modelling the interactions between landscape structure and spatio-temporal dynamics of pest natural enemies: Implications for conservation biological control," *Ecological modelling*, vol. 420, p. 108 912, 2020.

[250] J.-P. Sarthou, A. Badoz, B. Vaissière, A. Chevallier, and A. Rusch, "Local more than landscape parameters structure natural enemy communities during their overwintering in semi-natural habitats," *Agriculture, ecosystems & environment*, vol. 194, pp. 17–28, 2014.

[251] E. Commission, *Circabc document repository: Agricultural policy documents*, https://circabc.europa.eu/ui/group/befb6055-ab0c-4305-84fe-0c80c1c0553d/library/26cf03c0-c30a-4c19-8f46-bd56bfc59549?p=1&n=10&sort=modified_DESC, Accessed: 2025-10-10, 2025.

[252] T. De Ponti, B. Rijk, and M. K. Van Ittersum, "The crop yield gap between organic and conventional agriculture," *Agricultural systems*, vol. 108, pp. 1–9, 2012.

[253] European Commission, *Fertiliser input estimates in farms: An overview of costs and quantities of the three main fertilizer components used in the eu farms based on fadn data*, 2021. Accessed: May 8, 2025. [Online]. Available: https://agriculture.ec.europa.eu/document/download/f4c46068-c8d6-424b-a932-97f158ead6e8_en?filename=agri-farm-economics-brief-19_en.pdf.

[254] E. Commission, *Analytical brief n°3: Explore farm incomes in the eu: Farm economics overview based on 2021 fadn data*, Accessed: 2025/05/19, 2023. [Online]. Available: https://agriculture.ec.europa.eu/document/download/bc9e6d8c-5450-4c3a-884e-7198b44e371a_en?filename=analytical-brief-3-feo-brief_en.pdf.

[255] Y. Clough, A. Kruess, and T. Tscharntke, "Local and landscape factors in differently managed arable fields affect the insect herbivore community of a non-crop plant species," *Journal of Applied Ecology*, vol. 44, no. 1, pp. 22–28, 2007.

[256] I. D. Jonsen and L. Fahrig, "Response of generalist and specialist insect herbivores to landscape spatial structure," *Landscape Ecology*, vol. 12, pp. 185–197, 1997.

[257] R. Cloyd, "Indirect effects of pesticides on natural enemies," in *Pesticides-Advances in chemical and botanical pesticides*, IntechOpen, 2012.

[258] IPBES, *Global assessment report on biodiversity and ecosystem services of the intergovernmental science-policy platform on biodiversity and ecosystem services*, 2019.

[259] I. R. Staude et al., "Prioritize grassland restoration to bend the curve of biodiversity loss," *Restoration Ecology*, vol. 31, no. 5, e13931, 2023.

[260] S. Muller, T. Dutoit, D. Alard, and F. Grevilliot, "Restoration and rehabilitation of species-rich grassland ecosystems in france: A review," *Restoration Ecology*, vol. 6, no. 1, pp. 94–101, 1998.

[261] R. Duflot et al., "Adjacent woodlands rather than habitat connectivity influence grassland plant, carabid and bird assemblages in farmland landscapes," *Biodiversity and Conservation*, vol. 27, no. 8, pp. 1925–1942, 2018.

[262] A. Villemey et al., "Mosaic of grasslands and woodlands is more effective than habitat connectivity to conserve butterflies in french farmland," *Biological Conservation*, vol. 191, pp. 206–215, 2015.

[263] A. Veres, S. Petit, C. Conord, and C. Lavigne, "Does landscape composition affect pest abundance and their control by natural enemies? a review," *Agriculture, Ecosystems & Environment*, vol. 166, pp. 110–117, 2013.

[264] C. MacLaren et al., "Long-term evidence for ecological intensification as a pathway to sustainable agriculture," *Nature Sustainability*, vol. 5, no. 9, pp. 770–779, 2022.

[265] C. M. Kennedy et al., "A global quantitative synthesis of local and landscape effects on wild bee pollinators in agroecosystems," *Ecology letters*, vol. 16, no. 5, pp. 584–599, 2013.

[266] J. K. Boyce, "A future for small farms? biodiversity and sustainable agriculture," *Human development in the era of globalization: Essays in honor of Keith B. Griffin*, pp. 83–104, 2006.

[267] M. Tschumi, M. Albrecht, M. H. Entling, and K. Jacot, "High effectiveness of tailored flower strips in reducing pests and crop plant damage," *Proceedings of the Royal Society B: Biological Sciences*, vol. 282, no. 1814, p. 20 151 369, 2015.

[268] R. F. Pywell et al., "Wildlife-friendly farming increases crop yield: Evidence for ecological intensification," *Proceedings of the Royal Society B: Biological Sciences*, vol. 282, no. 1816, p. 20 151 740, 2015.

[269] L. A. Garibaldi, B. Gemmill-Herren, R. D'Annolfo, B. E. Graeub, S. A. Cunningham, and T. D. Breeze, "Farming approaches for greater biodiversity, livelihoods, and food security," *Trends in ecology & evolution*, vol. 32, no. 1, pp. 68–80, 2017.

[270] D. Serebrennikov, F. Thorne, Z. Kallas, and S. N. McCarthy, "Factors influencing adoption of sustainable farming practices in europe: A systemic review of empirical literature," *Sustainability*, vol. 12, no. 22, p. 9719, 2020.

[271] J. M. Rodriguez, J. J. Molnar, R. A. Fazio, E. Sydnor, and M. J. Lowe, "Barriers to adoption of sustainable agriculture practices: Change agent perspectives," *Renewable agriculture and food systems*, vol. 24, no. 1, pp. 60–71, 2009.

[272] L. Arnalte-Mur et al., "The drivers of change for the contribution of small farms to regional food security in europe," *Global Food Security*, vol. 26, p. 100 395, 2020.

[273] H. Wu, H. Hao, H. Lei, Y. Ge, H. Shi, and Y. Song, "Farm size, risk aversion and overuse of fertilizer: The heterogeneity of large-scale and small-scale wheat farmers in northern china," *Land*, vol. 10, no. 2, p. 111, 2021.

[274] T. Marsden, P. Lowe, and S. Whatmore, *Labour and locality: uneven development and the rural labour process*. Taylor & Francis, 2023.

[275] J. Bremmer, A. G. Martinez, R. Jongeneel, H. Huiting, and R. Stokkers, "Impact assessment study on ec 2030 green deal targets for sustainable food production: Effects of farm to fork and biodiversity strategy 2030 at farm, national and eu level," Wageningen Economic Research, Tech. Rep., 2021.

[276] J. Barreiro Hurle et al., "Modelling environmental and climate ambition in the agricultural sector with the capri model," Joint Research Centre, Tech. Rep., 2021.

[277] J. Cimon-Morin, M. Darveau, and M. Poulin, "Fostering synergies between ecosystem services and biodiversity in conservation planning: A review," *Biological conservation*, vol. 166, pp. 144–154, 2013.

[278] I. Herzon et al., "Time to look for evidence: Results-based approach to biodiversity conservation on farmland in europe," *Land use policy*, vol. 71, pp. 347–354, 2018.

[279] D. Mazzi and S. Dorn, "Movement of insect pests in agricultural landscapes," *Annals of Applied Biology*, vol. 160, no. 2, pp. 97–113, 2012.

[280] A. Bras, A. Roy, D. G. Heckel, P. Anderson, and K. Karlsson Green, "Pesticide resistance in arthropods: Ecology matters too," *Ecology letters*, vol. 25, no. 8, pp. 1746–1759, 2022.

[281] J. R. Prasifka, R. L. Hellmich, G. Dively, and L. C. Lewis, "Assessing the effects of pest management on nontarget arthropods: The influence of plot size and isolation," *Environmental Entomology*, vol. 34, no. 5, pp. 1181–1192, 2005.

[282] M. Nthambi et al., "Economic incentives for woodland creation on farmland: Modelling the impacts on biodiversity," *Ecological Economics*, vol. 224, p. 108 265, 2024.

[283] T. Václavík et al., "Farming system archetypes help explain the uptake of agri-environment practices in europe," *Environmental Research Letters*, vol. 19, no. 7, p. 074 004, 2024.

[284] R. Finger, N. Möhring, and P. Kudsk, "Glyphosate ban will have economic impacts on european agriculture but effects are heterogenous and uncertain," *Communications Earth & Environment*, vol. 4, no. 1, p. 286, 2023.

[285] D. R. Paini, A. W. Sheppard, D. C. Cook, P. J. De Barro, S. P. Worner, and M. B. Thomas, "Global threat to agriculture from invasive species," *Proceedings of the National Academy of Sciences*, vol. 113, no. 27, pp. 7575–7579, 2016.

[286] C. de MENTHIÈRE, P. Falcone, V. Piveteau, and X. Ory, "La haie, levier de la planification écologique," *CGAAER Rapport*, no. 22114, 2023.

[287] European Environment Agency, "Forest dynamics in europe and their ecological consequences," European Environment Agency, Copenhagen, Denmark, Tech. Rep., 2018. [Online]. Available: https://www.eea.europa.eu/publications/forest-dynamics-in-europe-and.

[288] Eurostat. "Extra-EU trade in agricultural goods." Statistics Explained, European Commission, Accessed: Jun. 1, 2026. [Online]. Available: https://ec.europa.eu/eurostat/statistics-explained/index.php?title=Extra-EU_trade_in_agricultural_goods.

[289] P. Meyfroidt, T. K. Rudel, and E. F. Lambin, "Forest transitions, trade, and the global displacement of land use," *Proceedings of the National Academy of Sciences*, vol. 107, no. 49, pp. 20 917–20 922, 2010.

[290] C. Singh and U. M. Persson, "Global patterns of commodity-driven deforestation and associated carbon emissions," *Nature Food*, vol. 7, no. 2, pp. 138–151, 2026.

[291] V. Guye, "Indirect land use change mechanisms: Tests from biofuel mandates and pantropical agriculture," *Environmental and Resource Economics*, pp. 1–37, 2025.

[292] D. M. Lapola et al., "Indirect land-use changes can overcome carbon savings from biofuels in brazil," *Proceedings of the national Academy of Sciences*, vol. 107, no. 8, pp. 3388–3393, 2010.

[293] D. Ramírez-Mejía, Y. Zinngrebe, E. C. Ellis, and P. H. Verburg, "Land-use spillovers from environmental policy interventions," *Global Environmental Change*, vol. 92, p. 103 013, 2025.

[294] S. A. de Sá, C. Palmer, and S. Di Falco, "Dynamics of indirect land-use change: Empirical evidence from brazil," *Journal of Environmental Economics and Management*, vol. 65, no. 3, pp. 377–393, 2013.

[295] E. Barona, N. Ramankutty, G. Hyman, and O. T. Coomes, "The role of pasture and soybean in deforestation of the brazilian amazon," *Environmental Research Letters*, vol. 5, no. 2, p. 024 002, 2010.

[296] N. Myers, R. A. Mittermeier, C. G. Mittermeier, G. A. Da Fonseca, and J. Kent, "Biodiversity hotspots for conservation priorities," *Nature*, vol. 403, no. 6772, pp. 853–858, 2000.

[297] D. M. Lapola et al., "The drivers and impacts of amazon forest degradation," *Science*, vol. 379, no. 6630, eabp8622, 2023.

[298] F. Chaddad, *The economics and organization of Brazilian agriculture: Recent evolution and productivity gains*. Academic Press, 2015.

[299] M. F. Basso, M. F. Neves, and M. F. Grossi-de-Sa, "Agriculture evolution, sustainability and trends, focusing on brazilian agribusiness: A review," *Frontiers in Sustainable Food Systems*, vol. 7, p. 1 296 337, 2024.

[300] A. Recalde Miranda, *Green is the new red*, Documentary film; France, Italy, Paraguay, Sweden, 2024.

[301] F. Schierhorn, P. Meyfroidt, T. Kastner, T. Kuemmerle, A. V. Prishchepov, and D. Müller, "The dynamics of beef trade between brazil and russia and their environmental implications," *Global Food Security*, vol. 11, pp. 84–92, 2016.

[302] H. Ritchie, P. Rosado, and M. Roser, "Soybean production," *Our World in Data*, 2024, https://ourworldindata.org/grapher/soybean-production.

[303] OECD/FAO, "Oecd-fao agricultural outlook 2025-2034," OECD Publishing, Paris, Tech. Rep., 2025.

[304] N. Søndergaard, "Food regime transformations and structural rebounding: Brazilian state–agribusiness relations," *Territory, Politics, Governance*, vol. 11, no. 1, pp. 60–79, 2023.

[305] K. de Jesus Boaventura, C. M. Da Silva, and S. D. Silva, "Building soil fertility: Embrapa and the agronomic development for the "conquest" of the brazilian cerrado (1975-95)," *História Agrária: revista de agricultura e história rural*, no. 89, pp. 247–278, 2023.

[306] N. Rada, "Assessing brazil's cerrado agricultural miracle," *Food Policy*, vol. 38, pp. 146–155, 2013.

[307] L. Gomes, S. J. Simões, E. L. Dalla Nora, E. R. de Sousa-Neto, M. C. Forti, and J. P. H. Ometto, "Agricultural expansion in the brazilian cerrado: Increased soil and nutrient losses and decreased agricultural productivity," *Land*, vol. 8, no. 1, p. 12, 2019.

[308] A. L. P. Nunes, O. J. G. Abi-Saab, and R. Ralisch, "Customer relationship management in the agricultural machinery market," *Ciência Rural*, vol. 47, no. 7, e20160974, 2017.

[309] F. Moffette and H. K. Gibbs, "Agricultural displacement and deforestation leakage in the brazilian legal amazon," *Land Economics*, vol. 97, no. 1, pp. 155–179, 2021.

[310] H. K. Gibbs et al., "Brazil's soy moratorium," *Science*, vol. 347, no. 6220, pp. 377–378, 2015.

[311] A. C. Soterroni et al., "Expanding the soy moratorium to brazil's cerrado," *Science advances*, vol. 5, no. 7, eaav7336, 2019.

[312] C. A. Klink and R. B. Machado, "Conservation of the brazilian cerrado," *Conservation biology*, vol. 19, no. 3, pp. 707–713, 2005.

[313] G. R. Colli, C. R. Vieira, and J. C. Dianese, "Biodiversity and conservation of the cerrado: Recent advances and old challenges," *Biodiversity and Conservation*, vol. 29, no. 5, pp. 1465–1475, 2020.

[314] L. Ferraz, L. de Sousa, L. da Silva, R. de Jesus, C. Santos, and F. Rocha, "Land use changes and hydrological trend analysis in a brazilian cerrado basin," *International Journal of Environmental Science and Technology*, vol. 19, no. 8, pp. 7469–7482, 2022.

[315] M. C. Terra et al., "The inverted forest: Aboveground and notably large belowground carbon stocks and their drivers in brazilian savannas," *Science of The Total Environment*, vol. 867, p. 161 320, 2023.

[316] A. A. Rodrigues et al., "Cerrado deforestation threatens regional climate and water availability for agriculture and ecosystems," *Global Change Biology*, vol. 28, no. 22, pp. 6807–6822, 2022.

[317] E. E. Sano, I. A. L. Magalhães, L. N. Rodrigues, and É. L. Bolfe, "Spatio-temporal dynamics of center pivot irrigation systems in the brazilian tropical savanna (1985–2020)," *Water*, vol. 16, no. 13, p. 1897, 2024.

[318] A. O. Santos Filho, J. M. Ramos, K. Oliveira, T. N. Nascimento, et al., "A evolução do código florestal brasileiro," *Caderno de Graduação-Ciências Humanas e Sociais-UNIT-SERGIPE*, vol. 2, no. 3, pp. 271–290, 2015.

[319] B. Soares-Filho et al., "Cracking brazil's forest code," *Science*, vol. 344, no. 6182, pp. 363–364, 2014.

[320] P. H. Verburg et al., "Beyond land cover change: Towards a new generation of land use models," *Current Opinion in Environmental Sustainability*, vol. 38, pp. 77–85, 2019.

[321] G. Câmara et al., "Modelling land use change in brazil: 2000–2050," INPE, IPEA, IIASA, UNEP-WCMC, São José dos Campos, Brasília, Laxenburg, Cambridge, Tech. Rep., 2015. DOI: 10.22022/REDD/08-2016.12115.

[322] B. Cultice, E. Irwin, and M. Jones, "Accounting for spatial economic interactions at local and meso scales in integrated assessment model (iam) frameworks: Challenges and recent progress," *Environmental Research Letters*, vol. 18, no. 3, p. 035 009, 2023.

[323] H. Van Delden et al., "Integrated assessment of agricultural policies with dynamic land use change modelling," *Ecological Modelling*, vol. 221, no. 18, pp. 2153–2166, 2010.

[324] A. Popp et al., "Land-use futures in the shared socio-economic pathways," *Global Environmental Change*, vol. 42, pp. 331–345, 2017.

[325] M. D. Rounsevell et al., "Identifying uncertainties in scenarios and models of socio-ecological systems in support of decision-making," *One Earth*, vol. 4, no. 7, pp. 967–985, 2021.

[326] C. B. Colman et al., "Modeling the brazilian cerrado land use change highlights the need to account for private property sizes for biodiversity conservation," *Scientific Reports*, vol. 14, no. 1, p. 4559, 2024.

[327] R. H. Day and I. Singh, "A dynamic model of regional agricultural development," *International Regional Science Review*, vol. 1, no. 1, pp. 27–48, 1975.

[328] S. Elsawah et al., "Eight grand challenges in socio-environmental systems modeling," *Socio-Environmental Systems Modelling*, vol. 2, p. 16 226, 2020.

[329] Z. Sun et al., "Multi-level agent-based modelling of social-ecological systems: Bridging the gap between the micro and macro levels," *Socio-Environmental Systems Modelling*, vol. 8, pp. 1–20, 2026.

[330] A. Schmidt et al., "Reflections on linking economic equilibrium models with agent-based models in the context of agricultural land use," *Socio-Environmental Systems Modelling*, vol. 8, pp. 1–18, 2026.

[331] G. Ravaioli, T. Domingos, and R. F. Teixeira, "A framework for data-driven agent-based modelling of agricultural land use," *Land*, vol. 12, no. 4, p. 756, 2023.

[332] D. S. Utomo, B. S. Onggo, and S. Eldridge, "Applications of agent-based modelling and simulation in the agri-food supply chains," *European Journal of Operational Research*, vol. 269, no. 3, pp. 794–805, 2018.

[333] J. Wang, M. Bretz, M. A. A. Dewan, and M. A. Delavar, "Machine learning in modelling land-use and land cover-change (lulcc): Current status, challenges and prospects," *Science of The Total Environment*, vol. 822, p. 153 559, 2022.

[334] J. M. Epstein and R. Axtell, *Growing artificial societies: social science from the bottom up*. Brookings Institution Press, 1996.

[335] M. Carauta, A. A. Dalla Libera, A. Hampf, R. F. Fan Chen, J. M. da Silveira, and T. Berger, "On-farm trade-offs for optimal agricultural practices in mato grosso, brazil.," *Brazilian Review of Economics & Agribusiness/Revista de Economia e Agronegócio*, vol. 15, no. 3, 2017.

[336] F. Dias, N. Suhadolnik, H. Camargo, and S. Da Silva, "Predicting the pulse of the amazon: Machine learning insights into deforestation dynamics," *Journal of Environmental Management*, vol. 362, p. 121 359, 2024.

[337] G. Larrea-Gallegos and I. Vazquez-Rowe, "Exploring machine learning techniques to predict deforestation to enhance the decision-making of road construction projects," *Journal of Industrial Ecology*, vol. 26, no. 1, pp. 225–239, 2022.

[338] National Research Council, *Advancing Land Change Modeling: Opportunities and Research Requirements*. Washington, DC: The National Academies Press, 2014, ISBN: 978-0-309-29177-4. DOI: 10.17226/18385.

[339] J.-F. Mas, M. Kolb, M. Paegelow, M. T. C. Olmedo, and T. Houet, "Inductive pattern-based land use/cover change models: A comparison of four software packages," *Environmental Modelling & Software*, vol. 51, pp. 94–111, 2014.

[340] W. R. Tobler, "Cellular geography," in *Philosophy in geography*, Springer, 1979, pp. 379–386.

[341] R. White and G. Engelen, "Cellular automata as the basis of integrated dynamic regional modelling," *Environment and Planning B: Planning and design*, vol. 24, no. 2, pp. 235–246, 1997.

[342] B. S. Soares-Filho, G. C. Cerqueira, and C. L. Pennachin, "Dinamica—a stochastic cellular automata model designed to simulate the landscape dynamics in an amazonian colonization frontier," *Ecological modelling*, vol. 154, no. 3, pp. 217–235, 2002.

[343] I. Santé, A. M. García, D. Miranda, and R. Crecente, "Cellular automata models for the simulation of real-world urban processes: A review and analysis," *Landscape and urban planning*, vol. 96, no. 2, pp. 108–122, 2010.

[344] I. Marcovici, "Cellular automata and percolation: An overview of selected connections," in *International Workshop on Cellular Automata and Discrete Complex Systems*, Springer, 2025, pp. 27–42.

[345] A. T. Leite-Filho, B. S. Soares-Filho, J. L. Davis, G. M. Abrahão, and J. Börner, "Deforestation reduces rainfall and agricultural revenues in the brazilian amazon," *Nature Communications*, vol. 12, no. 1, p. 2591, 2021.

[346] A. T. Leite-Filho, B. S. Soares-Filho, U. Oliveira, and M. Coe, "Intensification of climate change impacts on agriculture in the cerrado due to deforestation," *Nature Sustainability*, vol. 8, no. 1, pp. 34–43, 2025.

[347] W. Oliveira et al., "Yield vulnerability of low-income smallholders to pollinator declines in brazil is biome-dependent," *PLoS One*, vol. 20, no. 11, e0337328, 2025.

[348] J. C. Cardoso et al., "Pollination and plant reproduction in the cerrado, the world's most biodiverse savanna," *Biological Reviews*, vol. 101, no. 1, pp. 74–105, 2026.

[349] P. Hunke, E. N. Mueller, B. Schröder, and P. Zeilhofer, "The brazilian cerrado: Assessment of water and soil degradation in catchments under intensive agricultural use," *Ecohydrology*, vol. 8, no. 6, pp. 1154–1180, 2015.

[350] E. R. d. Oliveira, J. R. Silva, L. R. F. Baumann, F. Miziara, L. G. Ferreira, and L. R. d. O. Merelles, "Technology and degradation of pastures in livestock in the brazilian cerrado," *Sociedade & natureza*, vol. 32, pp. 585–596, 2022.

[351] L. Rattis et al., "Climatic limit for agriculture in brazil," *Nature Climate Change*, vol. 11, no. 12, pp. 1098–1104, 2021.

[352] J. Pompeu, T. O. Assis, and J. P. Ometto, "Landscape changes in the cerrado: Challenges of land clearing, fragmentation and land tenure for biological conservation," *Science of The Total Environment*, vol. 906, p. 167 581, 2024.

[353] L. F. S. Commar, G. M. Abrahão, and M. H. Costa, "A possible deforestation-induced synoptic-scale circulation that delays the rainy season onset in amazonia," *Environmental Research Letters*, vol. 18, no. 4, p. 044 041, 2023.

[354] G. C. Carrero, R. T. Walker, C. S. Simmons, and P. M. Fearnside, "Land grabbing in the brazilian amazon: Stealing public land with government approval," *Land Use Policy*, vol. 120, p. 106 133, 2022.

[355] G. Sparovek et al., "Who owns brazilian lands?" *Land use policy*, vol. 87, p. 104 062, 2019.

[356] A. Pacheco and C. Meyer, "Land tenure drives brazil's deforestation rates across socio-environmental contexts," *Nature communications*, vol. 13, no. 1, p. 5759, 2022.

[357] IBGE, "Censo agropecuário 1995-1996," Instituto Brasileiro de Geografia e Estatística (IBGE), Rio de Janeiro, Tech. Rep., 1996.

[358] J. G. Gasques, E. T. Bastos, C. Valdes, and M. R. P. Bacchi, "Total factor productivity in brazilian agriculture.," in *Productivity growth in agriculture: an international perspective*, CABI Wallingford UK, 2012, pp. 145–161.

[359] L. C. Dias, F. M. Pimenta, A. B. Santos, M. H. Costa, and R. J. Ladle, "Patterns of land use, extensification, and intensification of brazilian agriculture," *Global change biology*, vol. 22, no. 8, pp. 2887–2903, 2016.

[360] D. d. L. Ramos et al., "Ecosystem services provided by insects in brazil: What do we really know? ramos et al," *Neotropical entomology*, vol. 49, no. 6, pp. 783–794, 2020.

[361] E. Uuemaa, M. Antrop, J. Roosaare, R. Marja, and Ü. Mander, "Landscape metrics and indices: An overview of their use in landscape research," *Living reviews in landscape research*, vol. 3, no. 1, pp. 1–28, 2009.

[362] A. E. Frazier and P. Kedron, "Landscape metrics: Past progress and future directions," *Current Landscape Ecology Reports*, vol. 2, no. 3, pp. 63–72, 2017.

[363] X. Fu, Z. Li, J. Ma, M. Zhou, L. Chen, and J. Peng, "Ecosystem resilience response to forest fragmentation in china: Thresholds identification," *Journal of Environmental Management*, vol. 380, p. 125 180, 2025.

[364] H. Geist, W. McConnell, E. F. Lambin, E. Moran, D. Alves, and T. Rudel, "Causes and trajectories of land-use/cover change," in *Land-use and land-cover change: Local processes and global impacts*, Springer, 2006, pp. 41–70.

[365] M. Coronese, M. Occelli, F. Lamperti, and A. Roventini, "Agrilove: Agriculture, land-use and technical change in an evolutionary, agent-based model," *Ecological Economics*, vol. 208, p. 107 756, 2023.

[366] K. Happe, K. Kellermann, and A. Balmann, "Agent-based analysis of agricultural policies: An illustration of the agricultural policy simulator agripolis, its adaptation and behavior," *Ecology and Society*, vol. 11, Jan. 2006. DOI: 10.5751/ES-01741-110149.

[367] S. M. Helfand and E. S. Levine, "Farm size and the determinants of productive efficiency in the brazilian center-west," *Agricultural economics*, vol. 31, no. 2-3, pp. 241–249, 2004.

[368] S. M. Helfand and M. P. Taylor, "The inverse relationship between farm size and productivity: Refocusing the debate," *Food Policy*, vol. 99, p. 101 977, 2021.

[369] A. S. Cohn, J. Gil, T. Berger, H. Pellegrina, and C. Toledo, "Patterns and processes of pasture to crop conversion in brazil: Evidence from mato grosso state," *Land use policy*, vol. 55, pp. 108–120, 2016.

[370] V. Zalles et al., "Near doubling of brazil's intensive row crop area since 2000," *Proceedings of the National Academy of Sciences*, vol. 116, no. 2, pp. 428–435, 2019.

[371] I. M. Rosa, D. Purves, C. Souza Jr, and R. M. Ewers, "Predictive modelling of contagious deforestation in the brazilian amazon," *PloS one*, vol. 8, no. 10, e77231, 2013.

[372] J. Miranda, J. Börner, M. Kalkuhl, and B. Soares-Filho, "Land speculation and conservation policy leakage in brazil," *Environmental Research Letters*, vol. 14, no. 4, p. 045 006, 2019.

[373] L. L. Rausch et al., "Soy expansion in brazil's cerrado," *Conservation letters*, vol. 12, no. 6, e12671, 2019.

[374] F. F. Goulart, M. J. Chappell, F. Mertens, and B. Soares-Filho, "Sparing or expanding? the effects of agricultural yields on farm expansion and deforestation in the tropics," *Biodiversity and Conservation*, vol. 32, no. 3, pp. 1089–1104, 2023.

[375] M. G. Ceddia, S. Sedlacek, N. Bardsley, and S. Gomez-y-Paloma, "Sustainable agricultural intensification or jevons paradox? the role of public governance in tropical south america," *Global Environmental Change*, vol. 23, no. 5, pp. 1052–1063, 2013.

[376] M. G. Ceddia, "The impact of income, land, and wealth inequality on agricultural expansion in latin america," *Proceedings of the National Academy of Sciences*, vol. 116, no. 7, pp. 2527–2532, 2019.

[377] T. R. Silva, S. B. Rodrigues, J. B. de Azevedo Bringel, A. B. Sampaio, E. E. Sano, and D. L. M. Vieira, "Factors affecting savanna and forest regeneration in pastures across the cerrado," *Journal of Environmental Management*, vol. 330, p. 117 185, 2023.

[378] Secretaria de Estado de Meio Ambiente e Desenvolvimento Sustentável (Semad), *Psa cerrado em pé*, https://goias.gov.br/meioambiente/psa-cerrado-em-pe/, Accessed: 2026-06-02, 2026.

[379] Sistema FAEG/SENAR, *Expedição safra goiás aponta queda na produtividade da soja, custos altos de produção e redução de lucro*, https://sistemafaeg.com.br/noticias/expedicao-safra-goias-aponta-queda-na-produtividade-da-soja-custos-altos-de-producao-e-reducao-de-lucro, Acessado em: 10 de junho de 2026, Federação da Agricultura e Pecuária de Goiás (FAEG), Jan. 2026.

[380] Confederação da Agricultura e Pecuária do Brasil (CNA), "Ativos da pecuária de corte: Projeto campo futuro," CNA, Relatório Técnico, Jan. 2026, Acessado em: 10 de junho de 2026. [Online]. Available: https://www.cnabrasil.org.br/storage/arquivos/ativos_Pecuaria_corte_campo_futuro_janeiro.pdf.

[381] L. Eloy, K. Y. Kato, V. J. W. Junior, and S. Hecht, "Behind the myth: Land sparing and deforestation in brazil," *Journal of Agrarian Change*, vol. 26, no. 1, e70045, 2026.

[382] I. Carreira, F. Costa, and J. P. Pessoa, "The deforestation effects of trade and agricultural productivity in brazil," *Journal of development economics*, vol. 167, p. 103 217, 2024.

[383] J. Brandão, F. C. Cardoso, and R. Garrett, "Why has the brazilian cerrado been left behind by voluntary environmental policies?" *Global Environmental Change*, vol. 92, p. 103 005, 2025.

[384] G. Bennett and K. J. Mulongoy, "Review of experience with ecological networks, corridors and buffer zones," in *Secretariat of the convention on biological diversity, Montreal, Technical Series*, Secretariat of the Convention on Biological Diversity Montreal, QC, Canada, vol. 23, 2006, p. 100.

[385] I. R. Salviano, F. R. Gardon, and R. F. dos Santos, "Ecological corridors and landscape planning: A model to select priority areas for connectivity maintenance," *Landscape Ecology*, vol. 36, no. 11, pp. 3311–3328, 2021.

[386] P. Delacote, E. J. Robinson, and S. Roussel, "Deforestation, leakage and avoided deforestation policies: A spatial analysis," *Resource and Energy Economics*, vol. 45, pp. 192–210, 2016.

[387] M. M. Bustamante et al., "Ecological restoration as a strategy for mitigating and adapting to climate change: Lessons and challenges from brazil," *Mitigation and Adaptation Strategies for Global Change*, vol. 24, no. 7, pp. 1249–1270, 2019.

[388] F. M. Resende, J. Cimon-Morin, M. Poulin, L. Meyer, and R. Loyola, "Consequences of delaying actions for safeguarding ecosystem services in the brazilian cerrado," *Biological Conservation*, vol. 234, pp. 90–99, 2019.

[389] C. M. Kennedy et al., "Optimizing land use decision-making to sustain brazilian agricultural profits, biodiversity and ecosystem services," *Biological Conservation*, vol. 204, pp. 221–230, 2016.

[390] Instituto Chico Mendes de Conservação da Biodiversidade (ICMBio), *Dados geoespaciais*, https://www.gov.br/icmbio/pt-br/dados-icmbio/dados_geoespaciais, Acessado em: 9 de junho de 2026, Ministério do Meio Ambiente e Mudança do Clima, Governo do Brasil, 2026.

[391] F. S. Nunes et al., "Lessons from the historical dynamics of environmental law enforcement in the brazilian amazon," *Scientific Reports*, vol. 14, no. 1, p. 1828, 2024.

[392] C. C. Pereira et al., "The cerrado crisis review: Highlighting threats and providing future pathways to save brazil's biodiversity hotspot," *Nature Conservation*, vol. 61, pp. 29–70, 2026.

[393] Y. E. Shimabukuro, J. R. dos Santos, A. R. Formaggio, V. Duarte, and B. F. T. Rudorff, "The brazilian amazon monitoring program: Prodes and deter projects," in *Global forest monitoring from earth observation*, vol. 2012, CRC Press Boca Raton, FL, 2012, pp. 153–169.

[394] M. de O. Milfont, E. E. M. Rocha, A. O. N. Lima, and B. M. Freitas, "Higher soybean production using honeybee and wild pollinators, a sustainable alternative to pesticides and autopollination," *Environmental chemistry letters*, vol. 11, no. 4, pp. 335–341, 2013.

[395] M. Monasterolo, M. L. Musicante, G. R. Valladares, and A. Salvo, "Soybean crops may benefit from forest pollinators," *Agriculture, Ecosystems & Environment*, vol. 202, pp. 217–222, 2015.

[396] A. Santone, M. P. Mazzei, J. Vesprini, C. Torres, L. D. Amarilla, and L. Galetto, "Pollination service and soybean yields," *Acta Oecologica*, vol. 116, p. 103 846, 2022.

[397] F. de Souza Batista, C. Duku, and L. Hein, "Deforestation-induced changes in rainfall decrease soybean-maize yields in brazil," *Ecological Modelling*, vol. 486, p. 110 533, 2023.

[398] R. Flach et al., "Conserving the cerrado and amazon biomes of brazil protects the soy economy from damaging warming," *World Development*, vol. 146, p. 105 582, 2021.

[399] I. Dreoni, Z. Matthews, and M. Schaafsma, "The impacts of soy production on multi-dimensional well-being and ecosystem services: A systematic review," *Journal of Cleaner Production*, vol. 335, p. 130 182, 2022.

[400] L. Hunt et al., "Insecticide concentrations in stream sediments of soy production regions of south america," *Science of the Total Environment*, vol. 547, pp. 114–124, 2016.

[401] S. K. Ahmad et al., "Evapotranspiration declines prolonged by deforestation and fire in south american biomes," *Nature Geoscience*, pp. 1–7, 2026.

[402] J. A. Marengo, J. C. Jimenez, J.-C. Espinoza, A. P. Cunha, and L. E. Aragão, "Increased climate pressure on the agricultural frontier in the eastern amazonia–cerrado transition zone," *Scientific reports*, vol. 12, no. 1, p. 457, 2022.

[403] C. Li, A. Harris, B. S. Marimon, B. H. Marimon Junior, M. Dennis, and P. da Conceição Bispo, "Three decades of habitat fragmentation dynamics and landscape transformation in the cerrado–amazon transition," *Landscape Ecology*, 2026.

[404] F. M. Carvalho, P. D. M. Júnior, and L. G. Ferreira, "The cerrado into-pieces: Habitat fragmentation as a function of landscape use in the savannas of central brazil," *Biological conservation*, vol. 142, no. 7, pp. 1392–1403, 2009.

[405] T. G. Santos, R. Battisti, D. Casaroli, J. Alves Jr, and A. W. P. Evangelista, "Assessment of agricultural efficiency and yield gap for soybean in the brazilian central cerrado biome," *Bragantia*, vol. 80, e1821, 2021.

[406] Companhia Nacional de Abastecimento (CONAB), *Informações agropecuárias*, https://www.gov.br/conab/pt-br/atuacao/informacoes-agropecuarias, Acessado em: 10 de junho de 2026, Ministério do Desenvolvimento Agrário e Agricultura Familiar, Governo do Brasil, 2026.

[407] Associação Brasileira das Indústrias Exportadoras de Carnes (ABIEC), "Beef report 2024: Brazilian beef profile," ABIEC, Tech. Rep., 2024, Accessed: June 10, 2026. [Online]. Available: https://www.abiec.com.br/wp-content/uploads/beefreport_v2024-ENG.pdf.

[408] AgDev, *The economics of deforestation and the degraded pasture solution*, https://agdevinvest.com/2023/09/20/the-economics-of-deforestation-and-the-degraded-pasture-solution/, Accessed: June 10, 2026, Sep. 2023.

[409] T. S. Telles, A. W. A. Palludeto, and B. P. Reydon, "Price movement in the brazilian land market (1994-2010): An analysis in the light of post-keynesian theory," *Revista de Economia Política*, vol. 36, no. 1, pp. 109–129, 2016.

[410] Instituto Brasileiro de Geografia e Estatística (IBGE), *Censo agropecuário 2017: Resultados definitivos*, https://sidra.ibge.gov.br/pesquisa/censo-agropecuario/censo-agropecuario-2017/resultados-definitivos, Acessado em: 10 de junho de 2026, SIDRA - Sistema IBGE de Recuperação Automática, 2019.

[411] W. R. Catton, *Overshoot: The ecological basis of revolutionary change*. University of Illinois Press, 1982.

[412] P. R. Ehrlich and A. H. Ehrlich, "Can a collapse of global civilization be avoided?" *Proceedings of the Royal Society B: Biological Sciences*, vol. 280, no. 1754, p. 20 122 845, 2013. DOI: 10.1098/rspb.2012.2845. eprint: https://royalsocietypublishing.org/doi/pdf/10.1098/rspb.2012.2845. [Online]. Available: https://royalsocietypublishing.org/doi/abs/10.1098/rspb.2012.2845.

[413] P. Turchin and S. A. Nefedov, *Secular Cycles*. Princeton: Princeton University Press, 2009, ISBN: 9781400830688. DOI: doi:10.1515/9781400830688. [Online]. Available: https://doi.org/10.1515/9781400830688.

[414] S. Shennan et al., "Regional population collapse followed initial agriculture booms in mid-holocene europe," *Nature communications*, vol. 4, no. 1, p. 2486, 2013.

[415] L. J. Lucero, "The collapse of the classic maya: A case for the role of water control," *American Anthropologist*, vol. 104, no. 3, pp. 814–826, 2002. DOI: https://doi.org/10.1525/aa.2002.104.3.814. eprint: https://anthrosource.onlinelibrary.wiley.com/doi/pdf/10.1525/aa.2002.104.3.814. [Online]. Available: https://anthrosource.onlinelibrary.wiley.com/doi/abs/10.1525/aa.2002.104.3.814.

[416] Z. Li, C. Yaning, Y. Wang, and W. Li, "Drought promoted the disappearance of civilizations along the ancient silk road," *Environmental Earth Sciences*, vol. 75, Jul. 2016. DOI: 10.1007/s12665-016-5925-6.

[417] Z. Jingyun, L. Xiao, X. Fang, Z. Hao, Q. Ge, and B. Li, "How climate change impacted the collapse of the ming dynasty," *Climatic Change*, vol. 127, pp. 169–182, Nov. 2014. DOI: 10.1007/s10584-014-1244-7.

[418] L. Kehoe, A. Romero-Muñoz, E. Polaina, L. Estes, H. Kreft, and T. Kuemmerle, "Biodiversity at risk under future cropland expansion and intensification," *Nature Ecology and Evolution*, vol. 1, Jul. 2017. DOI: 10.1038/s41559-017-0234-3.

[419] P. M. Kopittke, R. C. Dalal, D. Finn, and N. W. Menzies, "Global changes in soil stocks of carbon, nitrogen, phosphorus, and sulphur as influenced by long-term agricultural production," *Global change biology*, vol. 23, no. 6, pp. 2509–2519, 2017.

[420] P. Borrelli et al., "An assessment of the global impact of 21st century land use change on soil erosion," *Nature Communications*, vol. 8, no. 1, p. 2013, Dec. 8, 2017, ISSN: 2041-1723. DOI: 10.1038/s41467-017-02142-7. Accessed: Jul. 7, 2023. [Online]. Available: https://www.nature.com/articles/s41467-017-02142-7.

[421] J. Bruinsma, *World agriculture: towards 2015/2030: an FAO study*. Routledge, 2017.

[422] D. R. Montgomery, "Soil erosion and agricultural sustainability," *Proceedings of the National Academy of Sciences*, vol. 104, no. 33, pp. 13 268–13 272, 2007. DOI: 10.1073/pnas.0611508104. eprint: https://www.pnas.org/doi/pdf/10.1073/pnas.0611508104. [Online]. Available: https://www.pnas.org/doi/abs/10.1073/pnas.0611508104.

[423] D. H. Meadows, D. L. Meadows, J. Randers, and W. W. Behrens, "The limits to growth," in *Green planet blues*, Routledge, 2018, pp. 25–29.

[424] D. Brozović, "Societal collapse: A literature review," *Futures*, vol. 145, p. 103 075, 2023, ISSN: 0016-3287. DOI: https://doi.org/10.1016/j.futures.2022.103075. [Online]. Available: https://www.sciencedirect.com/science/article/pii/S0016328722001768.

[425] D. Steel, C. T. DesRoches, and K. Mintz-Woo, "Climate change and the threat to civilization," *Proceedings of the National Academy of Sciences*, vol. 119, no. 42, e2210525119, 2022. DOI: 10.1073/pnas.2210525119. eprint: https://www.pnas.org/doi/pdf/10.1073/pnas.2210525119. [Online]. Available: https://www.pnas.org/doi/abs/10.1073/pnas.2210525119.

[426] S. Motesharrei, J. Rivas, and E. Kalnay, "Human and nature dynamics (HANDY): Modeling inequality and use of resources in the collapse or sustainability of societies," *Ecological Economics*, vol. 101, pp. 90–102, May 2014, ISSN: 09218009. DOI: 10.1016/j.ecolecon.2014.02.014. Accessed: Aug. 28, 2023. [Online]. Available: https://linkinghub.elsevier.com/retrieve/pii/S0921800914000615.

[427] G. M. Turner, "A comparison of the limits to growth with 30 years of reality," *Global Environmental Change*, vol. 18, no. 3, pp. 397–411, 2008, ISSN: 0959-3780. DOI: https://doi.org/10.1016/j.gloenvcha.2008.05.001. [Online]. Available: https://www.sciencedirect.com/science/article/pii/S0959378008000435.

[428] G. M. Turner, "On the cusp of global collapse? updated comparison of the limits to growth with historical data," *GAIA - Ecological Perspectives for Science and Society*, vol. 21, no. 2, pp. 116–124, 2012, ISSN: 0940-5550. DOI: 10.14512/gaia.21.2.10. [Online]. Available: https://www.ingentaconnect.com/content/oekom/gaia/2012/00000021/00000002/art00010.

[429] D. Meadows and J. Randers, *The limits to growth: the 30-year update*. Routledge, 2012.

[430] E. Gómez-Baggethun, "More is more: Scaling political ecology within limits to growth," *Political Geography*, vol. 76, p. 102 095, 2020, ISSN: 0962-6298. DOI: https://doi.org/10.1016/j.polgeo.2019.102095. [Online]. Available: https://www.sciencedirect.com/science/article/pii/S0962629819304263.

[431] J. Diamond, *Collapse: how societies choose to fail or succeed: revised edition*. Penguin, 2011.

[432] J. Diamond, "Two views of collapse," *Nature*, vol. 463, pp. 880–1, Feb. 2010. DOI: 10.1038/463880a.

[433] P. Turchin et al., "Disentangling the evolutionary drivers of social complexity: A comprehensive test of hypotheses," *Science Advances*, vol. 8, no. 25, eabn3517, 2022. DOI: 10.1126/sciadv.abn3517. eprint: https://www.science.org/doi/pdf/10.1126/sciadv.abn3517. [Online]. Available: https://www.science.org/doi/abs/10.1126/sciadv.abn3517.

[434] I. M. Fanuel, D. Kajunguri, and F. Moyo, "Modelling the impact of human population and its associated pressure on forest biomass and forest-dependent wildlife population," *Journal of Applied Mathematics*, vol. 2023, Q. Song, Ed., pp. 1–9, Jan. 12, 2023, ISSN: 1687-0042, 1110-757X. DOI: 10.1155/2023/4826313. Accessed: Sep. 6, 2023. [Online]. Available: https://www.hindawi.com/journals/jam/2023/4826313/.

[435] J. Peñuelas and S. Nogué, "Catastrophic climate change and the collapse of human societies," *National Science Review*, vol. 10, no. 6, nwad082, Mar. 2023, ISSN: 2095-5138. DOI: 10.1093/nsr/nwad082. eprint: https://academic.oup.com/nsr/article-pdf/10/6/nwad082/50928491/nwad082.pdf. [Online]. Available: https://doi.org/10.1093/nsr/nwad082.

[436] J. Gan and B. A. McCarl, "Measuring transnational leakage of forest conservation," *Ecological Economics*, vol. 64, no. 2, pp. 423–432, 2007.

[437] D. Tilman, C. Balzer, J. Hill, and B. L. Befort, "Global food demand and the sustainable intensification of agriculture," *Proceedings of the national academy of sciences*, vol. 108, no. 50, pp. 20 260–20 264, 2011.

[438] W. Willett et al., "Food in the anthropocene: The eat–lancet commission on healthy diets from sustainable food systems," *The lancet*, vol. 393, no. 10170, pp. 447–492, 2019.

[439] J. P. Reganold and J. M. Wachter, "Organic agriculture in the twenty-first century," *Nature plants*, vol. 2, no. 2, pp. 1–8, 2016.

[440] V. Seufert, N. Ramankutty, and J. A. Foley, "Comparing the yields of organic and conventional agriculture," *Nature*, vol. 485, no. 7397, pp. 229–232, 2012.

[441] P. Havlík et al., "Climate change mitigation through livestock system transitions," *Proceedings of the National Academy of Sciences*, vol. 111, no. 10, pp. 3709–3714, 2014.

[442] E. Stehfest, D. van Vuuren, L. Bouwman, T. Kram, et al., *Integrated assessment of global environmental change with IMAGE 3.0: Model description and policy applications*. Netherlands Environmental Assessment Agency (PBL), 2014.

[443] H. Lotze-Campen, C. Müller, A. Bondeau, S. Rost, A. Popp, and W. Lucht, "Global food demand, productivity growth, and the scarcity of land and water resources: A spatially explicit mathematical programming approach," *Agricultural Economics*, vol. 39, no. 3, pp. 325–338, 2008.

[444] C. Bone, S. Dragicevic, and R. White, "Modeling-in-the-middle: Bridging the gap between agent-based modeling and multi-objective decision-making for land use change," *International Journal of Geographical Information Science*, vol. 25, no. 5, pp. 717–737, 2011.

[445] J. A. Brander and M. S. Taylor, "The simple economics of easter island: A ricardo-malthus model of renewable resource use," *American economic review*, pp. 119–138, 1998.

[446] M. Scheffer, W. Brock, and F. Westley, "Socioeconomic mechanisms preventing optimum use of ecosystem services: An interdisciplinary theoretical analysis," *Ecosystems*, vol. 3, no. 5, pp. 451–471, 2000.

[447] P. Meyfroidt et al., "Ten facts about land systems for sustainability," *Proceedings of the National Academy of Sciences*, vol. 119, no. 7, e2109217118, 2022.

[448] L. Fahrig, "Effects of habitat fragmentation on biodiversity," *Annual review of ecology, evolution, and systematics*, vol. 34, no. 1, pp. 487–515, 2003.

[449] D. Bengochea Paz, K. Henderson, and M. Loreau, "Habitat percolation transition undermines sustainability in social-ecological agricultural systems," *Ecology Letters*, vol. 25, no. 1, pp. 163–176, 2022.

[450] A. Angelsen, "Policies for reduced deforestation and their impact on agricultural production," *Proceedings of the national Academy of Sciences*, vol. 107, no. 46, pp. 19 639–19 644, 2010.

[451] E. F. Lambin and P. Meyfroidt, "Land use transitions: Socio-ecological feedback versus socio-economic change," *Land use policy*, vol. 27, no. 2, pp. 108–118, 2010.

[452] K. Henderson and M. Loreau, "Unequal access to resources undermines global sustainability," *Science of The Total Environment*, vol. 763, p. 142 981, 2021.

[453] B. Phalan, M. Onial, A. Balmford, and R. E. Green, "Reconciling food production and biodiversity conservation: Land sharing and land sparing compared," *science*, vol. 333, no. 6047, pp. 1289–1291, 2011.

[454] J. Fischer et al., "Land sparing versus land sharing: Moving forward," *Conservation Letters*, vol. 7, no. 3, pp. 149–157, 2014.

[455] M. Bologna and G. Aquino, "Deforestation and world population sustainability: A quantitative analysis," *Scientific reports*, vol. 10, no. 1, p. 7631, 2020.

[456] J. Rockström, O. Edenhofer, J. Gaertner, and F. DeClerck, "Planet-proofing the global food system," *Nature food*, vol. 1, no. 1, pp. 3–5, 2020.

[457] M. A. Clark et al., "Global food system emissions could preclude achieving the 1.5 and 2 c climate change targets," *Science*, vol. 370, no. 6517, pp. 705–708, 2020.

[458] D. Rigby and D. Cáceres, "Organic farming and the sustainability of agricultural systems," *Agricultural systems*, vol. 68, no. 1, pp. 21–40, 2001.

[459] J. Michelsen, "Recent development and political acceptance of organic farming in europe," *Sociologia ruralis*, vol. 41, no. 1, pp. 3–20, 2001.

[460] A. Chai and A. Moneta, "Retrospectives: Engel curves," *Journal of Economic Perspectives*, vol. 24, no. 1, pp. 225–240, 2010.

[461] J. Banks, R. Blundell, and A. Lewbel, "Quadratic engel curves and consumer demand," *Review of Economics and statistics*, vol. 79, no. 4, pp. 527–539, 1997.

[462] H.-s. Chang, "Functional forms and the demand for meat in the united states," *The Review of Economics and Statistics*, pp. 355–359, 1977.

[463] C. A. Gallet, "The income elasticity of meat: A meta-analysis," *Australian Journal of Agricultural and Resource Economics*, vol. 54, no. 4, pp. 477–490, 2010.

[464] R. E. Evenson and D. Gollin, "Assessing the impact of the green revolution, 1960 to 2000," *science*, vol. 300, no. 5620, pp. 758–762, 2003.

[465] P. L. Pingali, "Green revolution: Impacts, limits, and the path ahead," *Proceedings of the national academy of sciences*, vol. 109, no. 31, pp. 12 302–12 308, 2012.

[466] F. J. Pierce and P. Nowak, "Aspects of precision agriculture," *Advances in agronomy*, vol. 67, pp. 1–85, 1999.

[467] I. Soto et al., *The contribution of precision agriculture technologies to farm productivity and the mitigation of greenhouse gas emissions in the EU*. Publications Office of the European Union Luxembourg, 2019.

[468] S. Heckbert, T. Baynes, and A. Reeson, "Agent-based modeling in ecological economics," *Annals of the new York Academy of Sciences*, vol. 1185, no. 1, pp. 39–53, 2010.

[469] A. L. Katchova and M. C. Ahearn, "Farm entry and exit from us agriculture," *Agricultural Finance Review*, vol. 77, no. 1, pp. 50–63, 2017.

[470] G. Breustedt and T. Glauben, "Driving forces behind exiting from farming in western europe," *Journal of Agricultural economics*, vol. 58, no. 1, pp. 115–127, 2007.

[471] J. M. Rey Benayas, A. Martins, J. M. Nicolau, and J. J. Schulz, "Abandonment of agricultural land: An overview of drivers and consequences.," *CABI Reviews*, no. 2007, 14–pp, 2007.

[472] G. A. De Leo and S. Levin, "The multifaceted aspects of ecosystem integrity," *Conservation ecology*, vol. 1, no. 1, 1997.

[473] J. E. Watson et al., "The exceptional value of intact forest ecosystems," *Nature ecology & evolution*, vol. 2, no. 4, pp. 599–610, 2018.

[474] O. Blumetto et al., "Ecosystem integrity index, an innovative environmental evaluation tool for agricultural production systems," *Ecological indicators*, vol. 101, pp. 725–733, 2019.

[475] J. E. Clapcott et al., "Quantifying relationships between land-use gradients and structural and functional indicators of stream ecological integrity," *Freshwater Biology*, vol. 57, no. 1, pp. 74–90, 2012.

[476] D. Montoya, B. Haegeman, S. Gaba, C. De Mazancourt, and M. Loreau, "Habitat fragmentation and food security in crop pollination systems," *Journal of Ecology*, vol. 109, no. 8, pp. 2991–3006, 2021.

[477] D. Montoya, B. Haegeman, S. Gaba, C. De Mazancourt, V. Bretagnolle, and M. Loreau, "Trade-offs in the provisioning and stability of ecosystem services in agroecosystems," *Ecological Applications*, vol. 29, no. 2, e01853, 2019.

[478] M. Loreau, "Biodiversity and ecosystem functioning: Recent theoretical advances," *Oikos*, vol. 91, no. 1, pp. 3–17, 2000.

[479] M. G. Mitchell, E. M. Bennett, and A. Gonzalez, "Forest fragments modulate the provision of multiple ecosystem services," *Journal of Applied Ecology*, vol. 51, no. 4, pp. 909–918, 2014.

[480] Food and Agriculture Organization of the United Nations, *Yearly per capita supply of all meat [dataset]*, https://archive.ourworldindata.org/20250925-235133/grapher/meat-supply-per-person.html, Processed by Our World in Data. Original data: "Food Balances: Food Balances (-2013, old methodology and population)" and "Food Balances: Food Balances (2010-)". Retrieved October 1, 2025 (archived on September 25, 2025)., 2024.

[481] J. Han, J. Trienekens, T. Tan, S. Omta, and K. Wang, "Vertical coordination, quality management and firm performance of the pork processing industry in china," in *International agrifood chains and networks*, Wageningen Academic, 2006, pp. 319–332.

[482] G. Wang, J. Wang, S. Chen, and C. e. Zhao, "Vertical integration selection of chinese pig industry chain under african swine fever-from the perspective of stable pig supply," *Plos one*, vol. 18, no. 2, e0280626, 2023.

[483] J. A. Foley et al., "Solutions for a cultivated planet," *Nature*, vol. 478, no. 7369, pp. 337–342, 2011.

[484] T. D. Searchinger et al., "Creating a sustainable food future," *World Resources Report*, 2019, World Resources Institute. [Online]. Available: https://www.wri.org/research/creating-sustainable-food-future.

[485] M. Springmann et al., "Options for keeping the food system within environmental limits," *Nature*, vol. 562, no. 7728, pp. 519–525, 2018.

[486] T. Searchinger et al., "Use of us croplands for biofuels increases greenhouse gases through emissions from land-use change," *Science*, vol. 319, no. 5867, pp. 1238–1240, 2008.

[487] J. Poore and T. Nemecek, "Reducing food's environmental impacts through producers and consumers," *Science*, vol. 360, no. 6392, pp. 987–992, 2018.

[488] M. Springmann, H. C. J. Godfray, M. Rayner, and P. Scarborough, "Analysis and valuation of the health and climate change cobenefits of dietary change," *Proceedings of the National Academy of Sciences*, vol. 113, no. 15, pp. 4146–4151, 2016.

[489] B. Bajželj et al., "Importance of food-demand management for climate mitigation," *Nature Climate Change*, vol. 4, no. 10, pp. 924–929, 2014.

[490] P. Smith and P. J. Gregory, "Climate change and sustainable food production," *Proceedings of the nutrition society*, vol. 72, no. 1, pp. 21–28, 2013.

[491] B. M. Campbell et al., "Agriculture production as a major driver of the earth system exceeding planetary boundaries," *Ecology and society*, vol. 22, no. 4, 2017.

[492] T. Garnett et al., "Sustainable intensification in agriculture: Premises and policies," *Science*, vol. 341, no. 6141, pp. 33–34, 2013.

[493] I. Perfecto, J. Vandermeer, and A. Wright, *Nature's matrix: linking agriculture, biodiversity conservation and food sovereignty*. Routledge, 2019.

[494] P. H. Verburg, K. Neumann, and L. Nol, "Challenges in using land use and land cover data for global change studies," *Global change biology*, vol. 17, no. 2, pp. 974–989, 2011.

[495] M. Lippe et al., "Using agent-based modelling to simulate social-ecological systems across scales," *GeoInformatica*, vol. 23, no. 2, pp. 269–298, 2019.

[496] C. Kremen and A. Miles, "Ecosystem services in biologically diversified versus conventional farming systems: Benefits, externalities, and trade-offs," *Ecology and society*, vol. 17, no. 4, 2012.

[497] P. Meyfroidt et al., "Ten facts about land systems for sustainability," *Proceedings of the National Academy of Sciences*, vol. 119, no. 7, e2109217118, 2022.

[498] F. Zabel, R. Delzeit, J. M. Schneider, R. Seppelt, W. Mauser, and T. Václavík, "Global impacts of future cropland expansion and intensification on agricultural markets and biodiversity," *Nature communications*, vol. 10, no. 1, p. 2844, 2019.

[499] J. Clapp, "Food security and nutrition: Building a global narrative towards 2030," 2020.

[500] M. Scheffer, S. Carpenter, J. A. Foley, C. Folke, and B. Walker, "Catastrophic shifts in ecosystems," *Nature*, vol. 413, no. 6856, pp. 591–596, 2001.

[501] H.-O. P. Mbow, A. Reisinger, J. Canadell, and P. O'Brien, "Special report on climate change, desertification, land degradation, sustainable land management, food security, and greenhouse gas fluxes in terrestrial ecosystems (sr2)," *Ginevra, IPCC*, vol. 650, 2017.

[502] V. A. Cramer, R. J. Hobbs, and R. J. Standish, "What's new about old fields? land abandonment and ecosystem assembly," *Trends in ecology & evolution*, vol. 23, no. 2, pp. 104–112, 2008.

[503] K. Henderson and M. Loreau, "A model of sustainable development goals: Challenges and opportunities in promoting human well-being and environmental sustainability," *Ecological modelling*, vol. 475, p. 110 164, 2023.

[504] M. Leach et al., "Equity and sustainability in the anthropocene: A social–ecological systems perspective on their intertwined futures," *Global Sustainability*, vol. 1, e13, 2018.

[505] E. Starbird, M. Norton, and R. Marcus, "Investing in family planning: Key to achieving the sustainable development goals," *Global health: science and practice*, vol. 4, no. 2, pp. 191–210, 2016.

[506] M. Obersteiner et al., "Assessing the land resource–food price nexus of the sustainable development goals," *Science advances*, vol. 2, no. 9, e1501499, 2016.

[507] H. C. J. Godfray et al., "Meat consumption, health, and the environment," *Science*, vol. 361, no. 6399, eaam5324, 2018.

[508] B. T. Milne, "The utility of fractal geometry in landscape design," *Landscape and Urban Planning*, vol. 21, no. 1-2, pp. 81–90, 1991.

[509] B. Zeide, "Fractal geometry in forestry applications," *Forest Ecology and Management*, vol. 46, no. 3-4, pp. 179–188, 1991.

[510] D. Evans, J. N. Quinton, J. A. Davies, J. Zhao, and G. Govers, "Soil lifespans and how they can be extended by land use and management change," *Environmental Research Letters*, vol. 15, no. 9, 0940b2, 2020.

[511] J. M. García-Ruiz, S. Beguería, E. Nadal-Romero, J. C. González-Hidalgo, N. Lana-Renault, and Y. Sanjuán, "A meta-analysis of soil erosion rates across the world," *Geomorphology*, vol. 239, pp. 160–173, 2015.

[512] R. Crouzeilles, M. Curran, M. S. Ferreira, D. B. Lindenmayer, C. E. Grelle, and J. M. Rey Benayas, "A global meta-analysis on the ecological drivers of forest restoration success," *Nature communications*, vol. 7, no. 1, p. 11 666, 2016.

[513] R. E. Evenson and P. Pingali, *Handbook of agricultural economics*. Elsevier, 2009, vol. 4.

[514] K. G. Cassman, "Ecological intensification of cereal production systems: Yield potential, soil quality, and precision agriculture," *Proceedings of the National Academy of Sciences*, vol. 96, no. 11, pp. 5952–5959, 1999.

[515] J. Pretty et al., "Policy challenges and priorities for internalizing the externalities of modern agriculture," *Journal of environmental planning and management*, vol. 44, no. 2, pp. 263–283, 2001.

[516] H. Sandhu et al., "The future of agriculture and food: Evaluating the holistic costs and benefits," *The Anthropocene Review*, vol. 6, no. 3, pp. 270–278, 2019.

[517] M. N. Khan and F. Mohammad, "Eutrophication: Challenges and solutions," in *Eutrophication: causes, consequences and control: volume 2*, Springer, 2013, pp. 1–15.

[518] P. J. Withers, C. Neal, H. P. Jarvie, and D. G. Doody, "Agriculture and eutrophication: Where do we go from here?" *Sustainability*, vol. 6, no. 9, pp. 5853–5875, 2014.

[519] F. N. Tubiello, M. Salvatore, S. Rossi, A. Ferrara, N. Fitton, and P. Smith, "The faostat database of greenhouse gas emissions from agriculture," *Environmental Research Letters*, vol. 8, no. 1, p. 015 009, 2013.

[520] J. J. Sigurdarson, S. Svane, and H. Karring, "The molecular processes of urea hydrolysis in relation to ammonia emissions from agriculture," *Reviews in Environmental Science and Bio/Technology*, vol. 17, no. 2, pp. 241–258, 2018.

[521] G. Mancuso, G. F. Bencresciuto, S. Lavrnić, and A. Toscano, "Diffuse water pollution from agriculture: A review of nature-based solutions for nitrogen removal and recovery," *Water*, vol. 13, no. 14, p. 1893, 2021.

[522] K. E. Wyer, D. B. Kelleghan, V. Blanes-Vidal, G. Schauberger, and T. P. Curran, "Ammonia emissions from agriculture and their contribution to fine particulate matter: A review of implications for human health," *Journal of environmental management*, vol. 323, p. 116 285, 2022.

[523] J. Shortle and R. D. Horan, "Policy instruments for water quality protection," *Annu. Rev. Resour. Econ.*, vol. 5, no. 1, pp. 111–138, 2013.

[524] H. L. Tuomisto, I. D. Hodge, P. Riordan, and D. W. Macdonald, "Does organic farming reduce environmental impacts?—a meta-analysis of european research," *Journal of Environmental Management*, vol. 112, pp. 309–320, 2012. DOI: 10.1016/j.jenvman.2012.08.018.

[525] J. P. Reganold and J. M. Wachter, "Organic agriculture in the twenty-first century," *Nature Plants*, vol. 2, no. 2, p. 15 221, 2016. DOI: 10.1038/nplants.2015.221.

[526] J. Bengtsson, J. Ahnström, and A.-C. Weibull, "The effects of organic agriculture on biodiversity and abundance: A meta-analysis," *Journal of Applied Ecology*, vol. 42, no. 2, pp. 261–269, 2005. DOI: 10.1111/j.1365-2664.2005.01005.x.

[527] V. Seufert, N. Ramankutty, and T. Mayerhofer, "What is this thing called organic?–how organic farming is codified in regulations," *Food Policy*, vol. 68, pp. 10–20, 2017.

[528] P. Migliorini and A. Wezel, "Converging and diverging principles and practices of organic agriculture regulations and agroecology. a review," *Agronomy for sustainable development*, vol. 37, no. 6, p. 63, 2017.

[529] S. L. Tuck, C. Winqvist, F. Mota, and et al., "Land-use intensity and the effects of organic farming on biodiversity: A hierarchical meta-analysis," *Journal of Applied Ecology*, vol. 51, pp. 746–755, 2014.

[530] J. Bengtsson, J. Ahnström, and A.-C. Weibull, "The effects of organic agriculture on biodiversity and abundance: A meta-analysis," *Journal of Applied Ecology*, vol. 42, pp. 261–269, 2005.

[531] A. Gattinger, A. Muller, M. Haeni, and et al., "Enhanced top soil carbon stocks under organic farming," *Proceedings of the National Academy of Sciences*, vol. 109, no. 44, pp. 18 226–18 231, 2012.

[532] European Food Safety Authority, *The 2023 european union report on pesticide residues in food*, EFSA Journal 22(3):e08012, Accessed 15 June 2025, 2024.

[533] M. Clark and D. Tilman, "Comparative analysis of environmental impacts of agricultural production systems, agricultural input efficiency, and food choice," *Environmental Research Letters*, vol. 12, no. 6, p. 064 016, 2017.

[534] European Commission, DG AGRI, *Eu organic market overview 2025*, Brussels: Market Brief, Accessed 15 June 2025, 2025.

[535] European Commission, *A farm to fork strategy for a fair, healthy and environmentally-friendly food system*, COM(2020) 381 final, Brussels, Accessed 15 June 2025, 2020.

[536] European Court of Auditors, *Special report 16/2024: Eu support to organic farming—positive but lacking measurement of results*, Luxembourg: EU Publications Office, Accessed 15 June 2025, 2024.

[537] O. Bommelaer and J. Devaux, "Coûts des principales pollutions agricoles de l'eau," *Études et documents*, vol. 52, pp. 1–28, 2011, Ministère de l'Écologie, du Développement durable, des Transports et du Logement.

[538] V. Marcus and O. Simon, "Les pollutions par les engrais azotés et les produits phytosanitaires : Coûts et solutions," *Études et Documents*, vol. 136, 2015, Décembre 2015.

[539] A. Quinet et al., "La valeur de l'action pour le climat : Une référence pour évaluer et agir," France Stratégie, Mar. 2025, Rapport de la commission présidée par Alain Quinet.

[540] CITEPA, "Rapport secten : Séries temporelles des émissions de gaz à effet de serre et de polluants atmosphériques en france," Centre Interprofessionnel Technique d'Études de la Pollution Atmosphérique, 2025. [Online]. Available: https://www.citepa.org/explorateur-de-donnees/.

[541] Eurostat, *Agri-environmental indicators—land-use statistics*, Accessed 14 June 2025, 2024. [Online]. Available: https://ec.europa.eu/eurostat.

[542] FSDN Public Database SO, *FSDN public database SO*, Accessed: 17 March 2026, 2025. [Online]. Available: https://agridata.ec.europa.eu/extensions/FSDNPublicDatabase/%20FSDNPublicDatabase.html.

[543] Agence Bio, *Observatoire de la production bio nationale*, https://www.agencebio.org/observatoire-de-la-production-bio-nationale/, Accessed: 2026-06-26, 2026.

[544] J. N. Pretty et al., "An assessment of the total external costs of uk agriculture," *Agricultural systems*, vol. 65, no. 2, pp. 113–136, 2000.

[545] J. N. Pretty, A. S. Ball, T. Lang, and J. I. Morison, "Farm costs and food miles: An assessment of the full cost of the uk weekly food basket," *Food policy*, vol. 30, no. 1, pp. 1–19, 2005.

[546] European Commission, *Infosheet C33: Farming intensity*, https://agridata.ec.europa.eu/Qlik_Downloads/InfoSheetEnvironmental/infoC33.html, Accessed: 2026-06-26, 2026.

INSTITUT POLYTECHNIQUE DE PARIS

Titre : Une analyse multi-échelles du déclin de la biodiversité : des décisions des agriculteurs aux systèmes alimentaires mondiaux

Mots clés : Modélisation à base d'agents, Gestion de la biodiversité, Changement d'affectation des sols

Résumé : L'effondrement en cours de la biodiversité mondiale est inextricablement lié à l'expansion agricole. Faire face à cette crise nécessite de dépasser les approches monodisciplinaires. Cette thèse développe des modèles bioéconomiques parcimonieux et adaptés à l'échelle — établissant un pont entre la science de la complexité et l'écologie — pour analyser trois domaines interconnectés : l'Europe, le Cerrado brésilien et le système alimentaire mondial. En Europe, un modèle à base d'agents démontre que les obligations environnementales isolées (comme les réductions générales de pesticides) accélèrent paradoxalement la perte de biodiversité en provoquant la faillite des petits exploitants et la concentration foncière. De plus, la lutte écologique contre les ravageurs se heurte à de fortes contraintes spatiales au sein des grandes exploitations remembrées.

À la frontière agricole brésilienne, la modélisation spatiale prouve que les politiques de conservation isolées sont facilement contournées. L'arrêt de la déforestation exige impérativement des interventions synergiques : le couplage d'une friction économique (la suppression des subventions sur les terres nouvellement défrichées) avec des incitations ciblées à la conservation. À l'échelle mondiale, la recherche démontre que les seules améliorations technologiques du côté de l'offre déclenchent le paradoxe de Jevons, élargissant ainsi involontairement l'empreinte agricole. En fin de compte, la véritable durabilité défie les solutions isolées. Elle exige des interventions socio-économiques à toutes les échelles — en répondant aux contraintes individuelles des agriculteurs, en gérant les flux de capitaux à la frontière, et en réduisant activement la demande mondiale pour les produits à forte intensité de ressources.

Title : A multi-scale analysis of biodiversity decline: From farmer decisions to global food systems

Keywords : Agent-based modelling, Biodiversity management, Land-use change

Abstract : The ongoing collapse of global biodiversity is inextricably linked to agricultural expansion. Addressing this crisis requires moving beyond single-discipline approaches. This thesis develops parsimonious, scale-adapted bio-economic models—bridging complexity science and ecology—to analyze three interconnected domains: Europe, the Brazilian Cerrado, and the global food system.

In Europe, an Agent-Based Model shows that isolated environmental mandates (e.g., blanket pesticide reductions) paradoxically accelerate biodiversity loss by driving smallholder bankruptcy and land consolidation. Furthermore, ecological pest control faces hard spatial limits on large, consolidated farms.

At the Brazilian agricultural frontier, spatial modeling proves standalone conservation policies are easily bypassed. Halting deforestation strictly requires synergistic interventions: coupling economic friction (removing subsidies on newly cleared land) with targeted conservation incentives. Globally, the research demonstrates that supply-side technological improvements alone trigger the Jevons Paradox, inadvertently expanding the agricultural footprint.

Ultimately, true sustainability defies isolated fixes. It demands socio-economic interventions across all scales—addressing individual farmer constraints, managing frontier capital flow, and actively curtailing global demand for resource-intensive commodities.

Institut Polytechnique de Paris
91120 Palaiseau, France